Non-Invasive Molecular Assessment to Determine Embryonic Viability and Reproductive Success

A thesis submitted to the University of Kent for the degree of

DOCTOR OF PHILOSOPHY

In the Division of Natural Sciences

2020

Jason C Parks

School of Biosciences

1.0 Declaration

No part of this thesis has been submitted in support of an application for any degree or qualification of the University of Kent or any other University or Institute of Learning.

Jason C Parks

December 2020

2.0 Acknowledgements

First, I would like to thank my scientific director, Dr. Mandy Katz-Jaffe, with whom I have had the distinct pleasure of working under for the entirety of my professional career. Dr. Katz-Jaffe has contributed immensely to my overall development as a scientist, author and presenter. She has also been a wonderful mentor and friend to me for over a decade. Without her encouragement, tutelage and (most importantly) patience, this thesis would have proved impossible. I look forward to many more years of waking up eager to arrive at work every day, where I get to play and enjoy my time in her laboratory. I would also like to thank Dr. Darren Griffin for his support throughout the entirety of my time spent within the Genetics program at the University of Kent. He has never failed to offer a steady and patient hand when I needed it, and has provided me with an amazing opportunity to grow and develop as a student and professional scientist. Furthermore, I would be remiss to overlook Dr. Bill Schoolcraft and my wonderful colleagues and co-authors at the Colorado Center for Reproductive Medicine, for creating a culture of excellence and always striving to engage in top quality scientific research and care that benefits the patients they serve. Especially my good friends Blair McCallie and Michelle Denomme who have been an absolute pleasure to collaborate with and always willing to share their strengths and offer insights into any issue that may arise in the lab. Finally, I would like to thank my supportive and loving friends and family for seeing me through these rigorous years of study, specifically I'd like to thank my wonderful wife Jill, who, no matter how busy she may have been, she was always available to listen to yet another

practice presentation or listen to me excitedly explain my results to her without ever once rolling her eyes.

3.0 Peer Reviewed Journal Articles

The substantive thesis incorporates the following published and/or submitted articles in which I was first (or joint-first) author:

Parks JC, Patton AL, McCallie BR, Griffin DK, Schoolcraft WB, Katz-Jaffe MG. *Corona cell RNA sequencing from individual oocytes revealed transcripts and pathways linked to euploid oocyte competence and live birth***.** Reprod Biomed Online. 2016 May;32(5):518-26. doi: 10.1016/j.rbmo.2016.02.002. Epub 2016 Feb 24.

Parks JC, McCallie BR, Patton AL, Al-Safi ZA, Polotsky AJ, Griffin DK, Schoolcraft WB, Katz-Jaffe MG. *The impact of infertility diagnosis on embryo-endometrial dialogue.* Reproduction. 2018 Jun;155(6):543-552. doi: 10.1530/REP-17-0566. Epub 2018 Apr 10.

Denomme MM*, **Parks JC*,** McCallie BR, McCubbin NI, Schoolcraft WB, Katz-Jaffe MG. *Advanced paternal age directly impacts mouse embryonic placental imprinting.* PLoS One. 2020 Mar 6;15(3):e0229904. doi: 10.1371/journal.pone.0229904. eCollection 2020.

- *Joint first authors

Published manuscripts where I was the primary author have been inserted as text, mostly unchanged, but modified for the thesis format.

The following articles are also presented for consideration. In each case, they are annexed at the back of the thesis. My contribution to each of them is outlined below *in italics***.**

McCallie BR*, **Parks JC***, Griffin DK, Schoolcraft WB, Katz-Jaffe MG. Infertility diagnosis has a significant impact on the transcriptome of developing blastocysts. Mol Hum Reprod. 2017 Aug 1;23(8):549-556. doi: 10.1093/molehr/gax034.

- *Provided input with regard to the study design and results interpretation.*
- *Coordinated collection of study materials between the research department and the IVF laboratory.*
- *Warmed vitrified embryos, confirmed viability and prepared samples for -80oC storage and downstream transcriptome experiments.*
- **Co-first authored manuscript.*

Katz-Jaffe MG, Lane SL, **Parks JC,** McCallie BR, Makloski R, Schoolcraft WB. Antioxidant Intervention Attenuates Aging-Related Changes in the Murine Ovary and Oocyte. Life (Basel). 2020 Oct 22;10(11):E250. doi: 10.3390/life10110250.

- *Provided input with regard to the study design and results interpretation.*
- *Maintained and monitored the health of the mouse colony and worked with first author to coordinate ordering animals and reagents as needed.*
- *Sacrificed animals in accordance with the experimental timeline and collected all study materials including oocytes & ovaries for -80oC storage.*

• *Contributed to writing of Materials and Methods.*

Denomme MM, McCallie BR, **Parks JC,** Schoolcraft WB, Katz-Jaffe MG. Epigenetic Dysregulation Observed in Monosomy Blastocysts Further Compromises Developmental Potential. PLoS One. 2016 Jun 7;11(6):e0156980. doi: 10.1371/journal.pone.0156980. eCollection 2016.

• *Coordinated collection of study materials between the research department and the IVF laboratory.*

• *Warmed vitrified embryos, confirmed viability and prepared samples for -80oC storage and downstream molecular experiments.*

• *Contributed to writing of Materials and Methods.*

Denomme MM, McCallie BR, **Parks JC,** Schoolcraft WB, Katz-Jaffe MG. Alterations in the sperm histone-retained epigenome are associated with unexplained male factor infertility and poor blastocyst development in donor oocyte IVF cycles. Hum Reprod. 2017 Dec 1;32(12):2443-2455. doi: 10.1093/humrep/dex317.

•*Coordinated collection of study materials between the research department and the IVF laboratory.*

• *Performed sperm count and motility, and prepared them for -80oC storage and downstream epigenetic experiments.*

• *Contributed to writing of Materials and Methods.*

Denomme MM, McCallie BR, **Parks JC,** Booher K, Schoolcraft WB, Katz-Jaffe MG. Inheritance of epigenetic dysregulation from male factor infertility has a direct impact on reproductive potential. Fertil Steril. 2018 Aug;110(3):419-428.e1. doi: 10.1016/j.fertnstert.2018.04.004. Epub 2018 Jun 28.

- *Coordinated collection of study materials between the research department and the IVF laboratory.*
- *Performed sperm count and motility, and prepared them for -80oC storage and downstream epigenetic experiments.*
- *Contributed to writing of Materials and Methods.*

Pini T, **Parks J,** Russ J, Dzieciatkowska M, Hansen KC, Schoolcraft WB, Katz-Jaffe M. Obesity significantly alters the human sperm proteome, with potential implications for fertility. J Assist Reprod Genet. 2020 Apr;37(4):777-787. doi: 10.1007/s10815-020-01707-8. Epub 2020 Feb 5.

- *Coordinated collection of study materials between the research department and the IVF laboratory.*
- *Performed sperm count and motility and morphological assessment of samples, and prepared them for -80oC storage and downstream proteomics.*
- *Contributed to writing of Materials and Methods.*

The following articles on which I was a co-author are <u>not</u> submitted as part of this thesis as they form the substantive part of Blair McCallie's thesis (recently submitted). Nonetheless they were published during the time of registration and I contributed to them with technical input

McCallie BR, Haywood M, Denomme MM, Makloski R, **Parks JC,** Griffin DK, Schoolcraft WB, Katz-Jaffe MG. Forecasting early onset diminished ovarian reserve for young reproductive age women. Submitted and under review to J Assist Reprod Genet. Sept 2020

McCallie BR, **Parks JC,** Trahan GD, Jones KL, Coate BD, Griffin DK, Schoolcraft WB, Katz-Jaffe MG Compromised global embryonic transcriptome associated with advanced maternal age. J Assist Reprod Genet. 2019 May;36(5):915-924

McCallie BR, **Parks JC,** Patton AL, Griffin DK, Schoolcraft WB, Katz-Jaffe MG. Hypomethylation and Genetic Instability in Monosomy Blastocysts May Contribute to Decreased Implantation Potential. PLoS One. 2016 Jul 19;11(7):e0159507

McCallie BR, **Parks JC,** Strieby AL, Schoolcraft WB, Katz-Jaffe MG. Human blastocysts exhibit unique microrna profiles in relation to maternal age and chromosome constitution. J Assist Reprod Genet. 2014 Jul;31(7):913-9

4.0 Published abstracts during the period of registration

Jason C. Parks, Alyssa L. Patton, Blair R. McCallie, William B. Schoolcraft, Mandy G. Katz-Jaffe. *Aspirate and lavage prior to mouse embryo transfer indicates secretome miRNA expression as an early predictor of embryo implantation potential*. Presented at 2015 ASRM Conference in Baltimore, Maryland.

Jason C Parks, Blair McCallie, Julie A Reisz, Matthew Wither, William B Schoolcraft, Mandy G Katz-Jaffe. *Maternal endometrial secretions 24 hours prior to frozen embryo transfer is predictive of implantation outcome*. Presented at 2016 ASRM Conference in Salt Lake City, Utah.

Jason C Parks, Michelle Denomme Tignanelli, Nathan McCubbin, Blair McCallie, William Schoolcraft, Mandy Katz-Jaffe. *Advanced paternal age directly impacts placental epigenetic mechanisms*. Presented at 2017 ASRM Conference in San Antonio, Texas.

Jason C. Parks, Blair R. McCallie, Alyssa L. Patton, Nathan I. McCubbin, William B. Schoolcraft, Mandy G. Katz-Jaffe. *Antioxidant intervention promotes cell survival and redox balance within the ovary and subsequent oocyte resulting in improved IVF outcomes*. Presented at 2018 ASRM Conference in Denver, Colorado.

JC Parks, BR McCallie, NI McCubbin, DK Griffin, WB Schoolcraft, MG Katz-Jaffe. *Uterine miRNAs reflect the unique microenvironment in an individual murine horn during the window of implantation*. Presented at 2018 SSR Conference in New Orleans, Louisiana.

Jason C Parks, Blair McCallie, Mary Sweet, Taylor Pini, William B Schoolcraft, Mandy G Katz-Jaffe. *Miniminally invasive uterine aspiration 24 hours ahead of embryo transfer characterizes the compromised RIF uterine microenvironment and is predictive of reproductive outcome*. Presented at 2019 ASRM Conference in Philadelphia, Pennsylvania.

Jason C Parks, Mary E Haywood, Blair McCallie, Sue McCormick, William B Schoolcraft, Mandy Katz-Jaffe. *Disruption of NFR2-mediated stress response and DNA repair pathways are associated with limited developmental potential of trisomy embryos.* Presented at 2020 ASRM Virtual Conference.

*Note ASRM = American Society of Reproductive Medicine; SSR = Society for the Study of Reproduction

5.0 Table of Contents

6.0 Abbreviations

AMA	Advanced Maternal Age
AMH	Anti-Müllerian hormone
ANOVA	Analysis of variance
APA	Advanced paternal age
APC	Adenomatosis polyposis coli
ART	Assisted Reproductive Technology
ART	Assisted Reproductive Technologies
ATP	Adenosine triphosphate
AUC	Area under the curve
CC	Corona cells
CD	Fertile control endometrium/fertile control blastocyst
CDC	Centers for Disease Control and Prevention
CI	Confidence interval
CK1α	Casein kinase 1α
COC	Cumulus-oocyte-complexes
Cox	Cyclooxygenase
CpG	Regions DNA where a cytosine is followed by a guanine nucleotide
CSF-1	Colony-stimulating factor-1
ED	Endometriosis endometrium/fertile control blastocyst
EDTA	Ethylenediaminetetraacetic acid
EE	Endometriosis endometrium/endometriosis blastocyst
EEC	Endometrial Epithelial Cells
EGF	Epidermal growth factor
ERA	Endometrial Receptivity Array
ESHRE	European Society for Reproduction and Embryology
FET	Frozen embryo transfer
fPN	Female pronuclei
FSH	Follicle stimulating hormone
GnRH	Gonadotrophin releasing hormone
GSK3	Glycogen synthase kinase 3
HB-EGF	Heparin-binding epidermal growth factor-like growth factor
hCG	Human Chorionic Gonadotropin
hDP	Human decidua-associated protein
hMG	Human menopausal gonadotrophin
ICI	Intracervical insemination
ICM	Inner cell mass
ICR	Imprinting control region
ICSI	Intracytoplasmic sperm injection
IGN	Imprinted gene networks
IL-1	Interleukin 1
IL-6	Interleukin 6

IUI	Intrauterine insemination
IVF	In Vitro Fertilization
LH	Luteinising hormone
LIF	Leukemia-inhibitory factor
MDA	Malon-di-aldehyde
miRNA	Micro-ribonucleic acid
MLID	Multi-locus imprinting disturbances
mPN	Male pronuclei
MUC1	Mucin 1
NGS	Next generation sequencing
NICS	Non-invasive chromosome screening
NIH	National Institute of Health
P4	Progesterone
PBS-BSA	Phosphate buffered saline-bovine serum albumin
PCR	Polymerase chain reaction
PGT-A	Pre-genetic testing for aneuploidy
PP2A	Protein phosphatase 2A
Q RT-PCR	Quantitative real-time PCR
RCT	Randomised controlled trial
REI	Reproduction Endocrinology and Infertility
RIF	Repeated implantation failure
RNA	Ribonucleic Acid
ROS	Reactive oxygen species
SART	Society for Assisted Reproductive Technologies
SCD	Sperm chromatin dispersion
SCM	Spent Culture Media
SCSA	Sperm chromatin structure assay
SIAH1A	E3 ubiquitin ligase seven in absentia homologue 1A
TAC	Total antioxidant capacity
TCA	The citric acid cycle
TE	Trophectoderm
TMS	Time-lapse monitoring systems
TUNEL	Terminal deoxynucleotidyl transferase dUTP nick-end labeling
VEGF	Vascular endothelial growth factor
WHO	World Health Organization

7.0 Abstract

The success of human IVF is essentially determined by the quality of the embryo (itself a function of the quality of the oocyte and sperm), the endometrium and of the interaction between them. While there are established means of establishing the quality of each individually, some of these are limited and, in particular, the embryo-endometrial dialogue is difficult to capture and observe. As a result, it is under-studied and, with this in mind, the aims of this thesis were threefold:

First, to investigate the corona cell transcriptome of euploid oocytes, RNA sequencing of corona cells from individual cumulus oocyte complexes that developed into euploid blastocysts was employed. Alongside bioinformatic and statistical analysis to compare IVF outcomes, a mean number of sequence reads of 21.2 million were produced. Differentially expressed gene analysis revealed 343 statistically significant transcripts and enriched pathway analysis showed WNT signaling, MAPK signaling, focal adhesion and TCA cycle to be related to IVF outcome. Specifically, key genes within the WNT/beta-catenin signaling pathway, including AXIN, were associated with oocyte competence. Furthermore, key genes and signaling pathways were identified in corona cell profiles in association with IVF outcome following the transfer of euploid blastocysts previously vitrified in a frozen embryo transfer.

A second study investigated an association between advanced maternal age (AMA) and endometriosis on the embryo-endometrial molecular dialogue before implantation. Co-culture experiments were performed with endometrial epithelial cells (EEC) and cryopreserved day 5 blastocysts from AMA or endometriosis patients. Extracellular vesicles isolated from the co-culture supernatant were analyzed for miRNA expression and revealed significant alterations correlating to AMA or endometriosis. Functional annotation analysis of miRNA-target genes revealed enriched pathways for both infertility etiologies, including disrupted cell cycle regulation and proliferation. These extracellular vesicle-bound secreted miRNAs are key transcriptional regulators in embryo-endometrial dialogue.

The third study was concerned with the placental epigenome, which plays a critical role in regulating mammalian growth and development. Alterations to placental methylation, often observed at imprinted genes, can lead to adverse pregnancy complications such as intrauterine growth restriction and preterm birth. Similar associations have been observed in offspring derived from advanced paternal age fathers. As parental age at time of conception continues to rise, the impact of advanced paternal age on these reproductive outcomes is a growing concern, but limited information is available on the molecular mechanisms affected in utero. This longitudinal murine research study investigated the impact of paternal aging on genomic imprinting. Paternal age significantly impacted embryonic placental weight, fetal weight and length, significant

hypermethylation was observed upon natural paternal aging and several transcript level alterations attributable to advanced paternal age were identified.

This thesis also presents a series of co-authored studies on related subjects such as embryonic epigenetic dysregulation, unexplained male factor and the sperm epigenome, the dynamic transcriptome of IVF blastocysts in association with infertility, redox balance and aging-related changes in the mouse ovary/oocyte, obesity and the human sperm proteome.

Collectively, these data could inform the development novel biomarkers for non-invasive assessment of oocyte competence and implantation success. They also demonstrate a paternal age effect with dysregulation at numerous imprinted loci, providing a mechanism for future adverse placental and offspring health conditions.

8.0 List of Figures

9.0 List of Tables

10.0 General Introduction

Infertility is a disease defined by the World Health Organization as "failure to achieve a clinical pregnancy after 12 months or more of regular unprotected sexual intercourse" (Zegers-Hochschild et al. 2009). According to the European Society for Reproduction and Embryology (ESHRE) and National Institute of Health and (NIH) its prevalence is ~ 1 in 6 of couples trying to conceive. https://medlineplus.gov/infertility.html

According to the most recent data provided by the Centers for Disease Control and Prevention, within the United States 35% of couples are diagnosed with infertility due to a combination of male and female influences, with 8% of couples experiencing infertility as male factor infertility as the principle cause (https://www.cdc.gov/reproductivehealth/infertility/index.htm). There are many factors contributing to the infertility phenotype including advanced maternal age, male factor, uterine factors, endometriosis, tubal factor, ovulatory disorders, luteal phase defects, repeated pregnancy loss, idiopathic (i.e. unknown), health and lifestyle, as well as specific oocyte related factors including mitochondrial health, metabolomic processes, spindle assembly functionality and meiotic success (Prates, Nunes, and Pereira 2014; Keefe, Kumar, and Kalmbach 2015). Infertility treatment regimes are similarly numerous e.g. intrauterine (IUI) or intracervical insemination (ICI) for patients with sufficient motile sperm available, normal hormone profiles and a functional uterus. Other interventions include optimal timing of intercourse, clomiphene citrate treatment to stimulate follicle

growth, human chorionic gonadotrophin administration to trigger ovulation or low dose gonadotropin administration to encourage ovarian follicular growth. Assisted Reproductive Technology (ART) is a generally applied term applied to indicate when oocytes, sperm and embryos are handled outside of the body including, significantly, in vitro Fertilization (IVF).

10.1. In-vitro fertilization (IVF)

Louise Brown and Alastair MacDonald in 1978 - 1979 are credited as the world's first IVF babies (Steptoe and Edwards 1978) and the approach has significantly improved over the years to one that is routine. Within the United States, it is currently estimated that 1 in 6 couples will have difficulty conceiving a child through conventional means, and will require the use of ART in order to be successful (Thoma et al. 2013). According to the Society for Assisted Reproductive Technology, In 2017, 248,086 total IVF treatment cycles had been performed in the United States. According to the Final National Summary Report for 2017, the overall IVF birth rate for first embryo transfers in 2017 is estimated to be 31.6 % for women aged 35-37, 21.5 % for women aged 38-40 and 11.2% for women aged 41-42 (sartcorsonline.com).

There are essentially three factors that ensure IVF success, namely the quality of the oocyte/embryo, uterus and sperm of the infertility patients. IVF begins with hyper-stimulation of the ovaries, and the subsequent capture of ~10-20 oocytes. To do this, the

pituitary gland is downregulated by administration of a dose of a gonadotrophin releasing hormone (GnRH) analogue (agonist or antagonist) to suppress endogenous hormone expression ahead of cycle commencement. Administration of follicle stimulating hormone (FSH) and/or human menopausal gonadotrophin (hMG) results in the recruitment and development of multiple antral follicles. Once follicles start to grow, they produce estrogen, which causes the endometrial proliferation. Once the follicle reaches a diameter of around 17mm, an artificial luteinising hormone (LH) surge is usually generated by either a dose of human Chorionic Gonadotropin (hCG) or a combination of a high dose agonist/low dose hCG to achieve the same effect. If an embryo transfer is to occur in the same cycle (fresh transfer), then progesterone is administered after oocyte retrieval to prepare the endometrium and maintain it. On the male side, semen is collected by the male partner or donor either by masturbation or more invasive means, including testicular sperm aspiration (TESA), percutaneous epididymal sperm aspiration (PESA), testicular sperm extraction (TESE), microepididymal sperm aspiration (MESA) or microdissection TESE (microTESE) (Coward and Mills 2017). Next, the sperm is purified and concentrated prior to its quality/quantity is analysed. Specifically, the viscosity, volume, color, pH, concentration, motility, vitality, the presence of leukocytes and the morphology of the sperm are recorded (Cooper et al. 2010) Next, to ensure fertilization, insemination is performed in the laboratory and sperm are either mixed with the collected oocytes (IVF), or injected (intracytoplasmic sperm injection (ICSI)) directly. Following fertilisation assessment, the following day (presence of 2 pronuclei), the

embryos that have been generated are kept in culture with the hope that a proportion will reach blastocyst stage.

Blastocyst transfer usually happens on day 5 post fertilization, and the remaining embryos can be vitrified to be transferred in either a later natural or artificial cycle. In a natural cycle, embryo transfer is timed either at 7 days following hCG trigger or 6 days following LH surge. In an artificial cycle, pituitary gland down-regulation and administration of exogenous oestrogen is applied to prepare the endometrium for implantation. When the thickness and pattern of the endometrium are appropriate, progesterone administration commences.

10.2. Endometrial factors affecting fertility

Implantation is an incredibly complex process determined by both embryonic and endometrial factors. Gene expression studies demonstrate noticeable changes during the cycle and, at the most receptive phase, growth factors, cytokines, glycoproteins and immunosuppressive agents are secreted into the uterine cavity (Melford, Taylor, and Konje 2014). The most receptive phase is usually termed the “window of Implantation” (WOI) at around 5-7 days post ovulation (Lessey 2000). To ensure appropriate timing for embryo transfer timing the WOI, which may differ between patients may be (Ruiz-Alonso

et al. 2013; Mahajan 2015). Commercial assays to measure endometrial receptivity and the WOI include “ERA” from Igenomix and “ER Peak” from Cooper Surgical. These have been developed by analysing a series of genes that are differentially expressed at different stages of the cycle. An algorithm is applied to accurately predict a personal WOI for women with repeated implantation failure (RIF) (Ruiz-Alonso, Blesa, and Simon 2012). Gomez *et al* (2015) (Gomez et al. 2015) reported that 25% of patients with RIF have an altered WOI. A recent randomised controlled trial (RCT) established evidence of proof of principle for the potential of using an ERA assay, demonstrating a significant increase in cumulative pregnancy rate (intention to treat criteria) when the ERA was used (Simon et al. 2020).

This thesis is concerned in part with the genetic quality of the embryo and partly its interaction with the endometrium.

10.3. Factors affecting the quality of the Sperm

Recently, there have been several meta-analysis studies that show male factors are present in 20-70% of all infertility cases. Furthermore, the overall quality of sperm among men appears to be in decline (Agarwal et al. 2015; Sengupta et al. 2018; Levine et al. 2017). Male fertility is influenced by a variety of factors including environmental, occupational and lifestyle choices as well as genetics, which may contribute to deteriorating sperm quality. An example of an external factor that can affect male fertility is smoking tobacco. Cigarette smoke for example contains over 7000 chemicals including known carcinogens and volatile organic compounds. Smoking has been shown to affect

male fertility and is associated with leucocytospermia, a major endogenous source of reactive oxygen species (ROS). At elevated levels, these ROS can overwhelm endogenous antioxidant defences leading to increased oxidative stress within the spermatozoa, compromising male fertility (Harlev et al. 2015). Specifically smoking has been negatively associated with sperm count, concentration motility as well as morphology (Adashi et al. 1994; Sharma, Harlev, et al. 2016). Additionally, the use of smoking tobacco products is also associated with increases in DNA damage, aneuploidies and mutations in sperm (Beal, Yauk, and Marchetti 2017). Similarly, frequent alcohol use also has negative consequences for semen volume and sperm morphology and motility (Li et al. 2011; Donnelly et al. 1999).

Males that have excessive fat accumulation resulting in a body mass index >30 have been shown to have decreased sperm quality and increased risk of infertility and elevated levels of ROS. A review of 30 studies including a total of 115,158 males found that paternal obesity was associated with significantly reduced reproductive potential. Obese men were found to have a higher percentage of sperm with DNA fragmentations, abnormal morphology and low mitochondrial membrane potential (Campbell et al. 2015; Lobascio et al. 2015). Additionally, obese men are also more likely to be oligozoospermic or azoospermic compared to men of a healthy weight range (Sermondade et al. 2013).

High levels of psychological stress can have serious side effects on the reproductive hormones and sperm quality in males. The HPA axis and gonadotrophin-inhibitory

hormone (GnIH) exert an inhibitory effect on the HPG axis and testicular Leydig cells. The resulting inhibition of the HPG axis reduces testosterone levels, which leads to changes in sertoli cells and the blood–testis barrier. The consequences, cause spermatogenesis to be suppressed, and further impairs testosterone secretion (Nargund 2015).

Another known contributor to male infertility is advanced paternal age. Advanced paternal age is not particularly well defined, with most studies estimating it to start between 35-50 years of age (Wu, Lipshultz, and Kovac 2016). A meta-analysis of 90 studies investigating the effects of advanced paternal age, involving 93 839 participants reported a paternal age associated decline in semen volume, sperm total, and progressive motility, normal sperm morphology as well as an increase in DNA fragmentation (Johnson et al. 2015). As men advance in age, testicular function and metabolism deteriorates once the testis undergoes morphological changes associated with aging, such as a decrease in the number of germ cells, leydig and sertoli cells, as well as structural changes, which include the narrowing of seminiferous tubules (Gunes et al. 2016). Concentrations of free and total testosterone also steadily decline with advanced paternal age, leading to primary hypogonadism. Regulation of the HPG axis is also shown to change as men get older. Furthermore, accumulation of ROS in male germ cells throughout the course of aging leads to oxidative stress, apoptosis and damage to sperm DNA (Gunes et al. 2016).

Finally, genetic factors have been found to contribute up to 15-30% of male infertility. Spermatazoa occurs in a sequential manner, and genes are in control of programming the

mitotic, meiotic, and postmeiotic differentiation phases (Shamsi, Kumar, and Dada 2011). Genetic factors affecting the viability of sperm include chromosomal abnormalities which can include both numerical errors and chromosomal anomalies, and account for 5-10% of oligozoospermia (which may be balanced or unbalanced), to 15%–25% cases with unobstructed azoospermia. An example of a numerical chromosome error found in male infertility is 47, XXY Klinefelter syndrome which is the most common cause of azoospermia (11% of cases), and is due to seminiferous tubule dysgenesis. Interestingly studies on the sperm chromosome of Kilenefelter men have shown that the extra chromosome is excluded during spermatogenesis, and that these men are able to have normal offspring, however there is also an increased risk of aneuploidy (Martin 2008; Selice et al. 2010; Rives et al. 2000).

Structural aberrations that can affect male fertility include Robertsonian and reciprocal translocations. Robertsonian translocations result in the fusion long arm of 2 acrocentric (Group D chromosomes: 13, 14, 15 and Group G chromosomes: 21, 22, and Y) chromosomes. The fused short arms are typically lost, so the carrier has a chromosomal constitution with 45 chromosomes. When the chromosomes pair during meiosis, they do so as a trivalent, and the resulting gametes can be chromosomally normal or aneuploid with an extra or missing long arm of chromosome (Kumar et al. 2007). Reciprical translocations occur due to an interchange in genetic material between nonhomologous chromosomes, and affects ~1% of infertile men (Meza-Espinoza, Anguiano, and Rivera 2008). During meiosis, chromosomes pair as quadravalents resulting in a higher

frequency of unbalanced chromosomes as compared with carriers of Roberstsonian translocations. Many of these imbalances lead to fetal mortality, with approximately 12% of translocation imbalances at prenatal diagnosis being paternally derived (Boue and Gallano 1984). Another structural aberration that may lead to male infertility are inversions. Inversions are balanced structural rearrangements that occurs when 2 chromosome breaks occur on the same chromosome and join after a 180° rotation, and are found within 0.1% of infertile men (Meza-Espinoza, Anguiano, and Rivera 2008). Inversions can be paracentric, with both breakpoints are on one chromosome arm and exclude the centromere or pericentric, when chromosome breaks include the centromere and the short and long arm of the chromosome.

The Y chromosome is the smallest of the human chromosomes, and is polymorphic in length, and divided into 7 deletion intervals. Microdeletions on the long arm of the Y chromosome (Yq) is one of the most significant defects associated with male infertility. Yq microdeletions are found within 13% azoospermic men, 1%-7% severely oligozoospermic men (sperm count less than 0.5 million/mL). These deletions are clustered in interval 5 and 6 of the Y chromosome (Colaco and Modi 2018).

Epigenetic modifications control a number of systems found within the body, and epigenetic dysregulation/modifications can have significant effects on male fertility. Two modifications that occur in chromatin are DNA methylation and post-translational histone modifications. DNA methylation involves an additional methyl group at the 5’ position of

the cytosine pyrimidine ring typically occurring in a CpG dinucleotide (Talbert and Henikoff 2006). Histone modifications include acetylation, methylation, ubiquitylation and phosphorylation and are believed to be major contributors to epigenetic regulatory mechanisms(Lachner, O'Sullivan, and Jenuwein 2003). The acetylation of histones marks active, transcriptionally competent regions, contrasted by hypoacetylated histones that are found in transcriptionally inactive euchromatic or heterochromatic regions. In contrast, histone methylation may be a marker for both active and inactive regions of chromatin (Tamaru and Selker 2001; Tariq et al. 2003). During gametogenesis, germ cells undergo extensive epigenetic reprograming which involves the establishment of sex specific patterns in the sperm and oocytes(Loukinov et al. 2002). These reprograming events can be affected by environmental factors which can cause idiopathic male infertility and affect implantation potential, placentation, as well as fetal growth (Emery and Carrell 2006; Dada et al. 2012; Jenkins et al. 2016).

10.4. Factors affecting the quality of the embryo or oocyte

Heavy emphasis is placed on the metric of oocyte/embryo competence, however this remains an elusive factor to quantify accurately. Culturing and handling IVF embryos, of course, exposes them to environmental stresses to which they otherwise would not have been subject. An important objective in all IVF clinics is to generate a stress-free environment for IVF and embryo growth, as close to natural conditions as can be made

possible (Swain 2010; Swain et al. 2016). Factors to consider include the culture medium, the surrounding gaseous environment, the laboratory consumables, pH and temperature.

The culture media currently in use has been continually modified over time, but is still based more or less on mouse embryo culture media that formed the basis of model species "work up" studies. Principally, it is a balanced salt solution (Chronopoulou and Harper 2015). Manufacturers rely on the abundant supply of mouse embryos to assess each batch (Quinn and Horstman 1998). This standard practice has limitations, however, as mouse embryos have different needs and sensitivity to human ones (Ackerman et al. 1985; Ackerman et al. 1984). Such tests ensure that media has no obvious toxins and that it is able to support growth of mouse embryos to blastocyst.

The precise composition of commercially available culture media are often a trade secret, however, they incorporate varying concentrations of glucose, pyruvate, and lactate to help embryo development (Gardner and Lane 1996). Contemporary formulations include amino acids, chelating agents (EDTA) and growth factors.

In a review by Mantikou the efficacy of different culture media was compared, concluding that there was no evidence to demonstrate the superiority of one medium over another (Mantikou et al. 2013). Some studies do however demonstrate differences in clinical outcomes between different media. For example, an RCT performed by (Kleijkers et al. 2016) demonstrated an increase in the incidence of low birthweight offspring using once

commercially available medium. Whether or not media constituents or culture environment generally affects the dynamics and rate of cell divisions and embryo development is still a topic of much debate (Ciray et al. 2012; Meseguer et al. 2012).

As culture conditions have continued to improve, in part because of media development, as well as improved knowledge and more sophisticated and reliable incubators, the ability to culture embryos beyond day 3, to day 5 has led to blastocyst stage transfer becoming more the norm in most quality IVF clinics.

10.5. Estimating embryo viability by conventional means

Most commonly, the "best" available embryo for transfer are chosen for their morphology and kinetics alone. If an embryo has successfully developed beyond day 3 when the embryonic genome is activated (Niakan et al. 2012) and undergone blastulation, is seems reasonable to suggest that it has better chance of implantation compared to one that has not. Failure to select a viable embryo for transfer will of course limit the chance of a pregnancy in a given treatment cycle. Taking into account highly successful vitrification regimes, it is is now thought that "freeze all" strategies and transferring the patients' embryos consecutively (following vitrification and warming) "one by one" can have the same end result as selection of the morphologically "best looking" embryo on the basis that, at some point, the best embryo will be transferred. However, to minimise both the financial and emotional burden on patients, identification and selection of the

most viable embryo should be prioritised. Visual observations (including time lapse) creates a picture of the quality, or viability of the embryo and the focus is heavily weighted on the embryo's appearance and its progression from fertilisation and through development. Given that many of the developing embryo's morphological features are more accurately assessed compared to time (morphokinetics) the assessment should be performed within designated, evidence-based time windows.

10.6. Non-Invasive Analysis: Viability and Developmental Competence in Assisted Reproduction

There is a fundamental need within the clinical laboratories of Reproduction Endocrinology and Infertility (REI) practices to continually improve and expedite assessment methods for the health and overall viability of oocytes and embryos in an IVF cycle. Current standards and practices within a modern IVF laboratory primarily use extended day 5/6 culture, combined with grading systems based on morphology (Gardner and Schoolcraft 1999b), and though widely integrated within daily use, it is unfortunately imperfect in regards to questions pertaining to competence and viability. To date, studies specifically investigating the embryo attrition rates associated with IVF (from oocyte retrieval throughout embryo development to live birth) are scarce. This may be due to individual clinics being reluctant to share the exact breakdown of their loss rate at each individual stage of daily embryo development (Zhao et al. 2020). However, based on

clinical data reported to the Society for Assisted Reproductive Technology (SART), the likelihood of a single aspirated oocyte to successfully develop and result in a live birth is merely ~5% (Patrizio and Caplan 2010). A recent study by Abe et al. found that the live birth rate per matured ooctyte in clomiphene citrate only minimal stimulation cycle IVF to vary heavily based on infertility etiology, as well as maternal age. However the loss to attrition from oocyte to live birth was exceptionally high in patients of advanced maternal age at ~2% (Table 1) (Abe et al. 2020).

	Total	Group A (age: ≤34 years)	Group B (age: 35–37 years)	Group C (age: 38–40 years)	Group D (age: 41–42 years)	Group E (age: ≥43 years)	*P* value
Number of patients	713	99	134	238	135	107	–
Number of oocytes retrieved	3264	304	476	1167	758	559	–
Number of live births	312	73	73	118	37	11	–
Live birth rate per oocyte (%)	9.6	24.0[a]	15.3[b]	10.1[c]	4.9[d]	2.0[e]	$P<0.01$

Different letters represent significant differences between groups ($P<0.01$)

Table 1: Live birth rate per matured oocyte in clomiphene citrate only minimal stimulation cycle IVF.

This extremely low efficiency translates to higher cost per patient due to the reality that IVF technicians must devote extra time, materials and resources on each oocyte/embryo, as it is impossible to select which developing embryo is competent to successfully implant and develop following an embryo transfer.

One of the greatest developments in the field of ART, has been the advancement and development of pre-genetic testing for aneuploidy (PGT-A), as many studies have demonstrated that embryo aneuploidy is the most important factor of IVF failure

(Litwicka et al. 2018; Dahdouh, Balayla, and Garcia-Velasco 2015; Sahin et al. 2014). Recent 2018 Data from the Society for Assisted Reproductive Technologies (SART)/U.S. Centers for Disease Control and Prevention (CDC) reveals that PGT-A improved live birth rates by approximately 19.0% from embryos chosen for transfer in women who underwent their first embryo transfer (D5/D6 day of transfer; frozen embryo transfer only) aged 35-37, and by 25.1% in women aged 38-40 relative to their peers who did not utilize PGT-A. This dramatic increase in live birth has revolutionized treatment strategies, especially in women presenting with advanced maternal age (defined as women >37 years of age), where the live birth rate is improved approximately 36.5% (National Summary Report. Atlanta: U.S. Department of Health and Human Services, 2018).

Though many IVF laboratories around the world have adopted PGT-A technologies, it remains a controversial subject. Specifically, several studies utilizing PGT-A on cleavage stage embryos had somewhat ambiguous or contrarian results with several studies finding it to be useful (Munne et al. 1993; Gianaroli et al. 2005) while other RCTs found no benefit from the practice (Mastenbroek et al. 2007; Schoolcraft et al. 2009). Performing blastomere biopsies at this stage of embryo development (~8 cell stage) is very invasive for the growing embryo, and the loss of ~25% of its cells retards its development as it now has to regenerate the lost cells. Although it is considered much less invasive, trophectoderm biopsy of blastocysts at the hatching stage is still an invasive procedure that injures the embryo. Often after performing laser assisted biopsy, the embryo will pulse in reaction to the large influx of energy, and may take an hour or more

to re-expand. Several studies have questioned whether PGT-A on trophectoderm biopsies is necessary at all, as by means of natural selection and attrition, blastocysts tend to have a higher euploidy rate than cleavage stage embryos (Kokkali et al. 2007; Fragouli et al. 2008). Finally, for a large proportion of patients, PGT-A may be unnecessary, it is prohibitively expensive for many, and for patient populations outside of those presenting with advanced maternal age, especially women under 38 years of age, the benefit may not be worth the cost as the likelihood of having a transfer grade, euploid embryo within a given cycle is high (Murphy et al. 2019; Doyle et al. 2020; Goldman et al. 2018).

A retrospective analysis of 15,162 trophectoderm biopsies with PGT-A, showed that beginning at age 26, the rate of aneuploidy begins to notably increase. From a clinical perspective, women aged 26-37 seeking ART treatment with PGT-A had at least one euploid embryo available for transfer ~96% of the time. Women classified as advanced maternal age had less favorable prognoses, with women aged 42 having one or more euploid embryos in ~77% of cases. By age 44, the number of patients that produced at least one euploid embryo fell to approximately 47% (Figure 1)(Franasiak and Scott 2014).

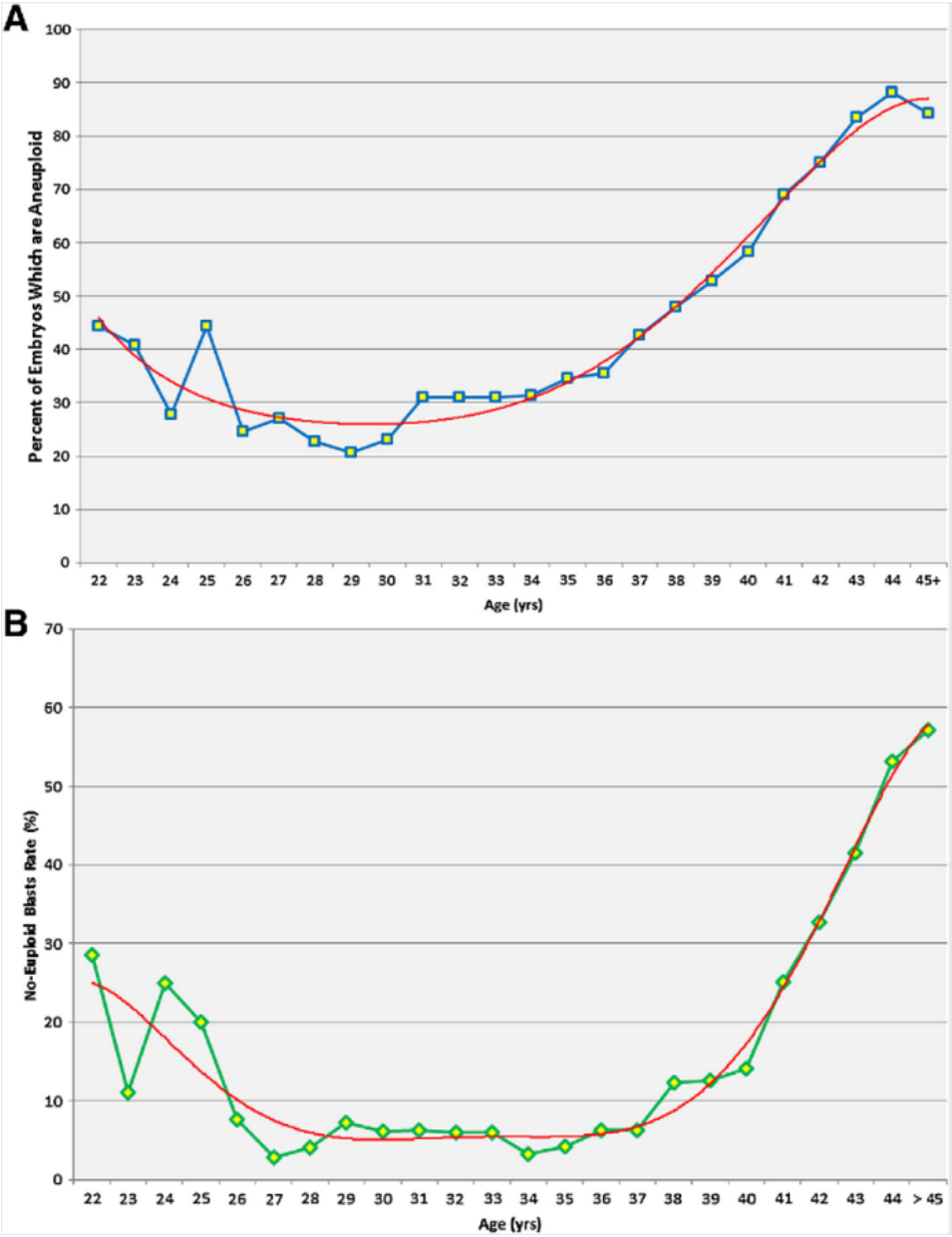

Figure 1: **A**) Prevalence of aneuploidy in embryos relative to the maternal age of the female partner. **B**) The odds of an ART cycle resulting in no-euploid blastocysts available for transfer (adapted from Franasiak JM et al, 2014)(Franasiak and Scott 2014).

However, even with these improved rates of positive clinical pregnancy and live birth, there remains room for improvement. One ongoing question that researchers continue to examine is, what additional factors are causing implantation failure and pregnancy loss in the instance of a morphologically top quality, euploid blastocyst embryo transfer into a seemingly healthy and receptive endometrium? Any extraneous factors affecting the quality of care, once known and addressed, will help further increase success rates in modern ART laboratories, as well as provide additional information for patients. This will allow them to make more informed decisions regarding their care, and give them a more accurate representation of their probabilities for success. The integration of additional accurate, non-invasive means by which to measure developmental competence would be a boon to the ART community, and it would potentially reduce the time to conception, and increase pregnancy rates and clinical success.

10.6.1. Time-lapse Monitoring Systems

Simple monitoring of morphological characteristics and cleavage rates are the most widely used criteria for embryo selection in clinical ART laboratories, used worldwide as a selection tool prior to blastocyst transfer (Bromer and Seli 2008). Traditionally, embryos are observed and removed from culture incubators every 24-48 hours to limit the developing embryos exposure to light and atmospheric changes, giving embryologists only select time points of observation. However, up to 70% of embryos created through IVF treatment are considered unusable for transfer based on their morphological

characteristics, and by some estimations, up to 84.9% of embryos considered selectable for transfer based on their morphological characteristics and cleavage rates fail to produce a live birth (Min et al. 2010; Kovalevsky and Patrizio 2005; Guerif et al. 2007; Racowsky et al. 2009).

Technological advancements have led to the development of time-lapse monitoring systems (TMS) that have been integrated into conventional gassed incubator systems. TMS generate a developmental time-line specific to each individual embryo, capturing images every 10-20 minutes, and do not require periodic removal of embryos from the incubator. This provides a non-invasive source of embryo specific morphokinetic information, allowing clinicians to capture subtle differences in development between embryos of the same cohort, in an effort to discern the top quality blastocyst for transfer (Figure 2) (Otsuki et al. 2019).

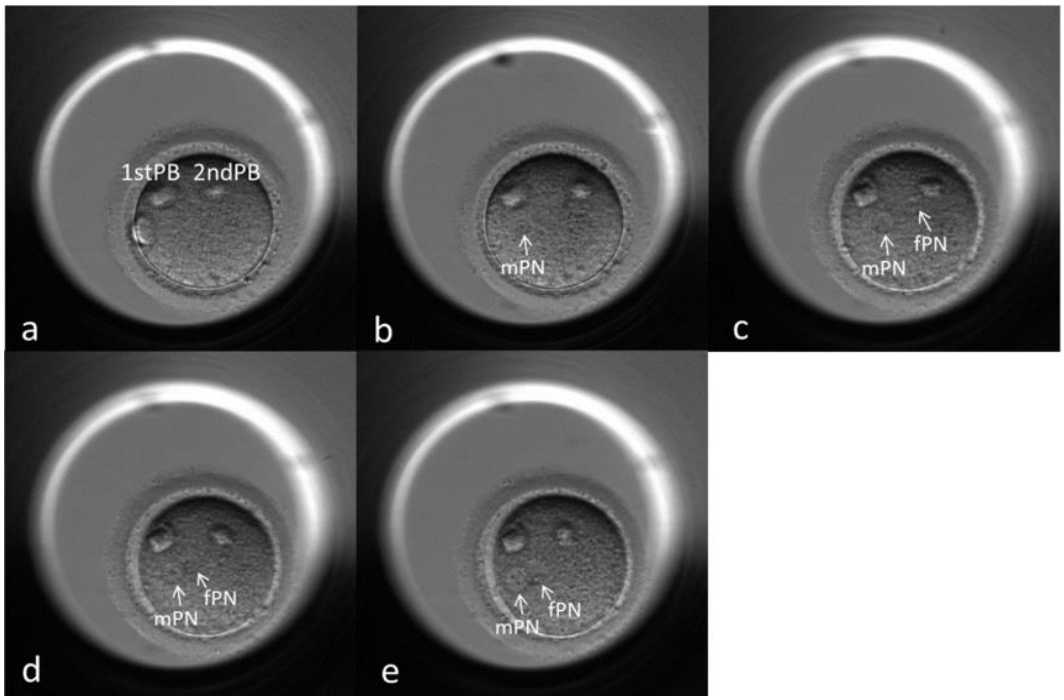

Figure 2: Example of images taken of a zygote in which the female (fPN) and male (mPN) pronuclei were successfully tracked. (**a**) First and second polar body become visible. (**b**) A male pronuclei (mPN) is formed has moved toward the center of the oocyte. (**c–e**) A female pronuclei fPN has formed close to the second polar body and is being drawn toward the mPN. (adapted from Otsuki J et al., 2019)(Otsuki et al. 2019).

An initial randomized control trial investigated use of a TMS with a novel morphokinetic algorithm and compared it to a standard cabinet culture incubator combined with routine morphological assessment. The results exhibited a significant increase in implantation and ongoing pregnancy rates in the TMS group, with a significant decrease in early pregnancy loss (Meseguer et al. 2011). The algorithm utilized previously un-used morphokinetic time points including duration of the first cytokinesis as well as duration of the 3-cell stage, and was determined to be a better oocyte and embryo selection

method than standard culture practices. However, after additional studies into the technology, the usefulness of TMS remains controversial, with some researchers concluding that fully integrating time-lapse imaging technologies into their already established daily routines, would not result in a net benefit (Armstrong et al. 2015; Wong, Repping, and Mastenbroek 2014). Recently, a meta-analysis of time-lapse culture, incorporating morphokinetic embryo selection, was published. This meta-analysis examined five randomized control trials including 1637 ART patients. The authors concluded that although the studies did not weight equally within the combined dataset, all showed some degree of benefit from TMS, with a total increase in ongoing pregnancy rates from 39.9% to 51.0% (Pribenszky, Nilselid, and Montag 2017).

One of the noted limitations of the initial TMS studies was the subjective nature of the annotations created by individual embryologists monitoring the time lapse data. Although embryologists within a single lab may show high levels of congruency, morphokinetic milestone annotation becomes much more difficult to normalize across multiple locations, with intrinsic inter-reader and intra-reader variability (Storr et al. 2017). In an effort to address some of these concerns and integrate new technologies into the existing platform, deep learning (a subfield of machine learning) has been utilized to remove as much subjectivity from the platform as possible. Combined retrospective data, including time lapse imaging and individual annotations from eight IVF laboratories across four countries, was incorporated into a deep learning model, which was then able to predict positive pregnancy with an average area under the curve (AUC) of 0.90-.95, despite the

data coming from different laboratories with different culture and laboratory practices (Tran et al. 2019). This model, combining TMS with robust machine learned algorithms can provide insight, non-invasively, into the predicted viability of individual embryos, giving embryologists additional selection criteria when choosing single transferable grade embryos out of a larger cohort of potential candidates.

10.6.2. Spent Culture Media (SCM): Secretomics, Metabolomics & Non-Invasive Screening

Another potentially valuable resource capable of providing developmental information for growing embryos, is the excess and often discarded media an embryo has been grown in. As an embryo develops and interacts with its environment, it absorbs and releases key nutrients found within the media. Previous studies have shown it is possible to observe an individual embryos metabolism (metabolome) by measuring the uptake of amino acids and carbohydrates from the surrounding media, and creating a unique, individual metabolic profile (Lane and Gardner 1996). It has been demonstrated that for the earliest stages of embryo development pyruvate is the primary substrate (1-8 cell stage), which later shifts to an increasingly glucose driven metabolism during the post compaction stages (Leese and Barton 1984; Gott et al. 1990). Embryonic glucose consumption results in subsequent lactate production, and it is by this glucose consumption to lactate production ratio that we can quantify an embryos glycolytic rate (Lane and Gardner 1996). Other important amino acids such as serine and potentially proline, may be

predictive of embryo viability, and embryos above a cutoff value for serine showed a statistically significant increase in pregnancy rates in a double embryo transfer, 62.5% vs 12.5% respectively (Zivi et al. 2014).

An embryos secretome is defined as the protein production of an embryo which is then sometimes secreted into the surrounding media. Secretome analysis of protein profiles of individual blastocysts have shown potential, and researchers have found that increased levels of ubiquitin were associated with increased implantation potential (Katz-Jaffe, Gardner, and Schoolcraft 2006; Katz-Jaffe, Schoolcraft, and Gardner 2006). Furthermore, the secretome from spent media has also been studied in conjunction with aneuploidy screening to determine if aneuploid embryos exhibit a different secretomic profile compared to euploid embryos. Lipocalin-1 is a protein that is secreted by embryos under stress, infection or inflammation and was discovered to be significantly increased in the spent media of aneuploid embryos (McReynolds et al. 2011). Embryo metabolism may also be used to observe effects of external factors, for example maternal obesity, which has been shown to impact embryo metabolism and embryonic development, resulting in a reduction of saturated fatty-acids in obese women compared to non-obese women (Bellver et al. 2015).

Researchers have also discovered that over the course of their development embryos also release genomic DNA and mitochondrial DNA into the surrounding media. In a study of 699 day 3 SCM samples, this ratio of mitochondrial DNA to genomic DNA was significantly

higher in viable embryos associated with successful implantation (Stigliani et al. 2014). Other molecules, including MicroRNAs have also been observed in the spent media of cultured embryos, including several microRNA profiles associated with positive IVF outcomes including miR-191 and miR-372 (Rosenbluth et al. 2014). Non-invasive detection of Mendelian genetic disorders such as alpha-thalassemia, has also been investigated by the quantification of cell-free DNA within spent media. When the SCM results were compared to traditional biopsy based PGD, researchers found a high rate of efficiency for diagnosis of this disorder (Wu et al. 2015).

One principal concern when considering spent media as a non-invasive tool is the requirement that embryos must be cultured individually, as it has been established that embryos have improved development when cultured together in groups (Holm et al. 1999; Hoelker et al. 2009). Individual embryo culture in low volumes is important so that the metabolic signature it leaves behind in the spent media is not diluted out by excess media and remains detectable. A low volume tool to measure glycolytic activity has been under development which utilizes a fused-silica capillary (Madr et al. 2015). This technology requires a relatively small volume of media, 2uL, to accurately measure pyruvate and lactate substrates, which would be advantageous for single embryo culture where low volume media drops allow for a more concentrated substrate for molecular analysis.

Although promising, there are limitations of metabolomics and spent media analysis, as the results have not always been easily reproducible. A study by the Aarhus University of Denmark found that NMR analysis of day 3 and day 5 spent media was unable to link the embryonic metabolome of good prognosis patients to embryo viability and subsequent embryo selection outcome (Kirkegaard et al. 2014). However, metabolomics combined with other analysis, such as when used in conjunction with time-lapse imaging software may prove to be a useful tool for research. For example, studies have found that morphokinetically advanced embryos demonstrated a higher metabolic rate, and resulted in higher fetal survival post-implantation compared to embryos with lower metabolic rates (Figure 3) (Lee, Thouas, and Gardner 2015).

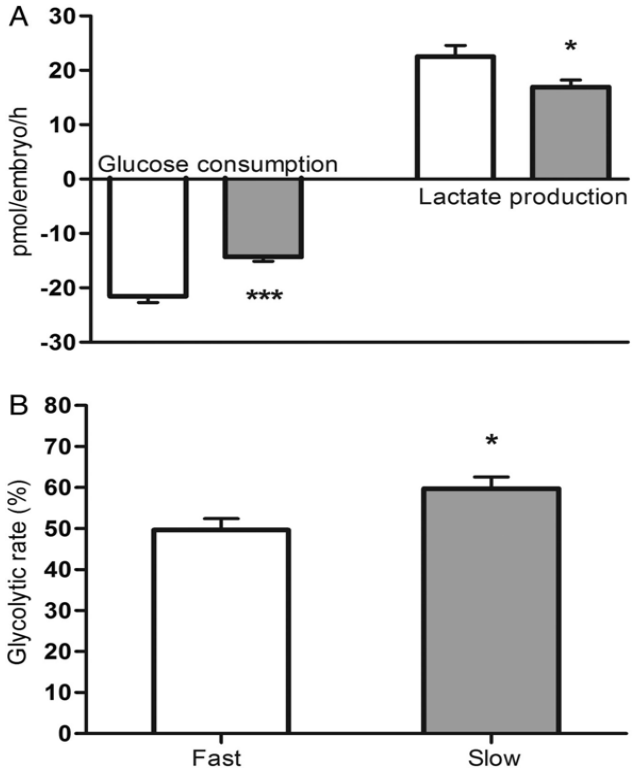

Figure 3: Correlation between morphokinetic activity and blastocyst carbohydrate metabolism. (A) Glucose consumption and lactate production (B) Glycolytic rate of

blastocysts, % of glucose converted to lactate. n ≥ 30 embryos per group, 12 biological replicates, *P < 0.05, ***P < 0.001. White bars represent 'fast' cleaving embryos and dark bars represent 'slow' cleaving embryos as observed with time lapse imaging (adapted from Lee et al., 2015)(Lee, Thouas, and Gardner 2015).

Beyond traditional secretomics and metabolomics investigating culture media, is a newly developed a non-invasive PGT-A technique utilizing SCM. As an embryo grows and divides throughout its development, small amounts of genomic DNA and mitochondrial DNA are shed into the surrounding environment, allowing detection as early as day 2-3 of development (Hammond et al. 2017; Yang et al. 2017). It has also been shown that this is more than mere DNA contamination, and that the genetic information leaked into the culture medium increases during embryo culture (Vera-Rodriguez et al. 2018). The source of this genomic DNA is still a cause of debate. Apoptosis of cells is one proposed theory, although many healthy embryos display none of the hallmarks of apoptosis as they grow and develop, despite this increase of genomic DNA found within SCM (Chi et al. 2011). However, SCM samples with the highest concentration of genomic and mitochondrial DNA was found in samples associated with poor to average quality blastocysts, with top quality blastocysts displaying less on average (Stigliani et al. 2013). Researchers have been attempting to use SCM proactively in conjunction with traditional trophectoderm biopsy based PGT-A to look for concordance between the two techniques. There are ongoing clinical trials investigating SCM use as an alternative source of genomic DNA, and initial results from a few pilot studies have been interesting. One report used vitrified embryos

combined with next generation sequencing (NGS) and evaluated the results found within the day 3-5 SCM and compared it to the corresponding whole blastocyst and discovered 100% chromosome copy number evaluation in 42 embryos obtained from 17 couples, representing the highest rate achieved by a study to date (Figure 4) (Xu et al. 2016).

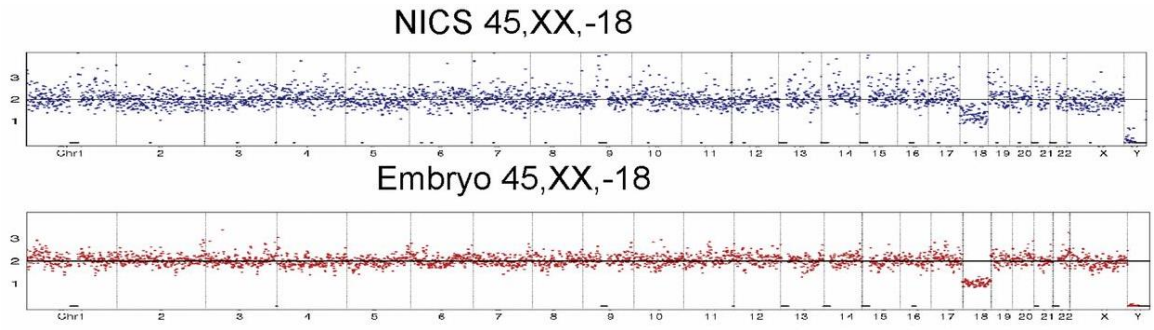

Figure 4: Example of validation of results from the comparison of non invasive chromosome screening (NICS) with spent media, versus the whole-blastocyst embryos (adapted figure from Xu J et al., 2016)(Xu et al. 2016).

Additional promising studies have concluded that although the techniques involved could use some additional refining, SCM is an alternative source of individual embryonic genomic DNA, and may be a promising alternative to more invasive, and technically difficult methods of blastocyst trophectoderm biopsy PGT-A screening (Fang et al. 2019; Rubio et al. 2019).

10.6.3. Follicular Fluid for Assessing Oocytes

During fetal development, primordial germ cells multiply, forming approximately 400,000 primordial follicles at birth within the ovary. These primordial follicles contain primary oocytes that will remain arrested within prophase stage of meiotic division I, until sexual maturity is reached. Upon reaching sexual maturity, two hormones, follicle stimulating hormone (FSH) and lutenising hormone (LH), are produced by the pituitary gland. The production of these hormones results in primary follicle development. In each subsequent ovarian cycle, approximately 20 primordial follicles are activated to begin maturation and development throughout the stages of folliculogenesis.

Within the standard operating procedure for oocyte retrieval during an ART cycle, follicular fluid is aspirated at the time of oocyte retrieval and is generally discarded post cumulus oocyte complex isolation (Figure 5). Prior to aspiration, this fluid is contained within the follicular antrum which surrounds the oocyte and changes its composition throughout the process of folliculogenesis. The intimate proximity of follicular fluid to the developing cumulus oocyte complex is important for follicular development, and the follicular fluid contains vital nutrients, including proteins associated with lipid transport, complement pathways, blood coagulation as well as plasma proteins (Schweigert et al. 2006; Jarkovska et al. 2010).

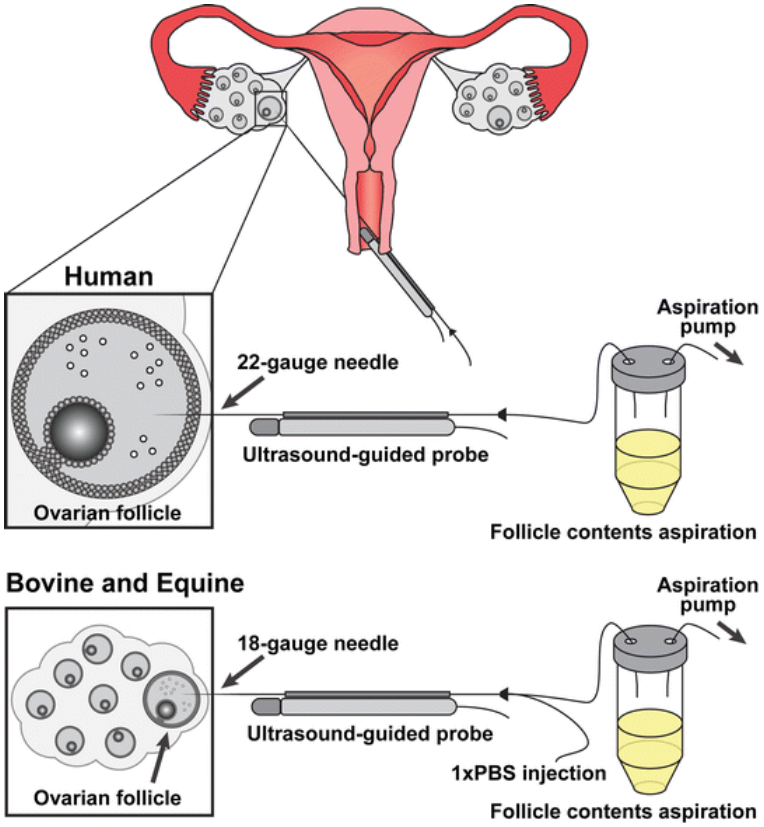

Figure 5: Follicular fluid aspiration is performed using transvaginal ultrasound guidance and a 22-gauge needle in human subjects. The collected fluid contains an abundance of cellular messages exchanged during follicle development (adapted from Kenigsberg S et al., 2017)(Kenigsberg et al. 2017).

This makes follicular fluid analysis an attractive prospect for the non-invasive analysis of oocytes because it reflects the metabolism of the developing follicle and is routinely discarded within an IVF lab. A recent investigation into the protein composition of follicular fluid identified a subset of 75 follicular fluid proteins that were linked with IVF outcome. Within the 75 proteins, 13 were involved in acute response signaling, coagulation, prothrombin activity, compliment system and growth hormone pathways

(Kushnir et al. 2012). Interestingly, follicular fluid protein composition appears to be dynamic, and studies have shown, that by using MALDI-TOF/TOF-MS technologies, observable differences are found in the follicular fluid proteins from women of advanced maternal age (38-42 years old), as compared to younger women (20-32 years old), with both groups of patients exhibiting normal FSH levels. The proteins serotransferrin, hemopexin precursor, complement C3, C4 and kininogen were uniquely down regulated in follicular fluid obtained from patients of advanced maternal age (Hashemitabar et al. 2014).

One theory pertaining to the cause and effect regarding changes within the ovary as it ages and the follicular metabolic age, states that improper levels of reactive oxygen species in follicular fluid may have the adverse effect of gradually distorting the levels of hydrogen peroxide in the follicles. By assessing the levels of ROS and H2O2 within the follicular fluid, it may be possible to determine the follicular metabolic state as a result of ovarian aging (Elizur et al. 2014). Outside of maternal age, oxidative stresses can also be induced by other factors such as high-fat diets, which can affect the levels of Malon-di-aldehyde (MDA) and total antioxidant capacity (TAC) within follicular fluid, which then has a negative effect on oocyte fertilization, and future developmental competence (Kazemi, Ramezanzadeh, Nasr-Esfahani, et al. 2013; Kazemi, Ramezanzadeh, Esfahani, et al. 2013). Follicular fluid also contains a number of exosomes, which are small vesicles used for transferring molecules in cell-to-cell signaling. A recent investigation into the function of exosomes within the follicular fluid discovered that exosomes contain a total of 35

microRNAs (small non-protein nucleotide chains of RNA) which were not present in serum derived from the same patient. Of the 35 microRNAs, 32 were transported by microvesicles containing exosomal biomarkers CD63 and CD81. These follicular fluid microRNAs are involved in critical pathways including follicle growth and oocyte maturation (Santonocito et al. 2014). Additionally, specific metabolites (arginine, glutamate, isoleucine and valine) found within follicular fluid are associated with oocyte developmental stage and maturity based upon their consumption and release (Hemmings et al. 2013).

Clinically, specific metabolic profiles of follicular fluids have also been correlated to cycle outcomes in patients who utilized ART. Researchers were able to correlate the metabolic profiles of follicular fluid containing variable concentrations of glucose, lactose, choline/phosphocholine and lipoproteins, to pregnancy outcome in patients undergoing an ART cycle (Wallace et al. 2012). Fatty acid ratios and carbohydrate concentrations have been associated with specific developmental stages including embryogenesis. Follicular fluid also contains cytokines and additional growth factors, including BMP2, interleukins 6, 8, 12 and 18, GDF-9, GCSF and amphiregulin (Sugiyama et al. 2010; Sarapik et al. 2012; Bedaiwy et al. 2007; Gode et al. 2011; Ledee et al. 2013; Liu et al. 2012). Several studies have used this information to develop multifactorial, individual, predictive values for oocytes to assess developmental potential and subsequent viability (Matoba et al. 2014; Wallace et al. 2012; O'Gorman et al. 2013).

Recently, the predictive values of follicular fluid profiles have been investigated, prospectively. One prospective analysis investigated the concentrations of anti-Müllerian hormone (AMH) and progesterone (P4) levels in follicular fluid, where it was discovered that elevated levels of these two molecules were correlated with increased oocyte viability and competence, and were able to predict which fertilized oocytes were developmentally competent enough to grow to the blastocyst stage (O'Brien, Wingfield, and O'Shea 2019). Another prospective analysis of 322 oocytes paired with follicular fluid samples found that increased levels of AMH and decreased levels of FSH were correlated with top quality blastocysts, whose transfer led to a live birth, compared with oocytes that failed to fertilize (91.2% sensitivity; 91.7% specificity) (Ciepiela et al. 2019). Follicular fluid collection and molecular biomarker analysis remains a promising, yet underutilized resource for the non-invasive assessment of oocyte developmental potential, which may be integrated into the standard operating protocols of ART laboratories in the future.

10.6.4. Cumulus Cells

During oocyte retrieval, follicles are aspirated from the ovary, and cumulus-oocyte-complexes (COC) are retrieved and isolated (Figure 6). Given ample time to complete maturation and development, the cumulus is then mechanically separated from the oocyte. To remove the remaining corona cells, the innermost collection of cells immediately surrounding the oocyte, diluted hyaluronidase is used to denude the corona

cells so the oocyte may be washed and held separately for future fertilization. The cumuli, as well as the corona cells, are then discarded.

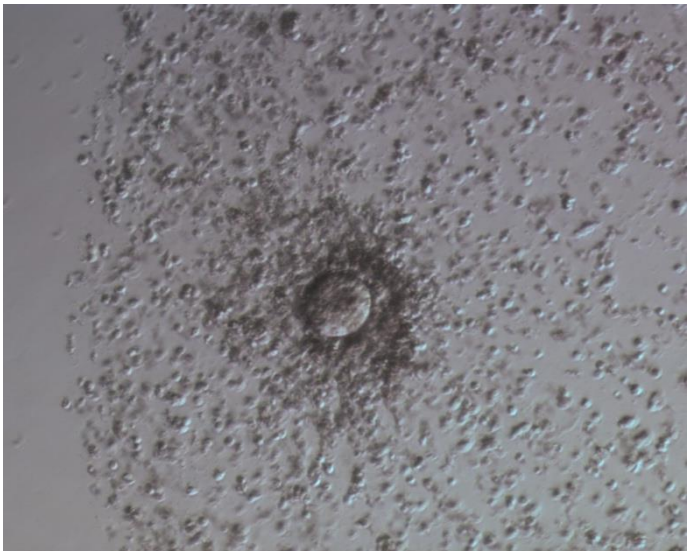

Figure 6: Cumulus oocyte complex before denudation, with compact, non-radiating cumulus cells. (100× magnification) (image adapted from Rienzi L et al., Atlas of Human Embryology atlas@eshre.eu 2020).

The molecular analysis of these follicular cells is another potential source for non-invasive oocyte viability assay development. Cumulus cells (CC) are nurse cells that surround the oocyte during development, and maintain a close bond through transzonal processes and gap junctions. These bonds serve to provide key nutrients and additional factors to the oocyte, which are crucial for oocyte development and maturation (Anderson and Albertini 1976).

This discarded material had been developing in conjunction with the oocyte, and may provide valuable information pertaining to the oocytes developmental potential. Gene

expression of CCs has been conducted, and found specific profiles able to predict oocyte maturation, cumulus expansion and fertilization potential (McKenzie et al. 2004; Assou et al. 2006; Anderson et al. 2009; Ouandaogo et al. 2011; Feuerstein et al. 2012; Yerushalmi et al. 2014). Gene expression within cumulus cells is very active, and is affected by specific events including maternal age (Al-Edani et al. 2014) as well as specific ovarian stimulation gonadatropin regimens (Assou, Al-edani, et al. 2013). CC gene profiles have also been investigated with regard to oocyte competence, and several CC genes were identified as potential developmental biomarkers, including BCL2L11, PCK1 and NFIB (Assou et al. 2008). Following this initial study, a panel of 45 CC genes associated with oocyte and embryo developmental potential were utilized in a prospective study by the researchers. The test group included patients receiving a day 3 transfer based solely on the gene expression of the panel of 45 genes, while the control group consisted of patients who received a day 3 transfer based on the standard morphological grading practices. Implantation rates and ongoing pregnancy rates were then observed between the two groups of subjects. The test group exhibited a statistically significant increase in pregnancy outcome as compared to control (40% vs 26.7% for implantation and 70% vs 47.7% for ongoing pregnancy rates). The study included the analysis of 267 CC samples, of which 27% had a gene expression profile predicting positive pregnancy outcome, 42% that predicted negative pregnancy outcome and 13% that predicted early arrested development. It is also noteworthy that no link between the gene expression of CCs and the morphological grades of the subsequent embryos was observed (Assou et al. 2010).

There have also been several retrospective studies of CC gene expression, and the following genes have been correlated with positive pregnancy outcome: NRP1, UBQLN1, PSMD6, HIST1H4C, CALM1, PTGS2, EFNB2 and CAMK1D. Alternatively, TOM1 has been correlated to negative pregnancy outcome (Assidi et al. 2011; Wathlet et al. 2012). Researchers have also looked beyond genes purely associated with developmental potential, and investigated a combinatorial panel of 12 genes found in CCs involved in glucose metabolism, transcription, gonadotropin regulation and apoptosis. By analyzing the gene expression of the specific 12 genes, researchers were able to predict pregnancy outcome for 55 patients with 78% accuracy (Iager et al. 2013). Although these studies show great potential, there are many inconsistencies between gene expression data. This may be due to differences in experimental design, or failure to take into account important parameters such as maternal age, IVF laboratory practices and specific ovarian stimulation protocols, all of which may affect embryo development.

10.6.5. Endometrial Environment

Although the oocyte and subsequent embryo remains the primary contributor to a failed IVF cycle, it is also important to consider the environment it is being transferred into. The embryo-endometrium interface represents the initial stages of implantation with blastocyst adhesion to a receptive uterus. Specifically, the endometrium is the compromised of mucosa and multiple tissue types including reticular connective tissue, secreted proteins, epithelial cells as well as a proliferation of blood vessels which supply

nutrients to the cells (Beier and Beier-Hellwig 1998). The endometrial cycle is tightly regulated by physiological alterations caused by changes in expression of genes and proteins. This cycle is composed of three specific phases which are marked by physiological changes controlled by circulating levels of estrogen and progesterone secreted and synthesized by the ovary (Ruiz-Alonso, Blesa, and Simon 2012).

The first phase of the endometrial cycle is the proliferative phase. During the proliferative phase, estradiol derived from growing follicles leads to the regeneration of the functionalis layer with re-epithelialization, which occurs on approximately day 5 of the menstrual cycle (Makieva et al. 2018). This phase is primarily characterized by the proliferation and hypertrophy of glands, increased stromal matrix and elongation of the terminal arterioles of the luminal epithelium (Gray et al. 2001; Taylor et al. 2001). Estrogen also upregulates the progesterone receptors, which alters the environment for the subsequent secretory phase (Fox et al. 2016; Gellersen and Brosens 2014). The cellular structure of the endometrial stromal cells during the proliferative phase, resemble a fibroblast-like appearance with developed rough endoplasmic reticulum and Golgi apparatus elongated nuclei and reduced cytoplasm (Cornillie and Lauweryns 1984). During decidual transformation, the nucleus of the stromal cells becomes rounded, the endoplasmic reticulum of the Golgi systems become dilated, and the cytoplasm begins to accumulate lipids and glycogens (Kajihara et al. 2014). Progesterone also induces the formation of pinopodes, the epithelial cells that lose their polarity and microvilli through down regulation of cell-to-cell adhesion molecules, producing a smooth apical surface

(Thie et al. 1995). This is critical for all future implantation, as the introduction of pinopodes also serves to decrease surface glycoprotein mucin 1 (MUC1), a mucus secretion responsible for forming a barrier against pathogens, which is inhibitory during the subsequent window of implantation (Haller-Kikkatalo et al. 2014; Redzovic et al. 2013).

The secretory phase is the second phase of the endometrial cycle. During the early and mid-secretory phase, cytoplasmic processes extend within the edematous connective tissue, releasing secretory products into the extracellular space. In the late-secretory phase, decidualizing cells display pseudopodia extensions engulfing the extracellular matrix. This phase of extreme remodeling may be attributed to the exhibition of phagocytotic activity during stromal cell decidualization (Cornillie, Lauweryns, and Brosens 1985). During this phase it is vital that the intercellular communication between the endometrial stromal cells is established in order to create the surface that will function as the site of embryo implantation along the fetomaternal interface (Figure 7). This communication is established by either direct cell to cell contact, or through intracellular junctions which mediate selective paracellular and intracellular transport of molecules (Garcia, Nelson, and Chavez 2018). Extensive communication networks are established which exert influence on the tissue, allowing physiological alterations as well as changes in homeostasis and tissue remodeling, making the endometrial surface one of great plasticity (Grund and Grummer 2018).

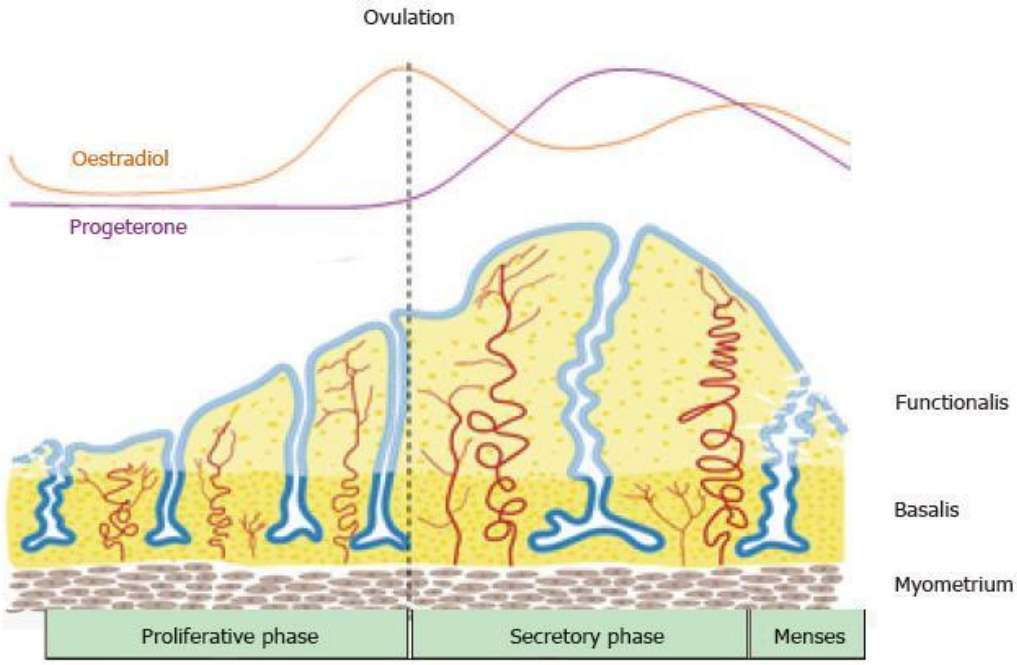

Figure 7: Changes within the human endometrium during the menstrual cycle, illustrating the growth, differentiation and shedding of the functionalis layer. The functionalis layer regenerates 4-10 mm during the proliferative phase (10 days) as cells proliferate in response to rising circulation of estrogen levels. During the secretory phase, progesterone induces differentiation of the luminal epithelium and stroma to generate an environment that is receptive to the implantation of an embryo (adapted from Gargett CE et al., 2007)(Gargett, Chan, and Schwab 2007).

The subsequent window of implantation occurs naturally between day six and day ten post ovulation (Figure8). Endometrial receptivity is characterized by changes in the endometrial layer and secretion of nutrients, including numerous vitamins and steroid-dependent proteins (Martin et al. 2002). During this period of endometrial receptivity, molecular dialogue is exchanged between the implanting blastocyst and the luminal

epithelium of the endometrial layer (Cuman et al. 2015). As the embryo approaches the uterine luminal epithelium near the future sight of implantation (usually near the upper posterior wall in the midsaggittal plane), a pro inflammatory reaction occurs causing endometrial vascular permeability to increase at the implantation site, mediated by Cyclooxygenase (Cox)-derived prostaglandins (van der Weiden, Helmerhorst, and Keirse 1991). Next, prostaglandin E_2 is increased in both the luminal epithelium and surrounding stromal cells, which has the added benefit of activating a multitude of other signaling proteins (Nicola, Lala, and Chakraborty 2008).

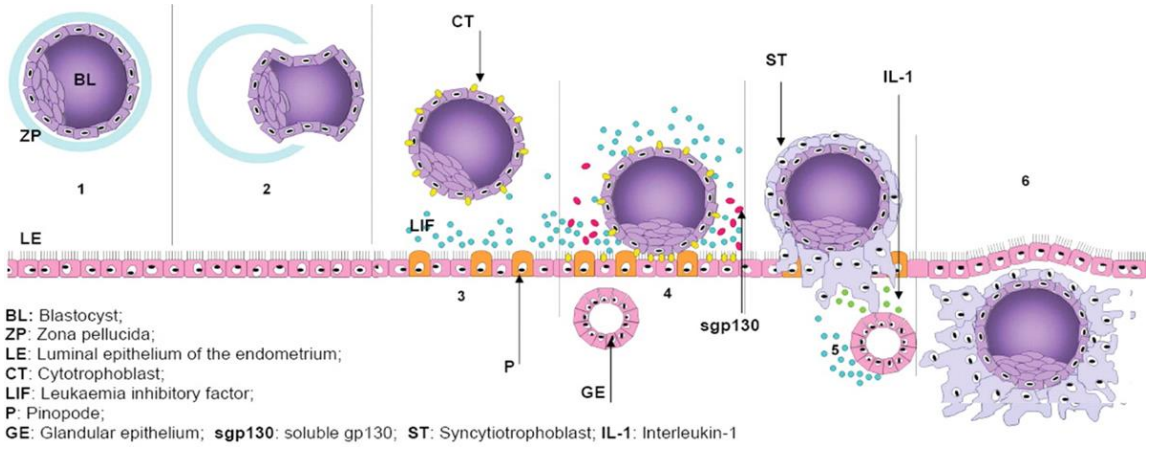

Figure 8: The blastocyst and uterus establish intimate physical and physiological contact resulting in the penetration of the basal membrane and controlled invasion of the stromal endometrium (adapted from Fitzgerald JS et al., 2008)(Fitzgerald et al. 2008).

Recently, researchers have benefited from transcriptomic studies investigating the endometrial window of implantation, which enabled the development of several commercial endometrial receptivity assays to diagnose the receptivity window including the Endometrial Receptivity Array (ERA) (Igenomix®), ERPeak^{SM} Endometrial Receptivity Test (CooperSurgical®) and the ReceptDivaDX (CiceroDX, Inc.). The ERA is a customized array containing 238 genes that are known to be differentially expressed depending on the receptivity status of the sample, is highly reproducible and more accurate than histologic dating (Garrido-Gomez et al. 2013). Likewise, the CooperSurgial and CiceroDX offerings also examine the expression of hormone-regulated genes to help determine a patients individual and uniquely timed window of implantation or identifies potential problems based on the upregulation of inflammatory genes, such as BCL6, based on a previously regulated cycle (Ruiz-Alonso et al. 2013; Tan et al. 2018; Almquist et al. 2017).

Researchers are also interested in alternative methods for evaluating the uterine environment, as these assays require an endometrial biopsy from a previously regulated cycle, and may not always accurately represent future endometrial receptivity profiles.

One of the more prolific types of signaling molecules found to be biologically active during the window of implantation are cytokines, which are regulatory peptides or glycoproteins. Cytokines act as local autocrine or paracrine signals, and occasionally have more distant effects as endocrine mediators (McEwan et al. 2009). Cytokines critical for successful implantation include Leukemia-inhibitory factor (LIF), a member of the interleukin-6 family of cytokines responsible for mediating estrogen actions. Knockout

studies investigating the Lif gene in mice found animals lacking this gene have a defect in implantation and decidualization that can be rescued by adding recombinant LIF into the environment (Stewart et al. 1992). LIF is also important for driving stromal proliferation by regulating epidermal growth factor (EGF) (Hantak, Bagchi, and Bagchi 2014). Another active cytokine during the window of implantation within the uterine environment is colony-stimulating factor-1 (CSF-1), believed to be involved in molecular dialogue between the implanting embryo and the endometrium due to both cell types having CSF-1 receptor mRNA (Pollard et al. 1991). Other cytokines involved in implantation and pre-implantation cellular development include interleukin 1 (IL-1), interleukin 6 (IL-6) and Heparin-binding epidermal growth factor-like growth factor (HB-EGF) (Krussel et al. 2003; Dominguez et al. 2015; Cha, Sun, and Dey 2012).

One minimally invasive method used to study the extracellular signaling molecules found within the endometrial environment, in-vitro, was the development and use of an endometrial co-culture system. This method involves taking a small endometrial biopsy from a subject prior to any further ART treatment, separating endometrial and stromal cells for culture, and finally growing a monolayer of these cell types in order to explore the molecular interactions between the culture media and the cells either in the presence or absence of an embryo (Figure 9) (Simon et al. 1997; Dominguez et al. 2010).

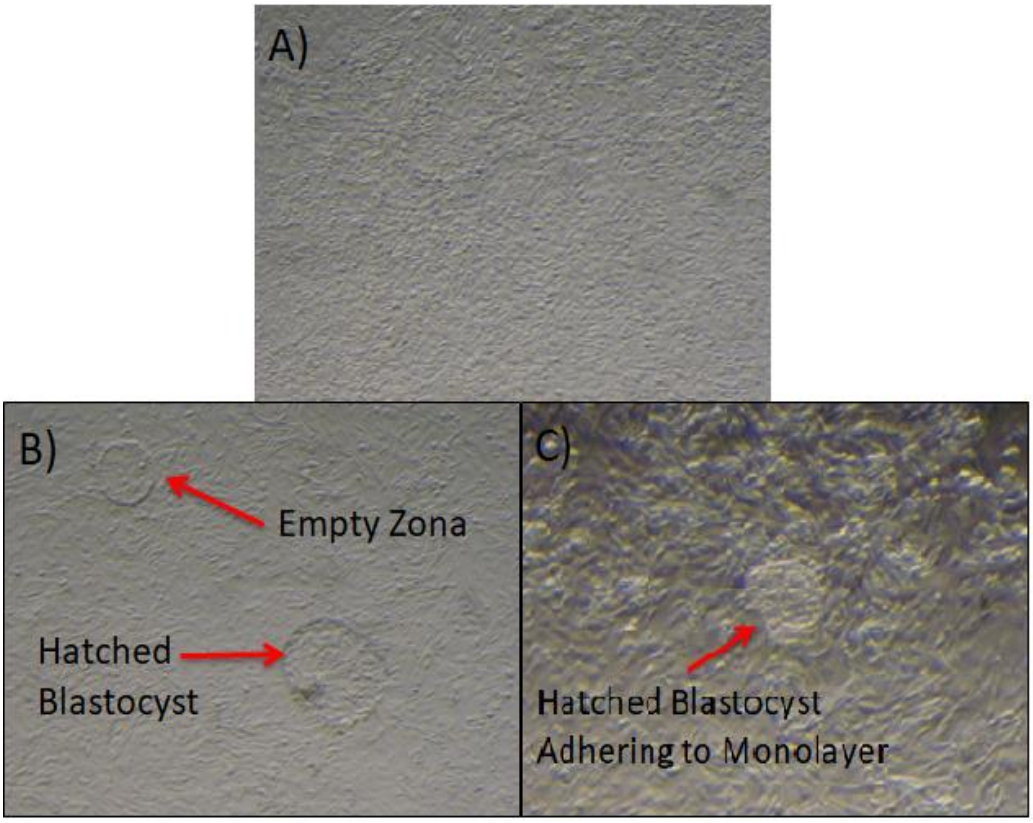

Figure 9: A) Confluent monolayer of epithelial endometrial primary cells. B) Example of a co-cultured fully hatched blastocyst. C) Co-cultured hatched blastocyst adhering to the monolayer on day 7 of embryo development (images Presented at ASRM by Parks et al., 2014).

To further study the molecular interaction between a developing embryo and a monolayer of endometrial epithelial cells (EECs), researchers co-cultured the cell types together and performed embryo transfer with the co-cultured blastocyst, and correlated the clinical outcome with the secreted molecules found within the co-cultured spent media. When compared with the spent media of embryos grown sans EECs, they discovered increased concentrations of IL-6, PLGF, and BCL (CXCL13) (indicating they were

secreted by the EECs in the presence of an embryo), and decreased levels of FGF-4, IL-12p40, VEGF, and uPAR (indicating EEC consumption) (Dominguez et al. 2010). These minimally invasive techniques offer insight into the molecular dialogue that occurs in the moments prior to implantation, and allows researchers to further investigate the beneficial, and the mandatory signalling molecules involved during this critical time.

Finally, the third phase of endometrial cycle consists of menstruation. When hormone levels are decreased during this final phase, the modified endometrium is unable to be maintained, and menses begins, and is considered to be day 0 to day 5 of the next menstrual cycle. The duration of menses is variable, but the usual duration of the menstrual flow is 3-5 days, and the amount of blood loss can vary, with the average being 30mL. Menstrual blood is mostly arterial in nature, and contains prostaglandins, tissue debris, and relatively large amounts of fibrinolysis from endometrial tissue. The fibrinolysis lyses clot so that menstrual blood does not contain clots typically unless the flow is particularly heavy. On average, a woman will experience 450 menses throughout her lifetime (Thiyagarajan, Basit, and Jeanmonod 2021).

10.6.6. Uterine Environment Aspiration

A common criticism of extrapolating data from endometrial co-culture data is that it oversimplifies the complex nature of the in-vivo environment. Furthermore, inter cycle reliability may be a concern, where uterine conditions may subtly vary from cycle to cycle,

and one brief snapshot may not perfectly represent all cycles going forward. In an attempt to address these concerns, a technique called uterine fluid aspiration has been developed to, non-invasively, study the in-vivo uterine microenvironment during the window of implantation. This method involves a transfer catheter and gentle suction to sample one isolated location of the uterine luminal endometrium, adjacent to potential implantation sites (Figure 10).

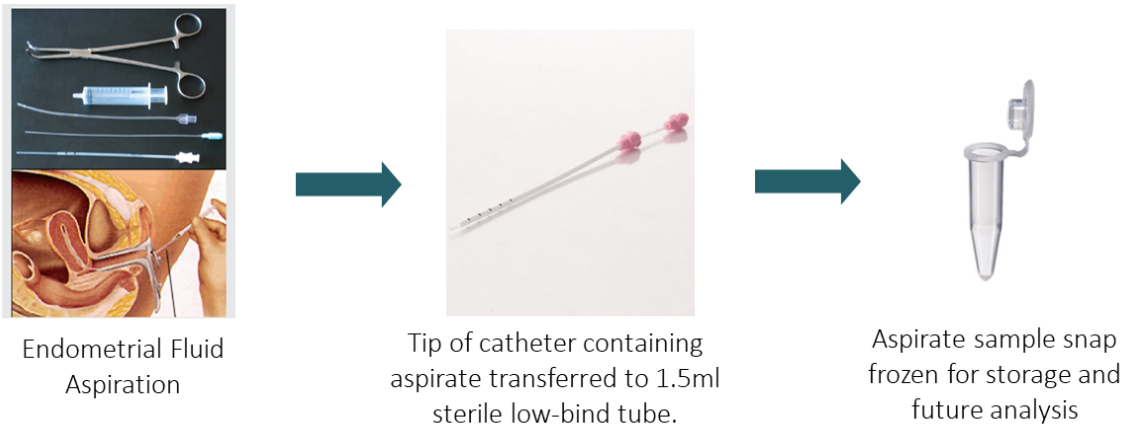

Figure 10: Endometrial aspirations taken at the time of embryo transfer, offer a brief snapshot into the uterine microenvironment the embryo is likely to encounter as it searches for a potential implantation site (images presented at ASRM by Parks JC et al., 2019).

The superficial uterine environment is composed of a protein-rich histotroph, made up of specific glandular secretions. It contains cytokines, anti-proteases, transport proteins, nutrients and enzymes (Hannan et al. 2010; Leese et al. 2008). Studies have shown uterine secretion aspiration at the time of transfer is a minimally invasive technique, capable of safely sampling the endometrial microenvironment (van der Gaast et al. 2003; Hannan et

al. 2012). Endometrial aspirations taken 24 hours prior to embryo transfer are an effective, minimally invasive means of sampling the endometrial micro-environment of a patients' current embryo transfer cycle. Studies, have demonstrated that endometrial aspirates collected 24 hours prior to embryo transfer contained specific prostaglandin levels that were correlated with successful implantation (Vilella et al. 2013).

Although this technique seems promising, in practice successful integration into ART laboratories has been thus far unconvincing. Based on the literature and previous studies, researchers have unsuccessfully attempted to use pre-determined cut-off values for a panel of promising molecular biomarkers (including urocortin, activin A, human decidua-associated protein (hDP) and interleukin-18), to predict endometrial receptivity and subsequent implantation success (Ledee-Bataille et al. 2004; Florio et al. 2008; Florio et al. 2010). Similarly, additional studies investigated other molecular biomarkers found within the uterine fluid milieu, including the mean levels of cytokines, glycodelin, isoforms of leucine-rich alpha2-glycoprotein, LIF and TNF, interleukin-1β, TNF-α, interferon gamma-induced protein 10 and monocyte chemoattractant protein. These levels were then categorized based on fertility treatments and outcomes to search for commonalities between patients who experienced successful implantation (Gillott et al. 2008; Boomsma, Kavelaars, Eijkemans, Amarouchi, et al. 2009; Boomsma, Kavelaars, Eijkemans, Lentjes, et al. 2009; Bentin-Ley et al. 2011; Rahiminejad et al. 2015; Rahiminejad et al. 2016). The results of these studies indicate that the individual levels of these potential molecular biomarkers are far too variable from one subject to the next, and that the use of uterine

aspirate assays are thus inadequate for determining implantation receptivity, so their use in a clinical setting is very limited.

10.6.7. Sperm Analysis

An integral component of an ART cycle is the analysis of the male gamete. However, the standard operating protocols focus more on simple, superficial observations. The methods for the evaluation of semen is described in World Health Organization (WHO) manuals, and includes viscosity, volume, color, pH, concentration, motility, vitality, the presence of leukocytes and the morphology of the sperm (Cooper et al. 2010). These parameters are used to standardize male subfertility in the population, and while they are correlated with successful oocyte fertilization and embryonic development, collectively, they do not produce a definitive predictive threshold of whether or not a patient will be able to conceive within an ART setting (van der Steeg et al. 2011; van Weert et al. 2004).

One factor limiting the usefulness of conventional semen analysis is that it fails to account for the integrity of sperm genome constitution and DNA integrity. There are many causes of sperm DNA damage and fragmentation, including defective apoptosis, excessive reactive oxygen species (ROS) production, toxic effects of drugs, pollution, cigarette use and even high testicular temperature (Boissonneault 2002; Moustafa et al. 2004; Saalu 2010; Sakkas et al. 2002; Colagar, Jorsaraee, and Marzony 2007). Several techniques have

been developed to investigate the sperm DNA integrity of patients including the sperm chromatin structure assay (SCSA) which utilizes specific staining techniques and a flow cytometer to quantitate the percentage of sperm with intact vs. fragmented chromatin. Another technique is the sperm chromatin dispersion (SCD) detects DNA fragmentation by incubating spermatozoa in a thin inert matrix with an acid solution that denatures the DNA, followed by an adapted lysing solution that removes the majority of nuclear proteins. This procedure results in DNA loops spreading out into the inert matrix, producing halos of chromatin, which will be largely absent in samples with DNA fragmentation. Alternatively, the single cell gel electrophoresis (Comet) assay embeds sperm cells in a thin layer of agarose on a microscope slide and subsequently lysed with detergent under high salt conditions. This process removes protamines and histones allowing the nucleus to form a nucleoid-like structure containing supercoiled loops of DNA. Alkaline pH conditions result in unwinding of double-stranded DNA, and subsequent electrophoresis results in the migration of broken strands towards the anode, forming a comet tail, when observed under fluorescence microscope. The amount of DNA in the head and tail is reflected by its fluorescent intensity. The relative fluorescence in the tail compared with its head serves as a measure of the level of DNA damage (Simon and Carrell 2013). Finally the terminal deoxynucleotidyl transferase mediated deoxyuridine triphosphate nick end labelling (TUNEL) assay analyzes DNA fragmentation by measuring the number of breaks or nicks in the DNA of the sperm. It can be performed on as few as 1,000 sperm, even on sperm retrieved from a small testis biopsy (Sharma et al. 2010). Of the four clinical assays developed, the COMET and TUNEL assays have been

the most successful at reliably predicting the DNA integrity of sub fertile men (Figure 11) (Cissen, Wely, et al. 2016). These assays have been integrated into many ART laboratories to evaluate sperm genome integrity, and have been successful at detecting damaged DNA within sperm. These assays are helpful for counseling patients regarding the cause of their infertility, however the predictive value of DNA fragmentation on evaluating the chances of achieving a successful pregnancy may need further research and analysis (Cissen, Bensdorp, et al. 2016).

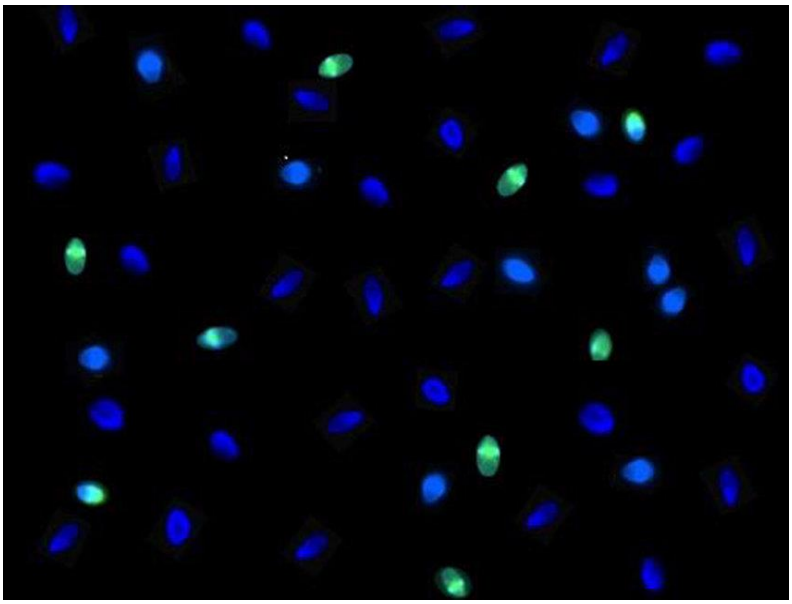

Figure 11: Terminal deoxynucleotidyl transferase dUTP nick-end labeling (TUNEL) immunofluorescent staining of human spermatozoa aids in detection of DNA fragmentation. Cells which fluoresce green are indicative of DNA fragmentation which takes place during late stages of apoptosis. Spermatozoa are considered TUNEL positive if approximately 40% or more of the head is fluorescent (adapted from Palermo GD et al., 2017)(Palermo et al. 2017).

Investigation into genome wide mutation rates reveal up to 80% originating in the paternal lineage (Acuna-Hidalgo, Veltman, and Hoischen 2016), and studies analyzing multi-generational sperm genomic DNA have observed an increase in de novo point mutations over the course of a males lifetime at a rate of 2 base pair changes per year on average (Kong et al. 2012; O'Roak et al. 2012) There are several mechanisms responsible for these de novo base substitutions sometimes acting in combination, including errors in replication and damage induction. As male germ cells undergo continuous mitotic cell divisions (800 rounds of division and replication by age 50), this leads to increased mutation rates as men age, although many remain fertile well past middle age. Mutations may also occur when the template or free nucleotides are damaged prior to replication. Interestingly, not all mutations found within the paternal genome are correlated with paternal age; in fact, a recent study found that a significant proportion of human germline mutations were correlated with maternal age at conception. As a woman reaches advanced maternal age, there is an accumulation of damage in oocytes and the subsequent number of postzygotic mutations in the embryo and the oocyte is no longer able to repair the damage introduced by the fertilizing sperm, as is seen in younger women (Gao et al. 2019). The known effects of these mutations are accumulating , and a recent publication of a parallel two-group, randomised trial indicated that although poor quality sperm can successfully fertilize and produce transfer grade blastocysts, the subsequent pregnancies have a much higher incidence of miscarriage following clinical pregnancy (Miller et al. 2019). Furthermore, evidence also points to a correlation

between de novo point mutations in sperm and adverse health effects in offspring, including increased risks of birth defects and neurodevelopmental and psychological disorders (Kojima et al. 2018; Kimura et al. 2018). Although not currently practical due to cost and techniques involved, screening for DNA mutations found within sperm may be incorporated into ART laboratories in the future, which would provide potential parents with additional information and assist with potential offspring health risk evaluation.

10.6.8. Placental Epigenetics

One of the earliest events which occurs during embryonic development, is the differentiation of the inner cell mass (ICM) and the trophectoderm cells (TE). This stage in development is the first period during which two distinct tissue types can be observed after successful fertilization has occurred. The TE cells make up the periphery of the blastocyst, while the ICM is located on a single side within the blastocoel cavity (Niwa et al. 2005). These two tissue types also give rise to two distinct types of stem cells, the embryonic stem cells that will eventually develop into the subsequent fetus, while the trophoblast stem cells will continue to develop and differentiate into the placenta, which is the first fetal organ to develop as well as the largest. Proper development and growth of the placenta is critical to the health of the fetus and the mother, and defects can lead to several major disease etiologies found within pregnancy including pre-eclampsia, fetal growth restriction, still birth and recurrent miscarriage, which can result in long term

health consequences for the mother and subsequent offspring (Brosens et al. 2011; Salam, Das, and Bhutta 2014; Amaral et al. 2015).

Epigenetics is the study of inherited changes in gene expression, whose mechanisms do not involve changes to a specific DNA sequence. This may be accomplished by several distinct mechanisms, including DNA methylation, acetylation, phosphorylation, ubiquitylation, and sumolyation (Weinhold 2006).

Recently, studies focusing on the importance of epigenetics and placental development by way of genome-wide methylome sequencing have revealed large partially methylated domains within the human placenta, interspersed with highly methylated domains (Schroeder and LaSalle 2013). These partially methylated domains are developmentally dynamic, and usually cover tissue-specific genes that are transcriptionally repressed. There are several factors that make placental tissue appealing as a study material for investigating epigenetic disturbances in methylation patterns. A 2015 study concluded that hypomethylation found within the placenta is likely derived from the hypomethylated state of an early embryo and trophectoderm. Thus, large-scale methylation disturbances found within the placenta may be indicative of methylation perturbations present in the embryo, and subsequent fetal development (Bianco-Miotto et al. 2016). Upon closer observation, researchers discovered that some of the genes statistically overrepresented by these partially methylated domains, include genes associated with neuronal development and synaptic transmission, making them excellent

candidate biomarker genes for autism spectrum disorder in at risk patient populations (Schroeder et al. 2016).

Genomic imprinting is a form of epigenetic modification in which gene expression differs in an allele-specific manner depending on parent of origin. Imprinting restricts gene expression to only one of the parental alleles, from either the sperm or egg. While 99% of the genes in our genome are bi-allelically expressed from both chromosomes, imprinted genes are a small subset of genes that are expressed only from one chromosome (sperm or egg).

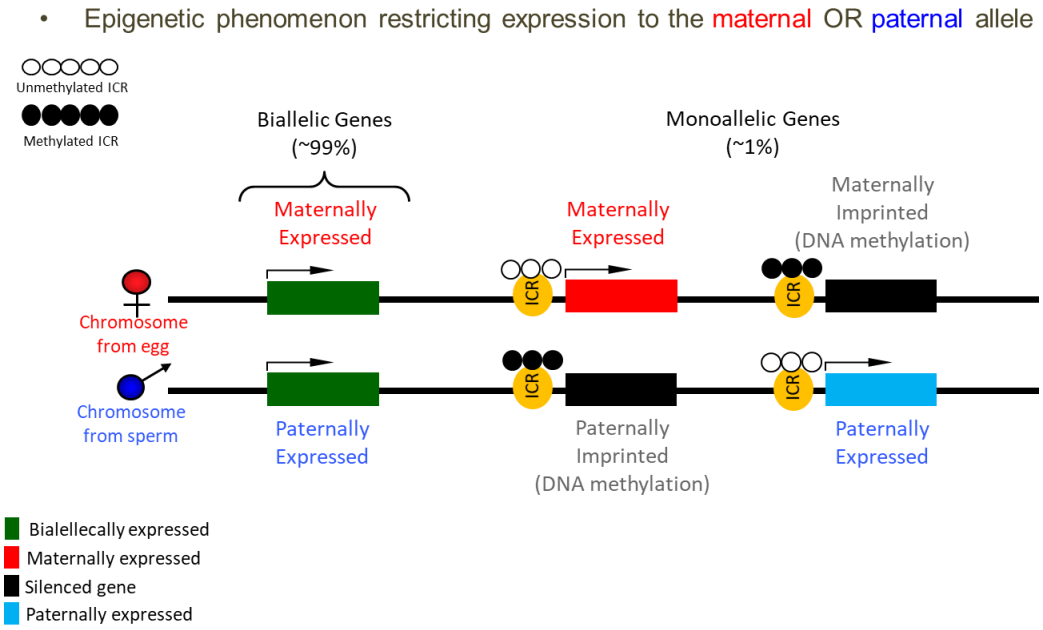

Figure 12: Genomic imprinting is an epigenetic phenomenon resulting from differences in methylation depending on whether the allele originated from the maternal allele (egg), or paternal allele (sperm) (Presented by Parks et al., at the 2017 ASRM conference).

In this diagram (Figure 12), methylated, or silenced imprinting regions are represented by the closed circles, whereas an unmethylated imprinting region is indicated by open circles. For example if a gene is paternally imprinted and silenced by DNA methylation on the chromosome from the sperm, it results in that gene being maternally expressed from the egg. Genomic imprinting offers an opportunity to study the expression of genes that may be transient and highly tissue specific. The placenta contains a high number of imprinted genes compared to many mammalian organs (Frost and Moore 2010). Within

the context of ART, researchers have studied placental tissue samples derived from murine embryos cultured in an in-vitro setting and discovered aberrant DNA methylation of imprinted genes after in vitro preimplantation culture of mouse embryos when compared to in-vivo derived controls, specifically the loss of imprinted expression of H19 and Snrpn imprinting control regions (Mann et al. 2004). This led to questions regarding the safety of extended embryo culture and ART practices, however it is difficult to replicate such a study in humans, as many IVF patients have a number of different infertility etiologies which act as confounding variables in relation to any aberrant epigenetic imprinting (Litzky and Marsit 2019).

10.6.9. Perspectives On The Potential To Improve ART Standard Operating Protocols

Although the field of ART has come a very long way in a relatively short amount of time, it also has ample room for improvement. In order to continue to advance and increase clinical excellence, we must build upon our great, but ultimately inadequate, base of knowledge. Non-invasive methods for evaluating fertility constitution should be focused on materials that are considered excess, and are commonly discarded, for its low-risk high-reward potential. If we can develop additional techniques and skills to incorporate into our clinical practices, we will get closer to our ultimate goal of providing top quality

care to sub fertile and infertile couples, assisting them to achieve their goal of having a successful and healthy pregnancy, and build their family.

As pointed out in section 10.5.4., the gene expression profiling of cumulus cells has revealed cumulus cell gene expression involved in glucose metabolism, transcription, gonadotropin regulation and apoptosis, and although promising, so far this data has had limited success predicting pregnancy outcome. Although cumulus cells are a potential window into oocyte competence and viability, inconsistency in the methodology and subjects studied has resulted in a need for a study investigating individual cumulus cell transcriptomes of chromosomally normal (euploid) embryos, to eliminate aneuploidy as a confounding variable, and finally, utilizing RNA sequencing to identify novel biological pathways associated with implantation outcome.

As pointed out in section 10.5.5, the co-culture model, taking an endometrial biopsy, isolating and culturing the endometrial cells into a monolayer with a late-stage blastocyst, is a great way to study the molecular dialogue that occurs between the luminal epithelial cells of the endometrium and the implanting blastocyst. However, the literature has not explored the differences in the secretomic dialogue that occurs between the blastocysts and endometrium of specific infertility etiologies that may have sub-optimal implantation rates. Such a study would be beneficial, as it may help doctors and clinicians understand the effects of infertility etiologies on the window of implantation, and provide them with information for counselling as well as potential treatment opportunities.

As pointed out in section 10.5.8, studies investigating the effects of ART and prolonged embryo culture on genomic imprinting, have found correlations with deficiencies in the subsequent placenta and offspring in murine studies. However, there is insufficient evidence as to the causal nature of these correlations, and there is limited information available overall on the direct effects of external influences on epigenetics and genomic imprinting. Specifically, due to the bi-allelic nature of genomic imprinting within the placenta, this offers an opportunity to investigate any potential paternal lifestyle choices and their impact, especially in a mouse model by controlling for any female factors that may be present. Furthermore, patients seeking fertility treatment are older on average, and especially in men, the effects of this advanced age etiology on their offspring is poorly understood. Therefore, an investigation into the effects of advanced paternal age on the epigenetics of the placenta, and viability and health of the subsequent offspring would be beneficial to the field, in an effort to better understand and treat this patient population.

11.0 Specific aims of this thesis

With the above in mind, the purpose of this thesis was to perform basic and applied research with the aim, ultimately, of providing underlying data to support the improvement of IVF:

Specific aim 1. To test the hypothesis, through corona cell RNA sequencing from individual oocytes, that transcripts and pathways are linked to euploid oocyte competence and live birth**.**

Specific aim 2. To investigate the impact of infertility diagnosis on embryo-endometrial dialogue.

Specific aim 3. To test the hypothesis that advanced paternal age directly impacts mouse embryonic placental imprinting.

The specific aims are supported by a series of published works to which I contributed (see page 5) with a similar overall purpose.

11.1. Specific aim 1

This chapter is based on published work from the following publication.

Parks JC, Patton AL, McCallie BR, Griffin DK, Schoolcraft WB, Katz-Jaffe MG. **Corona cell RNA sequencing from individual oocytes revealed transcripts and pathways linked to euploid oocyte competence and live birth.** Reprod Biomed Online. 2016 May;32(5):518-26. doi: 10.1016/j.rbmo.2016.02.002. Epub 2016 Feb 24.

11.1.1. My contribution to the work

I worked closely with Dr. Katz-Jaffe to develop and implement the experimental design of this experiment. I coordinated corona cell collection with the embryologists within the IVF lab at the Colorado Center for Reproductive Medicine during their routine IVF procedures. I performed the subsequent experiments, results analysis and interpretation, and wrote and edited the manuscript for publication.

11.1.2. Chapter summary

Capsule. RNA-sequencing of corona cells identified differentially expressed transcripts and observed numerous signaling pathways in association with euploid oocyte competence, including live birth and negative IVF outcome.

Purpose: To investigate the corona cell transcriptome of euploid oocytes utilizing RNA sequencing technologies.

Methods: Corona cell samples from individual cumulus oocyte complexes that developed into euploid blastocysts and were transferred in a frozen embryo transfer (n=10), were collected during oocyte retrieval. RNA-Sequencing was performed on corona cell samples alongside bioinformatics and statistical analysis to compare IVF outcomes.

Results: RNA-Sequencing of corona cell samples, produced a mean number of sequence reads of 21.2 million. Statistical analysis of differentially expressed genes revealed 343 statistically significant transcripts ($P<0.05$; fold change >=2). Enriched pathway analysis showed WNT signalling, MAPK signalling, focal adhesion and TCA cycle to be impacted by IVF outcome. Specifically, key genes within the WNT/beta-catenin signalling pathway, including AXIN, were associated with oocyte competence.

Conclusions: Oocyte-specific transcriptomic corona cell profiles were successfully generated by RNA-sequencing. Key genes and signalling pathways were identified in association with IVF outcome following the transfer of a euploid blastocyst in a frozen embryo transfer. This new information could provide novel biomarkers for the non-invasive assessment of oocyte competence.

11.1.3. Introduction

Current estimates state that 1 in 6 couples in the United States will require the use of Assisted Reproductive Technologies (ART) to successfully conceive a child (Thoma et al.

2013). For many infertile couples treatment will involve in vitro fertilization (IVF) and a subsequent embryo transfer. The oocyte is a major contributor to the success of an IVF cycle with oocyte competence tightly linked to embryo viability. Numerous factors determine oocyte competence including mitochondrial health, metabolomic processes, functional spindle assembly and successful meiotic division (Prates, Nunes, and Pereira 2014), (Keefe, Kumar, and Kalmbach 2015). Based on current IVF protocols, the likelihood of a single aspirated oocyte being fertilized, successfully developing, implanting and resulting in a healthy live birth is ~5% (Patrizio and Sakkas 2009). Consequently, additional non-invasive methods to measure oocyte competence could represent a valuable asset to improve embryo selection and IVF outcomes.

Follicular fluid is a potential non-invasive source of oocyte information. The fluid is aspirated at the time of oocyte retrieval and discarded following oocyte isolation. Follicular fluid is contained within the follicular antrum surrounding the oocyte and the composition of this fluid changes throughout folliculogenesis. Protein analysis of follicular fluid revealed diverse protein compositions containing mostly plasma proteins and proteins associated with lipid transport, complement pathways and blood coagulation (Schweigert et al. 2006), (Jarkovska et al. 2010). A recent study identified a subset of 75 follicular fluid proteins correlated with IVF outcome. Thirteen of these proteins were involved in acute response signaling, coagulation, prothrombin activation, complement system and growth hormone pathways, uniquely associated with IVF outcome (Kushnir et al. 2012). Metabolic analysis of follicular fluid has revealed metabolites that are

correlated with oocyte maturity based on the depletion/appearance of specific amino acids: arginine, glutamate, glutamine, isoleucine and valine (Hemmings et al. 2013). In addition to amino acids, carbohydrates and fatty acid ratios have been shown to correlate with developmental milestones including embryogenesis and form an overall predictive value of oocyte quality and developmental potential (Matoba et al. 2014), (Wallace et al. 2012), (O'Gorman et al. 2013). However, it is important to understand that many of these predictive studies are based on retrospective data, and are not equivalent to a truly independent prediction/replication experiment. Additional studies have linked oocyte quality with cytokines and growth factors in follicular fluid, including increased BMP2, interleukins (6, 8, 12 and 18), GDF-9, GCSF and amphiregulin (Sugiyama et al. 2010), (Sarapik et al. 2012), (Bedaiwy et al. 2007), (Gode et al. 2011), (Ledee et al. 2013), (Liu et al. 2012). Although follicular fluid molecular profiling appears promising, to date, there are no prospective studies utilizing a panel of follicular fluid biomarkers to determine potential clinical value in identifying oocyte competence.

Another promising area of research into oocyte competence has been the molecular analysis of follicular cells. Corona cells (CC) surrounding the oocyte maintain a close relationship via transzonal processes and gap junctions, providing key nutrients and other factors essential for oocyte maturation and future developmental competence (Anderson and Albertini 1976). CC's remain in close proximity to the oocyte throughout development through gap junctions which are formed by transzonal cytoplasmic projections transverse the zona pelucida matrix (ERICKSON et al. 1985). This in turn

results in the cumulus-oocyte-complex development(Plancha et al. 2005). Cumulus cells surround the oocyte and form the cumulus oophorus and corona radiata inner cell layer. Gap junctions connect the corona cells to the oocyte and allow bi-directional communication and the exchange of nutrients and metabolites. This results in the stimulation of the oocyte, triggering maturation (Saeed-Zidane et al. 2017; Mora et al. 2012). Transzonal projections, which penetrate the zona pelucida surrounding the oocyte allow the corona cells to maintain contact with the oocyte through and are believed to be involved in paracrine gap junctional communication and adhesion between the oocyte and corona cells (Simon and Goodenough 1998). Amino acids are transported through these gap junctions enhancing uptake of glycine, alanine, lysine and taurine required for oocyte development(Pelland, Corbett, and Baltz 2009). Specific profiles of cumulus cell gene expression have been able to predict oocyte maturation, cumulus expansion and fertilization (McKenzie et al. 2004), (Assou et al. 2006), (Anderson et al. 2009), (Ouandaogo et al. 2011), (Feuerstein et al. 2012), (Yerushalmi et al. 2014). CC gene expression is dynamic and can be affected by specific events such as maternal aging (Al-Edani et al. 2014) and ovarian gonadotropin treatments (Assou, Haouzi, et al. 2013). One of the first studies to investigate oocyte competence identified several CC genes as biomarkers for assessing developmental potential including BCL2L11, PCK1 and NFIB (Assou et al. 2008). Follow up investigations identified 45 CC genes of interest to be considered biomarkers of successful embryo development and pregnancy outcomes that were tested in a prospective study. The test group received a day 3 embryo transfer based on the 45 CC gene expression profiles, while the control group had a day 3 embryo

transfer based on traditional embryo grading selection. Both implantation and ongoing pregnancy rates were significantly higher in the test group after embryos were chosen based upon their CC gene expression profile (40% vs control = 26.7% and 70% vs control = 46.7% respectively). Of the 267 CC samples studied, 27% had a CC gene expression profile that predicted positive pregnancy outcome, 42% that predicted negative pregnancy outcome and 13% that predicted early arrested development. Remarkably, no relationship between traditional morphological grading and CC gene expression was observed (Assou et al. 2010). Other retrospective studies have shown a significant correlation between the cumulus transcriptome and subsequent pregnancy outcome where NRP1, UBQLN1, PSMD6, DPP8, HIST1H4C, CALM1, PTGS2, EFNB2 and CAMK1D gene expression correlated with pregnancy and TOM1 with negative outcome (Assidi et al. 2011), (Wathlet et al. 2012). Recently the combinatorial expression of 12 CC genes involved in glucose metabolism, transcription, gonadotropin regulation and apoptosis were utilized to estimate pregnancy outcome for 55 patients with 78% accuracy for an independent sample (Iager et al. 2013). Together, these studies indicate cumulus cells are a potential valuable source of information relative to the oocyte competence. However, there exists inconsistency in the CC transcriptome data to date primarily due to differences in experimental design and methodology including factors such as maternal age, ovarian stimulation protocols and various in vitro laboratory protocols.

The purpose of this study was to investigate the individual CC transcriptome of chromosomally normal (euploid) embryos utilizing RNA sequencing to identify novel

biological pathways associated with implantation outcome. Results demonstrated that the WNT-Canonical pathway and AXIN transcription are strong indicators of oocyte developmental competence and subsequent chromosomally normal live birth.

11.1.4. Materials and Methods

11.1.4.1. Corona Cell Collection

Corona cells were donated from individual cumulus oocyte complexes (COC's) (n=10) with patient and consent by the Western Institutional Review Board, Inc (WIRB® Protocol #20142383). Female subjects presented with normal ovarian reserve (AMH>1.0, FSH<10, AFC>6) and advanced maternal age (36-43 years old) but no other infertility diagnosis. Cumulus cells were collected and stored at -80 degrees Celsius from up to 10 oocytes per patient (30 patients, n=300 total), only cumulus cell samples that met the following criteria were analysed for this study, and oocytes that failed to fertilize or develop to the blastocyst stage were excluded from further experimentation. Next, patients underwent routine IVF with embryos individually cultured to the blastocyst stage for a trophectoderm (TE) biopsy prior to vitrification. Only embryos graded 3BB or better were chosen for TE biopsy, based on the Gardner Schoolcraft grading system (Gardner and Schoolcraft 1999a). Comprehensive chromosome screening (CCS) was performed on biopsied TE cells, and following the identification of a euploid blastocyst, patients were scheduled for a frozen embryo transfer (FET). Cumulus samples were chosen based upon

the previously described criteria and were subsequently randomized and grouped based on implantation outcome (live birth n=5 and negative implantation n=5).

Following routine oocyte retrieval, cumulus cells were mechanically separated from each individual COC without disturbing the inner corona cells. Oocyte maturity was visually confirmed and individual oocyte corona complexes were allowed to recover for 4 hours in an incubator at 7% CO_2, 5% O_2. Corona cells were removed prior to ICSI using a media solution containing 0.33mg/mL hyaluronidase and rinsed through sequential 3x20uL drops of PBS/BSA before transfer into 10 uL of Extraction Buffer (PicoPure® RNA-isolation kit, Life Technologies, Carlsbad CA). All CC samples were snap-frozen in liquid nitrogen and stored at -80°C until later analysis.

11.1.4.2. RNA Sequencing

Purified cDNA libraries were constructed from 50ng of rRNA-depleted Total RNA using the Ion Total RNA-Seq Kit v2, Whole Transcriptome Library Prep protocol (Life Technologies, Carlsbad CA). rRNA-depleted Total RNA was fragmented using RNase III and purified by Agencourt Ampure XP micro-beads (Beckman Coulter Inc., Brea CA). The fragmented RNA was then hybridized and ligated prior to reverse transcription and addition of multiplexing barcode adaptor. The subsequent cDNA was then amplified via PCR and purified again. Barcoded libraries were equalized and pooled into an evenly represented final library consisting of 100pM cDNA, which was then coupled onto templated capture beads and enriched using the Ion OneTouch 2 and OneTouch ES systems (Life Technologies, Carlsbad

CA). Final libraries were prepped for loading on the ION PI v2 chip and then sequenced on the Ion Proton with a P1 200 v2 Sequencing kit (Life Technologies, Carlsbad CA).

11.1.4.3. RNA-Sequencing Data and Bioinformatic analysis

Raw reads in FASTQ format were trimmed and filtered with FastQC (https://www.bioinformatics.babraham.ac.uk/projects/fastqc/) such that only reads with Phred Q-scores > 20 and read lengths > 35 bp were retained. Duplicate reads were removed thus retaining unique reads with higher average base quality. Strand NGS v.2.1 (Strand Life Sciences Inc., Aurora CO) was used for subsequent RNA-Seq data analysis. The trimmed/filtered reads were aligned to NCBI RefSeq human reference genome (GRCh37/hg19) and human transcriptome. Transcript isoform assembly, abundance estimation and quantification were performed with Strand NGS. Differential gene expression was performed with DESeq v.3.0 normalization and Fold Change > 2.0 (bioconductor.org). Strand NGS identified significantly differentially expressed up- and down-regulated genes. Gene annotations were provided by NCBI Entrez Gene database. Biological pathway analysis was performed with Strand NGS based on WikiPathways Analysis, Reactome, GenMAPP and Other pathway databases and the BioCyc pathway database (Martens et al. 2018; Fabregat et al. 2017; Prickett and Watson 2009; Paley and Karp 2017). Significantly enriched pathways were identified with a threshold Fold Change > 2.0.

11.1.4.4. RNA-Sequencing Gene Expression Validation

Additional individual CC samples (n = 10) were collected for RNA-sequencing validation using the PicoPure® RNA Isolation Kit (Life Technologies, Carlsbad CA) with modifications. Briefly, samples were lysed and bound to a silica-based filter, treated with RNase-free DNase I (Qiagen, Valencia CA) and washed several times before recovered in 20 µL elution solution. Reverse transcription was performed using the High Capacity Reverse Transcription cDNA kit (Life Technologies, Carlsbad CA) to generate cDNA template for real-time polymerase chain reaction (PCR).

Quantitative real-time PCR (Q RT-PCR) was performed using the ABI 7300 Real Time PCR System with the Power SYBR Green PCR Master Mix (Life Technologies, Carlsbad CA). After a 10-minute incubation at 95°C, amplification was performed for 40 cycles at 95°C for 15 seconds and 60°C for 1 minute, then a dissociation stage for 15 seconds at 95°C, 1 minute at 60°C, 15 seconds at 95°C, and 15 seconds at 60°C. The quantification of two genes, AXIN1 (GenBank NM_003502.3) and TNFRSF10A (GenBank NM_003844.3), was calculated relative to the constant level of transcription in every sample of the housekeeping gene, RPL19. The PCR reaction efficiency recorded R^2 values ≥0.9, and the correlation coefficient was calculated to be >0.99. Statistical analysis was performed with REST-2008 software using bootstrap randomization techniques (Qiagen, Valencia CA). Gene expression fold differences with $P<0.05$ were considered statistically significant.

11.1.5. Results

Traditional oocyte and embryo morphology parameters were not predictors of chromosome constitution, or implantation outcome. Embryos of equivalent good blastocyst morphology resulted in both negative and positive implantation (Table 2).

COC #	Oocyte MII Morphology	Day 3 Cell # (Grade)	Blastocyst Grade at Biopsy	Embryo Transfer Outcome
1	Normal	9 (4-)	3BA	Negative
2	Normal	8 (4-C)	5BB	Negative
3	Normal	12(4-C)	5AA	Negative
4	Normal	8(4-)	5BA	Negative
5	Normal	9(3+)	4BB	Live Birth
6	Normal	10(4)	5AA	Live Birth
7	Normal	8(4)	4BB	Live Birth
8	Normal	8(4-)	5BB	Live Birth
9	Normal	8(3+)	3BB	Negative
10	Normal	8(4)	4AA	Live Birth

Table 2: Oocyte and embryo morphology with embryo transfer outcome.

RNA-sequencing was successfully performed for individual CC samples, with the mean number of sequence reads per individual CC sample, 21.2 million (range = 10.2 million to 29.8 million reads). Following CC gene expression quantification with DESeq normalization, an unpaired t-test was performed comparing live birth (n=5) with negative outcome (n=5) that identified 343 significantly differentially expressed genes ($P<0.05$; fold change >=2). Of these 343 differentially expressed CC genes, 82 were observed to have increased expression and 261 CC genes decreased expression in association with a live birth. A volcano plot was generated to visualize RNA-sequencing transcripts between live birth and negative outcome CC samples. Each dot on the volcano plot represents a transcript, red dots indicate transcripts that showed statistically significant differential expression between the two groups of CC samples, with p-value on the y-axis. The x-axis represents increased and decreased fold change reflecting differential gene expression observed between live birth and negative outcome (Figure 13).

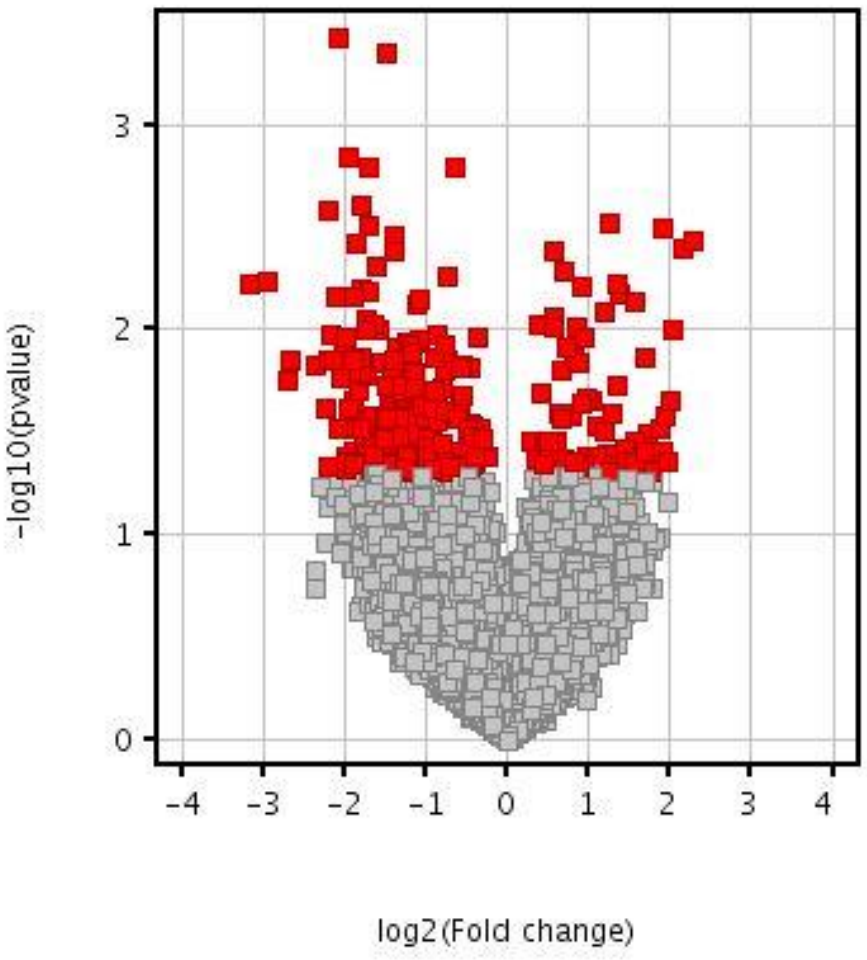

Figure 13: Volcano Plot for live birth vs. negative RNA-sequencing transcripts. Each dot represents a gene; red dots are significantly differentially expressed genes at $p < 0.05$ and fold change >=2. Up-regulated genes are shown as positive values on the x-axis, and down-regulated genes are shown as negative values on the x-axis.

Upon further examination of these differentially expressed genes, 87% were observed to be protein-coding, with the remaining 13% being either pseudo or small regulatory RNAs. Several genes were identified in the RNA-Sequencing data with differential expression

relative to live birth that have been published previously in association with oocyte competence including HDAC2, ANG and TNFRSF10A (data not shown) (Bessa et al. 2013), (Feuerstein et al. 2012), (Santonocito et al. 2013).

Gene Ontology analysis revealed significantly enriched biological processes among the differentially expressed transcripts including response to hormone stimulus, regulation of cellular protein metabolic processes, as well as, transcription and transmembrane transport in association with a live birth ($P<0.05$; >=2 fold). Pathway analysis of the differentially expressed transcripts identified enriched downstream biochemical signaling pathways. Table 3A displays the enriched signaling pathways with increased differentially expressed transcripts in association with live birth including WNT signaling, MAPK signaling, focal adhesion and TCA cycle (Table 3A).

Enriched Signaling Pathways with Increased Expression	**p-value**
Mitotic Prometaphase	0.00011
Mitotic Metaphase and Anaphase	0.00127
Hedgehog Signaling Pathway	0.00692
TCA cycle	0.00789
Glutamate removal from folates	0.00789
Methylglyoxal degradation VI	0.00789
Wnt Signaling Pathway and Pluripotency	0.00824
Toll-like receptor signaling pathway	0.00882

Nucleosome assembly	0.01291
Signal Transduction of S1P Receptor	0.01527
Focal Adhesion	0.01570
Histone Modifications	0.01607
Activation of Genes by ATF4	0.01651

Table 3A: Enriched signaling pathways with increased differentially expressed transcripts in association with live birth.

In contrast, Table 3B shows the enriched signaling pathways identified with decreased differentially expressed transcripts in association with live birth including degradation of beta-catenin, apoptosis, DNA damage response and the detoxification of reactive oxygen species (Table 3B).

Enriched Signaling Pathways with Decreased Expression	**p-value**
Degradation of beta-catenin by the destruction complex	0.000000367
Metabolism of non-coding RNA	0.000002327
Metabolism of amino acids and derivatives	0.000007400
MAPK Signaling Pathway	0.000016274
Mitotic Prophase	0.000024329
Wnt Signaling Pathway and Pluripotency	0.000046015
RNA Polymerase II Transcription	0.000046015

Apoptosis Modulation and Signaling	0.000049197
Cell Cycle Checkpoints	0.000053863
Synthesis of DNA	0.000055260
Metabolism of carbohydrates	0.000074778
Detoxification of Reactive Oxygen Species	0.000077281
M-G1 Transition	0.000115366

Table 3B: Enriched signaling pathways with decreased differentially expressed transcripts in association with live birth.

Further examination of both enriched signaling pathway lists revealed the WNT signaling pathway and the degradation of beta-catenin by the destruction complex pathway as two highly significant pathways associated with IVF outcome. These pathways are components of the WNT-canonical pathway, which is known to be functionally critical during development (Logan and Nusse 2004). It is important to note, FSH stimulates proliferation of granulosa cells; however, after the LH surge, granulosa cells stop dividing and exit the cell cycle (Baumgarten and Stocco 2018). This may account for the similarities in the observed cell signalling pathways and those expected within oocytes, such as a strong G2/M arrest, decrease of S phase and G1 genes etc.

A key gene of the WNT-canonical pathway is AXIN1, which showed differential expression in the RNA-sequencing data, and thus was chosen for qPCR validation. Additional CC

samples were collected and run individually using RT-PCR for AXIN1 gene expression relative to the internal constant housekeeping gene RPL19. AXIN1 showed significantly increased expression in individual CC samples that resulted in negative implantation versus live birth CC outcomes, in concordance with the RNA-sequencing data (Figure 14).

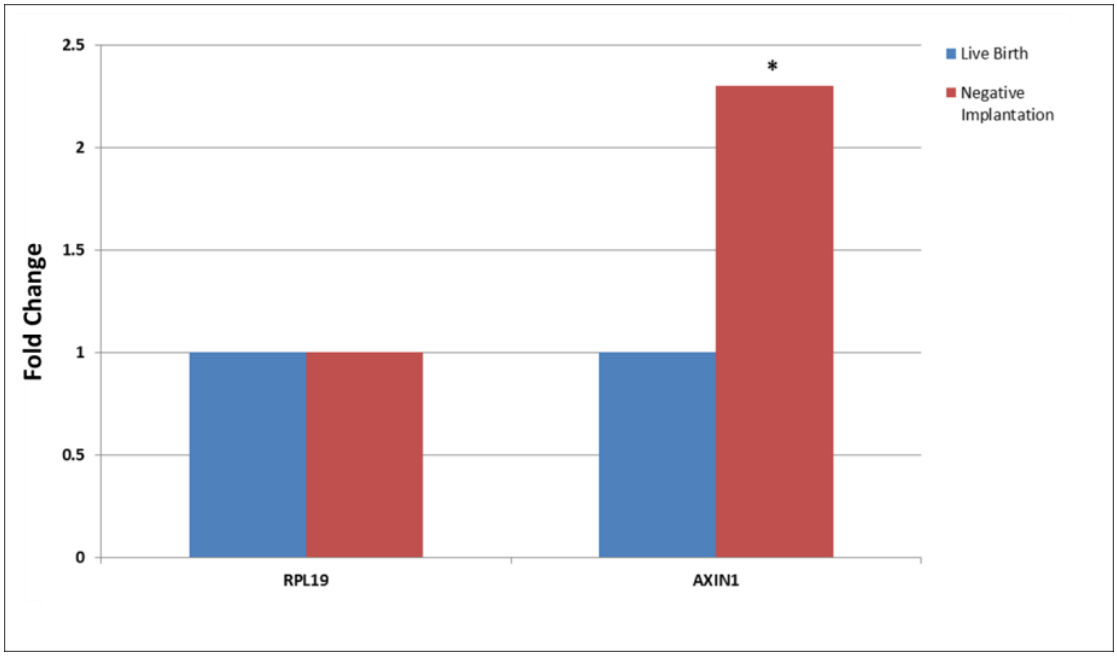

Figure 14: qPCR validation validated the RNA sequencing data showing a significant increase in AXIN1 expression with negative outcome relative to the internal housekeeping gene RPL19 ($P<0.05$; ≥2 fold).

11.1.6. Discussion

In this study RNA-sequencing technologies were utilized to generate an individual profile of corona cell (CC) gene expression in association with oocyte developmental potential and successful live birth following the transfer of a euploid blastocyst. This is the first

study to investigate CC gene expression in correlation with the frozen embryo transfer of a euploid blastocyst, thereby controlling for embryonic chromosomes and an unstimulated uterine environment. This ongoing research of cumulus cell gene expression biomarkers for non-invasive assessment of oocyte competence could represent a valuable tool in IVF.

Initial analysis of the CC RNA sequencing data confirmed genes previously published in association with oocyte competence including HDAC2, a member of the histone deacetylase family. This gene is responsible for the formation of large multi-protein complexes and the deacetylation of core histone complexes allowing for more compact histones wrapping around the DNA helix. HDAC2 gene expression has been shown to be vital for oocyte competence acquisition, and is critical for chromosomal segregation during maturation (Ma and Schultz 2013).

Another previously reported CC gene associated with oocyte competence that had increased expression levels relative to live birth is ANG. ANG is an angiogenesis stimulator promoter, responsible for transcribing the protein angiogenin, and stimulating the production of novel blood vessels. ANG expression in mechanically separated cumulus clouds has been observed to be a good predictor of oocyte development, and therefore a potential biomarker of oocyte competence (Feuerstein et al. 2012).

TNFRSF10A is a member of the TNF-receptor superfamily. The TNFRSF10A receptor is activated by the tumor necrosis factor-related apoptosis inducing ligand (TNFSF10/TRAIL), which is responsible for inducing apoptosis and cell death. In this study, decreased TNFRSF10A expression levels were observed in relation to live birth. Overexpression of TNFRSF10A is indicative of problematic cell regulation, which leads to increased apoptosis, and decreased developmental competence. Apoptosis is an essential pathway during folliculogenesis, however a balance between cell death and division is crucial with increased levels of apoptosis shown to be associated with impaired oocyte maturation, as well as fertilization and pregnancy outcome (Lee et al. 2001), (Host et al. 2002).

The WNT-Canonical Pathway was associated with both increased and decreased differentially expressed transcripts, suggesting this pathway may play a key role in oocyte developmental competence. When WNT binds to cell surface receptors, it turns off beta-catenin destruction, which in turn stabilizes beta-catenin, allowing translocation into the nucleus (Clevers 2006). Accumulation of beta catenin within the nucleus, activates genes by binding to transcriptional activators including transcription factors belonging to the TCF/LEF family (Clevers 2006), activating WNT target gene transcription (MacDonald, Tamai, and He 2009) (Figure 15).

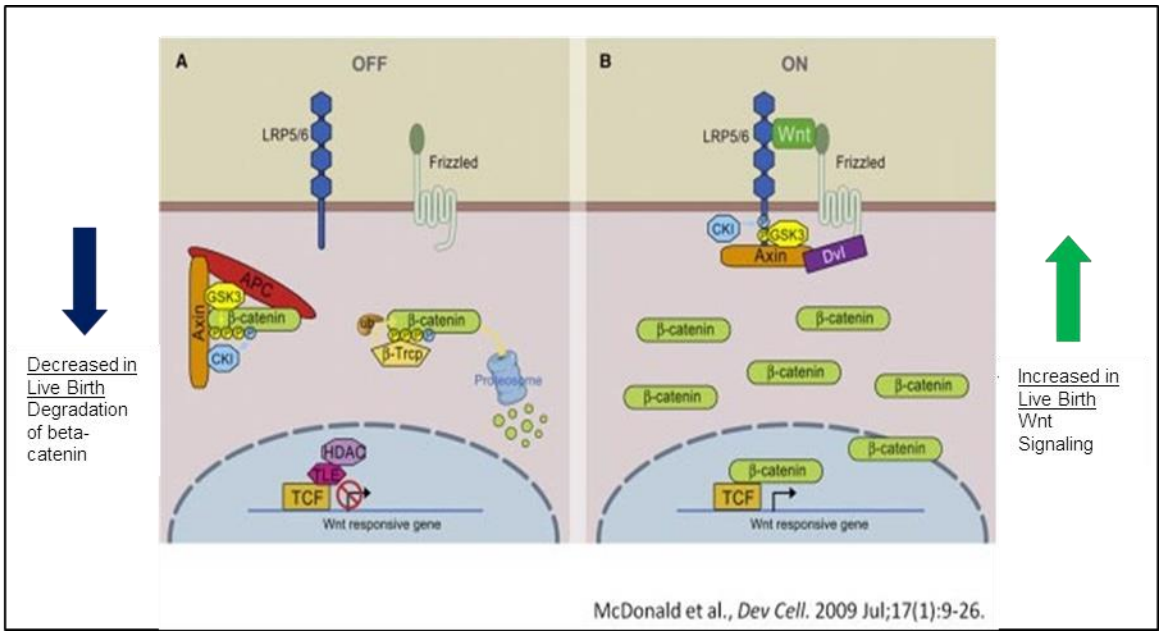

Figure 15: Wnt's are secreted extracellular signaling molecules that exert local control over diverse developmental processes including cell-fate specification, differentiation and regulation of cell-cell interactions.

WNT's are extracellular molecules that are secreted locally to exert control over a multitude of developmental processes including cell-to-cell interactions, differentiation, cell-fate specification and regulation. WNT signaling is vital for development, and is modulated by cytoplasmic, extracellular and nuclear regulations. Within the WNT signaling pathway WNT4 regulates a number of genes involved in late follicular development is required for normal antral follicular development (Boyer et al. 2010). In a mouse knock-out study, it was shown that inhibition of the Wnt4 gene led to a phenotype of compromised ovarian folliculogenesis and severely reduced fertility and premature ovarian failure (Prunskaite-Hyyrylainen et al. 2014). WNT signaling during embryogenesis participates in multiple processes including cell differentiation, regulation

and migration (Logan and Nusse 2004), and loss of even a single WNT gene can produce embryonic lethality (Gilbert et al. 2010). In the absence of WNT stimulus, cytoplasmic beta-catenin is targeted for proteolysis by a large multi-protein assembly called the beta-catenin destruction complex. Additionally the relative levels of the destruction proteins; Axin, adenomatosis polyposis coli (APC), protein phosphatase 2A (PP2A), glycogen synthase kinase 3 (GSK3) and casein kinase 1α (CK1α) are critical for both homeostasis as well as responsiveness to WNT (Minde et al. 2011). It has been suggested that WNT signaling in cumulus cells may act by recruiting beta-catenin and promoting the formation of adherens junctions, and may be important for folliculogenesis (Wang, Tekpetey, and Kidder 2009).

Key genes within the WNT/beta-catenin signaling pathway were observed in CC samples to be associated with oocyte competence. For example, AXIN which is expressed mostly within the cytoplasm can function as a negative regulator of the WNT signaling pathway, is capable of inducing apoptosis. AXIN acts by recruiting beta-catenin into plasma membranes and promotes the formation of adherens junctions (Wang, Tekpetey, and Kidder 2009). AXIN functions also as a scaffold protein capable of shuttling between the nucleus and cytoplasm, allowing beta-catenin to be transported from the nucleus to the cytoplasm where it is degraded (Wiechens et al. 2004). The increase of AXIN observed in CC samples with negative outcome may be indicative of a degradation of beta-catenin, causing a reduction in WNT-signaling, cellular proliferation, cellular migration and an increase in apoptosis.

Additional enriched CC signaling pathways in association with a live birth included the MAPK signaling pathway which moderates multiple cellular processes including differentiation, growth and proliferation (Ono and Han 2000). In oocytes the MAPK signaling pathway is associated with maintaining an arrested metaphase II, though recently it has been discovered that when it is inhibited during the transition from meiosis I and meiosis II, meiosis I is accelerated, leading to an increase in aneuploidy in the metaphase II stage of development (Nabti et al. 2014). MAPK signaling is mediated by FSH and EGF, essential for cumulus expansion which is critical for oocyte advancement (Dragovic et al. 2007). The Focal adhesion pathway similarly showed increased expression in CC's resulting in live birth. This pathway is responsible for the transmission of mechanical force and regulatory signaling between extracellular matrices and cells (Chen et al. 2003). The focal adhesion pathway has been linked to oocyte maturation thereby impacting oocyte developmental competence, and is partially involved in the communication between CCs and the developing oocyte (Ohtake et al. 2015). In cumulus cells, disruption of the MAPK/focal adhesion signaling pathways may affect critical processes involved in cumulus-oocyte communication, which may result in a less competent oocyte and embryo.

Finally, the citric acid (TCA) cycle and respiratory electron transport pathway were observed to have increased CC gene expression in association with a live birth. These pathways are responsible for generating energy in eukaryotic cells in the form of

adenosine triphosphate (ATP). Energy production can be glucose derived, or extracellular pyruvate may be metabolized by the mitochondria, producing most of the ATP found in the oocyte (Dumollard et al. 2007), (Dumollard et al. 2009). In the mouse, the oocyte controls intercellular metabolomic cooperation for energy production through the TCA cycle between the CCs and the developing oocyte. Sufficient energy production during development is crucial for oocyte competence (Sugiura, Pendola, and Eppig 2005).

In summary this study has demonstrated that RNA-Sequencing technologies can retrospectively generate a unique, oocyte-specific, transcriptomic corona cell profile on individual corona cell samples. This data looks promising, but more research, specifically an experiment designed around independent prediction and replication, must be performed to truly assess the value of the proposed developmental biomarkers highlighted in this study. Another limitation of this study is that the patients' stimulation protocols were not the same between the patients, nor the test groups, and the researchers did not perform any analysis of the stimulation protocol as a variable that may affect the molecular profiles discovered. However, the transfer of known euploid blastocysts into an unstimulated uterine environment strengthens this corona cell transcriptome data, specifically in relation to true negative outcomes. Ongoing research to elucidate the biological and signaling pathways of corona cells associated with oocyte competence could assist with advancements in embryo selection. A corona cell biomarker assay developed for the identification of oocyte viability, utilized in conjunction with

advanced morphological algorithms and comprehensive chromosome screening, could result in the routine use of single embryo transfers and overall improved IVF outcomes.

11.2. Specific aim 2

This chapter is based on published work from the following publication.

Parks JC, McCallie BR, Patton AL, Al-Safi ZA, Polotsky AJ, Griffin DK, Schoolcraft WB, Katz-Jaffe MG. *The impact of infertility diagnosis on embryo-endometrial dialogue.* Reproduction. 2018 Jun;155(6):543-552. doi: 10.1530/REP-17-0566. Epub 2018 Apr 10.

11.2.1. My contribution to this work

I worked closely with Dr. Katz-Jaffe to develop and implement the experimental design of this experiment. I coordinated endometrial biopsy collection taken at the time of oocyte retrieval with the physicians at the Colorado Center for Reproductive Medicine during their routine IVF procedures. I performed the subsequent experiments, results analysis and interpretation, and wrote and edited the manuscript for publication.

11.2.2. Chapter summary

Initial stages of implantation involve bi-directional molecular crosstalk between the blastocyst and endometrium. This study investigated an association between infertility

etiologies, specifically advanced maternal age (AMA) and endometriosis, on the embryo-endometrial molecular dialogue prior to implantation. Co-culture experiments were performed with endometrial epithelial cells (EEC) and cryopreserved day 5 blastocysts (*n* = 41 ≥ Grade 3BB) donated from patients presenting with AMA or endometriosis, compared to fertile donor oocyte controls. Extracellular vesicles isolated from co-culture supernatant were analyzed for miRNA expression and revealed significant alterations correlating to AMA or endometriosis. Specifically, AMA resulted in 16 miRNAs with increased expression ($P \leq 0.05$) and strong evidence for negative regulation toward 206 target genes. *VEGFA*, a known activator of cell adhesion, displayed decreased expression ($P \leq 0.05$), validating negative regulation by 4 of these increased miRNAs: miR-126; 150; 29a; 29b ($P \leq 0.05$). In endometriosis patients, a total of 10 significantly altered miRNAs displayed increased expression compared to controls (miR-7b; 9; 24; 34b; 106a; 191; 200b; 200c; 342-3p; 484) ($P \leq 0.05$), targeting 1014 strong evidence-based genes. Three target genes of miR-106a (*CDKN1A*, *E2F1* and *RUNX1*) were independently validated. Functional annotation analysis of miRNA-target genes revealed enriched pathways for both infertility etiologies, including disrupted cell cycle regulation and proliferation ($P \leq 0.05$). These extracellular vesicle-bound secreted miRNAs are key transcriptional regulators in embryo-endometrial dialogue and may be prospective biomarkers of implantation success. One of the limitations of this study is that it was a stimulated, *in vitro* model and therefore may not accurately reflect the *in-vivo* environment.

11.2.3. Chapter Introduction

The World Health Organization estimates that 10% of couples worldwide will struggle with infertility. Although a small number of these reproductive-age couples may succeed using conventional methods over many months and possibly years, most will require the use of assisted reproductive technologies (ARTs) and often *in vitro* fertilization (IVF) to establish a pregnancy (Thoma et al. 2013). Although considered relatively successful, 70% of IVF cycles will not result in a live birth (Weimar et al. 2013).

An intricate, bi-directional molecular dialogue between embryo and endometrium during the window of implantation, approximately 6–12 days post ovulation, is crucial for success (Wilcox, Baird, and Weinberg 1999). Without a precise interchange between the two, implantation will ultimately fail. Key genes involved with cell cycle regulation, as well as ion-binding and signal-transporting proteins, have been identified as contributors to the molecular dialogue between the embryo and a receptive endometrium by sampling the uterine microenvironment (Hannan et al. 2012; Ruiz-Alonso, Blesa, and Simon 2012). MicroRNAs (miRNAs) also play an important role during the window of implantation and are expressed by both the implanting embryo and the receptive endometrium (Blakaj and Lin 2008; Laurent 2008). Altered expression of miRNAs (including miR- 30b, miR-30d and miR-494) have been shown to regulate endometrial receptivity (Altmae et al. 2013).

An *in vitro* co-culture system can provide valuable insight into the initial bi-directional dialogue (Simon et al. 1998). *In vitro* studies utilizing an embryo/endometrial co-culture system have observed key components of the molecular crosstalk between the embryo and endometrial epithelial cells (EEC). However, limited information regarding this interaction is known (Barmat et al. 1999; Rubio et al. 2000; Simon et al. 1999).

Our unique study utilized a human uterine luminal endometrial epithelial cell and human blastocyst co-culture system to investigate the molecular dialogue at the time of adhesion, in association with two major causes of female factor infertility (endometriosis and advanced maternal age). The researchers specifically chose to investigate the role miRNAs within extracellular vesicles play during the window of implantation because of miRNAs ability to perform essential post-transcriptional regulation of gene expression. MiRNAs accomplish this through either the degradation of a transcript or the inhibition of translation and their involvement in key cellular processes, such as apoptosis, proliferation, or differentiation, all of which are occurring on a large scale within the uterine microenvironment during endometrial development and blastocyst implantation (Revel et al. 2011). By utilizing the miRNA data discovered within this study, the researchers hope to examine mRNA transcriptome and protein/protein communications in the future to get a more complete understanding of the intricate molecular dialogue during the window of implantation. Advanced maternal age (AMA) is associated with a substantial linear decline in reproductive potential and is the major cause of female infertility (Rosenwaks, Davis, and Damario 1995). There are many factors contributing to

the significant decrease in live births as women approach their 5th decade, including diminishing ovarian reserve (Zhang 2015), and the increase in oocyte chromosomal aneuploidy (Harton et al. 2013). Aneuploidy screening in IVF cycles has allowed for the transfer of euploid blastocysts, resulting in higher implantation rates, independent of maternal age (Schoolcraft et al. 2011). However, there are other variables beyond the oocyte/embryo chromosome constitution that impact the ability of a euploid blastocyst to successfully implant. Traditionally, AMA patients are shown to have a longer infertility duration and diminished ovarian reserve and require a higher dose of gonadotropins in controlled ovarian hyperstimulation, all resulting in poorer oocyte quality (Ocal et al. 2012).

Another pathological cause of infertility, widely diagnosed and treated within the field of reproductive medicine, is endometriosis. Endometriosis is a disease which causes tissue normally found within the uterus, to migrate and grow outside of it (Buck Louis et al. 2011). This debilitating disease is often painful, impacting a woman's quality of life, and greatly reduces the chances of conception. It is estimated that nearly half of all women with this diagnosis will have difficulty achieving a pregnancy (Practice Committee of the American Society for Reproductive Medicine 2006, (Ozkan, Murk, and Arici 2008)). The causes of endometriosis remain unclear; however a genetic predisposition is suspected as a common risk factor, including a family history of the condition (Wenzl et al. 2003). Several pathways have also been identified within patients diagnosed with endometriosis which may contribute to the poor oocyte quality associated with the disease (Shebl et al.

2017). Within infertile populations, it is estimated that the prevalence of patients diagnosed with endometriosis is approximately 26.13% in women undergoing laparoscopy (Garcia-Velasco and Quea 2005; Rizk et al. 2015).

The aim of this study is to investigate these different primary infertility etiologies within a controlled co-culture system, and to elucidate differences within the secretome that may offer insight, non-invasively, into the competence and viability of the blastocyst and endometrial monolayer. We found significant differences in the miRNA content within the extracellular vesicles of the supernatant, as well as differences in gene expression within the co-cultured endometrial cells and blastocysts which may impact endometrial function during the window of implantation.

11.2.4. Materials and Methods

11.2.4.1. Study Design

This study was conducted in two phases, each examining a distinct infertility etiology. This included women presenting with advanced maternal age, or endometriosis. These particular infertility etiologies were chosen due to their significant impact on implantation potential and the high number of patients presenting with these distinct phenotypes available to participate in the study. Both phases utilized surplus cryopreserved human blastocysts and endometrial biopsies, which were donated to research with consent by

current and prior IVF patients under the guidance of the Western Institutional Review Board, Inc (WIRB® Protocol #20140449).

Phase 1 incorporated blastocysts from infertile endometriosis patients, while phase two examined blastocysts from patients presenting with advanced maternal age (Figure 16). Our control group across both phases consisted of blastocysts from fertile oocyte donor cycles described below.

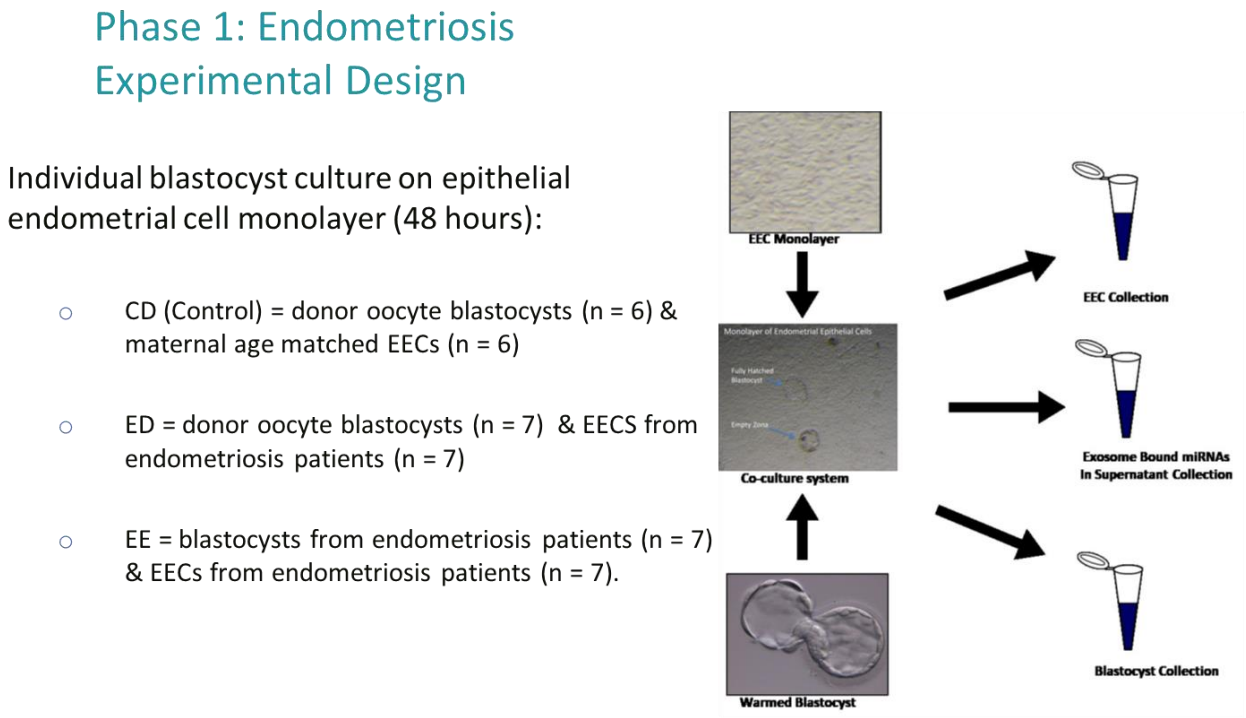

Figure 16: Phase 1 Experimental groups (CD = fertile control endometrium/fertile control blastocyst; ED = endometriosis endometrium/fertile control blastocyst; EE = endometriosis endometrium/endometriosis blastocyst) and the affected miRNAs for

embryos and endometrial cells derived from patients diagnosed with endometriosis compared with fertile control.

Phase 2 examined advanced maternal age by utilizing our co-culture model with two groups, a control which consisted of donor oocyte blastocysts co-cultured with donor endometrial cells, and an advanced maternal age group which consisted of AMA blastocysts co-cultured with donor endometrial cells. Following the establishment of the EEC monolayer, individual vitrified blastocysts that were donated to research were warmed and co-cultured with the EEC monolayer for 48 hours.

Similarly, following the 48 hour co-culture, the EEC monolayer was collected, as well as the supernatant and the associated blastocyst for analysis (Figure 17).

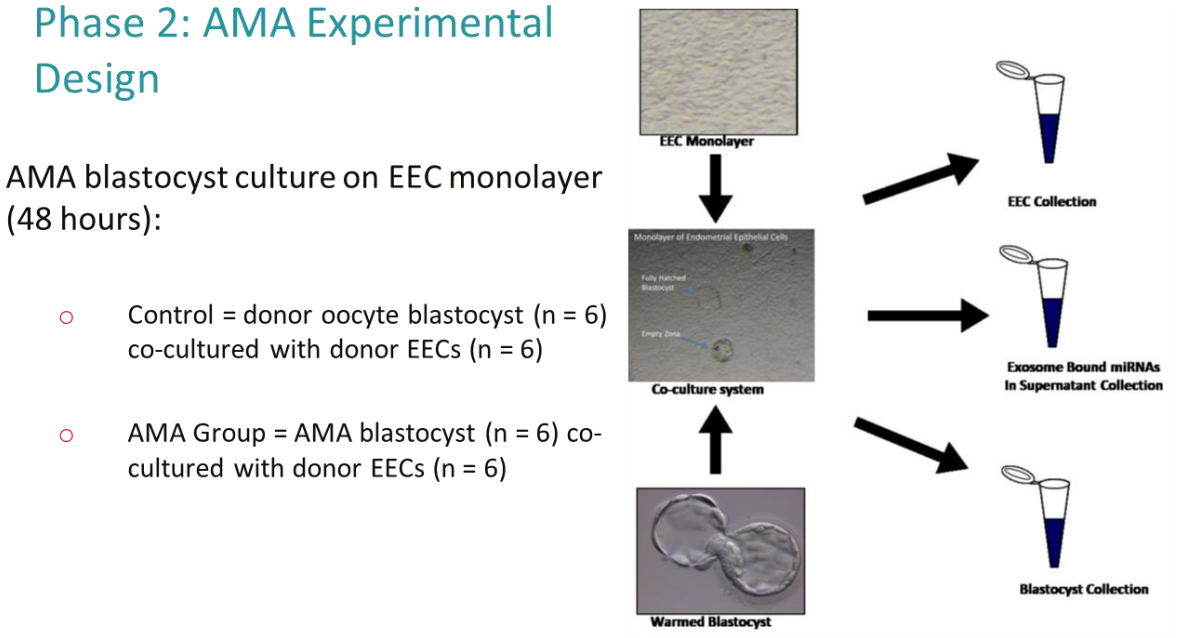

Figure 17: Phase 2 Experimental groups (Control = donor oocyte blastocyst co-cultured with donor EECs; AMA Group = AMA blastocyst co-cultured with donor EECs) and the affected miRNAs for embryos and endometrial cells derived from patients diagnosed with endometriosis compared with fertile control.

11.2.4.2. Embryos

Surplus, cryopreserved, hatching, transfer-grade blastocysts as identified by the Gardner & Schoolcraft grading system (Gardner & Schoolcraft 1999) as ≥Grade 3BB on day 5 of embryonic development (*n* = 41) were donated with patient consent and IRB approval. Blastocysts were derived from IVF cycles: young fertile oocyte donor controls (fertile control group) with no history of female or male factor infertility, based on WHO guidelines (maternal age ≤32 years old, BMI <29, non-smoker, non-drug user, with normal

ovarian reserve and regular menstrual cycles, *n* = 15), infertile women of AMA group without pre-implantation genetic diagnosis (≥39 years or older, with no other infertility diagnosis, *n* = 14), and younger female patients diagnosed with endometriosis as the only cause of infertility (mean maternal age of 34.3, with 11 of the 12 patients ≤33 years old, *n* = 12). Subjects underwent an ovarian stimulation protocol based on clinical discretion which included gonadotropin-releasing hormone (GnRH) agonist down-regulation, microdose GnRH agonist flare or GnRH antagonist with Menopur (Ferring Pharmaceuticals, Saint-Prex, Switzerland) or Bravelle (Ferring Pharmaceuticals) with or without clomiphene citrate. Final oocyte maturation trigger was induced when the lead follicle reached 20 mm mean diameter using an intramuscular injection of hCG, a subcutaneous injection of leuprolide acetate, or a combination of both, based on clinical judgment. Routine oocyte retrieval was performed transvaginally under ultrasound guidance 35 h post trigger. Patients within the endometriosis group were asymptomatic at the time of their oocyte retrieval and biopsy. Patients were excluded from the study if they had any other infertility comorbidities including polycystic ovary syndrome and depleted ovarian reserve. Embryos were vitrified and warmed according to routine laboratory procedures described previously (Kuwayama et al. 2005). Total time spent frozen varied, with an average time of approximately 4 years.

11.2.4.3. Endometrial Biopsies

Endometrial biopsies were collected from either young, fertile oocyte donors (fertile control group, *n* = 7) or from patients diagnosed with endometriosis who were currently

asymptomatic at the time of their oocyte retrieval (*n* = 2). Subjects were stimulated as described earlier. Endometrial biopsies measured 1.5–3.0 cm in length and approximately 0.5 cm in diameter. For every endometrial biopsy collected, tissue was minced into <1 mm sections and incubated at 4°C overnight in a 0.1% collagenase solution (Sigma-Aldrich). The primary epithelial endometrial cells (EEC) were isolated by vigorously vortexing and rinsing the cell milieu in 10 mL of room temperature DMEM (Sigma-Aldrich), prior to resting the cells for 5–10 min as they settled into distinct layers of EEC and stromal cells. The supernatant containing stromal cells was then removed and the process was repeated three times until no further stromal cells remained. 500 µL of the EEC/DMEM was then added to 6 wells of a Falcon Multiwell 24-well Tissue Culture Plate (Corning Incorporated) (Mercader et al. 2003). Cells were cultured in a media composed of 75% Dulbecco Modified Eagle Medium (Sigma) and 25% MCDB- 105 (Sigma) containing antibiotics, 5 µg/mL insulin (Sigma) and supplemented with 10% exosome-depleted fetal bovine serum (System Biosciences, Palo Alto, CA, USA) and observed daily to monitor the development of an EEC monolayer. The monolayer reached acceptable levels of well coverage at >65% after 4–6 days. The growth medium was then replaced with a serum-free medium for embryo development and supplemented with 4% recombinant human serum albumin (Vitrolife, Englewood, CO, USA). For each endometrial biopsy processed, 4–6 wells received an individual thawed blastocyst which was co-cultured for 48 h at 5% O2 and 6% CO2 at 37°C based on current laboratory practices for human blastocyst culture (Kovacic 2012).

11.2.4.4. Co-culture collection

Blastocysts were co-cultured together for 48 h prior to collection. AMA or fertile control donor blastocysts were co-cultured with fertile control donor endometrial tissue. Additionally, the endometriosis subjects were divided into three groups: fertile control donor blastocysts co-cultured with fertile control donor endometrium (CD), fertile control donor blastocysts co-cultured with endometrial cells from patients diagnosed with endometriosis (ED) and blastocysts and endometrial cells that were both obtained from patients diagnosed with endometriosis (EE). Adhesion by the blastocyst to the endometrial monolayer was observed twice in the AMA group, twice in the fertile control group and once in both of the endometriosis groups. Adhered blastocysts were gently scraped off the monolayer prior to collection. Following co-culture, blastocysts were graded and rinsed in 10% phosphate buffered saline-bovine serum albumin (PBS-BSA) before lysis in 10 µL of extraction buffer (PicoPureRNA Isolation Kit, Thermo Fisher Scientific). Co-culture supernatant was collected (500 µL) and snap-frozen in liquid nitrogen. The monolayer was visually measured for 100% confluence, then rinsed with DPBS (Thermo Fisher) and incubated at 37°C with 1× diluted TrypLESelect (10×) (Thermo Fisher) until cells lifted from the bottom of the plate (5–15 min). Each well of EEC were collected individually. The pelleted EEC were lysed with 50 µL Extraction Buffer (PicoPureRNA Isolation Kit, Thermo Fisher) and snap-frozen with liquid nitrogen. All samples were stored at −80°C until further analysis (Figure 16).

11.2.4.5. Supernatant extracellular vesicle miRNA analysis

Extracellular vesicles were isolated using Total Exosome Isolation Reagent (from cell culture media) kit (Thermo Fisher) which isolates small vesicles (30-120 nm) from water molecules. The reagent forces less-soluble components such as vesicles out of solution, allowing them to be collected by a short, low-speed centrifugation. The reagent is added to the cell media sample, and the solution is incubated overnight at 2°C to 8°C. The precipitated extracellular vesicles are recovered by standard centrifugation at 10,000 x g for 60 min. The pellet is then resuspended in PBS, and the extracellular vesicles are ready for downstream analysis or further purification by affinity methods. 350 µL of supernatant was combined with 175 µL of reagent and vortex-mixed prior to an overnight incubation at 4°C. Samples were centrifuged under refrigerated conditions for 1 h, then the supernatant was aspirated and discarded. The resulting pellet was lysed in 10 µL of lysis solution containing DNase (Taqman MicroRNA Cells-to-CT Kit, Thermo Fisher) and incubated at room temperature for 8 min. Lysed miRNA was reverse-transcribed using the Taqman MicroRNA Reverse Transcription Kit with MegaPlex RT Human Primer Pool A (Thermo Fisher) in a final volume of 7.5 µL under the following thermal cycling conditions: 40 cycles at 16°C for 2 min, 42°C for 1 min and 50°C for 1 s followed by a hold for 5 min at 85°C. cDNA was pre-amplified using the Taqman PreAmp Mastermix with MegaPlex PreAmp Human Primer Pool A (Thermo Fisher). 100 µL of the diluted pre-amplified product was added to each well of the Taqman Human MicroRNA Array Card A and was then run on the 7900HT Fast Real-Time PCR System (Thermo Fisher) under the following thermal cycling conditions: 50°C for 2 min, 94.5°C for 10 min and 40 cycles at 97°C for 30

s and 59.7°C for 1 min. Data were analyzed using the RQ Manager 1.2.1 (Thermo Fisher), and statistical analysis was performed using REST 2009 software (Qiagen). miRNAs that displayed significantly altered expression profiles were further investigated for target gene analysis using miRTarBase (http://mirtarbase.mbc.nctu.edu.tw/index.php), a database of experimentally validated miRNA-target interactions that are classified as strong evidence based if there is sufficient published empirical evidence.

11.2.4.6. Blastocyst gene expression

Individual blastocysts stored in 10 µL of extraction buffer (PicoPure RNA Isolation Kit, Thermo Fisher) were incubated at 42°C for 30 min prior to isolating RNA. This procedure entailed adding 1 volume of 70% EtOH to each sample before transferring to a pre-conditioned purification column. Samples were then DNase-treated using the RNase-Free DNase Set (Qiagen) and eluted in 20 µL following several washes. All 20 µL of purified total RNA was reverse-transcribed using the High-Capacity cDNA Reverse Transcription Kit (Thermo Fisher) in a final volume of 40 µL. The reaction occurred in a thermal cycler at 25°C for 10 min followed by 37°C for 2 h. cDNA samples were diluted 1:5 with nuclease-free water and a 5 µL template was used for real-time PCR using the Power SYBR Green PCR Master Mix (Thermo Fisher) and a 5 µM primer mix (forward + reverse) in a 25 µL final volume. Duplicates of each sample were performed on the ABI 7300 Real-Time PCR System under the following thermal cycling conditions: 95°C for 10 min, 40 cycles at 95°C for 15 s and 60°C for 1 min, followed by a dissociation stage to determine melt temperatures. Standard curves were also employed for each gene using Universal Human

Reference RNA (Agilent) in 10-fold serial dilutions and an internal housekeeping gene (*PPIA*) was used to normalize each sample.

11.2.4.7. Endometrial cell molecular analysis

EEC samples were lysed in 75 µL of lysis solution and miRNAs were isolated using the RNaqueous-Micro Kit (Thermo Fisher) which required the addition of 1.25 volumes of 100% EtOH prior to loading onto a micro filter cartridge assembly. Samples were DNase-treated in the same manner as the blastocyst samples, and washed several times before eluting in 10 µL of elution solution previously heated to 75°C (performed twice for maximum recovery, 20 µL final volume). miRNA samples were then concentrated down to a 10 µL volume using a vacuum concentrator (Vacufuge Plus, Eppendorf).

miRNA samples were pre-amplified, diluted and evaluated using the Taqman Human MicroRNA Array Card A (Thermo Fisher) as described in the earlier supernatant exosome miRNA analysis section. Data were analyzed using the RQ Manager 1.2.1 (Thermo Fisher) and statistical analysis was performed as described in the following.

11.2.4.8. Statistical analysis

A Mann–Whitney *U* test was used to compare differences in the age of the donor women (fertile control, AMA and endometriosis blastocysts), with significance at $P \leq 0.05$. The PCR reaction efficiencies recorded R^2 values ≥0.9 and correlation coefficients were calculated to be >0.99. Statistical analysis was performed with REST-2009 software (Qiagen) which uses bootstrap randomization techniques to correct for exact PCR efficiencies with mean crossing point deviations between sample and control groups to determine an expression ratio that is tested for significance by a pair wise fixed reallocation randomization test. The standard error and the 95% confidence interval (CI) given by REST-2009 software are not derived from Ct values. They are the standard error and the CI for the 50,000 iterations the program runs to calculate the *P* value; thus, no error bars are generated for graphical presentation. Gene expression fold differences with $P \leq 0.05$ were considered statistically significant.

11.2.5. Results

11.2.5.1. Co-culture of AMA blastocysts and fertile control blastocysts

The age of the donors in the fertile control blastocyst group were significantly different than those in the AMA blastocyst group ($P \leq 0.05$). Isolated cargo of extracellular vesicles from supernatant collected after co-culture of fertile endometrial epithelial cells with blastocysts from infertile AMA patients revealed altered miRNA expression profiles compared to fertile control blastocysts. A total of 16 miRNAs showed increased expression and 2 exhibited reduced expression in association with the maternal age of

the blastocyst relative to the internal housekeeping gene *RNU48* ($P \leq 0.05$, Figure 18). Target gene investigation of these 18 altered miRNAs using miRTarBase (http://mirtarbase. mbc.nctu.edu.tw/index.php) revealed 576 genes, 206 of which displayed strong evidence as defined by Western blot, qPCR or reporter assay as described previously. Of these strong evidence-based genes, *VEGFA* was identified as a target gene, specifically regulated by four of the altered miRNAs: miR-126, 150, 29a and 29b. Examination of *VEGFA* transcription by qPCR observed decreased expression in both the corresponding endometrial epithelial cells and blastocysts from infertile AMA patients following co-culture, specifically a 50% fold change reduction compared to fertile controls ($P \leq 0.05$; Figure 18).

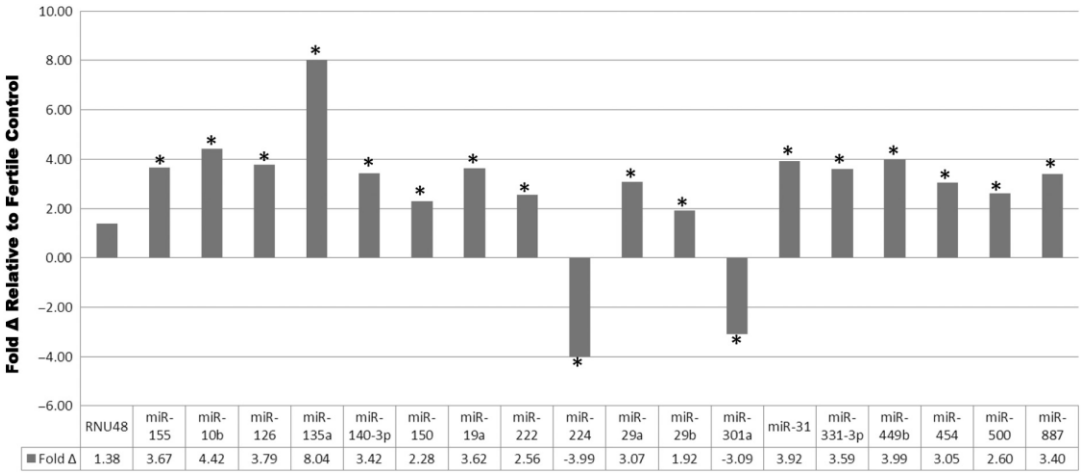

Figure 18: Differential expression of extracellular vesicle-bound miRNAs in co-culture supernatant in association with maternal age (*$P \leq 0.05$).

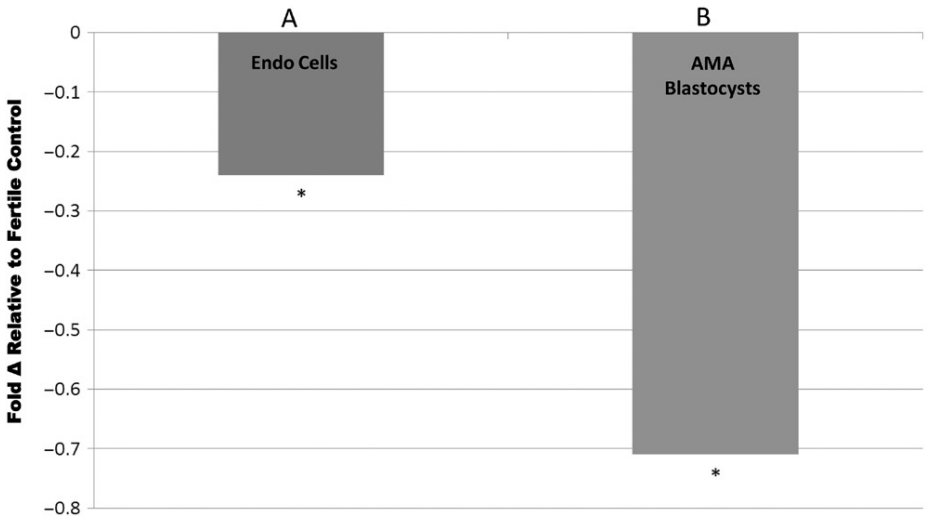

Figure 19: Target gene *VEGFA* expression in endometrial cells (A) and AMA blastocysts (B) compared to young fertile controls (*$P \leq 0.05$).

11.2.5.2. Co-culture of endometriosis blastocysts or fertile control blastocysts on donor endometrium or endometriosis endometrium

The ages of the donors in the fertile control blastocyst group were not significantly different from those in the endometriosis blastocyst group ($P \geq 0.05$; ns). Isolated extracellular vesicles from supernatant collected after co-culture of endometriosis EEC with blastocysts from endometriosis patients revealed an altered miRNAome compared to fertile controls. Specifically, 10 miRNAs showed significant decreased expression including miR-7b miR-24, miR-34b, miR-200c, miR- 342-3p, miR-9, miR-484, miR-200b, miR-106a and miR-191 ($P \leq 0.05$; Figures 18 and 19) compared to fertile control endometrium co-cultured with fertile control blastocysts. Using mirTarBase, strong evidence-based target genes were revealed, including, among others, 27 target genes for miR-106a. Of these 27 target genes *CDKN1A*, *E2F1* and *RUNX1* were chosen for further

investigation because of their known roles in association with implantation in murine (Cdkn1a) (Das 2009) and human models (E2F1 and RUNX1) (Tapia et al. 2011; Tapia-Pizarro et al. 2014). qPCR analysis observed increased expression of *CDKN1A* in endometriosis blastocysts compared to fertile controls when co-cultured with fertile control derived EEC ($P \leq 0.05$). This expression was further increased when endometriosis derived blastocysts were co-cultured with endometriosis derived EEC ($P \leq 0.05$; Figure 22A). Endometriosis EEC co-cultured with fertile control blastocysts displayed increased expression of *E2F1* and *RUNX1* ($P \leq 0.05$). This significant difference in expression was further increased when endometriosis derived blastocysts were co-cultured using endometriosis derived EEC($P \leq 0.05$; Figure. 20B).

11.2.5.3. Gene ontology and pathway analysis

DAVID Bioinformatics Resources 6.8 (https://david. ncifcrf.gov/) was utilized for functional annotation clustering analyses of differentially expressed miRNAs to explore the GO biological processes and pathways, common to both infertility etiologies, and included cellular development, proliferation and cell cycle regulation.

The enriched pathways and processes that were identified as being specific to only the AMA etiology included PI3K-Akt and vascular endothelial growth factor (VEGF) signaling, as well as biological processes involving cellular development and migration, adhesion

and cell cycle regulation ($P \leq 0.05$; Table S1, see section on supplementary data given at the end of this article).

For the endometriosis etiology group, enriched biological processes and pathways crucial for development and implantation were revealed within functional annotation clusters of the 1014 strong evidence-based target genes, including positive regulation of cell proliferation, G1/S transition of mitotic cell cycle and the p53 signaling pathway and angiogenesis ($P \leq 0.05$). Additionally, cell cycle regulation and arrest, positive regulation of cell proliferation, negative regulation of apoptotic processes and negative regulation of G1/S transition of mitotic cell cycles were also identified (Table S2).

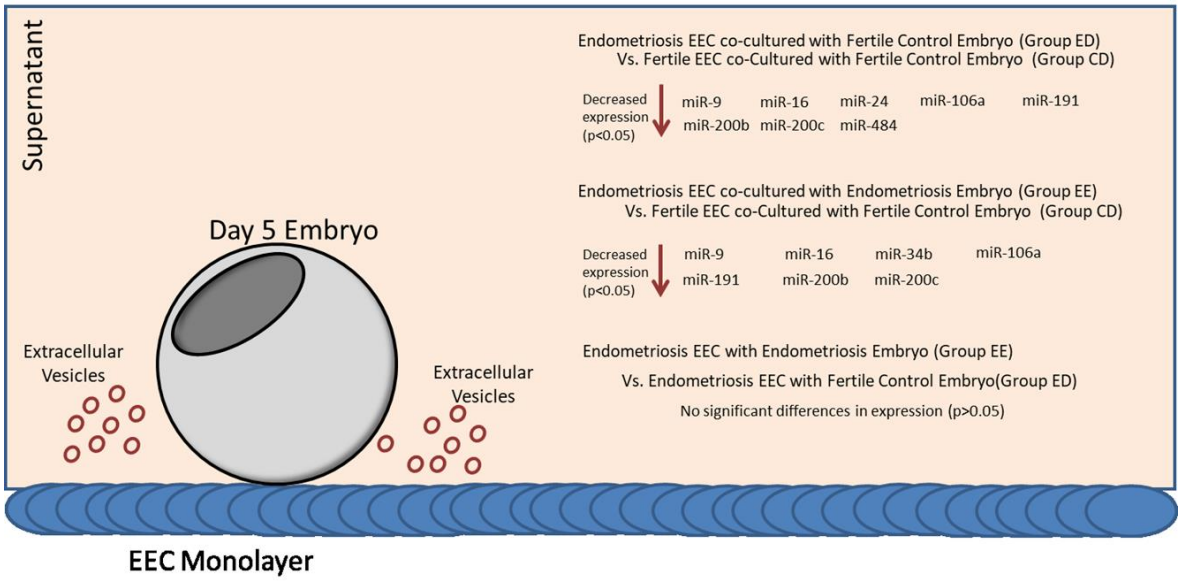

Figure 20: Experimental groups (CD = fertile control endometrium/fertile control blastocyst (n = 6); ED = endometriosis endometrium/fertile control blastocyst (n = 7); EE = endometriosis endometrium/endometriosis blastocyst (n = 7)) and the affected miRNAs for embryos and endometrial cells derived from patients diagnosed with endometriosis

compared with fertile control. No significant differences in expression were found between groups EE and ED ($p>0.05$).

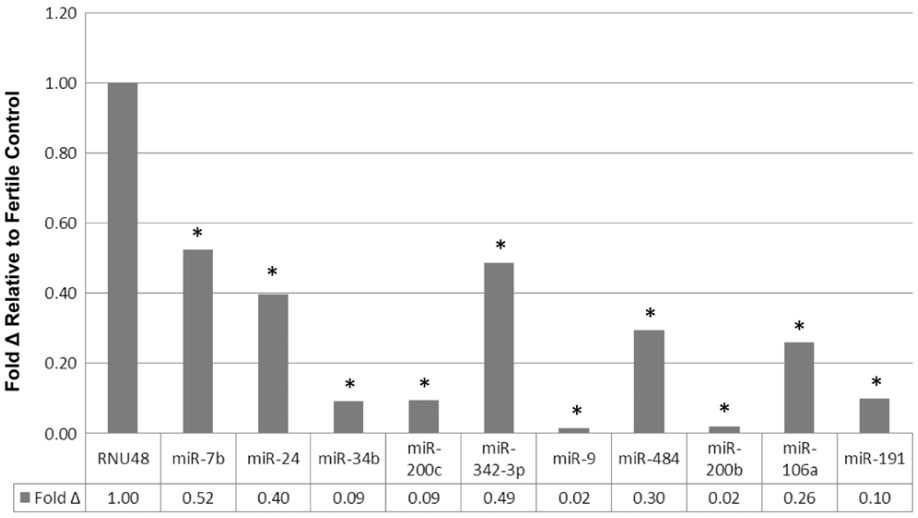

Figure 21: Extracellular vesicle-bound microRNA expression of co-culture supernatant. Endometriosis derived blastocysts cultured on a monolayer of endometriosis derived endometrial tissue and fertile control derived endometrial tissue, fertile control oocyte derived blastocysts (*$P \leq 0.05$).

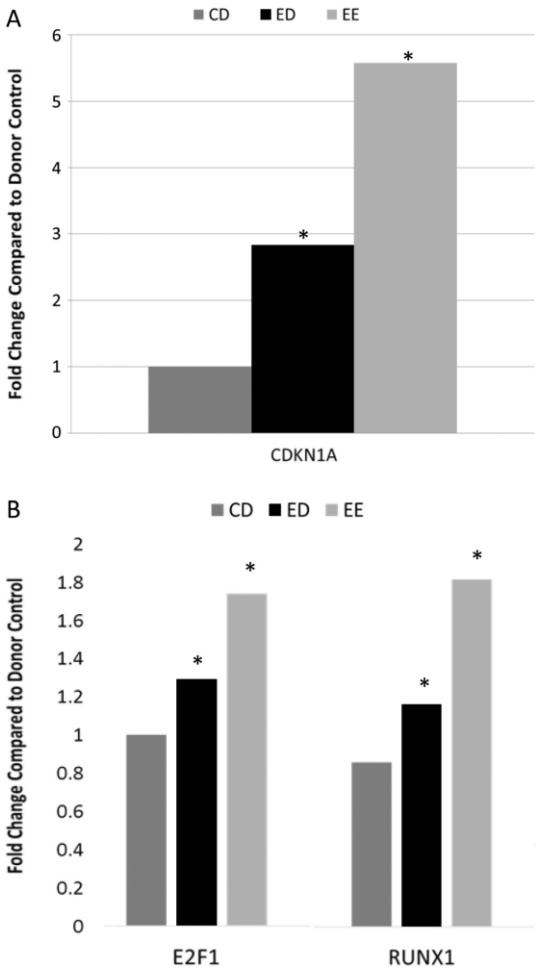

Figure 22: (A) miR-106a target gene validation of endometriosis derived blastocysts revealed significantly increased expression of *CDKN1A* when co-cultured with endometriosis derived endometrial cells compared to fertile control (CD = fertile control endometrium/ fertile control blastocyst (n = 6); ED = endometriosis endometrium/fertile control blastocyst (n = 7); EE = endometriosis endometrium/endometriosis blastocyst (n = 7)) (*$P \leq 0.05$). (B) miR-106a target gene validation of endometriosis derived endometrial cells co-cultured with endometriosis derived blastocysts revealed significantly increased expression of *E2F1* and *RUNX1* compared to fertile control derived controls (CD = fertile control endometrium/fertile control blastocyst (n = 6); ED =

endometriosis endometrium/fertile control blastocyst (n = 7); EE = endometriosis endometrium/endometriosis blastocyst (n = 7)) (*$P \leq 0.05$).

11.2.6. Discussion

This is a novel study investigating the bi-directional molecular communication at the time of implantation in association with infertility etiologies, a model which will offer a non-invasive way to identify deficiencies found within the secretome. Blastocysts from patients presenting with AMA or endometriosis were co-cultured on a monolayer of endometrial cells to capture the molecular dialogue between a blastocyst and the endometrium during the initial stages of implantation. Specific extracellular vesicle-bound miRNAs derived from co-culture supernatant were identified to have significantly altered expression in association with AMA or endometriosis, highlighted by the differences within embryo-endometrial communication depending on the source of the embryo or endometrium. This impacted downstream target gene expression in either blastocysts or endometrial cells during the window of implantation.

11.2.6.1. Advanced maternal age

It is well documented that infertile women presenting with advanced maternal age have some of the poorest prognoses with regard to oocyte and blastocyst quality. Additionally, there is some evidence that the endometrium is also affected by advanced age, resulting in embryo-endometrial asynchrony (Shapiro et al. 2016). The molecular dialogue between

the embryo and endometrium is crucial for successful implantation, and it is believed that miRNA-bound extracellular vesicles are involved in this bi-directional molecular communication.

A total of 18 extracellular vesicle-bound miRNAs displayed altered expression with the presence of AMA blastocysts. One example was miR-150, a critically important miRNA for lineage cell differentiation, which also plays a role in mediating an appropriate inflammatory response within the endometrial environment. This response includes not only the endometrial epithelial cells and stromal cells, but also the immune-related cells and vasculature (Elton et al. 2013; Goossens et al. 2013; Pan and Chegini 2008). Pregnancy is a pro-inflammatory state and molecular miscommunication may result in an improperly coordinated auto-immune response, leading to inflammation at the implantation site, causing implantation failure and embryonic death. This is a delicate balance, and if the immune response is too great or insufficient, implantation potential may be impacted (Clark 2008). miR-150 is also a regulatory miRNA for the platelet-derived growth factor/VEGF family of genes, responsible for both angiogenesis and vasculogenesis, and is vital for successful embryo implantation. It has also been shown that supplementing embryo culture media with VEGF had beneficial effects with regard to post-compaction mouse embryo development, outgrowth, implantation and fetal development (Binder et al. 2014; Binder et al. 2016).

VEGFA is a glycosylated mitogen that specifically acts on endothelial cells with various effects, including mediating vascular permeability, angiogenesis, cell growth and cell migration and inhibiting apoptosis. Treatment of human endometrial cells with recombinant human VEGFA protein has been found to significantly increase endometrial cell adhesion (Hannan et al. 2011). In this study, *VEGFA* displayed a significantly lower expression in AMA samples ($P \leq 0.05$), which may lead to dysregulated cellular function and increased apoptosis. This decrease in *VEGFA* expression may be indicative of the compromised communication between the AMA blastocyst and fertile control endometrium.

An additional altered miRNA observed in extracellular vesicles following co-culture was miR- 135a with an 8-fold decrease in expression in AMA blastocysts ($P \leq 0.05$). A previous study observed that increased expression of miR-135a during pre-implantation embryo development led to the down-regulation of E3 ubiquitin ligase seven in absentia homologue 1A (*SIAH1A*) expression (Pang et al. 2011). The SIAH1A protein is involved in many cellular processes including apoptosis, TNF-alpha signaling and cell cycle regulation (Relaix et al. 2000). Nearly a third of the zygotes injected with miR-135a inhibitor were observed to arrest in development. The mechanism for this disruption is believed to be due to dysregulated proteosomal degradation, possibly controlling the expression of chemokines in DNA-binding protein (Pang et al. 2011). miR-135a has also been correlated to increased apoptosis resistance in cancer cells by *BCL2* regulation, a protein which determines cell survival and death through the mitochondrial apoptotic signaling

pathway. Dysregulation of *BCL2* and disruption of the apoptotic pathway resulted in interference of not only the establishment of pregnancy, but also pregnancy maintenance if successful implantation was able to occur at all (Mathew et al. 2009; Pan et al. 2014). The dysregulation of miR-135a observed in our samples suggests that the cellular regulation of blastocysts derived from AMA patients may be compromised, thus decreasing their viability and implantation potential.

Another miRNA found in the extracellular vesicles of the supernatant that displayed significantly disrupted differential expression was miR-449b. One strong, evidence-based target gene for miR-449b is *NOTCH1* which has demonstrated its ability to act as a promoter of centriole multiplication multiciliogenesis by repressing the Delta/Notch pathway in *Xenopus laevis* embryonic dermis (Marcet et al. 2011). It is currently unknown precisely how mammalian cells are affected by this pathway; however it is hypothesized that, rather than the cilia found in *Xenopus* cells, it is the formation of the pseudopodia within the blastocyst trophectoderm that is being directly regulated (Goossens et al. 2013). miR-449b showed significantly increased expression in the co-culture supernatant of AMA blastocysts, which may indicate compromised trophectoderm formation, leading to an increase in failed implantation as observed clinically in this patient population.

11.2.6.2. Endometriosis

Endometriosis is a disease characterized by an abnormal, and in many cases, compromised endometrium. The impact this diagnosis bears on the bi-directional

embryo-endometrial dialogue at the time of implantation is largely unexplored. In our study, co-culture of endometriosis endometrium with blastocysts derived from patients diagnosed with endometriosis displayed significantly decreased extracellular miRNA, from within the isolated extracellular vesicles, when compared to fertile control endometrium with fertile control derived blastocysts for 10 key miRNAs ($P \leq 0.05$). Of particular interest was miR-106a, commonly associated with adherens junctions, receptor interactions, metabolic pathways and VEGF signaling. In one study utilizing a uterine cavity lavage, miR-106a was identified in the exosomes found within the mucus near the time implantation may occur. It is suspected that as the blastocyst transitions toward the implantation site and begins to adhere, exosomes trapped within the mucus on the luminal surface of the endometrium release miRNAs which contribute to endometrial-embryo crosstalk by binding to the trophectoderm cells themselves (Ng et al. 2013). miR-106a has also revealed itself to be a strong identifying biomarker for various types of cancer where it is often down-regulated (Wang 2016). MiRTarBase target gene analysis of miR-106a identified 29 strong evidence-based target genes, including *CDKN1A*, *E2F1* and *RUNX1*.

CDKN1A works in conjunction with *TP53* and is linked to stress response in the G1 phase. If this stress response continues to cascade, it causes arrested cell cycle, potentially compromising the viability of embryos, and also contributing to possible de-regulation of the endometrium itself (Sharma, Kubaczka, et al. 2016). *CDKN1A* expression has been shown to induce cellular growth, arrest, terminal differentiation or apoptosis (Ying et al.

2011). Altered aberrant *CDKN1A* expression is also believed to play a vital role in the pathogenesis of specific cancer types, including ovarian and uterine carcinomas (Elbendary et al. 1996). Our results demonstrate altered *CDKN1A* gene expression in blastocysts derived from patients diagnosed with endometriosis, which may negatively impact their viability, and also contribute to the reduced implantation potential of embryos derived from this patient population.

E2F1 is a transcription factor that plays a crucial role in the control of the cell cycle and can mediate apoptosis. Over-expression of *E2F1* in myoblasts has demonstrated proliferation stimulation while also inhibiting differentiation (Luo et al. 2016). *E2F1* induces the transcription of several genes involved in cell cycle entry, resulting in either the induction or inhibition of apoptosis. This influence leads to both negative and positive feedback loops, having a critical impact on the outcome of the cell's fate. The *E2F1* protein has also shown increased expression in patients diagnosed with endometrial cancer, where the cell cycle becomes accelerated and irregular (Mints et al. 2016). Decreased expression of miR-106a can increase p53 expression in human glioma cells by inhibiting *E2F1*, negatively effecting cell proliferation and inducing apoptosis (Feng, Cao, and Wang 2013; Yang et al. 2011). Within the endometrium derived from patients diagnosed with endometriosis, irregular feedback loops may lead to inhibited differentiation, compromising the viability of the implantation site.

RUNX1 is also a transcription factor that, when over expressed, increases apoptosis. In a mouse embryo knockout study, embryos with homozygous mutations on Runx1 terminated after 12.5 days of development, and suffered from a lack of fetal liver hematopoiesis as well as hemorrhaging of the central nervous system (Okuda et al. 1996; Wang et al. 1996). Similar to *E2F1*, over-expression of the *RUNX1* protein has been linked to various forms of cancer, including endometrial and endometrioid carcinomas (Abal et al. 2006; Planaguma et al. 2004). In mice, *Runx1* also plays an important role in regulating the gene expression of *Ada* in trophoblast cell lineage which is critical for embryo development (Schaubach, Wen, and Kellems 2006). In our study, endometriosis derived endometrium showed increased expression of *RUNX1* that may lead to decreased implantation potential by compromising hematopoiesis and influencing the gene expression of placental *ADA*.

DAVID functional annotation bioinformatics microarray analysis revealed further dysfunction within the expression of miRNAs for both infertility etiologies, in relation to GO biological processes and pathways. When comparing the three different design groups, we found that miR-24, 34b and 484 were not commonly expressed between the groups of ED vs CD and EE vs CD, highlighting a subset of developmental pathways that were affected by the presence of endometrial cells from patients diagnosed with endometriosis (Table S3). Interestingly, there were also no significant differences in miRNA expression between the groups of EE and ED ($P > 0.05$), which signifies that the endometriosis EEC are contributing the majority of the extracellular vesicles to the

supernatant and may affect the developmental potential of the implanting blastocyst. Target gene validation within the EE and ED endometrial cell samples did show significant differences in expression of CDKN1A, E2F1 and RUNX1, which may be indicative that the blastocysts from endometriosis phenotype may have an increased sensitivity to miRNA dysregulation found within the supernatant. One commonality between the endometriosis and AMA groups was the focus on cell cycle regulation. This may be indicative of compromised dialogue within the extracellular matrix. As the window of implantation approaches, specific auto-induction loops must occur to mediate the critical crosstalk between a competent blastocyst and the uterine epithelium at the implantation site (Hamatani et al. 2004). If these critical processes and pathways are disrupted, the resulting cell cycle dysregulation may contribute to a harsh environment, unsuitable for implantation and further development necessary for a viable pregnancy by preventing firm adhesion between the blastocyst and the uterine epithelium (Wang et al. 2008).

A few limitations of this study include the source of the endometrial biopsy. These biopsies were taken at the time of oocyte retrieval from women undergoing controlled ovarian stimulation. It has been shown that this leads to estrogen-dependent changes in the protein profiles of the endometrial compartments which may affect endometrial receptivity (Ullah et al. 2017). Most importantly, these biopsies were not taken during the window of implantation, and as such are not truly representative of endometrial micro environment found in vivo. Furthermore, due to the scarcity of research materials, these protein profile alterations were unable to be validated further by ELISA analysis.

In conclusion, our study displayed a theme of compromised cellular communication in blastocysts and endometrium derived from patients diagnosed with AMA or endometriosis. These alterations may account for the lower implantation potential and clinical outcomes observed for these infertile patient populations, and future studies utilizing a model that includes independent prediction and replication will be the best way to proactively test these molecular data for their usefulness as developmental biomarkers to be used clinically in the future. Any compromise in the delicate embryo-endometrial molecular dialogue, either autocrine or paracrine, may impact transcription levels of key miRNAs and their target signaling molecules, resulting in significantly lower potential for reproductive success. Further investigation of the bi-directional molecular dialogue may help elucidate important implantation biomarkers during this critical time point, and advance our understanding of reproductive success.

Supplementary data

This is linked to the online version of the paper at https://doi.org/10.1530/REP-17-0566.

Table S1: Enriched pathways of statistically significant miRNA target genes (p<0.05) increased or decreased in the Endometriosis group compared to donor controls

hsa-miR-106a

GO Term	Term	# of genes	P-Value
GO:0008284	positive regulation of cell proliferation	4	3.40E-02

GO:2000134	negative regulation of G1/S transition of mitotic cell cycle	3	6.80E-04
GO:0043066	negative regulation of apoptotic process	7	5.60E-05
GO:0051726	regulation of cell cycle	5	3.70E-05

KEGG Pathway	**Pathway**	**# of Genes**	**P-Value**
hsa04110	Cell cycle	5	3.10E-04

hsa-miR-let-7b

GO Term	**Term**	**# of genes**	**P-Value**
GO:2000766	negative regulation of cytoplasmic translation	3	8.30E-05
GO:0071230	cellular response to amino acid stimulus	4	1.16E-04
GO:0000082	G1/S transition of mitotic cell cycle	5	5.17E-05
GO:0051301	cell division	7	6.45E-05
GO:0001934	positive regulation of protein phosphorylation	3	0.027192
GO:0030335	positive regulation of cell migration	6	3.22E-05
GO:0008284	positive regulation of cell proliferation	5	0.014057

KEGG Pathway	**Pathway**	**# of Genes**	**P-Value**
hsa04914	Progesterone-mediated oocyte maturation	7	3.76E-07
hsa04152	AMPK signaling pathway	6	5.13E-05
hsa04914	Progesterone-mediated oocyte maturation	7	3.76E-07
hsa04114	Oocyte meiosis	4	0.006072

hsa04110	Cell cycle	5	7.95E-04
hsa04115	p53 signaling pathway	3	0.022282
hsa04151	PI3K-Akt signaling pathway	10	1.17E-06
hsa04068	FoxO signaling pathway	7	4.80E-06
hsa05213	Endometrial cancer	3	0.013792

hsa-miR-200c

GO Term	Term	# of genes	P-Value
GO:0001525	angiogenesis	7	6.36E-04
GO:0048010	vascular endothelial growth factor receptor signaling pathway	6	2.22E-05
GO:0010595	positive regulation of endothelial cell migration	4	0.001315
GO:0001701	in utero embryonic development	7	2.49E-04
GO:0035924	cellular response to vascular endothelial growth factor stimulus	4	1.66E-04
GO:0045766	positive regulation of angiogenesis	5	0.002113

KEGG Pathway	Pathway	# of Genes	P-Value
hsa04510	Focal adhesion	9	6.30E-05

Table S2: Enriched pathways of statistically significant miRNA target genes (p<0.05) increased or decreased in the AMA group

hsa-miR-126

GO Term	Term	# of genes	P-Value
GO:0001938	positive regulation of endothelial cell proliferation	5	3.13E-05
GO:0045766	positive regulation of angiogenesis	5	2.29E-04
GO:0001525	angiogenesis	5	2.70E-03
GO:0048010	vascular endothelial growth factor receptor signaling pathway	3	1.53E-02

KEGG Pathway	Pathway	# of Genes	P-Value
hsa04151	PI3K-Akt signaling pathway	10	1.32E-05
hsa04012	ErbB signaling pathway	6	3.70E-05
hsa04015	Rap1 signaling pathway	7	2.86E-04
hsa04370	VEGF signaling pathway	4	2.46E-03
hsa04210	Apoptosis	4	2.59E-03
hsa04668	TNF signaling pathway	4	1.15E-02
hsa04010	MAPK signaling pathway	5	2.60E-02
hsa04664	Fc epsilon RI signaling pathway	3	3.69E-02
hsa05213	Endometrial cancer	5	7.72E-05
hsa04152	AMPK signaling pathway	5	2.01E-03

miR-150

GO Term	Term	# of genes	P-Value
GO:0043066	negative regulation of apoptotic process	5	3.68E-03

GO:0008284	positive regulation of cell proliferation	5	4.00E-03

KEGG Pathway	Pathway	# of Genes	P-Value
hsa04110	Cell cycle	3	4.90E-02

miR-29a

GO Term	Term	# of genes	P-Value
GO:2000352	negative regulation of endothelial cell apoptotic process	4	2.80E-04
GO:0007160	cell-matrix adhesion	5	7.75E-04
GO:0030335	positive regulation of cell migration	9	1.97E-06
GO:0048010	vascular endothelial growth factor receptor signaling pathway	3	4.32E-02

KEGG Pathway	Pathway	# of Genes	P-Value
hsa04510	Focal adhesion	16	1.81E-11
hsa04151	PI3K-Akt signaling pathway	18	3.14E-10
hsa04068	FoxO signaling pathway	7	5.17E-04
hsa04115	p53 signaling pathway	5	1.65E-03
hsa05213	Endometrial cancer	4	7.22E-03
hsa04370	VEGF signaling pathway	4	1.12E-02

miR-29b

GO Term	Term	# of genes	P-Value
GO:0030335	positive regulation of cell migration	11	8.74E-09

GO:0051781	positive regulation of cell division	7	6.01E-08
GO:0043406	positive regulation of MAP kinase activity	7	2.42E-07
GO:0016477	cell migration	6	1.03E-03
GO:0050680	negative regulation of epithelial cell proliferation	4	2.00E-02
GO:0016049	cell growth	4	2.00E-02
GO:0043065	positive regulation of apoptotic process	7	2.22E-02
GO:0007050	cell cycle arrest	4	2.52E-02
GO:0007160	cell-matrix adhesion	8	1.48E-07
GO:0050714	positive regulation of protein secretion	6	5.25E-07
GO:2000352	negative regulation of endothelial cell apoptotic process	5	6.93E-06
GO:0048010	vascular endothelial growth factor receptor signaling pathway	3	4.11E-02

KEGG Pathway	**Pathway**	**# of Genes**	**P-Value**
hsa04510	Focal adhesion	22	2.71E-19
hsa04151	PI3K-Akt signaling pathway	24	4.96E-17
hsa04014	Ras signaling pathway	9	2.51E-04
hsa04068	FoxO signaling pathway	7	4.65E-04
hsa05213	Endometrial cancer	4	6.85E-03
hsa04110	Cell cycle	6	2.27E-03
hsa04350	TGF-beta signaling pathway	5	3.53E-03
hsa04370	VEGF signaling pathway	4	1.06E-02
hsa04390	Hippo signaling pathway	5	2.64E-02
hsa05213	Endometrial cancer	4	6.85E-03

hsa04370	VEGF signaling pathway	4	1.06E-02
hsa04668	TNF signaling pathway	4	4.51E-02

Table S3: Enriched pathways of statistically significant miRNA target genes (p<0.05) increased or decreased in Combined Differentially expressed miRNA in Association with Endometriosis Diagnosis Endometrial Cells

GO Term	Term	# of genes	P-Value
GO:0000082	G1/S transition of mitotic cell cycle	12	4.01E-12
GO:0051301	cell division	8	0.002112036
GO:0001701	in utero embryonic development	7	3.96E-04
GO:0060070	canonical Wnt signaling pathway	4	0.00887545
GO:0016055	Wnt signaling pathway	4	0.071185563
GO:0048599	oocyte development	3	0.001949408
GO:2001234	negative regulation of apoptotic signaling pathway	3	0.002969315
GO:0045766	positive regulation of angiogenesis	6	3.09E-04
GO:0001525	angiogenesis	6	0.005756441

KEGG Pathway	Pathway	# of Genes	P-Value
hsa04151	PI3K-Akt signaling pathway	16	3.01E-07
hsa04110	Cell cycle	13	8.02E-10
hsa04115	p53 signaling pathway	7	2.92E-05
hsa04390	Hippo signaling pathway	8	4.11E-04

hsa05213	Endometrial cancer	5	0.001224143
hsa04310	Wnt signaling pathway	6	0.008213403
hsa04510	Focal adhesion	9	5.15E-04
hsa04370	VEGF signaling pathway	4	0.017862483
hsa04350	TGF-beta signaling pathway	5	0.007023653
hsa04068	FoxO signaling pathway	5	0.033410186
hsa04010	MAPK signaling pathway	6	0.081996404

11.3. Specific aim 3

This chapter is based on published work from the following publication.

Denomme MM*, **Parks JC*,** McCallie BR, McCubbin NI, Schoolcraft WB, Katz-Jaffe MG. *Advanced paternal age directly impacts mouse embryonic placental imprinting.* PLoS One. 2020 Mar 6;15(3):e0229904. doi: 10.1371/journal.pone.0229904. eCollection 2020.

11.3.1. My personal contribution to the work

I worked closely with Dr. Katz-Jaffe and Dr. Denomme to develop and implement the design of this experiment. I worked in tandem with Dr. Denomme to perform the subsequent experiments, results analysis and interpretation, and co-wrote and edited the manuscript for publication as a co-first author.

11.3.2. Chapter summary

The placental epigenome plays a critical role in regulating mammalian growth and development. Alterations to placental methylation, often observed at imprinted genes, can lead to adverse pregnancy complications such as intrauterine growth restriction and preterm birth. Similar associations have been observed in offspring derived from advanced paternal age fathers. As parental age at time of conception continues to rise,

the impact of advanced paternal age on these reproductive outcomes is a growing concern, but limited information is available on the molecular mechanisms affected *in utero*. This longitudinal murine research study thus investigated the impact of paternal aging on genomic imprinting in viable F1 embryonic portions of the placentas derived from the same paternal males when they were young (4-6 months) and when they aged (11-15 months). The use of a controlled outbred mouse model (male and female) enabled analysis of offspring throughout the natural lifetime of the same paternal males and excluded confounding factors like female age or infertility. It was also the researcher's opinion that the use of an outbred model more accurately mimics the genetic diversity found within an analogous homo sapien population (please note that this is a limitation that will be discussed in section 11.3.6). Firstly, paternal age significantly impacted embryonic placental weight, fetal weight and length. Targeted bisulfite sequencing was utilized to examine imprinted methylation at the *Kcnq1ot1* imprinting control region, with significant hypermethylation observed upon natural paternal aging. Quantitative real-time PCR assessed imprinted gene expression levels at various imprinting clusters, resulting in transcript level alterations attributable to advanced paternal age. In summary, our results demonstrate a paternal age effect with dysregulation at numerous imprinted loci, providing a mechanism for future adverse placental and offspring health conditions.

11.3.3. Introduction

As couples delay childbearing to later stages in life, the impact of increasing parental age on reproductive outcomes has become a significant concern (Kimura, Yoshizaki, and Osumi 2018). Advanced paternal age (APA) is associated with various pregnancy complications including increased risks for placental abruption, miscarriage, premature birth and low birth weight (Alio et al. 2012; Brandt et al. 2019; Khandwala et al. 2018). Long-term effects from delayed fatherhood have also been reported in mice, including reproductive fitness and longevity (Garcia-Palomares, Navarro, et al. 2009) as well as postnatal development and behavioural traits in offspring (Garcia-Palomares, Pertusa, et al. 2009). However, limited information is available on the direct influence of APA on the molecular mechanisms driving embryonic development *in utero*.

Our preceding murine study showed an adverse effect of APA on *in vivo* and *in vitro* reproductive outcomes commencing at paternal midlife (Katz-Jaffe et al. 2013). The use of a murine model comes with some inherent limitations, as they are such a short-lived species when compared to homo sapiens. Because of this, the underlying mechanisms that cause epigenetic perturbations caused by aging may be different. It has been well established that in human beings, epigenetic alterations in sperm can be caused by environmental stressors individuals are exposed to throughout their lifetime including metals, air pollution, benzene, organic pollutants, and electromagnetic radiation (Baccarelli and Bollati 2009; Berthaut et al. 2013; Miao et al. 2014) in addition to any change in epigenetics associated with natural aging. To date, most human studies have studied the epigenetics of aging sperm as populations of young individuals vs those of

aged individuals, rather than across the same males natural lifetime, (Jenkins, Aston, and Carrell 2018). However, quantifying exposure risks of environmental stressors within an aged individual is extremely difficult to assess, especially over the course of a man's natural lifetime. This makes the prospect of using a short-lived species more attractive, as it is much easier to control their environment. This allows researchers to choose to eliminate environmental confounding variables to focus instead on epigenetic permutations that occur naturally sans environmental exposures. One potential underlying mechanism involves perturbations in epigenetic modifications, such as DNA methylation, which regulate gene expression without alterations to the DNA sequence. Gametogenesis and embryogenesis are important stages for the establishment and maintenance of epigenetic marks. It is thus hypothesized that epigenetic errors during spermatogenesis can occur over time as males age. In fact, age-related methylation errors have already been identified in human sperm (Atsem et al. 2016; Jenkins et al. 2014) as well as mouse sperm (Kobayashi et al. 2016; Milekic et al. 2015). Evidence has shown a critical role for the paternal epigenome in embryo development, and so temporal alterations to the sperm epigenetic landscape as fathers age may be inherited by progeny and subsequently affect offspring development.

The placental epigenome plays a key role in regulating embryonic growth and development. Alterations in embryonic placental DNA methylation, frequently occurring at imprinted genes, have been associated with adverse pregnancy complications including preterm birth, intrauterine growth restriction and preeclampsia (Tilley et al.

2018; Toure et al. 2016). Genomic imprinting is a phenomenon that leads to monoallelic gene expression based on parental-origin (Bartolomei and Ferguson-Smith 2011). Imprinted domains often comprise of multiple genes under coordinated epigenetic control. The *Kcnq1ot1* imprinting cluster consists of a maternally-methylated imprinting control region (ICR) with paternally-expressed *Kcnq1ot1* non-coding RNA and numerous maternally-expressed protein-coding genes (Mancini-DiNardo et al. 2003). Importantly, a large proportion of imprinted genes are involved in growth, development and metabolism, and play critical roles in both the placenta and the brain.

The aim of this longitudinal research study was to investigate the impact of paternal aging in a controlled outbred murine model on the imprinted methylation of the *Kcnq1ot1* ICR and gene expression at various imprinting clusters in viable embryonic placentas. An outbred mouse model was utilized as previous research has found that it more accurately mimics the genetic diversity found within an analogous aging homo sapien population (Kõks et al. 2016). The use of a mouse model enabled analysis throughout the natural lifetime of the paternal males and excluded confounding factors like female age or infertility. The placenta tissue used to conduct these experiments represents another tissue commonly discarded at birth that can be used to non-invasively assess the health of the accompanying new life. Our results demonstrate a paternal age effect on embryonic placental and fetal weight, likely due to widespread dysregulation of imprinted genes restricted to the paternal allele, providing a mechanism for future adverse offspring health conditions.

11.3.4. Materials and methods

11.3.4.1. Ethics Statement

This study conducted in a privately-owned corporate setting followed national ethical guidelines for humane animal treatment and complied with relevant legislation. All experimental designs including studies involving animals were approved by an Internal Research Committee (IRC Protocol #990205, 5/11/2010) , adhering to a high standard of animal care in strict accordance with the recommendations in the Guide for the Care and Use of Laboratory Animals (8th Edition). Euthanasia was performed by cervical dislocation, and all efforts were made to minimize suffering.

11.3.4.2. Animals and male aging

Eight 6-8 week old outbred CF1 male mice (Charles River) with proven fertility were randomly selected for this study. Throughout the study, only young fertile 6-8 week old outbred CF1 female mice were selected for mating.

11.3.4.3. Placenta collection

Young male CF1 mice with proven fertility (“paternal males”) were mated routinely from 4-15 months of age with superovulated young CF1 females (6-8 week old). Before mating,

females underwent an ovarian superovulation protocol as described previously (Larman et al. 2011), by an injection of 5 IU PMSG (Sigma) followed 48 hours later by 5 IU hCG (Sigma). The females were superovulated in both young and aged groups to ensure that the authors were able to collect an appropriate number of pregnancies. This is common practice for many murine studies. The pregnant females were sacrificed each month at E16 of fetal development and the F1 embryonic portions of the placentas ("embryonic placentas"; n=8 males, 96 placentas total) were carefully dissected by excising the superficial portion of the chorion/chorionic plate and stored at -80^{o}C; this tissue has been shown to contain no maternal cells (Sood et al. 2006). Embryonic placental weight (g), fetal weight (g) and crown-rump length (mm) were also measured and recorded. Student's t-test was performed, with differences considered to be significant at $p<0.05$. DNA and RNA were concurrently isolated from embryonic placentas derived from the same males in their youth (4-6 months) and aged (11-15 months) (All-in-One Purification Kit, Norgen) and stored at -80^{o}C for further processing.

11.3.4.4. Targeted bisulfite sequencing

F1 embryonic placenta samples derived from the same males (n=8) in their youth (6/male; 48 total placentas) and aged (6/male; 48 total placentas). The overall number of fetuses varied by mating and male. Exactly 6 were randomly chosen from each young and aged mating per male. Collected samples were analyzed for targeted DNA methylation analysis as previously described (Denomme et al. 2016). Briefly, DNA isolation of individual embryonic placenta samples using the QiaAmp DNA Mini kit (Qiagen) was followed by

bisulfite mutagenesis using the EZ DNA Methylation-Direct kit (Zymo Research). PCR amplification involved the addition of 4 ng converted DNA directly to Hot Start Ready-To-Go (RTG) (GE Healthcare) PCR beads that each contained 0.4 µM *Kcnq1ot1* primers, 1 µL of 240 ng/mL transfer RNA and water up to 25 µL, with 25 µL mineral oil overlay. Methylation primers and PCR parameters are outlined in the supplementary data (Table S4A). PCR products were gel extracted, ligated into the pGEM-T EASY vector system (Promega), and transformed into Z-competent DHα *Escherichia coli* cells (Zymo Research). Following colony PCR amplification, 30 µL of individual clone samples were sent for sequencing at Bio Basic Inc. (Markham, ON, Canada). Approximately 26-28 clones were sequenced for each of the 96 samples. Methylation patterns were determined using two online software programs (BISMA and QUMA). Identical clones with the same CpG methylation and unconverted cytosines were considered to be representative of one individual DNA strand, and thus were included only once. Total DNA methylation for each gene was calculated as a percentage of the total number of methylated CpGs divided by the total number of CpG dinucleotides. Two-way ANOVA statistical assessments were used to examine significance for methylation between paternal age groups and individual paternal males for 4-6 vs. 11-15 months (n=8) and aged subgroups 4-6 vs. 11-12 months (n=5), and 4-6 vs. 14-15 months (n=3), while a one-way ANOVA test was used to evaluate significance between the young group and the two aged subgroups (4-6 vs. 11-12 vs. 14-15 months). A reanalysis was also performed by calculating total DNA methylation for each gene as a percentage of the total number of methylated clones divided by total

clones in each placenta. Percent methylation differences with $p<0.05$ were considered to be statistically significant.

11.3.4.5. Quantitative real-time PCR

Analysis of transcript abundance on isolated RNA from the same individual embryonic placenta samples (96 placentas from 8 males) was performed as previously described (Denomme et al. 2018). Briefly, RNase-free DNase I (Qiagen) treated samples were reverse transcribed using the High Capacity Reverse Transcription cDNA kit (Thermo Fisher Scientific). Quantitative real-time PCR was performed with Power SYBR Green PCR Master Mix (ThermoFisher Scientific) on the ABI 7300 Real Time PCR System. Quantification of nineteen imprinted genes within five imprinting clusters were calculated relative to a constant internal housekeeping gene, *Ppia*, and the embryonic placenta samples derived from aged males (11-15 months, and subdivided into 11-12 months and 14-15 months) were analyzed relative to those derived from when the same males were in their youth (4-6 months). Expression primers and PCR parameters are outlined in the supplementary data (Table S4B). The Relative Expression Software Tool (REST 2009; Qiagen) was used for mRNA gene expression analysis. REST uses a mathematical model for gene expression which is based on the PCR efficiencies and the mean crossing point deviation between sample and control group and tested for significance relative to a housekeeping gene by a pairwise fixed reallocation randomization test (Pfaffl, Horgan, and Dempfle 2002). Gene expression fold differences with $p<0.05$ were considered to be statistically significant. Furthermore, two-way ANOVA statistical analysis was performed

on deltaCt values to evaluate the effects of both paternal age as well as the paternal male individual for 4-6 vs. 11-15 months (n=8), with $p<0.05$ considered statistically significant.

11.3.5. Results

11.3.5.1. Reproduction and Fetal Development

Outbred males (n=8) with proven fertility were mated every consecutive month with superovulated young outbred females throughout their natural lifetime. For purposes of this study, paired litters of offspring from the same individual males were assessed from young paternal males (4-6 months) and the same paternal males when aged (11-15 months). A secondary subdivision of the aged samples (11-12 months vs. 14-15 months) was executed to further characterize the timing of paternal age effects. The greatest age interval for a single male was 10 months, with the smallest age interval being 6 months (Table 4).

	Young paternal males (months)	**Same paternal males when aged (months)**	**Interval (months)**
Male1	5	15	10
Male2	4	14	10
Male3	6	14	8
Male4	4	11	7
Male5	4	11	7
Male6	6	12	6
Male7	5	11	6
Male8	5	11	6

Table 4: Paternal age at time of offspring embryonic placenta collection

Pregnancies conceived by the males when aged resulted in significantly smaller embryonic placentas (aged: 0.111g vs. young: 0.149g; $p<0.0001$), as well as significantly smaller fetuses in both weight (aged: 0.379g vs. young: 0.432g; $p<0.05$) and length (aged: 13.0mm vs. young: 13.7mm; $p<0.05$) compared to when the same males were in their youth (Table 5). The fetus:placenta weight ratio was significantly higher for offspring conceived by the males when aged (aged: 3.45 vs. young: 3.05; $p<0.05$) compared to when the same males were in their youth, indicating placental efficiency is increasingly compromised in the offspring following paternal aging. No statistical differences were observed for the three tissues upon aged subdivision of paternal males at 11-12 months

and 14-15 months. The sex of the fetuses was not examined and is a limitation to the study.

	Offspring from young paternal males (paternal age 4-6 months; n=48)	**Offspring from same males when aged (paternal age 11-15 months; n=48)**	**P-Value (4-6 vs 11-15 months)**	**Aged Subdivision (paternal age 11-12 months; n=30)**	**Aged Subdivision (paternal age 14-15 months; n=18)**	**P-Value (11-12 vs 14-15 months)**
Embryonic placental weight (g)	0.149 ± 0.04	0.111 ± 0.02	<0.0001	0.111 ± 0.02	0.111 ± 0.03	n.s.
Fetal weight (g)	0.432 ± 0.08	0.379 ± 0.11	0.0095	0.394 ± 0.11	0.355 ± 0.11	n.s.
Crown-rump length (mm)	13.7 ± 1.3	13.0 ± 1.6	0.0178	13.2 ± 1.6	12.6 ± 1.5	n.s.
Fetus:Placenta weight ratio (#)	3.05	3.45	0.0147	3.28	3.56	n.s.
Successful mating frequency (%)	54.2%	28.1%	0.0494	37.5%	18.8%	n.s.
Fetuses per paternal male (#)	14.8 ± 7.2	18.9 ± 10.3	n.s.	19.8 ± 10.2	17.0 ± 12.5	n.s.

Table 5: Average offspring development results from the same males in their youth and aged

While all eight males successfully mated in their youth, the frequency of mating activity significantly declined for the paternal males when aged (28% successful matings in months 11-15; $p<0.05$). This decline was exacerbated by increasing paternal age, with only 2/8 males resulting in a successful pregnancy at 14 months of age and only 1/8

resulting in a successful pregnancy at 15 months of age. Nevertheless, upon successful mating the litter size was unchanged between the paternal males in their youth (14.8 ± 7.2 fetuses) and when they aged (18.9 ± 10.3 fetuses; p=n.s.). Importantly, these averages include all matings from 4-6 months and all matings from 11-15 months, not just the 8 young and 8 aged matings that lead to the placentas we used for epigenetic profiling. Analysis of placental and fetal weight for litters of comparable sizes demonstrated an equivalent reduction for offspring conceived by the males when aged compared to their youth ($p<0.05$).

11.3.5.2. DNA methylation at the *Kcnq1ot1* imprinting control region

Several imprinted genes required for normal placentation are regulated by the *Kcnq1ot1* ICR and the non-coding RNA *Kcnq1ot1* specifically expressed on the paternal allele during development (Oh-McGinnis et al. 2010). Results from targeted bisulfite sequencing analyses at the *Kcnq1ot1* ICR revealed a significant DNA methylation difference in embryonic placentas based on the paternal age of individual males. A small but statistically significant increase in imprinted methylation was observed in the paternal aged group (59.3% average) compared to when the same males were in their youth (54.3% average; $p<0.05$; Figure 23A) due to paternal aging, with no statistical effect based on the individual paternal males (p=n.s.). Significance was calculated based on all young vs. all aged placenta methylation, with no separation based on male (P=0.0348, n=48 placentas). Average percent methylation increase after aging ranged from 0% to 11.5% for the 6 placentas per paternal male young vs. aged (P=0.0357, n=8 males) (Figure 23B,

Figure S1). This range correlated appropriately with age, such that the greatest methylation differences were observed in the embryonic placentas derived from the males with largest age intervals and oldest males (14-15 months). Of the twenty CpG sites analyzed within the *Kcnq1ot1* ICR, sixteen were found to be statistically significant between the two groups ($p<0.05$; Figure 23C). A reanalysis was performed based upon the methylated clones divided by total clones in each placenta, which resulted in a very similar outcome, though slightly higher methylated averages (56.2% Young vs. 61.4% Aged, $p=0.0375$). A clone was considered methylated when 50% or more of the CpGs were methylated (10 or more). The CpGs did not all change by the exact same methylation percentage. Therefore, the small but varying amounts of increased methylation argues for sporadic aberrant methylation on the paternal allele, rather than extra copies of the maternal allele which would appear as 100% methylation (all 20 CpGs would increase by the same amount).

To further characterize the timing of the methylation aberrations, the embryonic placentas from the paternal males when aged were subdivided into 11-12 months (n=5 males, 30 placentas) and 14-15 months (n=3 males, 18 placentas). Methylation at the *Kcnq1ot1* ICR was significantly increased only in the placentas derived from the 14-15 month aged males (63.9% average) compared to the 11-12 month aged males (56.6% average) and to the same males in their youth (4-6 months; 54.3% average; $p<0.05$), again with no statistical effect based on the individual paternal males (p=n.s.), demonstrating

the targeted increase in imprinted DNA methylation over time, specifically as the males aged past 12 months.

A) **Individual *Kcnq1ot1* ICR methylation for each embryonic placenta sample**

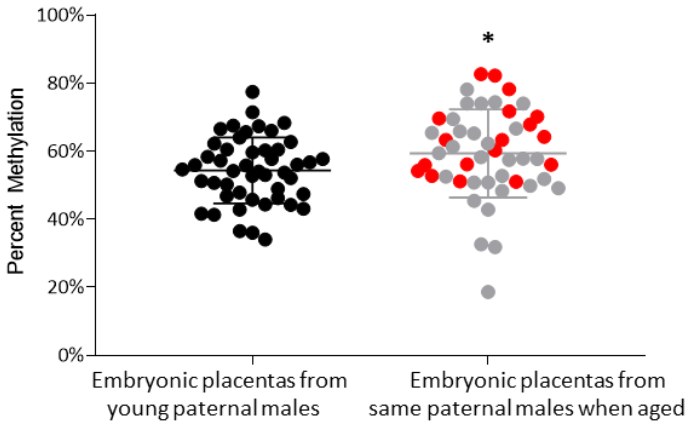

B) **Average *Kcnq1ot1* ICR methylation by paternal male**

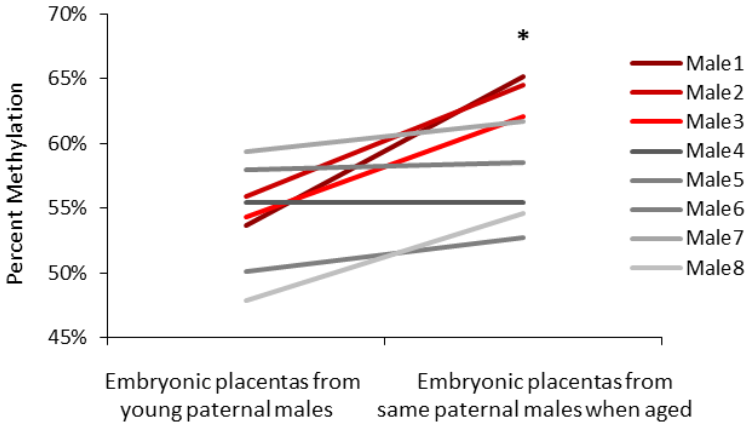

C) **Average *Kcnq1ot1* ICR methylation by CpG site**

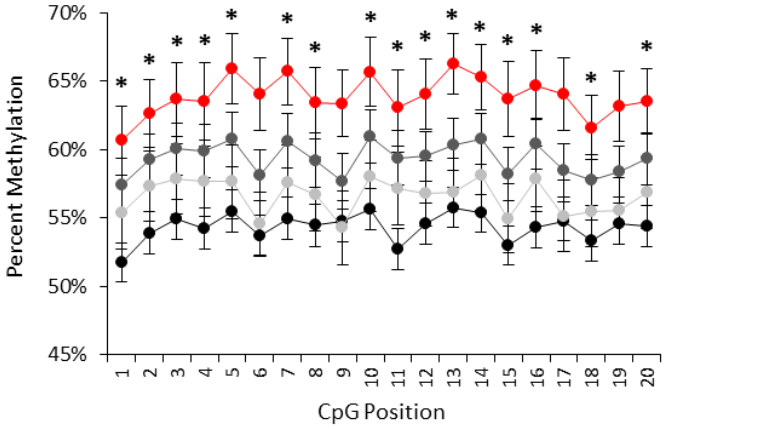

- Embryonic placentas from young paternal males (4-6 months)
- Embryonic placentas from same paternal males when aged (11-15 months)
- Paternal aged subdivision (11-12 months)
- Paternal aged subdivision (14-15 months)

Figure 23: A) Percent methylation at the *Kcnq1ot1* ICR in all individual embryonic placentas derived from all young paternal males at 4-6 months (black dots; n=48) compared to the same paternal males when aged (n=48); subdivided into 11-12 months (grey dots; n=30) and 14-15 months (red dots; n=18). Bolded middle line denotes the mean; error bars represent standard deviation. B) Average percent methylation at the *Kcnq1ot1* ICR for embryonic placentas from each of the eight young paternal males (n=6/male) and the same paternal males when aged (n=6/male), subdivided into 11-12 months (grey lines; n=5 males) and 14-15 months (red lines; n=3 males). C) Average percent methylation for all placenta samples at each of the 20 CpG sites within the amplified *Kcnq1ot1* ICR from embryonic placentas derived from young paternal males (black dots; n=48) compared to the same paternal males when aged (dark grey dots; n=48), subdivided into 11-12 months (light grey dots; n=30) and 14-15 months (red dots; n=18). Error bars represent standard error of the mean. Statistical significance of $p<0.05$ is denoted by a star.

No individual male resulted in statistical significance between young and aged placenta methylation. Importantly, taking all 8 males together, the 3 males that reach +14 months all experience a greater methylation change than the ~5% expected random variation (avg 9.3% increase, p=0.008 by 2-way ANOVA), while those at 11-12 months are all within the ~5% shift (avg 2.4% increase, p=0.609), supporting the concept that the methylation alterations occur after 12 months of aging and have biological relevance. Notably, we do not observe a decrease in average methylation for any of the 8 males after aging, an

added argument against random variation that would expect some males to show decrease.

11.3.5.3. Gene expression for the *Kcnq1ot1* imprinting cluster

Results from imprinted gene expression analyses revealed corresponding differences between embryonic placentas based on paternal age. Five genes analyzed within the maternally-methylated *Kcnq1ot1* imprinting cluster were all observed to be differentially expressed in the paternal aged group compared to when the same males were in their youth. A significant decrease in transcript abundance was observed due to paternal age for the paternally-expressed *Kcnq1ot1* non-coding RNA and a significant increase in expression for the paternally-silenced protein-coding genes *Nap1l4, Slc22a18, Cdkn1c*, and *Kcnq1* ($p<0.05$; Figure 24), with the individual paternal males resulting in a statistical effect at *Kcnq1ot1* and *Slc22a18* ($p<0.05$). Upon subdivision of the aged group, the paternally-expressed *Kcnq1ot1* non-coding RNA was found to be further significantly downregulated in the embryonic placentas derived from the paternal males when aged to 14-15 months ($p<0.05$). This pattern of expression combined with the observed hypermethylation is indicative of imprinting dysregulation restricted to the paternal allele based on paternal aging.

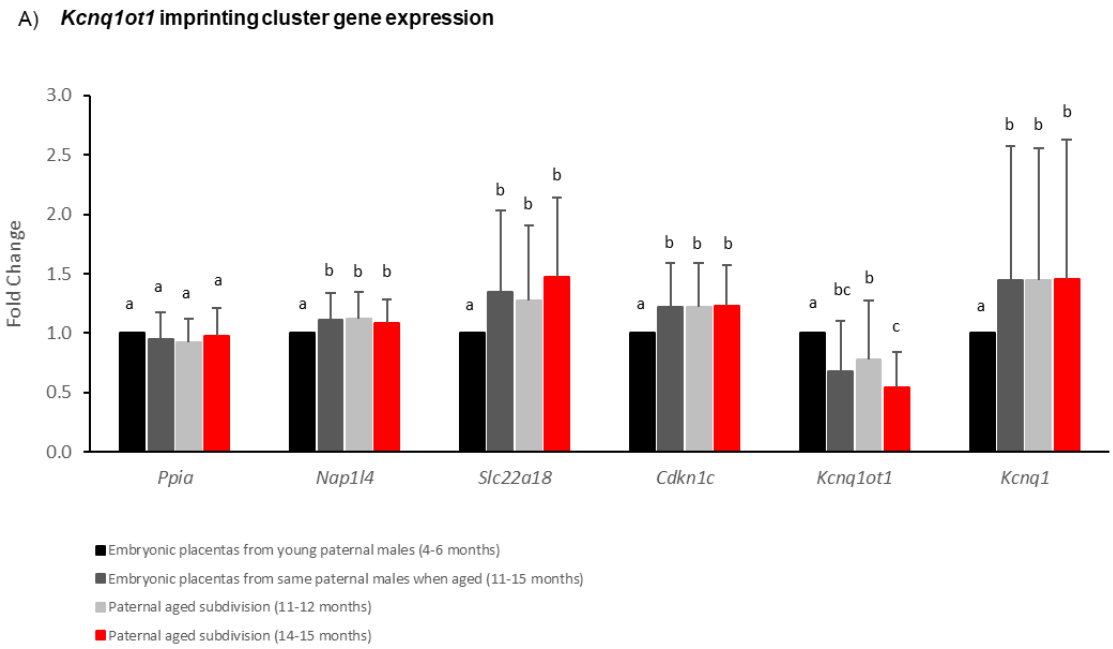

Figure 24: A) Expression results for imprinted genes within the *Kcnq1ot1* imprinting cluster for embryonic placentas derived from the same males in their youth (4-6 months, black bars; n=48) and aged (11-15 months, dark grey bars; n=48), subdivided into 11-12 months (light grey bars; n=30) and 14-15 months (red bars; n=18). Alphabetic letters indicate statistical significance of $p<0.05$ between groups.

11.3.5.4. Gene expression for additional imprinting clusters

Four additional imprinting clusters were analyzed for gene expression alterations in the same embryonic placentas. For the maternally-methylated *Mest* imprinted domain, *Mest* transcript abundance was significantly decreased, while *Copg2* and *Klf14* were significantly increased with paternal age ($p<0.05$; Figure 25A). Similarly, in the maternally-methylated *Airn/Igf2r* imprinted domain, the non-coding RNA *Airn* was significantly decreased, with significantly increased expression of *Igf2r* and *Slc22a3* ($p<0.05$; Figure

25B). In the paternally-methylated *H19* imprinted domain, the non-coding RNA *H19* transcript abundance was significantly increased, and *Ins2* was significantly decreased with paternal aging ($p<0.05$; Figure 25C). Finally, in the paternally-methylated *Dlk1/Dio3* imprinted domain, *Dlk1* expression was significantly decreased ($p<0.05$; Figure 25D). A statistical effect was also observed based on the individual paternal males at *Mest, Copg2* and *Slc22a3* ($p<0.05$). Upon subdivision of the aged group, *Mest, Klf14* and *Dio3* were significantly dysregulated in the embryonic placentas derived from the paternal males when aged to 14-15 months compared to those aged 11-12 months. *Airn, Ins2* and *Dlk1* reached statistical significance only in those aged 11-12 months, while *Meg3* was found to be significantly increased only in those aged 14-15 months; which did not reach significance when combined with the 11-12 months cohort. The subtle and varying effect of APA, combined with the reduced sample sizes when subdivided, may contribute to the variable statistical differences observed at certain imprinted genes. Significant decreases in gene expression for paternally-expressed imprinted genes, and corresponding significant increases in gene expression for paternally-silenced imprinted genes are indicative of imprinting dysregulation restricted to the paternal allele due to paternal aging.

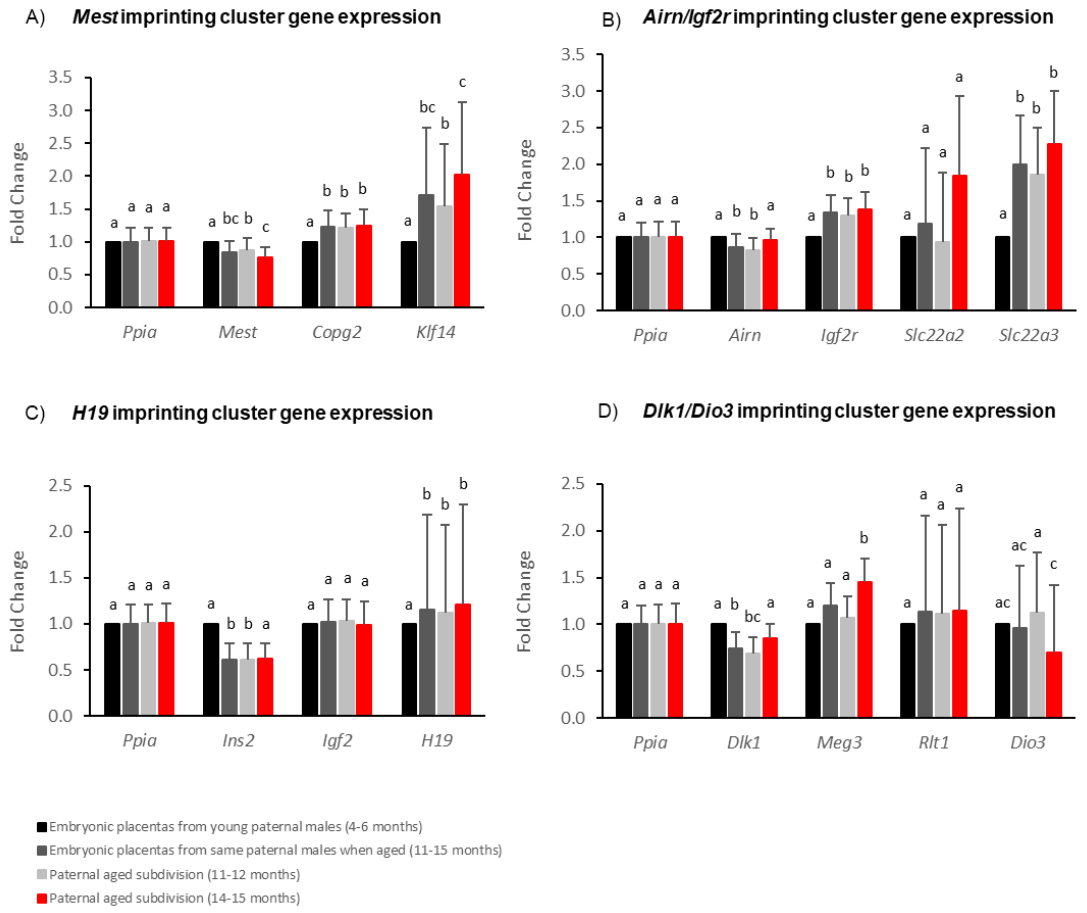

Figure 25: Expression results for imprinted genes within the A) *Mest* B) *Airn/Igf2r* C) *H19* D) *Dlk1/Dio3* imprinting clusters for embryonic placentas derived from the same males in their youth (4-6 months, black bars; n=48) and aged (11-15 months, dark grey bars; n=48), subdivided into 11-12 months (light grey bars; n=30) and 14-15 months (red bars; n=18). Alphabetic letters indicate statistical significance of $p<0.05$ between groups.

11.3.6. Discussion

While the genome is largely reprogrammed during gametogenesis and early embryogenesis, the epigenetic status at imprinted domains must be actively maintained,

and thus are highly susceptible to epigenetic perturbations. In our longitudinal research study, paternal aging during the natural lifetime of male mice was associated with significant dysregulation to both ICR DNA methylation and imprinted gene expression in embryonic placentas of their offspring, offering non-invasive insight into the health of the associated fetus.

The *Kcnq1ot1* ICR and the paternally-expressed non-coding RNA *Kcnq1ot1* regulate several imprinted genes required for normal placentation during development (Oh-McGinnis et al. 2010). *Kcnq1ot1* ICR methylation in eight sets of paired embryonic placenta samples showed overall hypermethylation upon advanced paternal age (APA) compared to when the same males were in their youth. While the average methylation was situated near expected for imprinting loci, the range of methylation between placenta samples was considerable even when the sperm contribution was from the males in their youth, highlighting variability between individuals (both F0 and F1). A larger placental methylation range was, nevertheless, observed when the same males aged during their natural lifetimes. Most embryonic placentas had increased methylation, but markedly decreased methylation was also observed in a few select samples, indicative of overall epigenetic perturbations in either direction by advanced paternal age. Hypermethylation of the *Kcnq1ot1* ICR was exacerbated in the embryonic placentas derived from the paternal males when they reached 14-15 months of age, demonstrating the targeted increase in imprinted DNA methylation over time, specifically as the males aged past 12 months. The gain of methylation in the majority of samples is presumed to

come from the unmethylated paternal allele, as the maternal allele is hypermethylated. This aberrant gain of methylation at a gametic imprinting control region may have originated in the APA sperm and been directly inherited by the offspring, or it may be attributable to a paternal factor(s) compromised in the aging sperm environment leading to inappropriate imprinting methylation maintenance in the trophectoderm of the embryo. The biological significance of the small methylation shift is unknown, though subtle epigenetic changes have been associated with complex disease phenotypes (Leenen, Muller, and Turner 2016), and may result in a cumulative effect on placentation and embryonic developmental capacity. As paternal aging is a subtle and varying effect, not every pregnancy from an APA father will be impacted. Indeed, a threshold of methylation alterations may be required to predispose placental dysfunction. As allelic identity was not feasible, overrepresentation of the maternal allele is also a possibility; a substantial number of samples were analyzed for both young and aged groups in order to overcome this technical limitation.

The subtle, yet statistically significant shift in DNA methylation at the *Kcnq1ot1* ICR based on advanced paternal age lead to subsequent transcription changes for five imprinted genes within the cluster, observed in both subdivisions of the paternally aged group. In particular, the embryonic placentas derived from males that aged to 14-15 months had the largest methylation increase, and this correlated with the largest *Kcnq1ot1* expression decrease, statistically. These alterations may be due to disrupted transcription factor binding. Within the amplified *Kcnq1ot1* ICR region, various binding sites exist

(MatInspector by Genomatix), many with direct binding motifs overlapping at least one CpG site. These transcription factors have potential to be impacted by compacted chromatin from increased methylation, including those that have been shown to be critical in genomic imprinting regulation. For example, the Kruppel-like zinc finger protein ZFP57 binds methylated DNA and is necessary for maintaining the methylation memory at imprinting control regions during replication in early mouse embryos (Quenneville et al. 2011). Binding of ZFP57 to the aberrantly methylated *Kcnq1ot1* ICR paternal allele would result in a more maternal-like phenotype by means of recruiting additional repressive factors. Evidence of this is the aberrant decrease in *Kcnq1ot1* gene expression, and the resulting aberrant increase in the surrounding imprinted genes, analogous to what is observed on the maternal allele. The loss of *Kcnq1ot1* transcript expression is presumed to occur on the paternal allele, as the maternal allele is innately silenced, supporting a paternally-inherited effect at the *Kcnq1ot1* imprinted domain from advanced paternal age.

A large proportion of imprinted genes are involved in growth, development and metabolism, and play important roles in both the placenta and the brain. Paternally-expressed genes often promote growth enhancement while maternally-expressed genes are involved in growth suppression. Loss of mouse paternally-expressed *Mest* causes placental growth restriction, while loss of maternally-expressed *Igf2r* or *Cdkn1c* results in placental enlargement (Coan, Burton, and Ferguson-Smith 2005). In the embryonic placentas derived from males in their old age, significantly decreased expression was

observed in paternally-expressed genes (*Kcnq1ot1, Mest, Airn, Ins2, Dlk1*) and aberrant expression in paternally-silenced genes (*Kcnq1, Cdkn1c, Slc22a18, Nap1l4, Copg2, Klf14, Igf2r, Slc22a3, H19*) compared to when the same males were in their youth. These results in combination with significantly reduced embryonic placental weight is indication of imprinting dysregulation restricted to the paternally-inherited allele due to paternal aging, despite the origin (sperm or oocyte) of methylation for the gametic imprinting control region. The main role of the placenta is the nutrition of the fetus, thus influencing the significant reduction in fetal weight and crown-rump length also observed in the offspring derived from the paternal males when they aged.

The majority of imprinted genes have been described as belonging to imprinted gene networks (IGN) involved in the control of embryonic growth, that are co-regulated during development (Al Adhami et al. 2015; Varrault et al. 2006). For example, *H19*, with dysregulated gene expression in our study, is a master regulator of an IGN impacting expression of other imprinted genes including several that were also dysregulated in our study (*Cdkn1c, Dlk1, Igf2r* (Gabory et al. 2009; Monnier et al. 2013), and *Mest, Meg3* (Monnier et al. 2013)). Interestingly, various reports of multi-locus imprinting disturbances (MLID) exist in individuals with human imprinting disorders, having epigenetic errors in auxiliary imprinted regions in addition to the disease-associated locus (Azzi et al. 2014; Mackay et al. 2015; Sanchez-Delgado et al. 2016). The statistically significant alterations to fourteen imprinted gene transcripts at five imprinting clusters in

our study support both IGN and MLID models and provide a translational consequence to the subtle epigenetic dysregulation observed.

It is hypothesized that epimutations in the male gamete may subsequently be generationally transmitted. Age-related imprinting errors have been identified in mouse spermatozoa (Kobayashi et al. 2016), as well as genome-wide sperm methylation alterations, transferring some methylation abnormalities to offspring and impacting offspring behavior (Milekic et al. 2015). Furthermore, placental imprinting perturbations have been shown to arise from other external insults to the paternal germline, including paternal folic acid exposure (Ly et al. 2017) and paternal obesity (Mitchell et al. 2017), presumably impacting imprinting on the paternal allele. In terms of aging, DNA methylation alterations were also observed at the *Kcnq1ot1* promoter in the brain of offspring of older fathers compared with the offspring of younger fathers (Smith et al. 2013). Our study further argues this generational epigenetic consequence to paternal aging.

There are several critical limitations to this study, and it is important to note that the researchers used superovulated female mice in the study which may have affected the results of the study. Specifically, the number of embryos that were generated and implanted per female, and how a higher number of implantations would affect the health of the placenta or fetal growth. The females were superovulated in both young and aged groups to ensure that the authors were able to collect an appropriate number of

pregnancies. This is common practice for many murine studies. As all females were superovulated, it is unlikely that superovulation contributed to the effects on placenta or fetal growth observed between young and aged paternal male groups. The current study performed in vivo matings and development only, thus we did not compute number of embryos generated. However, our previously published work that was the basis of this study (Katz-Jaffe et al. 2013) showed a significant decline in in vitro blastocyst development at +12 months of paternal age. Our earlier publication also noted that pregnancies from natural conceptions with paternal age >12 months resulted in significantly smaller fetuses in length and weight. In addition, placental weight was observed to be significantly smaller with paternal age >12 months, similar to this studies results. Another limitation of the study is the use of clone and sequence technology, rather than next-gen amplicon sequencing which would be more precise. The authors used clone and sequence as it is a traditional low-cost targeted bisulfite sequencing approach for imprinted methylation analysis, and has be published recently in other peer-reviewed articles using placenta samples (Vasconcelos et al. 2019; Monteagudo-Sánchez et al. 2019; Yamaguchi et al. 2019; Huo et al. 2020). The initial analysis of this study calculated the total DNA methylation as a percentage of the total number of methylated CpGs divided by the total number of CpG dinucleotides which we then reanalysed as methylated clones divided by total clones in each placenta which, resulted in a very similar outcome and importantly, still statistically significant. The researchers note that the statistical significance occurs only in the 14-15 month males, and did not see a decrease in average methylation for any of the 8 males after aging, which the authors believe is an

added argument against random chance of getting more or less maternal alleles in the aged samples. Finally, the use of outbred females in this study is also a very significant limitation, and makes it exceedingly difficult to assess the number of maternal vs paternal alleles cloned in this study, as the authors are unable to utilize SNPs to help determine parental origin, as the samples used in this study are no longer accessible. Future directions for this study include the introduction of a separate, inbred strain of female mice to strengthen this research, and eliminate this confounding variable.

In conclusion, the present study examined the contribution of male aging throughout their natural lifetime to genomic imprinting regulation in offspring embryonic placentas, with results demonstrating ICR epigenetic dysregulation, a widespread effect on imprinted expression, and a combined reduction in placental weight, fetal weight, crown-rump length and successful mating frequency. A key strength to the study is the longitudinal feature, enabling age comparisons during the natural lifetime of the same males without confounding factors including female aging or infertility. Imprinted genes play critical roles in growth, development and metabolism, and are highly essential to placental function. Understanding the causal relationship between sperm aging and placental genomic imprinting regulation is critical as developed countries continue to delay childbearing. If these epigenetic changes related to paternal aging are translational, they could be responsible for placental dysfunction as well as adverse pregnancy outcomes and childhood health conditions observed in the human population.

Supporting Material

SUPPLEMENTARY S1a TABLE: Primer and PCR parameters for targeted bisulfite sequencing						
GENE	**CHROMOSOME**	**FORWARD PRIMER**	**REVERSE PRIMER**	**LENGTH (BP)**	**# of CpGs**	
Kcnq1or1	Chr7	GGTTAGAAGTAGAGGTGATT	CAAAACCACCCCTACTTCTAT	206	20	
PCR Parameters:						
94°C for 10 min, 55 cycles of (94°C for 15 sec, 56°C for 20 sec, 72°C for 20 sec), 72°C for 10 min.						
SUPPLEMENTARY S1b TABLE: Primer and PCR parameters for targeted qRT-PCR						
GENE	**CHROMOSOME**	**FORWARD PRIMER**	**REVERSE PRIMER**	**LENGTH (BP)**		
Kcnq1ot1	Chr7	CACCCCAACCTGCTATTGCTA	CTGGGGAGAATGTACCAGCC	239		
Kcnq1	Chr7	GCTGAGAAAGATGCGGTGAAC	CATCTGCGTAGCTGCCAAAC	58		
Cdkn1c	Chr7	CCACGGTTTTGTGGAAATCTG	CGTACTCCTTGCACATGGTACAG	71		
Slc22a18	Chr7	CCTCTGCTTTGGCATTGGAA	ATCCCGTATGCGGTGTTAAGG	69		
Nap1l4	Chr7	TTCACTGTCCTCCCACTTACGA	CTCCCTCCACTTGGTGTCACA	71		
Mest	Chr6	CGGAAGCCCTGAGATAGTTGTG	CCTAAGAAATCAAGGGCGATCAC	120		
Copg2	Chr6	AAGAGGTGGGAGATGCCTTTG	ACCTCTCACATGGCTGCATACC	117		
Klf14	Chr6	ACCGAAGGAGGCAGATTACG	ACGACTTGTAGTAGGCCTTGTTG	81		
Airn	Chr17	GGGAAGTGGACCTGTTTAGAAG	CTGCCGATTTCCTGATAACAC	68		
Igf2r	Chr17	GGCACCACTCCTTCATGATC	TTGGCCGATTCAAGCAA	61		
Slc22a2	Chr17	CACACAACCCAACCTCACTTACC	TGGACACATCAGTGCAACAAAC	89		
Slc22a3	Chr17	AACTGCCTCTGATCATCTTTGG	CGTTTCAGGCAAAAGCATCAC	71		
H19	Chr7	ATGGTGCTACCCAGCTCATGTC	GTGGTTCTGATTGCAGCATCTTC	95		
Igf2	Chr7	CCTACATAACGGGAGCAGTGATC	CATTGTGGTAGCCGGTGTTG	85		
Ins2	Chr7	AGAAGCGTGGCATTGTAGATCAG	TGGTGGGTCTAGTTGCAGTAGTTC	82		
Dlk1	Chr12	CTAACCCATGCGAGAACGA	AGCGGCAACGGAAGTCA	60		
Meg3	Chr12	GAGTGGACTAAGCACGAAGCA	CACTTGTACGAGCATCCATCTC	173		
Rtl1	Chr12	GCAAGTCGCCCGTTCTCTA	TGACCCAGTGATGTCTGTTTCC	71		
Dio3	Chr12	ATCCAGAGTGGCACCATCATG	CGCAACTCAGACACCTGGTAAC	68		
PCR Parameters:						
95°c for 10 min, 40 cycles of (95°C for 15 sec, 60°C for 1 min),						
followed by 95°C for 15 sec, 60°C for 1 min, 95°C for 15 sec, 60°C for 15 sec						

Table S4: A) Primer and PCR parameters for targeted bisulfite sequencing. B) Primer and PCR parameters for targeted qRT-PCR.

Supplementary Figure S1

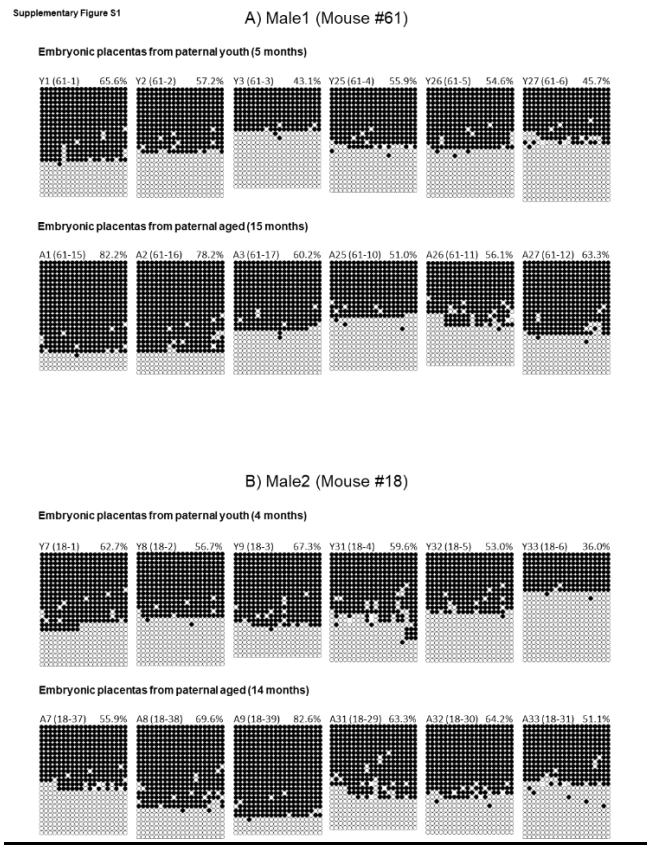

Supplementary Figure S1

C) Male3 (Mouse #116)

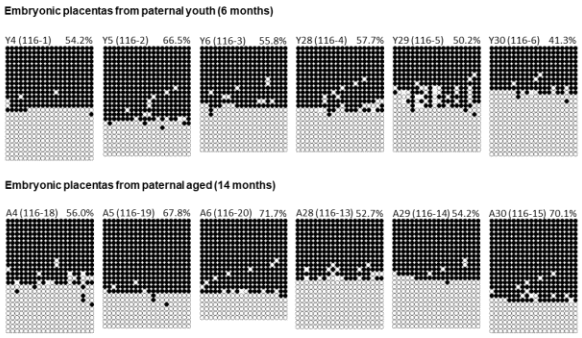

D) Male4 (Mouse #83)

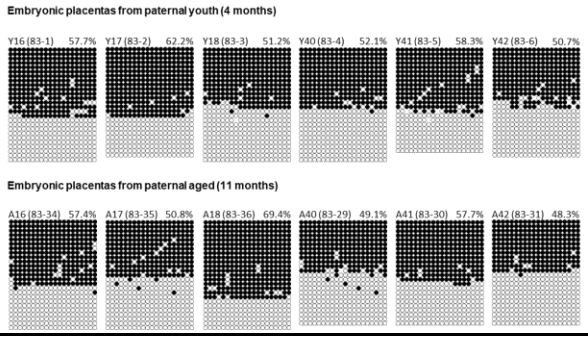

Supplementary Figure S1

E) Male5 (Mouse #90)

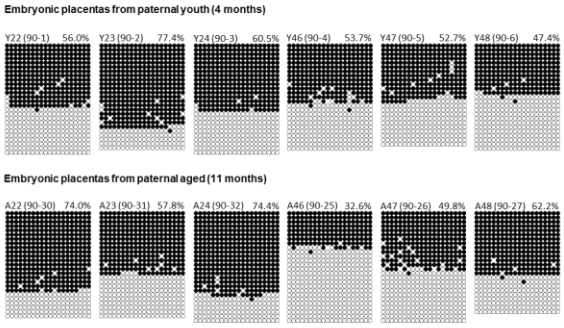

F) Male6 (Mouse #112)

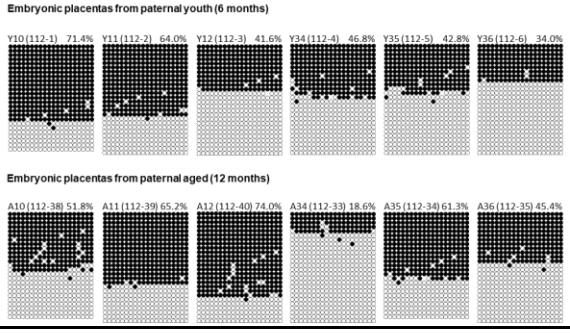

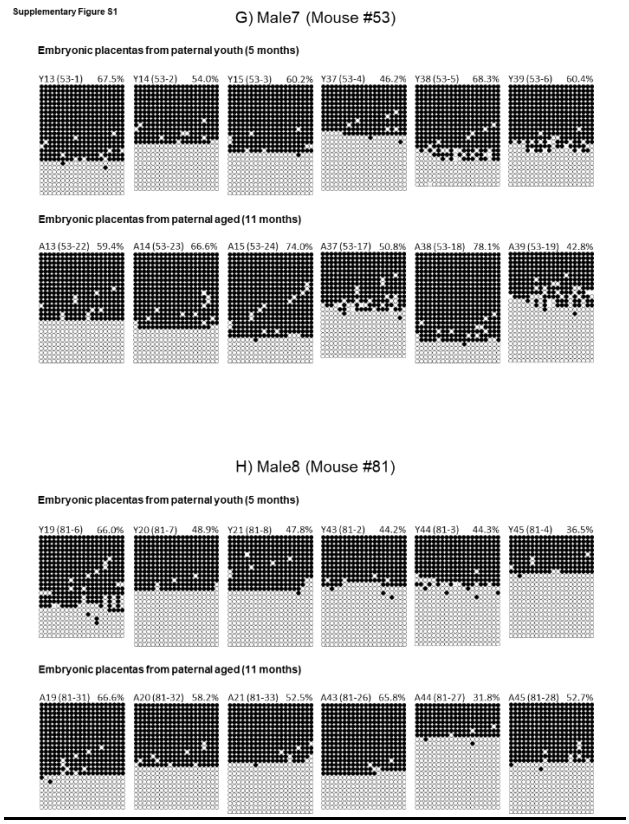

Figure S1: DNA methylation results for each embryonic placenta for the eight paternal males when young (n=6/male) and aged (n=6/male). A) Male1 (ID 61), B) Male2 (ID 18), C) Male3 (ID 116), D) Male4 (ID 83), E) Male5 (ID 90), F) Male6 (ID 112), G) Male7 (ID 53), H) Male8 (ID 81). Each group of circles represents one embryonic placenta sample, with the sample name indicated in the top left (Y=young, A=aged), and percent methylation indicated in the top right. Each row represents one DNA strand. Filled circles represent methylated CpG dinucleotides and unfilled circles represent unmethylated CpGs.

12.0 General Discussion

This thesis was largely successful in the fulfilment of its specific aims, first it investigated the individual CC transcriptome of chromosomally normal (euploid) embryos, and by utilizing RNA sequencing, was able to identify novel biological pathways associated which were associated with implantation outcome. The results of the corona cell transcriptome study demonstrated that the WNT-Canonical pathway and AXIN transcription are strong indicators of oocyte developmental competence and viability when correlated with a subsequent chromosomally normal live birth.

Next, this thesis utilized a comprehensive endometrial co-culture study to investigate the window of implantation in women presenting with advanced maternal age, and endometriosis. This second study displayed a theme of compromised cellular communication between blastocysts and endometrium derived from patients with compromised fertility. These variations may account for the lower implantation potential and clinical outcomes observed for these infertile patient populations. There must be a balance in the delicate embryo-endometrial molecular dialogue, and any alterations, either autocrine or paracrine, may affect transcription levels of key miRNAs and their target signalling molecules. This may then result in significantly lowered implantation potential and fertility.

Finally, the third study included in this thesis investigated the contribution of male aging throughout their natural lifetime to genomic imprinting regulation in their subsequent offspring's embryonic placentas. The results demonstrated ICR epigenetic dysregulation, as well as a widespread effect on placental imprinted expression, and a combined reduction in successful mating frequency, and fetal offspring parameters including placental weight, fetal weight and crown-rump length. A key strength to the study was its longitudinal nature, which allowed for age comparisons during the same subjects natural lifetime sans external confounding variables including female aging or infertility. The study concluded that imprinted genes play critical roles in growth, development and metabolism, and are highly essential to placental function. The investigation broadened our understanding the causal relationship between sperm aging and placental genomic imprinting regulation, which is critical, as developed countries continue to delay parenthood.

12.1. Common themes and insights

This thesis sought to utilize commonly discarded materials and incorporate them into non-invasive assays to monitor the health and development of a developing life through multiple stages of its development. As an oocyte, excess cumulus and corona cells that are commonly disregarded were collected and their molecular profile was examined in conjunction with their developmental potential.

Next, this thesis examined the maternal microenvironment a resulting developmentally competent embryo was likely to encounter after it was transferred to the luminal epithelial tissues of the endometrium within the uterine cavity. This investigation utilized a minimally invasive endometrial biopsy, which was performed at a time when it would not affect the health of the mother or the embryo. However, this provided us a window into this critical juncture, and the role of microvesicles were investigated in correlation to specific infertility diagnoses. Notably, aberrant expression was examined in relation to both the advanced maternal age and endometriosis phenotypes, which may lead to compromised implantation potential.

Finally, the health of the subsequent pregnancy was observed by studying the epigenetics and genomic imprinting of placenta tissue, a tissue that is intimately connected to both the mother and child and due to the bi-allelic nature of its imprinted status the father as well. Here it was discovered that over the natural lifetime of an aging male subject, their contribution to genomic imprinting regulation in the subsequent offspring's' embryonic placentas, demonstrated epigenetic dysregulation, which may have significant long term consequences on over the course of the progeny's life, and are potentially passed on to future generations.

When taken together, these studies provide a blueprint for a model underutilized in current ART practices, using specific discarded materials to assess the new life's vitality and viability throughout multiple stages of development. If this model is expanded upon,

and these practices and collected materials are used serially in conjunction with a single couple's infertility journey, it is this researchers belief we will see improvements in clinical ART success rates and enhanced patient counselling.

12.2. Future Work

Ongoing research to illuminate the biological and signalling pathways of corona cells associated with oocyte viability continues to be an appealing target for researchers as well as clinicians. Corona cells are intimately linked with their associated oocyte throughout development, and provide one of the earliest windows into the health and competence of a mature oocyte. However, the true value of these discovered molecular biomarkers will be realized when they are used in conjunction with conventional means of embryo selection in a prospective, randomized control trial. This will be the best way to assess the usefulness of a corona cell biomarker assay, combined with the routine use of single embryo transfers, which may lead to overall improved IVF outcomes. There are multiple ways of measuring molecular biomarkers of the maternal microenvironment secretome during the window if implantation including endometrial biopsy and uterine aspiration. When used together in a prospective trial, these studies will provide researchers further insight into the bi-directional molecular dialogue during this critical time point. Finally, a deeper understanding of the paternal contribution to the health and development of a viable pregnancy by examining the imprinting profile of the placenta will provide an early insight into the developmental future of the child, and may assist

parents by detecting risk factors, and preparing for any discovered health challenges. To expand our current understanding, investigations into the placenta profile of other paternal risk factors should be studied, including harmful environmental exposure as well as any familial history of disease.

12.3. Personal Perspectives and Final Conclusions

As of the writing of this thesis, despite a plethora of ongoing efforts to discover molecular biomarkers from non-invasive assays and incorporate them into a clinical IVF lab setting, relatively few have found any commercial success outside of those highlighted in the introduction. This may be due to multiple factors including the additional time associated with collecting and assessing biological materials, the necessity of culturing the embryos as singletons despite their survival being higher when cultured in a group setting, the technical expertise that such methods require and the high costs associated with the purchasing required equipment. Nonetheless, these efforts must continue if we are to achieve our collective goal within the field of ART for every infertile couple seeking treatment to attain successful conception.

13.0 References

Abal, M., J. Planaguma, A. Gil-Moreno, M. Monge, M. Gonzalez, T. Baro, A. Garcia, J. Castellvi, Y. Cajal S. Ramon, J. Xercavins, F. Alameda, and J. Reventos. 2006. 'Molecular pathology of endometrial carcinoma: transcriptional signature in endometrioid tumors', *Histol Histopathol*, 21: 197-204.

Abe, T., A. Yabuuchi, K. Ezoe, H. Skaletsky, J. Fukuda, S. Ueno, Y. Fan, S. Goldsmith, T. Kobayashi, S. Silber, and K. Kato. 2020. 'Success rates in minimal stimulation cycle IVF with clomiphene citrate only', *J Assist Reprod Genet*, 37: 297-304.

Ackerman, S. B., G. L. Stokes, R. J. Swanson, S. P. Taylor, and L. Fenwick. 1985. 'Toxicity testing for human in vitro fertilization programs', *J In Vitro Fert Embryo Transf*, 2: 132-7.

Ackerman, S. B., S. P. Taylor, R. J. Swanson, and L. H. Laurell. 1984. 'Mouse embryo culture for screening in human IVF', *Arch Androl*, 12 Suppl: 129-36.

Acuna-Hidalgo, R., J. A. Veltman, and A. Hoischen. 2016. 'New insights into the generation and role of de novo mutations in health and disease', *Genome Biol*, 17: 241.

Adashi, Eli Y, Marilyn F Vine, Barry H Margolin, Howard I Morrison, and Barbara S Hulka. 1994. 'Cigarette smoking and sperm density: a meta-analysis', *Fertility and sterility*, 61: 35-43.

Agarwal, Ashok, Aditi Mulgund, Alaa Hamada, and Michelle Renee Chyatte. 2015. 'A unique view on male infertility around the globe', *Reproductive Biology and Endocrinology*, 13: 37.

Al-Edani, T., S. Assou, A. Ferrieres, S. Bringer Deutsch, A. Gala, C. H. Lecellier, O. Ait-Ahmed, and S. Hamamah. 2014. 'Female aging alters expression of human cumulus cells genes that are essential for oocyte quality', *Biomed Res Int*, 2014: 964614.

Al Adhami, H., B. Evano, A. Le Digarcher, C. Gueydan, E. Dubois, H. Parrinello, C. Dantec, T. Bouschet, A. Varrault, and L. Journot. 2015. 'A systems-level approach to parental genomic imprinting: the imprinted gene network includes extracellular matrix genes and regulates cell cycle exit and differentiation', *Genome Res*, 25: 353-67.

Alio, A. P., H. M. Salihu, C. McIntosh, E. M. August, H. Weldeselasse, E. Sanchez, and A. K. Mbah. 2012. 'The effect of paternal age on fetal birth outcomes', *Am J Mens Health*, 6: 427-35.

Almquist, L. D., C. E. Likes, B. Stone, K. R. Brown, R. Savaris, D. A. Forstein, P. B. Miller, and B. A. Lessey. 2017. 'Endometrial BCL6 testing for the prediction of in vitro fertilization outcomes: a cohort study', *Fertil Steril*, 108: 1063-69.

Altmae, S., J. A. Martinez-Conejero, F. J. Esteban, M. Ruiz-Alonso, A. Stavreus-Evers, J. A. Horcajadas, and A. Salumets. 2013. 'MicroRNAs miR-30b, miR-30d, and miR-494 regulate human endometrial receptivity', *Reprod Sci*, 20: 308-17.

Amaral, L. M., M. W. Cunningham, Jr., D. C. Cornelius, and B. LaMarca. 2015. 'Preeclampsia: long-term consequences for vascular health', *Vasc Health Risk Manag*, 11: 403-15.

Anderson, E., and D. F. Albertini. 1976. 'Gap junctions between the oocyte and companion follicle cells in the mammalian ovary', *J Cell Biol*, 71: 680-6.

Anderson, R. A., R. Sciorio, H. Kinnell, R. A. Bayne, K. J. Thong, P. A. de Sousa, and S. Pickering. 2009. 'Cumulus gene expression as a predictor of human oocyte fertilisation, embryo development and competence to establish a pregnancy', *Reproduction*, 138: 629-37.

Armstrong, S., A. Vail, S. Mastenbroek, V. Jordan, and C. Farquhar. 2015. 'Time-lapse in the IVF-lab: how should we assess potential benefit?', *Hum Reprod*, 30: 3-8.

Assidi, M., M. Montag, K. Van der Ven, and M. A. Sirard. 2011. 'Biomarkers of human oocyte developmental competence expressed in cumulus cells before ICSI: a preliminary study', *J Assist Reprod Genet*, 28: 173-88.

Assou, S., T. Al-edani, D. Haouzi, N. Philippe, C. H. Lecellier, D. Piquemal, T. Commes, O. Ait-Ahmed, H. Dechaud, and S. Hamamah. 2013. 'MicroRNAs: new candidates for the regulation of the human cumulus-oocyte complex', *Hum Reprod*, 28: 3038-49.

Assou, S., T. Anahory, V. Pantesco, T. Le Carrour, F. Pellestor, B. Klein, L. Reyftmann, H. Dechaud, J. De Vos, and S. Hamamah. 2006. 'The human cumulus--oocyte complex gene-expression profile', *Hum Reprod*, 21: 1705-19.

Assou, S., D. Haouzi, J. De Vos, and S. Hamamah. 2010. 'Human cumulus cells as biomarkers for embryo and pregnancy outcomes', *Mol Hum Reprod*, 16: 531-8.

Assou, S., D. Haouzi, H. Dechaud, A. Gala, A. Ferrieres, and S. Hamamah. 2013. 'Comparative gene expression profiling in human cumulus cells according to ovarian gonadotropin treatments', *Biomed Res Int*, 2013: 354582.

Assou, S., D. Haouzi, K. Mahmoud, A. Aouacheria, Y. Guillemin, V. Pantesco, T. Reme, H. Dechaud, J. De Vos, and S. Hamamah. 2008. 'A non-invasive test for assessing embryo potential by gene expression profiles of human cumulus cells: a proof of concept study', *Mol Hum Reprod*, 14: 711-9.

Atsem, S., J. Reichenbach, R. Potabattula, M. Dittrich, C. Nava, C. Depienne, L. Bohm, S. Rost, T. Hahn, M. Schorsch, T. Haaf, and N. El Hajj. 2016. 'Paternal age effects on sperm FOXK1 and KCNA7 methylation and transmission into the next generation', *Hum Mol Genet*, 25: 4996-5005.

Azzi, S., A. Blaise, V. Steunou, M. D. Harbison, J. Salem, F. Brioude, S. Rossignol, W. A. Habib, N. Thibaud, C. D. Neves, M. L. Jule, C. Brachet, C. Heinrichs, Y. L. Bouc, and I. Netchine. 2014. 'Complex tissue-specific epigenotypes in Russell-Silver Syndrome associated with 11p15 ICR1 hypomethylation', *Hum Mutat*, 35: 1211-20.

Baccarelli, A., and V. Bollati. 2009. 'Epigenetics and environmental chemicals', *Curr Opin Pediatr*, 21: 243-51.

Barmat, L. I., H. C. Liu, S. D. Spandorfer, A. Kowalik, C. Mele, K. Xu, L. Veeck, M. Damario, and Z. Rosenwaks. 1999. 'Autologous endometrial co-culture in patients with repeated failures of implantation after in vitro fertilization-embryo transfer', *J Assist Reprod Genet*, 16: 121-7.

Bartolomei, M. S., and A. C. Ferguson-Smith. 2011. 'Mammalian genomic imprinting', *Cold Spring Harb Perspect Biol*, 3.

Baumgarten, Sarah C., and Carlos Stocco. 2018. 'Granulosa Cells.' in Michael K. Skinner (ed.), *Encyclopedia of Reproduction (Second Edition)* (Academic Press: Oxford).

Beal, Marc A, Carole L Yauk, and Francesco Marchetti. 2017. 'From sperm to offspring: Assessing the heritable genetic consequences of paternal smoking and potential public health impacts', *Mutation research/Reviews in mutation research*, 773: 26-50.

Bedaiwy, M., A. Y. Shahin, A. M. AbulHassan, J. M. Goldberg, R. K. Sharma, A. Agarwal, and T. Falcone. 2007. 'Differential expression of follicular fluid cytokines: relationship to subsequent pregnancy in IVF cycles', *Reprod Biomed Online*, 15: 321-5.

Beier, H. M., and K. Beier-Hellwig. 1998. 'Molecular and cellular aspects of endometrial receptivity', *Hum Reprod Update*, 4: 448-58.

Bellver, J., M. J. De Los Santos, P. Alama, D. Castello, L. Privitera, D. Galliano, E. Labarta, C. Vidal, A. Pellicer, and F. Dominguez. 2015. 'Day-3 embryo metabolomics in the spent culture media is altered in obese women undergoing in vitro fertilization', *Fertil Steril*, 103: 1407-15 e1.

Bentin-Ley, U., A. Lindhard, V. Ravn, H. Islin, and S. Sorensen. 2011. 'Glycodelin in endometrial flushing fluid and endometrial biopsies from infertile and fertile women', *Eur J Obstet Gynecol Reprod Biol*, 156: 60-6.

Berthaut, I., D. Montjean, L. Dessolle, K. Morcel, F. Deluen, C. Poirot, A. Bashamboo, K. McElreavey, and C. Ravel. 2013. 'Effect of temozolomide on male gametes: an epigenetic risk to the offspring?', *J Assist Reprod Genet*, 30: 827-33.

Bessa, I. R., R. C. Nishimura, M. M. Franco, and M. A. Dode. 2013. 'Transcription profile of candidate genes for the acquisition of competence during oocyte growth in cattle', *Reprod Domest Anim*, 48: 781-9.

Bianco-Miotto, T., B. T. Mayne, S. Buckberry, J. Breen, C. M. Rodriguez Lopez, and C. T. Roberts. 2016. 'Recent progress towards understanding the role of DNA methylation in human placental development', *Reproduction*, 152: R23-30.

Binder, N. K., J. Evans, D. K. Gardner, L. A. Salamonsen, and N. J. Hannan. 2014. 'Endometrial signals improve embryo outcome: functional role of vascular endothelial growth factor isoforms on embryo development and implantation in mice', *Hum Reprod*, 29: 2278-86.

Binder, N. K., J. Evans, L. A. Salamonsen, D. K. Gardner, T. J. Kaitu'u-Lino, and N. J. Hannan. 2016. 'Placental Growth Factor Is Secreted by the Human Endometrium and Has Potential Important Functions during Embryo Development and Implantation', *PLoS One*, 11: e0163096.

Blakaj, A., and H. Lin. 2008. 'Piecing together the mosaic of early mammalian development through microRNAs', *J Biol Chem*, 283: 9505-8.

Boissonneault, G. 2002. 'Chromatin remodeling during spermiogenesis: a possible role for the transition proteins in DNA strand break repair', *FEBS Lett*, 514: 111-4.

Boomsma, C. M., A. Kavelaars, M. J. Eijkemans, K. Amarouchi, G. Teklenburg, D. Gutknecht, B. J. Fauser, C. J. Heijnen, and N. S. Macklon. 2009. 'Cytokine profiling in endometrial secretions: a non-invasive window on endometrial receptivity', *Reprod Biomed Online*, 18: 85-94.

Boomsma, C. M., A. Kavelaars, M. J. Eijkemans, E. G. Lentjes, B. C. Fauser, C. J. Heijnen, and N. S. Macklon. 2009. 'Endometrial secretion analysis identifies a cytokine profile predictive of pregnancy in IVF', *Hum Reprod*, 24: 1427-35.

Boue, A, and P Gallano. 1984. 'A collaborative study of the segregation of inherited chromosome structural rearrangements in 1356 prenatal diagnoses', *Prenatal diagnosis*, 4: 45-67.

Boyer, A., E. Lapointe, X. Zheng, R. G. Cowan, H. Li, S. M. Quirk, F. J. DeMayo, J. S. Richards, and D. Boerboom. 2010. 'WNT4 is required for normal ovarian follicle development and female fertility', *FASEB J*, 24: 3010-25.

Brandt, J. S., M. A. Cruz Ithier, T. Rosen, and E. Ashkinadze. 2019. 'Advanced paternal age, infertility, and reproductive risks: A review of the literature', *Prenat Diagn*, 39: 81-87.

Bromer, J. G., and E. Seli. 2008. 'Assessment of embryo viability in assisted reproductive technology: shortcomings of current approaches and the emerging role of metabolomics', *Curr Opin Obstet Gynecol*, 20: 234-41.

Brosens, I., R. Pijnenborg, L. Vercruysse, and R. Romero. 2011. 'The "Great Obstetrical Syndromes" are associated with disorders of deep placentation', *Am J Obstet Gynecol*, 204: 193-201.

Buck Louis, G. M., M. L. Hediger, C. M. Peterson, M. Croughan, R. Sundaram, J. Stanford, Z. Chen, V. Y. Fujimoto, M. W. Varner, A. Trumble, L. C. Giudice, and Endo Study Working Group. 2011. 'Incidence of endometriosis by study population and diagnostic method: the ENDO study', *Fertil Steril*, 96: 360-5.

Campbell, Jared M, Michelle Lane, Julie A Owens, and Hassan W Bakos. 2015. 'Paternal obesity negatively affects male fertility and assisted reproduction outcomes: a systematic review and meta-analysis', *Reproductive biomedicine online*, 31: 593-604.

Cha, J., X. Sun, and S. K. Dey. 2012. 'Mechanisms of implantation: strategies for successful pregnancy', *Nat Med*, 18: 1754-67.

Chen, C. S., J. L. Alonso, E. Ostuni, G. M. Whitesides, and D. E. Ingber. 2003. 'Cell shape provides global control of focal adhesion assembly', *Biochem Biophys Res Commun*, 307: 355-61.

Chi, H. J., J. J. Koo, S. Y. Choi, H. J. Jeong, and S. I. Roh. 2011. 'Fragmentation of embryos is associated with both necrosis and apoptosis', *Fertil Steril*, 96: 187-92.

Chronopoulou, E., and J. C. Harper. 2015. 'IVF culture media: past, present and future', *Hum Reprod Update*, 21: 39-55.

Ciepiela, P., A. J. Duleba, A. Kario, K. Chelstowski, D. Branecka-Wozniak, and R. Kurzawa. 2019. 'Oocyte matched follicular fluid anti-Mullerian hormone is an excellent predictor of live birth after fresh single embryo transfer', *Hum Reprod*, 34: 2244-53.

Ciray, H. N., T. Aksoy, C. Goktas, B. Ozturk, and M. Bahceci. 2012. 'Time-lapse evaluation of human embryo development in single versus sequential culture media--a sibling oocyte study', *J Assist Reprod Genet*, 29: 891-900.

Cissen, M., A. Bensdorp, B. J. Cohlen, S. Repping, J. P. de Bruin, and M. van Wely. 2016. 'Assisted reproductive technologies for male subfertility', *Cochrane Database Syst Rev*, 2: CD000360.

Cissen, M., M. V. Wely, I. Scholten, S. Mansell, J. P. Bruin, B. W. Mol, D. Braat, S. Repping, and G. Hamer. 2016. 'Measuring Sperm DNA Fragmentation and Clinical Outcomes of Medically Assisted Reproduction: A Systematic Review and Meta-Analysis', *PLoS One*, 11: e0165125.

Clark, D. A. 2008. 'Immunological factors in pregnancy wastage: fact or fiction', *Am J Reprod Immunol*, 59: 277-300.

Clevers, H. 2006. 'Wnt/beta-catenin signaling in development and disease', *Cell*, 127: 469-80.

Coan, P. M., G. J. Burton, and A. C. Ferguson-Smith. 2005. 'Imprinted genes in the placenta--a review', *Placenta*, 26 Suppl A: S10-20.

Colaco, Stacy, and Deepak Modi. 2018. 'Genetics of the human Y chromosome and its association with male infertility', *Reproductive Biology and Endocrinology*, 16: 14.

Colagar, A. H., G. A. Jorsaraee, and E. T. Marzony. 2007. 'Cigarette smoking and the risk of male infertility', *Pak J Biol Sci*, 10: 3870-4.

Cooper, T. G., E. Noonan, S. von Eckardstein, J. Auger, H. W. Baker, H. M. Behre, T. B. Haugen, T. Kruger, C. Wang, M. T. Mbizvo, and K. M. Vogelsong. 2010. 'World Health Organization reference values for human semen characteristics', *Hum Reprod Update*, 16: 231-45.

Cornillie, F. J., and J. M. Lauweryns. 1984. 'Transendothelial channels in fenestrated endometrial blood capillaries of rats', *Cell Tissue Res*, 237: 371-3.

Cornillie, F. J., J. M. Lauweryns, and I. A. Brosens. 1985. 'Normal human endometrium. An ultrastructural survey', *Gynecol Obstet Invest*, 20: 113-29.

Coward, R. M., and J. N. Mills. 2017. 'A step-by-step guide to office-based sperm retrieval for obstructive azoospermia', *Transl Androl Urol*, 6: 730-44.

Cuman, C., M. Van Sinderen, M. P. Gantier, K. Rainczuk, K. Sorby, L. Rombauts, T. Osianlis, and E. Dimitriadis. 2015. 'Human Blastocyst Secreted microRNA Regulate Endometrial Epithelial Cell Adhesion', *EBioMedicine*, 2: 1528-35.

Dada, R., M. Kumar, R. Jesudasan, J. L. Fernandez, J. Gosalvez, and A. Agarwal. 2012. 'Epigenetics and its role in male infertility', *J Assist Reprod Genet*, 29: 213-23.

Dahdouh, E. M., J. Balayla, and J. A. Garcia-Velasco. 2015. 'Comprehensive chromosome screening improves embryo selection: a meta-analysis', *Fertil Steril*, 104: 1503-12.

Das, S. K. 2009. 'Cell cycle regulatory control for uterine stromal cell decidualization in implantation', *Reproduction*, 137: 889-99.

Denomme, M. M., B. R. McCallie, J. C. Parks, K. Booher, W. B. Schoolcraft, and M. G. Katz-Jaffe. 2018. 'Inheritance of epigenetic dysregulation from male factor infertility has a direct impact on reproductive potential', *Fertil Steril*, 110: 419-28 e1.

Denomme, M. M., B. R. McCallie, J. C. Parks, W. B. Schoolcraft, and M. G. Katz-Jaffe. 2016. 'Epigenetic Dysregulation Observed in Monosomy Blastocysts Further Compromises Developmental Potential', *PLoS One*, 11: e0156980.

Dominguez, F., B. Gadea, A. Mercader, F. J. Esteban, A. Pellicer, and C. Simon. 2010. 'Embryologic outcome and secretome profile of implanted blastocysts obtained after coculture in human endometrial epithelial cells versus the sequential system', *Fertil Steril*, 93: 774-82 e1.

Dominguez, F., M. Meseguer, B. Aparicio-Ruiz, P. Piqueras, A. Quinonero, and C. Simon. 2015. 'New strategy for diagnosing embryo implantation potential by combining proteomics and time-lapse technologies', *Fertil Steril*, 104: 908-14.

Donnelly, GP, N McClure, MS Kennedy, and SEM Lewis. 1999. 'Direct effect of alcohol on the motility and morphology of human spermatozoa', *Andrologia*, 31: 43-47.

Doyle, N., M. Gainty, A. Eubanks, J. Doyle, H. Hayes, M. Tucker, K. Devine, A. DeCherney, M. Levy, S. Jahandideh, and M. Hill. 2020. 'Donor oocyte recipients do not benefit from preimplantation genetic testing for aneuploidy to improve pregnancy outcomes', *Hum Reprod*, 35: 2548-55.

Dragovic, R. A., L. J. Ritter, S. J. Schulz, F. Amato, J. G. Thompson, D. T. Armstrong, and R. B. Gilchrist. 2007. 'Oocyte-secreted factor activation of SMAD 2/3 signaling enables initiation of mouse cumulus cell expansion', *Biol Reprod*, 76: 848-57.

Dumollard, R., J. Carroll, M. R. Duchen, K. Campbell, and K. Swann. 2009. 'Mitochondrial function and redox state in mammalian embryos', *Semin Cell Dev Biol*, 20: 346-53.

Dumollard, R., Z. Ward, J. Carroll, and M. R. Duchen. 2007. 'Regulation of redox metabolism in the mouse oocyte and embryo', *Development*, 134: 455-65.

Elbendary, A. A., F. D. Cirisano, A. C. Evans, Jr., P. L. Davis, J. D. Iglehart, J. R. Marks, and A. Berchuck. 1996. 'Relationship between p21 expression and mutation of the p53 tumor suppressor gene in normal and malignant ovarian epithelial cells', *Clin Cancer Res*, 2: 1571-5.

Elizur, S. E., O. Lebovitz, R. Orvieto, J. Dor, and T. Zan-Bar. 2014. 'Reactive oxygen species in follicular fluid may serve as biochemical markers to determine ovarian aging and follicular metabolic age', *Gynecol Endocrinol*, 30: 705-7.

Elton, T. S., H. Selemon, S. M. Elton, and N. L. Parinandi. 2013. 'Regulation of the MIR155 host gene in physiological and pathological processes', *Gene*, 532: 1-12.

Emery, B. R., and D. T. Carrell. 2006. 'The effect of epigenetic sperm abnormalities on early embryogenesis', *Asian J Androl*, 8: 131-42.

ERICKSON, GREGORY F, CHRIS HOFEDITZ, MICHAEL UNGER, W ROSS ALLEN, and RENATO DULBECCO. 1985. 'A monoclonal antibody to a mammary cell line recognizes two distinct subtypes of ovarian granulosa cells', *Endocrinology*, 117: 1490-99.

Fabregat, A., K. Sidiropoulos, G. Viteri, O. Forner, P. Marin-Garcia, V. Arnau, P. D'Eustachio, L. Stein, and H. Hermjakob. 2017. 'Reactome pathway analysis: a high-performance in-memory approach', *BMC Bioinformatics*, 18: 142.

Fang, R., W. Yang, X. Zhao, F. Xiong, C. Guo, J. Xiao, L. Chen, X. Song, H. Wang, J. Chen, X. Xiao, B. Yao, and L. Y. Cai. 2019. 'Chromosome screening using culture medium of embryos fertilised in vitro: a pilot clinical study', *J Transl Med*, 17: 73.

Feng, S., Z. Cao, and X. Wang. 2013. 'Role of aryl hydrocarbon receptor in cancer', *Biochim Biophys Acta*, 1836: 197-210.

Feuerstein, P., V. Puard, C. Chevalier, R. Teusan, V. Cadoret, F. Guerif, R. Houlgatte, and D. Royere. 2012. 'Genomic assessment of human cumulus cell marker genes as predictors of oocyte developmental competence: impact of various experimental factors', *PLoS One*, 7: e40449.

Fitzgerald, J. S., T. G. Poehlmann, E. Schleussner, and U. R. Markert. 2008. 'Trophoblast invasion: the role of intracellular cytokine signalling via signal transducer and activator of transcription 3 (STAT3)', *Hum Reprod Update*, 14: 335-44.

Florio, P., L. Bruni, C. De Falco, G. Filardi, M. Torricelli, F. M. Reis, L. Galleri, C. Voltolini, C. Bocchi, V. De Leo, and F. Petraglia. 2008. 'Evaluation of endometrial urocortin secretion for prediction of pregnancy after intrauterine insemination', *Clin Chem*, 54: 350-5.

Florio, P., L. Bruni, L. Galleri, F. M. Reis, L. E. Borges, C. Bocchi, P. Litta, V. De Leo, and F. Petraglia. 2010. 'Evaluation of endometrial activin A secretion for prediction of pregnancy after intrauterine insemination', *Fertil Steril*, 93: 2316-20.

Fox, C., S. Morin, J. W. Jeong, R. T. Scott, Jr., and B. A. Lessey. 2016. 'Local and systemic factors and implantation: what is the evidence?', *Fertil Steril*, 105: 873-84.

Fragouli, E., M. Lenzi, R. Ross, M. Katz-Jaffe, W.B. Schoolcraft, and D. Wells. 2008. 'Comprehensive molecular cytogenetic analysis of the human blastocyst stage', *Human Reproduction*, 23: 2596-608.

Franasiak, J. M., and R. T. Scott, Jr. 2014. 'Embryonic aneuploidy: overcoming molecular genetics challenges improves outcomes and changes practice patterns', *Trends Mol Med*, 20: 499-508.

Frost, J. M., and G. E. Moore. 2010. 'The importance of imprinting in the human placenta', *PLoS Genet*, 6: e1001015.

Gabory, A., M. A. Ripoche, A. Le Digarcher, F. Watrin, A. Ziyyat, T. Forne, H. Jammes, J. F. Ainscough, M. A. Surani, L. Journot, and L. Dandolo. 2009. 'H19 acts as a trans regulator of the imprinted gene network controlling growth in mice', *Development*, 136: 3413-21.

Gao, Z., P. Moorjani, T. A. Sasani, B. S. Pedersen, A. R. Quinlan, L. B. Jorde, G. Amster, and M. Przeworski. 2019. 'Overlooked roles of DNA damage and maternal age in generating human germline mutations', *Proc Natl Acad Sci U S A*, 116: 9491-500.

Garcia-Palomares, S., S. Navarro, J. F. Pertusa, C. Hermenegildo, M. A. Garcia-Perez, F. Rausell, A. Cano, and J. J. Tarin. 2009. 'Delayed fatherhood in mice decreases reproductive fitness and longevity of offspring', *Biol Reprod*, 80: 343-9.

Garcia-Palomares, S., J. F. Pertusa, J. Minarro, M. A. Garcia-Perez, C. Hermenegildo, F. Rausell, A. Cano, and J. J. Tarin. 2009. 'Long-term effects of delayed fatherhood in mice on postnatal development and behavioral traits of offspring', *Biol Reprod*, 80: 337-42.

Garcia-Velasco, J. A., and G. Quea. 2005. 'Medical treatment of endometriosis', *Minerva Ginecol*, 57: 249-55.

Garcia, M. A., W. J. Nelson, and N. Chavez. 2018. 'Cell-Cell Junctions Organize Structural and Signaling Networks', *Cold Spring Harb Perspect Biol*, 10.

Gardner, D. K., and M. Lane. 1996. 'Alleviation of the '2-cell block' and development to the blastocyst of CF1 mouse embryos: role of amino acids, EDTA and physical parameters', *Hum Reprod*, 11: 2703-12.

Gardner, D. K., and W. B. Schoolcraft. 1999a. *Towards reproductive certainty: fertility and genetics beyond.* (Parthenon: London).

Gardner, DK, and WB Schoolcraft. 1999b. 'In-vitro culture of human blastocysts.' in R. Jansen and D. Mortimer (eds.), *Towards Reproductive Certainty: Fertility and Genetics Beyond 1999* (Carnforth: Parthenon Press).

Gargett, C. E., R. W. Chan, and K. E. Schwab. 2007. 'Endometrial stem cells', *Curr Opin Obstet Gynecol*, 19: 377-83.

Garrido-Gomez, T., M. Ruiz-Alonso, D. Blesa, P. Diaz-Gimeno, F. Vilella, and C. Simon. 2013. 'Profiling the gene signature of endometrial receptivity: clinical results', *Fertil Steril*, 99: 1078-85.

Gellersen, B., and J. J. Brosens. 2014. 'Cyclic decidualization of the human endometrium in reproductive health and failure', *Endocr Rev*, 35: 851-905.

Gianaroli, L., M. C. Magli, A. P. Ferraretti, C. Tabanelli, V. Trengia, V. Farfalli, and G. Cavallini. 2005. 'The beneficial effects of preimplantation genetic diagnosis for aneuploidy support extensive clinical application', *Reprod Biomed Online*, 10: 633-40.

Gilbert, A. M., M. G. Bursavich, N. Alon, B. M. Bhat, F. J. Bex, M. Cain, V. Coleburn, V. Gironda, P. Green, D. B. Hauze, Y. Kharode, G. Krishnamurthy, M. Kirisits, H. S. Lam, Y. B. Liu, S. Lombardi, J. Matteo, R. Murrills, J. A. Robinson, S. Selim, M. Sharp, R. Unwalla, U. Varadarajan, W. Zhao, and P. J. Yaworsky. 2010. 'Hit to lead studies on (hetero)arylpyrimidines--agonists of the canonical Wnt-beta-catenin cellular messaging system', *Bioorg Med Chem Lett*, 20: 366-70.

Gillott, D. J., H. M. Al-Rumaih, K. Y. Leung, A. Eldib, and J. G. Grudzinskas. 2008. 'Specific isoforms of leucine-rich alpha2-glycoprotein detected in the proliferative endometrium of women undergoing assisted reproduction are associated with spontaneous pregnancy', *Fertil Steril*, 90: 761-8.

Gode, F., B. Gulekli, E. Dogan, P. Korhan, S. Dogan, O. Bige, D. Cimrin, and N. Atabey. 2011. 'Influence of follicular fluid GDF9 and BMP15 on embryo quality', *Fertil Steril*, 95: 2274-8.

Goldman, R. H., C. Racowsky, L. V. Farland, J. H. Fox, S. Munné, L. Ribustello, and E. S. Ginsburg. 2018. 'The cost of a euploid embryo identified from preimplantation genetic testing for aneuploidy (PGT-A): a counseling tool', *J Assist Reprod Genet*, 35: 1641-50.

Gomez, E., M. Ruiz-Alonso, J. Miravet, and C. Simon. 2015. 'Human Endometrial Transcriptomics: Implications for Embryonic Implantation', *Cold Spring Harb Perspect Med*, 5: a022996.

Goossens, K., P. Mestdagh, S. Lefever, M. Van Poucke, A. Van Zeveren, A. Van Soom, J. Vandesompele, and L. Peelman. 2013. 'Regulatory microRNA network identification in bovine blastocyst development', *Stem Cells Dev*, 22: 1907-20.

Gott, A. L., K. Hardy, R. M. Winston, and H. J. Leese. 1990. 'Non-invasive measurement of pyruvate and glucose uptake and lactate production by single human preimplantation embryos', *Hum Reprod*, 5: 104-8.

Gray, C. A., K. M. Taylor, W. S. Ramsey, J. R. Hill, F. W. Bazer, F. F. Bartol, and T. E. Spencer. 2001. 'Endometrial glands are required for preimplantation conceptus elongation and survival', *Biol Reprod*, 64: 1608-13.

Grund, S., and R. Grummer. 2018. 'Direct Cell(-)Cell Interactions in the Endometrium and in Endometrial Pathophysiology', *Int J Mol Sci*, 19.

Guerif, F., A. Le Gouge, B. Giraudeau, J. Poindron, R. Bidault, O. Gasnier, and D. Royere. 2007. 'Limited value of morphological assessment at days 1 and 2 to predict blastocyst development potential: a prospective study based on 4042 embryos', *Hum Reprod*, 22: 1973-81.

Gunes, Sezgin, Gulgez Neslihan Taskurt Hekim, Mehmet Alper Arslan, and Ramazan Asci. 2016. 'Effects of aging on the male reproductive system', *Journal of assisted reproduction and genetics*, 33: 441-54.

Haller-Kikkatalo, K., S. Altmae, A. Tagoma, R. Uibo, and A. Salumets. 2014. 'Autoimmune activation toward embryo implantation is rare in immune-privileged human endometrium', *Semin Reprod Med*, 32: 376-84.

Hamatani, T., T. Daikoku, H. Wang, H. Matsumoto, M. G. Carter, M. S. Ko, and S. K. Dey. 2004. 'Global gene expression analysis identifies molecular pathways distinguishing blastocyst dormancy and activation', *Proc Natl Acad Sci U S A*, 101: 10326-31.

Hammond, E. R., B. C. McGillivray, S. M. Wicker, J. C. Peek, A. N. Shelling, P. Stone, L. W. Chamley, and L. M. Cree. 2017. 'Characterizing nuclear and mitochondrial DNA in spent embryo culture media: genetic contamination identified', *Fertil Steril*, 107: 220-28 e5.

Hannan, N. J., G. Nie, A. Rainzcuk, L. J. Rombauts, and L. A. Salamonsen. 2012. 'Uterine lavage or aspirate: which view of the intrauterine environment?', *Reprod Sci*, 19: 1125-32.

Hannan, N. J., P. Paiva, K. L. Meehan, L. J. Rombauts, D. K. Gardner, and L. A. Salamonsen. 2011. 'Analysis of fertility-related soluble mediators in human uterine fluid identifies VEGF as a key regulator of embryo implantation', *Endocrinology*, 152: 4948-56.

Hannan, N. J., A. N. Stephens, A. Rainczuk, C. Hincks, L. J. Rombauts, and L. A. Salamonsen. 2010. '2D-DiGE analysis of the human endometrial secretome reveals differences between receptive and nonreceptive states in fertile and infertile women', *J Proteome Res*, 9: 6256-64.

Hantak, A. M., I. C. Bagchi, and M. K. Bagchi. 2014. 'Role of uterine stromal-epithelial crosstalk in embryo implantation', *Int J Dev Biol*, 58: 139-46.

Harlev, A., A. Agarwal, S. O. Gunes, A. Shetty, and S. S. du Plessis. 2015. 'Smoking and Male Infertility: An Evidence-Based Review', *World J Mens Health*, 33: 143-60.

Harton, G. L., S. Munne, M. Surrey, J. Grifo, B. Kaplan, D. H. McCulloh, D. K. Griffin, D. Wells, and P. G. D. Practitioners Group. 2013. 'Diminished effect of maternal age on implantation after preimplantation genetic diagnosis with array comparative genomic hybridization', *Fertil Steril*, 100: 1695-703.

Hashemitabar, M., M. Bahmanzadeh, A. Mostafaie, M. Orazizadeh, M. Farimani, and R. Nikbakht. 2014. 'A proteomic analysis of human follicular fluid: comparison between younger and older women with normal FSH levels', *Int J Mol Sci*, 15: 17518-40.

Hemmings, K. E., D. Maruthini, S. Vyjayanthi, J. E. Hogg, A. H. Balen, B. K. Campbell, H. J. Leese, and H. M. Picton. 2013. 'Amino acid turnover by human oocytes is influenced by gamete developmental competence, patient characteristics and gonadotrophin treatment', *Hum Reprod*, 28: 1031-44.

Hoelker, M., F. Rings, Q. Lund, N. Ghanem, C. Phatsara, J. Griese, K. Schellander, and D. Tesfaye. 2009. 'Effect of the microenvironment and embryo density on developmental characteristics and gene expression profile of bovine preimplantative embryos cultured in vitro', *Reproduction*, 137: 415-25.

Holm, P., P. J. Booth, M. H. Schmidt, T. Greve, and H. Callesen. 1999. 'High bovine blastocyst development in a static in vitro production system using SOFaa medium supplemented with sodium citrate and myo-inositol with or without serum-proteins', *Theriogenology*, 52: 683-700.

Host, E., A. Gabrielsen, S. Lindenberg, and S. Smidt-Jensen. 2002. 'Apoptosis in human cumulus cells in relation to zona pellucida thickness variation, maturation stage, and cleavage of the corresponding oocyte after intracytoplasmic sperm injection', *Fertil Steril*, 77: 511-5.

Huo, P., K. Deng, L. Wang, M. Li, J. Yao, J. Le, X. Lei, and S. Zhang. 2020. 'The effect of laser-assisted hatching on the methylation and expression pattern of imprinted gene IGF2/H19 in mouse blastocysts and offspring', *J Assist Reprod Genet*, 37: 3057-67.

Iager, A. E., A. M. Kocabas, H. H. Otu, P. Ruppel, A. Langerveld, P. Schnarr, M. Suarez, J. C. Jarrett, J. Conaghan, G. J. Rosa, E. Fernandez, R. G. Rawlins, J. B. Cibelli, and J. A. Crosby. 2013. 'Identification of a novel gene set in human cumulus cells predictive of an oocyte's pregnancy potential', *Fertil Steril*, 99: 745-52 e6.

Jarkovska, K., J. Martinkova, L. Liskova, P. Halada, J. Moos, K. Rezabek, S. J. Gadher, and H. Kovarova. 2010. 'Proteome mining of human follicular fluid reveals a crucial role of complement cascade and key biological pathways in women undergoing in vitro fertilization', *J Proteome Res*, 9: 1289-301.

Jenkins, T. G., K. I. Aston, and D. T. Carrell. 2018. 'Sperm epigenetics and aging', *Transl Androl Urol*, 7: S328-s35.

Jenkins, T. G., K. I. Aston, T. D. Meyer, J. M. Hotaling, M. B. Shamsi, E. B. Johnstone, K. J. Cox, J. B. Stanford, C. A. Porucznik, and D. T. Carrell. 2016. 'Decreased fecundity and sperm DNA methylation patterns', *Fertil Steril*, 105: 51-7.e1-3.

Jenkins, T. G., K. I. Aston, C. Pflueger, B. R. Cairns, and D. T. Carrell. 2014. 'Age-associated sperm DNA methylation alterations: possible implications in offspring disease susceptibility', *PLoS Genet*, 10: e1004458.

Johnson, Sheri L, Jessica Dunleavy, Neil J Gemmell, and Shinichi Nakagawa. 2015. 'Consistent age-dependent declines in human semen quality: a systematic review and meta-analysis', *Ageing research reviews*, 19: 22-33.

Kajihara, T., K. Tanaka, T. Oguro, H. Tochigi, J. Prechapanich, S. Uchino, A. Itakura, S. Sucurovic, K. Murakami, J. J. Brosens, and O. Ishihara. 2014. 'Androgens modulate the morphological characteristics of human endometrial stromal cells decidualized in vitro', *Reprod Sci*, 21: 372-80.

Katz-Jaffe, M. G., D. K. Gardner, and W. B. Schoolcraft. 2006. 'Proteomic analysis of individual human embryos to identify novel biomarkers of development and viability', *Fertil Steril*, 85: 101-7.

Katz-Jaffe, M. G., J. Parks, B. McCallie, and W. B. Schoolcraft. 2013. 'Aging sperm negatively impacts in vivo and in vitro reproduction: a longitudinal murine study', *Fertil Steril*, 100: 262-8 e1-2.

Katz-Jaffe, M. G., W. B. Schoolcraft, and D. K. Gardner. 2006. 'Analysis of protein expression (secretome) by human and mouse preimplantation embryos', *Fertil Steril*, 86: 678-85.

Kazemi, A., F. Ramezanzadeh, M. H. Esfahani, A. A. Saboor-Yaraghi, S. Nejat, and A. Rahimi-Foroshani. 2013. 'Impact of environmental tobacco smoke exposure in women on oxidative stress in the antral follicle and assisted reproduction outcomes', *J Res Med Sci*, 18: 688-94.

Kazemi, A., F. Ramezanzadeh, M. H. Nasr-Esfahani, A. A. Saboor Yaraghi, and M. Ahmadi. 2013. 'Does dietary fat intake influence oocyte competence and embryo quality by inducing oxidative stress in follicular fluid?', *Iran J Reprod Med*, 11: 1005-12.

Keefe, D., M. Kumar, and K. Kalmbach. 2015. 'Oocyte competency is the key to embryo potential', *Fertil Steril*, 103: 317-22.

Kenigsberg, S., B. A. Wyse, C. L. Librach, and J. C. da Silveira. 2017. 'Protocol for Exosome Isolation from Small Volume of Ovarian Follicular Fluid: Evaluation of Ultracentrifugation and Commercial Kits', *Methods Mol Biol*, 1660: 321-41.

Khandwala, Y. S., V. L. Baker, G. M. Shaw, D. K. Stevenson, Y. Lu, and M. L. Eisenberg. 2018. 'Association of paternal age with perinatal outcomes between 2007 and 2016 in the United States: population based cohort study', *BMJ*, 363: k4372.

Kimura, R., K. Yoshizaki, and N. Osumi. 2018. 'Risk of Neurodevelopmental Disease by Paternal Aging: A Possible Influence of Epigenetic Alteration in Sperm', *Adv Exp Med Biol*, 1012: 75-81.

Kimura, Y., M. Akahira-Azuma, N. Harada, Y. Enomoto, Y. Tsurusaki, and K. Kurosawa. 2018. 'Novel SYNGAP1 variant in a patient with intellectual disability and distinctive dysmorphisms', *Congenit Anom (Kyoto)*, 58: 188-90.

Kirkegaard, K., A. S. Svane, J. S. Nielsen, J. J. Hindkjaer, N. C. Nielsen, and H. J. Ingerslev. 2014. 'Nuclear magnetic resonance metabolomic profiling of Day 3 and 5 embryo culture medium does not predict pregnancy outcome in good prognosis patients: a prospective cohort study on single transferred embryos', *Hum Reprod*, 29: 2413-20.

Kleijkers, S. H., E. Mantikou, E. Slappendel, D. Consten, J. van Echten-Arends, A. M. Wetzels, M. van Wely, L. J. Smits, A. P. van Montfoort, S. Repping, J. C. Dumoulin, and S. Mastenbroek. 2016. 'Influence of embryo culture medium (G5 and HTF) on pregnancy and perinatal outcome after IVF: a multicenter RCT', *Hum Reprod*, 31: 2219-30.

Kobayashi, N., H. Okae, H. Hiura, H. Chiba, Y. Shirakata, K. Hara, K. Tanemura, and T. Arima. 2016. 'Genome-Scale Assessment of Age-Related DNA Methylation Changes in Mouse Spermatozoa', *PLoS One*, 11: e0167127.

Kojima, K., K. Shirai, M. Kobayashi, A. Miyauchi, H. Saitsu, N. Matsumoto, H. Osaka, and T. Yamagata. 2018. 'A patient with early myoclonic encephalopathy (EME) with a de novo KCNQ2 mutation', *Brain Dev*, 40: 69-73.

Kokkali, G., J. Traeger-Synodinos, C. Vrettou, D. Stavrou, G.M. Jones, D.S. Cram, E. Makrakis, A.O. Trounson, E. Kanavakis, and K. Pantos. 2007. 'Blastocyst biopsy versus cleavage stage biopsy and blastocyst transfer for preimplantation genetic diagnosis of β-thalassaemia: a pilot study', *Human Reproduction*, 22: 1443-49.

Kõks, Sulev, Soner Dogan, Bilge Guvenc Tuna, Herminia González-Navarro, Paul Potter, and Roosmarijn E. Vandenbroucke. 2016. 'Mouse models of ageing and their relevance to disease', *Mech Ageing Dev*, 160: 41-53.

Kong, A., M. L. Frigge, G. Masson, S. Besenbacher, P. Sulem, G. Magnusson, S. A. Gudjonsson, A. Sigurdsson, A. Jonasdottir, A. Jonasdottir, W. S. Wong, G. Sigurdsson, G. B. Walters, S. Steinberg, H. Helgason, G. Thorleifsson, D. F. Gudbjartsson, A. Helgason, O. T. Magnusson, U. Thorsteinsdottir, and K. Stefansson. 2012. 'Rate of de novo mutations and the importance of father's age to disease risk', *Nature*, 488: 471-5.

Kovacic, B. 2012. 'Culture systems: low-oxygen culture', *Methods Mol Biol*, 912: 249-72.

Kovalevsky, G., and P. Patrizio. 2005. 'High rates of embryo wastage with use of assisted reproductive technology: a look at the trends between 1995 and 2001 in the United States', *Fertil Steril*, 84: 325-30.

Krussel, J. S., P. Bielfeld, M. L. Polan, and C. Simon. 2003. 'Regulation of embryonic implantation', *Eur J Obstet Gynecol Reprod Biol*, 110 Suppl 1: S2-9.

Kumar, R, MB Shamsi, MI Gaznavi, M Jena, K Kucheria, and R Kumar. 2007. 'Structural chromosomal anomalies and their association with reproductive failure', *Obstet Gynecol Today*, 12: 152-4.

Kushnir, M. M., T. Naessen, K. Wanggren, A. L. Rockwood, D. K. Crockett, and J. Bergquist. 2012. 'Protein and steroid profiles in follicular fluid after ovarian hyperstimulation as potential biomarkers of IVF outcome', *J Proteome Res*, 11: 5090-100.

Kuwayama, M., G. Vajta, O. Kato, and S. P. Leibo. 2005. 'Highly efficient vitrification method for cryopreservation of human oocytes', *Reprod Biomed Online*, 11: 300-8.

Lachner, Monika, Roderick J O'Sullivan, and Thomas Jenuwein. 2003. 'An epigenetic road map for histone lysine methylation', *J Cell Sci*, 116: 2117-24.

Lane, M., and D. K. Gardner. 1996. 'Selection of viable mouse blastocysts prior to transfer using a metabolic criterion', *Hum Reprod*, 11: 1975-8.

Larman, M. G., M. G. Katz-Jaffe, B. McCallie, J. A. Filipovits, and D. K. Gardner. 2011. 'Analysis of global gene expression following mouse blastocyst cryopreservation', *Hum Reprod*, 26: 2672-80.

Laurent, L. C. 2008. 'MicroRNAs in embryonic stem cells and early embryonic development', *J Cell Mol Med*, 12: 2181-8.

Ledee-Bataille, N., S. Dubanchet, A. Coulomb-L'hermine, I. Durand-Gasselin, R. Frydman, and G. Chaouat. 2004. 'A new role for natural killer cells, interleukin (IL)-12, and IL-18 in repeated implantation failure after in vitro fertilization', *Fertil Steril*, 81: 59-65.

Ledee, N., V. Gridelet, S. Ravet, C. Jouan, O. Gaspard, F. Wenders, F. Thonon, N. Hincourt, M. Dubois, J. M. Foidart, C. Munaut, and S. Perrier d'Hauterive. 2013. 'Impact of follicular G-CSF quantification on subsequent embryo transfer decisions: a proof of concept study', *Hum Reprod*, 28: 406-13.

Lee, K. S., B. S. Joo, Y. J. Na, M. S. Yoon, O. H. Choi, and W. W. Kim. 2001. 'Cumulus cells apoptosis as an indicator to predict the quality of oocytes and the outcome of IVF-ET', *J Assist Reprod Genet*, 18: 490-8.

Lee, Y. S., G. A. Thouas, and D. K. Gardner. 2015. 'Developmental kinetics of cleavage stage mouse embryos are related to their subsequent carbohydrate and amino acid utilization at the blastocyst stage', *Hum Reprod*, 30: 543-52.

Leenen, F. A., C. P. Muller, and J. D. Turner. 2016. 'DNA methylation: conducting the orchestra from exposure to phenotype?', *Clin Epigenetics*, 8: 92.

Leese, H. J., and A. M. Barton. 1984. 'Pyruvate and glucose uptake by mouse ova and preimplantation embryos', *J Reprod Fertil*, 72: 9-13.

Leese, H. J., C. G. Baumann, D. R. Brison, T. G. McEvoy, and R. G. Sturmey. 2008. 'Metabolism of the viable mammalian embryo: quietness revisited', *Mol Hum Reprod*, 14: 667-72.

Lessey, B. A. 2000. 'Endometrial receptivity and the window of implantation', *Baillieres Best Pract Res Clin Obstet Gynaecol*, 14: 775-88.

Levine, H., N. Jørgensen, A. Martino-Andrade, J. Mendiola, D. Weksler-Derri, I. Mindlis, R. Pinotti, and S. H. Swan. 2017. 'Temporal trends in sperm count: a systematic review and meta-regression analysis', *Hum Reprod Update*, 23: 646-59.

Li, Ying, Hui Lin, Yafei Li, and Jia Cao. 2011. 'Association between socio-psycho-behavioral factors and male semen quality: systematic review and meta-analyses', *Fertility and sterility*, 95: 116-23.

Litwicka, K., C. Mencacci, C. Arrivi, M. T. Varricchio, A. Caragia, M. G. Minasi, and E. Greco. 2018. 'HCG administration after endogenous LH rise negatively influences pregnancy rate in modified natural cycle for frozen-thawed euploid blastocyst transfer: a pilot study', *J Assist Reprod Genet*, 35: 449-55.

Litzky, J. F., and C. J. Marsit. 2019. 'Epigenetically regulated imprinted gene expression associated with IVF and infertility: possible influence of prenatal stress and depression', *J Assist Reprod Genet*, 36: 1299-313.

Liu, N., Y. Ma, R. Li, H. Jin, M. Li, X. Huang, H. L. Feng, and J. Qiao. 2012. 'Comparison of follicular fluid amphiregulin and EGF concentrations in patients undergoing IVF with different stimulation protocols', *Endocrine*, 42: 708-16.

Lobascio, AM, M De Felici, M Anibaldi, P Greco, MG Minasi, and E Greco. 2015. 'Involvement of seminal leukocytes, reactive oxygen species, and sperm mitochondrial membrane potential in the DNA damage of the human spermatozoa', *Andrology*, 3: 265-70.

Logan, C. Y., and R. Nusse. 2004. 'The Wnt signaling pathway in development and disease', *Annu Rev Cell Dev Biol*, 20: 781-810.

Loukinov, Dmitri I, Elena Pugacheva, Sergei Vatolin, Svetlana D Pack, Hanlim Moon, Igor Chernukhin, Poonam Mannan, Erik Larsson, Chandrasekhar Kanduri, and Alexander A Vostrov. 2002. 'BORIS, a novel male germ-line-specific protein associated with epigenetic reprogramming events, shares the same 11-zinc-finger domain with CTCF, the insulator protein involved in reading imprinting marks in the soma', *Proceedings of the National Academy of Sciences*, 99: 6806-11.

Luo, W., G. Li, Z. Yi, Q. Nie, and X. Zhang. 2016. 'E2F1-miR-20a-5p/20b-5p auto-regulatory feedback loop involved in myoblast proliferation and differentiation', *Sci Rep*, 6: 27904.

Ly, L., D. Chan, M. Aarabi, M. Landry, N. A. Behan, A. J. MacFarlane, and J. Trasler. 2017. 'Intergenerational impact of paternal lifetime exposures to both folic acid

deficiency and supplementation on reproductive outcomes and imprinted gene methylation', *Mol Hum Reprod*, 23: 461-77.

Ma, P., and R. M. Schultz. 2013. 'Histone deacetylase 2 (HDAC2) regulates chromosome segregation and kinetochore function via H4K16 deacetylation during oocyte maturation in mouse', *PLoS Genet*, 9: e1003377.

MacDonald, B. T., K. Tamai, and X. He. 2009. 'Wnt/beta-catenin signaling: components, mechanisms, and diseases', *Dev Cell*, 17: 9-26.

Mackay, D. J., T. Eggermann, K. Buiting, I. Garin, I. Netchine, A. Linglart, and G. P. de Nanclares. 2015. 'Multilocus methylation defects in imprinting disorders', *Biomol Concepts*, 6: 47-57.

Madr, A., A. Cela, B. Klejdus, M. Pelcova, I. Crha, J. Zakova, and Z. Glatz. 2015. 'Determination of pyruvate and lactate as potential biomarkers of embryo viability in assisted reproduction by capillary electrophoresis with contactless conductivity detection', *Electrophoresis*, 36: 1244-50.

Mahajan, N. 2015. 'Endometrial receptivity array: Clinical application', *J Hum Reprod Sci*, 8: 121-9.

Makieva, S., E. Giacomini, J. Ottolina, A. M. Sanchez, E. Papaleo, and P. Vigano. 2018. 'Inside the Endometrial Cell Signaling Subway: Mind the Gap(s)', *Int J Mol Sci*, 19.

Mancini-DiNardo, D., S. J. Steele, R. S. Ingram, and S. M. Tilghman. 2003. 'A differentially methylated region within the gene Kcnq1 functions as an imprinted promoter and silencer', *Hum Mol Genet*, 12: 283-94.

Mann, M. R., S. S. Lee, A. S. Doherty, R. I. Verona, L. D. Nolen, R. M. Schultz, and M. S. Bartolomei. 2004. 'Selective loss of imprinting in the placenta following preimplantation development in culture', *Development*, 131: 3727-35.

Mantikou, E., M. A. Youssef, M. van Wely, F. van der Veen, H. G. Al-Inany, S. Repping, and S. Mastenbroek. 2013. 'Embryo culture media and IVF/ICSI success rates: a systematic review', *Hum Reprod Update*, 19: 210-20.

Marcet, B., B. Chevalier, G. Luxardi, C. Coraux, L. E. Zaragosi, M. Cibois, K. Robbe-Sermesant, T. Jolly, B. Cardinaud, C. Moreilhon, L. Giovannini-Chami, B. Nawrocki-Raby, P. Birembaut, R. Waldmann, L. Kodjabachian, and P. Barbry. 2011. 'Control of vertebrate multiciliogenesis by miR-449 through direct repression of the Delta/Notch pathway', *Nat Cell Biol*, 13: 693-9.

Martens, M., T. Verbruggen, P. Nymark, R. Grafstrom, L. D. Burgoon, H. Aladjov, F. Torres Andon, C. T. Evelo, and E. L. Willighagen. 2018. 'Introducing WikiPathways as a Data-Source to Support Adverse Outcome Pathways for Regulatory Risk Assessment of Chemicals and Nanomaterials', *Front Genet*, 9: 661.

Martin, J., F. Dominguez, S. Avila, J. L. Castrillo, J. Remohi, A. Pellicer, and C. Simon. 2002. 'Human endometrial receptivity: gene regulation', *J Reprod Immunol*, 55: 131-9.

Martin, R. H. 2008. 'Cytogenetic determinants of male fertility', *Hum Reprod Update*, 14: 379-90.

Mastenbroek, S., M. Twisk, J. van Echten-Arends, B. Sikkema-Raddatz, J. C. Korevaar, H. R. Verhoeve, N. E. Vogel, E. G. Arts, J. W. de Vries, P. M. Bossuyt, C. H.

Buys, M. J. Heineman, S. Repping, and F. van der Veen. 2007. 'In vitro fertilization with preimplantation genetic screening', *N Engl J Med*, 357: 9-17.

Mathew, S. J., D. Haubert, M. Kronke, and M. Leptin. 2009. 'Looking beyond death: a morphogenetic role for the TNF signalling pathway', *J Cell Sci*, 122: 1939-46.

Matoba, S., K. Bender, A. G. Fahey, S. Mamo, L. Brennan, P. Lonergan, and T. Fair. 2014. 'Predictive value of bovine follicular components as markers of oocyte developmental potential', *Reprod Fertil Dev*, 26: 337-45.

McEwan, M., R. J. Lins, S. K. Munro, Z. L. Vincent, A. P. Ponnampalam, and M. D. Mitchell. 2009. 'Cytokine regulation during the formation of the fetal-maternal interface: focus on cell-cell adhesion and remodelling of the extra-cellular matrix', *Cytokine Growth Factor Rev*, 20: 241-9.

McKenzie, L. J., S. A. Pangas, S. A. Carson, E. Kovanci, P. Cisneros, J. E. Buster, P. Amato, and M. M. Matzuk. 2004. 'Human cumulus granulosa cell gene expression: a predictor of fertilization and embryo selection in women undergoing IVF', *Hum Reprod*, 19: 2869-74.

McReynolds, S., L. Vanderlinden, J. Stevens, K. Hansen, W. B. Schoolcraft, and M. G. Katz-Jaffe. 2011. 'Lipocalin-1: a potential marker for noninvasive aneuploidy screening', *Fertil Steril*, 95: 2631-3.

Melford, S. E., A. H. Taylor, and J. C. Konje. 2014. 'Of mice and (wo)men: factors influencing successful implantation including endocannabinoids', *Hum Reprod Update*, 20: 415-28.

Mercader, A., J. A. Garcia-Velasco, E. Escudero, J. Remohi, A. Pellicer, and C. Simon. 2003. 'Clinical experience and perinatal outcome of blastocyst transfer after coculture of human embryos with human endometrial epithelial cells: a 5-year follow-up study', *Fertil Steril*, 80: 1162-8.

Meseguer, M., J. Herrero, A. Tejera, K. M. Hilligsoe, N. B. Ramsing, and J. Remohi. 2011. 'The use of morphokinetics as a predictor of embryo implantation', *Hum Reprod*, 26: 2658-71.

Meseguer, M., I. Rubio, M. Cruz, N. Basile, J. Marcos, and A. Requena. 2012. 'Embryo incubation and selection in a time-lapse monitoring system improves pregnancy outcome compared with a standard incubator: a retrospective cohort study', *Fertil Steril*, 98: 1481-9 e10.

Meza-Espinoza, Juan Pablo, Lilia Ortiz Anguiano, and Horacio Rivera. 2008. 'Chromosomal abnormalities in couples with reproductive disorders', *Gynecologic and obstetric investigation*, 66: 237-40.

Miao, M., X. Zhou, Y. Li, O. Zhang, Z. Zhou, T. Li, W. Yuan, R. Li, and D. K. Li. 2014. 'LINE-1 hypomethylation in spermatozoa is associated with Bisphenol A exposure', *Andrology*, 2: 138-44.

Milekic, M. H., Y. Xin, A. O'Donnell, K. K. Kumar, M. Bradley-Moore, D. Malaspina, H. Moore, D. Brunner, Y. Ge, J. Edwards, S. Paul, F. G. Haghighi, and J. A. Gingrich. 2015. 'Age-related sperm DNA methylation changes are transmitted to offspring and associated with abnormal behavior and dysregulated gene expression', *Mol Psychiatry*, 20: 995-1001.

Miller, D., S. Pavitt, V. Sharma, G. Forbes, R. Hooper, S. Bhattacharya, J. Kirkman-Brown, A. Coomarasamy, S. Lewis, R. Cutting, D. Brison, A. Pacey, R. West, K. Brian, D. Griffin, and Y. Khalaf. 2019. 'Physiological, hyaluronan-selected

intracytoplasmic sperm injection for infertility treatment (HABSelect): a parallel, two-group, randomised trial', *Lancet*, 393: 416-22.

Min, J. K., E. Hughes, D. Young, Committee Joint Sogc-Cfas Clinical Practice Guidelines, Endocrinology Reproductive, and Committee Infertility. 2010. 'Elective single embryo transfer following in vitro fertilization', *J Obstet Gynaecol Can*, 32: 363-77.

Minde, D. P., Z. Anvarian, S. G. Rudiger, and M. M. Maurice. 2011. 'Messing up disorder: how do missense mutations in the tumor suppressor protein APC lead to cancer?', *Mol Cancer*, 10: 101.

Mints, M., M. Mushtaq, N. Iurchenko, L. Kovalevska, M. C. Stip, D. Budnikova, S. Andersson, L. Polischuk, L. Buchynska, and E. Kashuba. 2016. 'Mitochondrial ribosomal protein S18-2 is highly expressed in endometrial cancers along with free E2F1', *Oncotarget*, 7: 22150-8.

Mitchell, M., R. Strick, P. L. Strissel, R. Dittrich, N. O. McPherson, M. Lane, G. Pliushch, R. Potabattula, T. Haaf, and N. El Hajj. 2017. 'Gene expression and epigenetic aberrations in F1-placentas fathered by obese males', *Mol Reprod Dev*, 84: 316-28.

Monnier, P., C. Martinet, J. Pontis, I. Stancheva, S. Ait-Si-Ali, and L. Dandolo. 2013. 'H19 lncRNA controls gene expression of the Imprinted Gene Network by recruiting MBD1', *Proc Natl Acad Sci U S A*, 110: 20693-8.

Monteagudo-Sánchez, A., M. Sánchez-Delgado, J. R. H. Mora, N. T. Santamaría, E. Gratacós, M. Esteller, M. L. de Heredia, V. Nunes, C. Choux, P. Fauque, G. P. de Nanclares, L. Anton, M. A. Elovitz, I. Iglesias-Platas, and D. Monk. 2019. 'Differences in expression rather than methylation at placenta-specific imprinted loci is associated with intrauterine growth restriction', *Clin Epigenetics*, 11: 35.

Mora, Jocelyn M, Mark A Fenwick, Laura Castle, Marianne Baithun, Timothy A Ryder, Margaret Mobberley, Raffaella Carzaniga, Stephen Franks, and Kate Hardy. 2012. 'Characterization and significance of adhesion and junction-related proteins in mouse ovarian follicles', *Biology of reproduction*, 86: 153, 1-14.

Moustafa, M. H., R. K. Sharma, J. Thornton, E. Mascha, M. A. Abdel-Hafez, A. J. Thomas, Jr., and A. Agarwal. 2004. 'Relationship between ROS production, apoptosis and DNA denaturation in spermatozoa from patients examined for infertility', *Hum Reprod*, 19: 129-38.

Munne, S., A. Lee, Z. Rosenwaks, J. Grifo, and J. Cohen. 1993. 'Diagnosis of major chromosome aneuploidies in human preimplantation embryos', *Hum Reprod*, 8: 2185-91.

Murphy, L. A., E. A. Seidler, D. A. Vaughan, N. Resetkova, A. S. Penzias, T. L. Toth, K. L. Thornton, and D. Sakkas. 2019. 'To test or not to test? A framework for counselling patients on preimplantation genetic testing for aneuploidy (PGT-A)', *Hum Reprod*, 34: 268-75.

Nabti, I., P. Marangos, J. Bormann, N. R. Kudo, and J. Carroll. 2014. 'Dual-mode regulation of the APC/C by CDK1 and MAPK controls meiosis I progression and fidelity', *J Cell Biol*, 204: 891-900.

Nargund, Vinod H. 2015. 'Effects of psychological stress on male fertility', *Nature Reviews Urology*, 12: 373-82.

Ng, Y. H., S. Rome, A. Jalabert, A. Forterre, H. Singh, C. L. Hincks, and L. A. Salamonsen. 2013. 'Endometrial exosomes/microvesicles in the uterine microenvironment: a new paradigm for embryo-endometrial cross talk at implantation', *PLoS One*, 8: e58502.

Niakan, K. K., J. Han, R. A. Pedersen, C. Simon, and R. A. Pera. 2012. 'Human pre-implantation embryo development', *Development*, 139: 829-41.

Nicola, C., P. K. Lala, and C. Chakraborty. 2008. 'Prostaglandin E2-mediated migration of human trophoblast requires RAC1 and CDC42', *Biol Reprod*, 78: 976-82.

Niwa, H., Y. Toyooka, D. Shimosato, D. Strumpf, K. Takahashi, R. Yagi, and J. Rossant. 2005. 'Interaction between Oct3/4 and Cdx2 determines trophectoderm differentiation', *Cell*, 123: 917-29.

O'Brien, Y., M. Wingfield, and L. C. O'Shea. 2019. 'Anti-Mullerian hormone and progesterone levels in human follicular fluid are predictors of embryonic development', *Reprod Biol Endocrinol*, 17: 47.

O'Gorman, A., M. Wallace, E. Cottell, M. J. Gibney, F. M. McAuliffe, M. Wingfield, and L. Brennan. 2013. 'Metabolic profiling of human follicular fluid identifies potential biomarkers of oocyte developmental competence', *Reproduction*, 146: 389-95.

O'Roak, B. J., L. Vives, S. Girirajan, E. Karakoc, N. Krumm, B. P. Coe, R. Levy, A. Ko, C. Lee, J. D. Smith, E. H. Turner, I. B. Stanaway, B. Vernot, M. Malig, C. Baker, B. Reilly, J. M. Akey, E. Borenstein, M. J. Rieder, D. A. Nickerson, R. Bernier, J. Shendure, and E. E. Eichler. 2012. 'Sporadic autism exomes reveal a highly interconnected protein network of de novo mutations', *Nature*, 485: 246-50.

Ocal, P., T. Cift, B. Bulut, E. Balcan, I. Cepni, B. Aydogan, and T. Irez. 2012. 'Recurrent implantation failure is more frequently seen in female patients with poor prognosis', *Int J Fertil Steril*, 6: 71-8.

Oh-McGinnis, R., A. B. Bogutz, K. Y. Lee, M. J. Higgins, and L. Lefebvre. 2010. 'Rescue of placental phenotype in a mechanistic model of Beckwith-Wiedemann syndrome', *BMC Dev Biol*, 10: 50.

Ohtake, J., M. Sakurai, Y. Hoshino, K. Tanemura, and E. Sato. 2015. 'Expression of focal adhesion kinase in mouse cumulus-oocyte complexes, and effect of phosphorylation at Tyr397 on cumulus expansion', *Mol Reprod Dev*.

Okuda, T., J. van Deursen, S. W. Hiebert, G. Grosveld, and J. R. Downing. 1996. 'AML1, the target of multiple chromosomal translocations in human leukemia, is essential for normal fetal liver hematopoiesis', *Cell*, 84: 321-30.

Ono, K., and J. Han. 2000. 'The p38 signal transduction pathway: activation and function', *Cell Signal*, 12: 1-13.

Otsuki, J., T. Iwasaki, N. Enatsu, Y. Katada, K. Furuhashi, and M. Shiotani. 2019. 'Noninvasive embryo selection: kinetic analysis of female and male pronuclear development to predict embryo quality and potential to produce live birth', *Fertil Steril*, 112: 874-81.

Ouandaogo, Z. G., D. Haouzi, S. Assou, H. Dechaud, I. J. Kadoch, J. De Vos, and S. Hamamah. 2011. 'Human cumulus cells molecular signature in relation to oocyte nuclear maturity stage', *PLoS One*, 6: e27179.

Ozkan, S., W. Murk, and A. Arici. 2008. 'Endometriosis and infertility: epidemiology and evidence-based treatments', *Ann N Y Acad Sci*, 1127: 92-100.

Palermo, G. D., C. L. O'Neill, S. Chow, S. Cheung, A. Parrella, N. Pereira, and Z. Rosenwaks. 2017. 'Intracytoplasmic sperm injection: state of the art in humans', *Reproduction*, 154: F93-F110.

Paley, S., and P. D. Karp. 2017. 'Update notifications for the BioCyc collection of databases', *Database (Oxford)*, 2017.

Pan, Q., and N. Chegini. 2008. 'MicroRNA signature and regulatory functions in the endometrium during normal and disease states', *Semin Reprod Med*, 26: 479-93.

Pan, Y., F. Ren, W. Zhang, G. Liu, D. Yang, J. Hu, K. Feng, and Y. Feng. 2014. 'Regulation of BGC-823 cell sensitivity to adriamycin via miRNA-135a-5p', *Oncol Rep*, 32: 2549-56.

Pang, R. T., W. M. Liu, C. O. Leung, T. M. Ye, P. C. Kwan, K. F. Lee, and W. S. Yeung. 2011. 'miR-135A regulates preimplantation embryo development through down-regulation of E3 Ubiquitin Ligase Seven In Absentia Homolog 1A (SIAH1A) expression', *PLoS One*, 6: e27878.

Patrizio, P., and A. L. Caplan. 2010. 'Ethical issues surrounding fertility preservation in cancer patients', *Clin Obstet Gynecol*, 53: 717-26.

Patrizio, P., and D. Sakkas. 2009. 'From oocyte to baby: a clinical evaluation of the biological efficiency of in vitro fertilization', *Fertil Steril*, 91: 1061-6.

Pelland, Amélie MD, Hannah E Corbett, and Jay M Baltz. 2009. 'Amino acid transport mechanisms in mouse oocytes during growth and meiotic maturation', *Biology of reproduction*, 81: 1041-54.

Pfaffl, M. W., G. W. Horgan, and L. Dempfle. 2002. 'Relative expression software tool (REST) for group-wise comparison and statistical analysis of relative expression results in real-time PCR', *Nucleic Acids Res*, 30: e36.

Planaguma, J., M. Diaz-Fuertes, A. Gil-Moreno, M. Abal, M. Monge, A. Garcia, T. Baro, T. M. Thomson, J. Xercavins, F. Alameda, and J. Reventos. 2004. 'A differential gene expression profile reveals overexpression of RUNX1/AML1 in invasive endometrioid carcinoma', *Cancer Res*, 64: 8846-53.

Plancha, Carlos E, Alexandra Sanfins, Patrícia Rodrigues, and David Albertini. 2005. 'Cell polarity during folliculogenesis and oogenesis', *Reproductive biomedicine online*, 10: 478-84.

Pollard, J. W., J. S. Hunt, W. Wiktor-Jedrzejczak, and E. R. Stanley. 1991. 'A pregnancy defect in the osteopetrotic (op/op) mouse demonstrates the requirement for CSF-1 in female fertility', *Dev Biol*, 148: 273-83.

Prates, E. G., J. T. Nunes, and R. M. Pereira. 2014. 'A role of lipid metabolism during cumulus-oocyte complex maturation: impact of lipid modulators to improve embryo production', *Mediators Inflamm*, 2014: 692067.

Pribenszky, C., A. M. Nilselid, and M. Montag. 2017. 'Time-lapse culture with morphokinetic embryo selection improves pregnancy and live birth chances and reduces early pregnancy loss: a meta-analysis', *Reprod Biomed Online*, 35: 511-20.

Prickett, D., and M. Watson. 2009. 'Use of GenMAPP and MAPPFinder to analyse pathways involved in chickens infected with the protozoan parasite Eimeria', *BMC Proc*, 3 Suppl 4: S7.

Prunskaite-Hyyrylainen, R., J. Shan, A. Railo, K. M. Heinonen, I. Miinalainen, W. Yan, B. Shen, C. Perreault, and S. J. Vainio. 2014. 'Wnt4, a pleiotropic signal for

controlling cell polarity, basement membrane integrity, and antimullerian hormone expression during oocyte maturation in the female follicle', *FASEB J*, 28: 1568-81.

Quenneville, S., G. Verde, A. Corsinotti, A. Kapopoulou, J. Jakobsson, S. Offner, I. Baglivo, P. V. Pedone, G. Grimaldi, A. Riccio, and D. Trono. 2011. 'In embryonic stem cells, ZFP57/KAP1 recognize a methylated hexanucleotide to affect chromatin and DNA methylation of imprinting control regions', *Mol Cell*, 44: 361-72.

Quinn, P., and F. C. Horstman. 1998. 'Is the mouse a good model for the human with respect to the development of the preimplantation embryo in vitro?', *Hum Reprod*, 13 Suppl 4: 173-83.

Racowsky, C., L. Ohno-Machado, J. Kim, and J. D. Biggers. 2009. 'Is there an advantage in scoring early embryos on more than one day?', *Hum Reprod*, 24: 2104-13.

Rahiminejad, M. E., A. Moaddab, M. Ebrahimi, S. Rabiee, A. Zamani, M. Ezzati, and A. Abdollah Shamshirsaz. 2015. 'The relationship between some endometrial secretion cytokines and in vitro fertilization', *Iran J Reprod Med*, 13: 557-62.

Rahiminejad, M. E., A. Moaddab, M. Ganji, N. Eskandari, M. Yepez, S. Rabiee, M. Wise, R. Ruano, and A. Ranjbar. 2016. 'Oxidative stress biomarkers in endometrial secretions: A comparison between successful and unsuccessful in vitro fertilization cycles', *J Reprod Immunol*, 116: 70-5.

Redzovic, A., G. Laskarin, M. Dominovic, H. Haller, and D. Rukavina. 2013. 'Mucins help to avoid alloreactivity at the maternal fetal interface', *Clin Dev Immunol*, 2013: 542152.

Relaix, F., Xj Wei, W. Li, J. Pan, Y. Lin, D. D. Bowtell, D. A. Sassoon, and X. Wu. 2000. 'Pw1/Peg3 is a potential cell death mediator and cooperates with Siah1a in p53-mediated apoptosis', *Proc Natl Acad Sci U S A*, 97: 2105-10.

Revel, Ariel, Hanna Achache, Juliet Stevens, Yoav Smith, and Reuven Reich. 2011. 'MicroRNAs are associated with human embryo implantation defects', *Human Reproduction*, 26: 2830-40.

Rives, N, G Joly, A Machy, N Simeon, P Leclerc, and B Mace. 2000. 'Assessment of sex chromosome aneuploidy in sperm nuclei from 47, XXY and 46, XY/47, XXY males: comparison with fertile and infertile males with normal karyotype', *Molecular human reproduction*, 6: 107-12.

Rizk, B., R. Turki, H. Lotfy, S. Ranganathan, H. Zahed, A. R. Freeman, Z. Shilbayeh, M. Sassy, M. Shalaby, and R. Malik. 2015. 'Surgery for endometriosis-associated infertility: do we exaggerate the magnitude of effect?', *Facts Views Vis Obgyn*, 7: 109-18.

Rosenbluth, E. M., D. N. Shelton, L. M. Wells, A. E. Sparks, and B. J. Van Voorhis. 2014. 'Human embryos secrete microRNAs into culture media--a potential biomarker for implantation', *Fertil Steril*, 101: 1493-500.

Rosenwaks, Z., O. K. Davis, and M. A. Damario. 1995. 'The role of maternal age in assisted reproduction', *Hum Reprod*, 10 Suppl 1: 165-73.

Rubio, C., L. Rienzi, L. Navarro-Sanchez, D. Cimadomo, C. M. Garcia-Pascual, L. Albricci, D. Soscia, D. Valbuena, A. Capalbo, F. Ubaldi, and C. Simon. 2019. 'Embryonic cell-free DNA versus trophectoderm biopsy for aneuploidy testing: concordance rate and clinical implications', *Fertil Steril*, 112: 510-19.

Rubio, C., C. Simon, A. Mercader, J. Garcia-Velasco, J. Remohi, and A. Pellicer. 2000. 'Clinical experience employing co-culture of human embryos with autologous human endometrial epithelial cells', *Hum Reprod*, 15 Suppl 6: 31-8.

Ruiz-Alonso, M., D. Blesa, P. Diaz-Gimeno, E. Gomez, M. Fernandez-Sanchez, F. Carranza, J. Carrera, F. Vilella, A. Pellicer, and C. Simon. 2013. 'The endometrial receptivity array for diagnosis and personalized embryo transfer as a treatment for patients with repeated implantation failure', *Fertil Steril*, 100: 818-24.

Ruiz-Alonso, M., D. Blesa, and C. Simon. 2012. 'The genomics of the human endometrium', *Biochim Biophys Acta*, 1822: 1931-42.

Saalu, L. C. 2010. 'The incriminating role of reactive oxygen species in idiopathic male infertility: an evidence based evaluation', *Pak J Biol Sci*, 13: 413-22.

Saeed-Zidane, Mohammed, Lea Linden, Dessie Salilew-Wondim, Eva Held, Christiane Neuhoff, Ernst Tholen, Michael Hoelker, Karl Schellander, and Dawit Tesfaye. 2017. 'Cellular and exosome mediated molecular defense mechanism in bovine granulosa cells exposed to oxidative stress', *PLoS One*, 12: e0187569.

Sahin, L., M. Bozkurt, H. Sahin, A. Gurel, and A. E. Yumru. 2014. 'Is preimplantation genetic diagnosis the ideal embryo selection method in aneuploidy screening?', *Kaohsiung J Med Sci*, 30: 491-8.

Sakkas, D., O. Moffatt, G. C. Manicardi, E. Mariethoz, N. Tarozzi, and D. Bizzaro. 2002. 'Nature of DNA damage in ejaculated human spermatozoa and the possible involvement of apoptosis', *Biol Reprod*, 66: 1061-7.

Salam, R. A., J. K. Das, and Z. A. Bhutta. 2014. 'Impact of intrauterine growth restriction on long-term health', *Curr Opin Clin Nutr Metab Care*, 17: 249-54.

Sanchez-Delgado, M., A. Riccio, T. Eggermann, E. R. Maher, P. Lapunzina, D. Mackay, and D. Monk. 2016. 'Causes and Consequences of Multi-Locus Imprinting Disturbances in Humans', *Trends Genet*, 32: 444-55.

Santonocito, M., M. R. Guglielmino, M. Vento, M. Ragusa, D. Barbagallo, P. Borzi, I. Casciano, P. Scollo, M. Romani, C. Tatone, M. Purrello, and C. Di Pietro. 2013. 'The apoptotic transcriptome of the human MII oocyte: characterization and age-related changes', *Apoptosis*, 18: 201-11.

Santonocito, M., M. Vento, M. R. Guglielmino, R. Battaglia, J. Wahlgren, M. Ragusa, D. Barbagallo, P. Borzi, S. Rizzari, M. Maugeri, P. Scollo, C. Tatone, H. Valadi, M. Purrello, and C. Di Pietro. 2014. 'Molecular characterization of exosomes and their microRNA cargo in human follicular fluid: bioinformatic analysis reveals that exosomal microRNAs control pathways involved in follicular maturation', *Fertil Steril*, 102: 1751-61 e1.

Sarapik, A., A. Velthut, K. Haller-Kikkatalo, G. C. Faure, M. C. Bene, M. de Carvalho Bittencourt, F. Massin, R. Uibo, and A. Salumets. 2012. 'Follicular proinflammatory cytokines and chemokines as markers of IVF success', *Clin Dev Immunol*, 2012: 606459.

Schaubach, B. M., H. Y. Wen, and R. E. Kellems. 2006. 'Regulation of murine Ada gene expression in the placenta by transcription factor RUNX1', *Placenta*, 27: 269-77.

Schoolcraft, W. B., M. G. Katz-Jaffe, J. Stevens, M. Rawlins, and S. Munne. 2009. 'Preimplantation aneuploidy testing for infertile patients of advanced maternal age: a randomized prospective trial', *Fertil Steril*, 92: 157-62.

Schoolcraft, W. B., N. R. Treff, J. M. Stevens, K. Ferry, M. Katz-Jaffe, and R. T. Scott, Jr. 2011. 'Live birth outcome with trophectoderm biopsy, blastocyst vitrification, and single-nucleotide polymorphism microarray-based comprehensive chromosome screening in infertile patients', *Fertil Steril*, 96: 638-40.

Schroeder, D. I., and J. M. LaSalle. 2013. 'How has the study of the human placenta aided our understanding of partially methylated genes?', *Epigenomics*, 5: 645-54.

Schroeder, D. I., R. J. Schmidt, F. K. Crary-Dooley, C. K. Walker, S. Ozonoff, D. J. Tancredi, I. Hertz-Picciotto, and J. M. LaSalle. 2016. 'Placental methylome analysis from a prospective autism study', *Mol Autism*, 7: 51.

Schweigert, F. J., B. Gericke, W. Wolfram, U. Kaisers, and J. W. Dudenhausen. 2006. 'Peptide and protein profiles in serum and follicular fluid of women undergoing IVF', *Hum Reprod*, 21: 2960-8.

Selice, R, A Di Mambro, A Garolla, V Ficarra, M Lafrate, A Ferlin, and Carlo Foresta. 2010. 'Spermatogenesis in Klinefelter syndrome', *Journal of endocrinological investigation*, 33: 789-93.

Sengupta, P., E. Borges, Jr., S. Dutta, and E. Krajewska-Kulak. 2018. 'Decline in sperm count in European men during the past 50 years', *Hum Exp Toxicol*, 37: 247-55.

Sermondade, N, C Faure, L Fezeu, AG Shayeb, Jens Peter Bonde, Tina Kold Jensen, Madelon Van Wely, J Cao, Ana Carolina Martini, and M Eskandar. 2013. 'BMI in relation to sperm count: an updated systematic review and collaborative meta-analysis', *Human reproduction update*, 19: 221-31.

Shamsi, M. B., K. Kumar, and R. Dada. 2011. 'Genetic and epigenetic factors: Role in male infertility', *Indian journal of urology : IJU : journal of the Urological Society of India*, 27: 110-20.

Shapiro, B. S., S. T. Daneshmand, J. Desai, F. C. Garner, M. Aguirre, and C. Hudson. 2016. 'The risk of embryo-endometrium asynchrony increases with maternal age after ovarian stimulation and IVF', *Reprod Biomed Online*, 33: 50-5.

Sharma, N., C. Kubaczka, S. Kaiser, D. Nettersheim, S. S. Mughal, S. Riesenberg, M. Holzel, E. Winterhager, and H. Schorle. 2016. 'Tpbpa-Cre-mediated deletion of TFAP2C leads to deregulation of Cdkn1a, Akt1 and the ERK pathway, causing placental growth arrest', *Development*, 143: 787-98.

Sharma, R. K., E. Sabanegh, R. Mahfouz, S. Gupta, A. Thiyagarajan, and A. Agarwal. 2010. 'TUNEL as a test for sperm DNA damage in the evaluation of male infertility', *Urology*, 76: 1380-6.

Sharma, Reecha, Avi Harlev, Ashok Agarwal, and Sandro C Esteves. 2016. 'Cigarette smoking and semen quality: a new meta-analysis examining the effect of the 2010 World Health Organization laboratory methods for the examination of human semen', *European urology*, 70: 635-45.

Shebl, O., I. Sifferlinger, A. Habelsberger, P. Oppelt, R. B. Mayer, E. Petek, and T. Ebner. 2017. 'Oocyte competence in in vitro fertilization and intracytoplasmic sperm injection patients suffering from endometriosis and its possible association with subsequent treatment outcome: a matched case-control study', *Acta Obstet Gynecol Scand*, 96: 736-44.

Simon, Alexander M, and Daniel A Goodenough. 1998. 'Diverse functions of vertebrate gap junctions', *Trends in cell biology*, 8: 477-83.

Simon, C., M. J. Gimeno, A. Mercader, J. E. O'Connor, J. Remohi, M. L. Polan, and A. Pellicer. 1997. 'Embryonic regulation of integrins beta 3, alpha 4, and alpha 1 in human endometrial epithelial cells in vitro', *J Clin Endocrinol Metab*, 82: 2607-16.

Simon, C., C. Gomez, S. Cabanillas, I. Vladimirov, G. Castillon, J. Giles, K. Boynukalin, N. Findikli, M. Bahceci, I. Ortega, C. Vidal, M. Funabiki, A. Izquierdo, L. Lopez, S. Portela, N. Frantz, M. Kulmann, S. Taguchi, E. Labarta, F. Colucci, S. Mackens, X. Santamaria, E. Munoz, S. Barrera, J. A. Garcia-Velasco, M. Fernandez, M. Ferrando, M. Ruiz, B. W. Mol, D. Valbuena, and Era-Rct Study Consortium Group. 2020. 'A 5-year multicentre randomized controlled trial comparing personalized, frozen and fresh blastocyst transfer in IVF', *Reprod Biomed Online*, 41: 402-15.

Simon, C., A. Mercader, J. Garcia-Velasco, G. Nikas, C. Moreno, J. Remohi, and A. Pellicer. 1999. 'Coculture of human embryos with autologous human endometrial epithelial cells in patients with implantation failure', *J Clin Endocrinol Metab*, 84: 2638-46.

Simon, C., C. Moreno, J. Remohi, and A. Pellicer. 1998. 'Molecular interactions between embryo and uterus in the adhesion phase of human implantation', *Hum Reprod*, 13 Suppl 3: 219-32; discussion 33-6.

Simon, L., and D. T. Carrell. 2013. 'Sperm DNA damage measured by comet assay', *Methods Mol Biol*, 927: 137-46.

Smith, R. G., A. Reichenberg, R. L. Kember, J. D. Buxbaum, L. C. Schalkwyk, C. Fernandes, and J. Mill. 2013. 'Advanced paternal age is associated with altered DNA methylation at brain-expressed imprinted loci in inbred mice: implications for neuropsychiatric disease', *Mol Psychiatry*, 18: 635-6.

Sood, R., J. L. Zehnder, M. L. Druzin, and P. O. Brown. 2006. 'Gene expression patterns in human placenta', *Proc Natl Acad Sci U S A*, 103: 5478-83.

Stewart, C. L., P. Kaspar, L. J. Brunet, H. Bhatt, I. Gadi, F. Kontgen, and S. J. Abbondanzo. 1992. 'Blastocyst implantation depends on maternal expression of leukaemia inhibitory factor', *Nature*, 359: 76-9.

Stigliani, S., P. Anserini, P. L. Venturini, and P. Scaruffi. 2013. 'Mitochondrial DNA content in embryo culture medium is significantly associated with human embryo fragmentation', *Hum Reprod*, 28: 2652-60.

Stigliani, S., L. Persico, C. Lagazio, P. Anserini, P. L. Venturini, and P. Scaruffi. 2014. 'Mitochondrial DNA in Day 3 embryo culture medium is a novel, non-invasive biomarker of blastocyst potential and implantation outcome', *Mol Hum Reprod*, 20: 1238-46.

Storr, A., C. A. Venetis, S. Cooke, S. Kilani, and W. Ledger. 2017. 'Inter-observer and intra-observer agreement between embryologists during selection of a single Day 5 embryo for transfer: a multicenter study', *Hum Reprod*, 32: 307-14.

Sugiura, K., F. L. Pendola, and J. J. Eppig. 2005. 'Oocyte control of metabolic cooperativity between oocytes and companion granulosa cells: energy metabolism', *Dev Biol*, 279: 20-30.

Sugiyama, R., A. Fuzitou, C. Takahashi, O. Akutagawa, H. Ito, K. Nakagawa, R. Sugiyama, and K. Isaka. 2010. 'Bone morphogenetic protein 2 may be a good

predictor of success in oocyte fertilization during assisted reproductive technology', *Hum Cell*, 23: 83-8.

Swain, J. E. 2010. 'Optimizing the culture environment in the IVF laboratory: impact of pH and buffer capacity on gamete and embryo quality', *Reprod Biomed Online*, 21: 6-16.

Swain, J. E., D. Carrell, A. Cobo, M. Meseguer, C. Rubio, and G. D. Smith. 2016. 'Optimizing the culture environment and embryo manipulation to help maintain embryo developmental potential', *Fertil Steril*, 105: 571-87.

Talbert, Paul B, and Steven Henikoff. 2006. 'Spreading of silent chromatin: inaction at a distance', *Nature Reviews Genetics*, 7: 793-803.

Tamaru, Hisashi, and Eric U Selker. 2001. 'A histone H3 methyltransferase controls DNA methylation in Neurospora crassa', *Nature*, 414: 277-83.

Tan, J., A. Kan, J. Hitkari, B. Taylor, N. Tallon, G. Warraich, A. Yuzpe, and G. Nakhuda. 2018. 'The role of the endometrial receptivity array (ERA) in patients who have failed euploid embryo transfers', *J Assist Reprod Genet*, 35: 683-92.

Tapia-Pizarro, A., P. Figueroa, J. Brito, J. C. Marin, D. J. Munroe, and H. B. Croxatto. 2014. 'Endometrial gene expression reveals compromised progesterone signaling in women refractory to embryo implantation', *Reprod Biol Endocrinol*, 12: 92.

Tapia, A., C. Vilos, J. C. Marin, H. B. Croxatto, and L. Devoto. 2011. 'Bioinformatic detection of E47, E2F1 and SREBP1 transcription factors as potential regulators of genes associated to acquisition of endometrial receptivity', *Reprod Biol Endocrinol*, 9: 14.

Tariq, Muhammad, Hidetoshi Saze, Aline V Probst, Jacek Lichota, Yoshiki Habu, and Jerzy Paszkowski. 2003. 'Erasure of CpG methylation in Arabidopsis alters patterns of histone H3 methylation in heterochromatin', *Proceedings of the National Academy of Sciences*, 100: 8823-27.

Taylor, R. N., D. I. Lebovic, D. Hornung, and M. D. Mueller. 2001. 'Endocrine and paracrine regulation of endometrial angiogenesis', *Ann N Y Acad Sci*, 943: 109-21.

Thie, M., B. Harrach-Ruprecht, H. Sauer, P. Fuchs, A. Albers, and H. W. Denker. 1995. 'Cell adhesion to the apical pole of epithelium: a function of cell polarity', *Eur J Cell Biol*, 66: 180-91.

Thiyagarajan, D. K., H. Basit, and R. Jeanmonod. 2021. 'Physiology, Menstrual Cycle.' in, *StatPearls* (StatPearls Publishing

Copyright © 2021, StatPearls Publishing LLC.: Treasure Island (FL)).

Thoma, M. E., A. C. McLain, J. F. Louis, R. B. King, A. C. Trumble, R. Sundaram, and G. M. Buck Louis. 2013. 'Prevalence of infertility in the United States as estimated by the current duration approach and a traditional constructed approach', *Fertil Steril*, 99: 1324-31 e1.

Tilley, S. K., E. M. Martin, L. Smeester, R. M. Joseph, K. C. K. Kuban, T. C. Heeren, O. U. Dammann, T. M. O'Shea, and R. C. Fry. 2018. 'Placental CpG methylation of infants born extremely preterm predicts cognitive impairment later in life', *PLoS One*, 13: e0193271.

Toure, D. M., L. Baccaglini, S. T. Opoku, D. Barnes-Josiah, R. Cox, T. Hartman, and D. Klinkebiel. 2016. 'Epigenetic dysregulation of Insulin-like growth factor (IGF)-related genes and adverse pregnancy outcomes: a systematic review', *J Matern Fetal Neonatal Med*, 29: 3542-52.

Tran, D., S. Cooke, P. J. Illingworth, and D. K. Gardner. 2019. 'Deep learning as a predictive tool for fetal heart pregnancy following time-lapse incubation and blastocyst transfer', *Hum Reprod*, 34: 1011-18.

Ullah, K., T. U. Rahman, H. T. Pan, M. X. Guo, X. Y. Dong, J. Liu, L. Y. Jin, Y. Cheng, Z. H. Ke, J. Ren, X. H. Lin, X. X. Qiu, T. T. Wang, H. F. Huang, and J. Z. Sheng. 2017. 'Serum estradiol levels in controlled ovarian stimulation directly affect the endometrium', *J Mol Endocrinol*, 59: 105-19.

van der Gaast, M. H., K. Beier-Hellwig, B. C. Fauser, H. M. Beier, and N. S. Macklon. 2003. 'Endometrial secretion aspiration prior to embryo transfer does not reduce implantation rates', *Reprod Biomed Online*, 7: 105-9.

van der Steeg, J. W., P. Steures, M. J. Eijkemans, F. Habbema JD, P. G. Hompes, J. A. Kremer, L. van der Leeuw-Harmsen, P. M. Bossuyt, S. Repping, S. J. Silber, B. W. Mol, F. van der Veen, and Group Collaborative Effort for Clinical Evaluation in Reproductive Medicine Study. 2011. 'Role of semen analysis in subfertile couples', *Fertil Steril*, 95: 1013-9.

van der Weiden, R. M., F. M. Helmerhorst, and M. J. Keirse. 1991. 'Influence of prostaglandins and platelet activating factor on implantation', *Hum Reprod*, 6: 436-42.

van Weert, J. M., S. Repping, B. J. Van Voorhis, F. van der Veen, P. M. Bossuyt, and B. W. Mol. 2004. 'Performance of the postwash total motile sperm count as a predictor of pregnancy at the time of intrauterine insemination: a meta-analysis', *Fertil Steril*, 82: 612-20.

Varrault, A., C. Gueydan, A. Delalbre, A. Bellmann, S. Houssami, C. Aknin, D. Severac, L. Chotard, M. Kahli, A. Le Digarcher, P. Pavlidis, and L. Journot. 2006. 'Zac1 regulates an imprinted gene network critically involved in the control of embryonic growth', *Dev Cell*, 11: 711-22.

Vasconcelos, S., C. Ramalho, C. J. Marques, and S. Doria. 2019. 'Altered expression of epigenetic regulators and imprinted genes in human placenta and fetal tissues from second trimester spontaneous pregnancy losses', *Epigenetics*, 14: 1234-44.

Vera-Rodriguez, M., A. Diez-Juan, J. Jimenez-Almazan, S. Martinez, R. Navarro, V. Peinado, A. Mercader, M. Meseguer, D. Blesa, I. Moreno, D. Valbuena, C. Rubio, and C. Simon. 2018. 'Origin and composition of cell-free DNA in spent medium from human embryo culture during preimplantation development', *Hum Reprod*, 33: 745-56.

Vilella, F., L. Ramirez, O. Berlanga, S. Martinez, P. Alama, M. Meseguer, A. Pellicer, and C. Simon. 2013. 'PGE2 and PGF2alpha concentrations in human endometrial fluid as biomarkers for embryonic implantation', *J Clin Endocrinol Metab*, 98: 4123-32.

Wallace, M., E. Cottell, M. J. Gibney, F. M. McAuliffe, M. Wingfield, and L. Brennan. 2012. 'An investigation into the relationship between the metabolic profile of follicular fluid, oocyte developmental potential, and implantation outcome', *Fertil Steril*, 97: 1078-84 e1-8.

Wang, B., J. Z. Sheng, R. H. He, Y. L. Qian, F. Jin, and H. F. Huang. 2008. 'High expression of L-selectin ligand in secretory endometrium is associated with better endometrial receptivity and facilitates embryo implantation in human being', *Am J Reprod Immunol*, 60: 127-34.

Wang, H. 2016. 'Predicting MicroRNA Biomarkers for Cancer Using Phylogenetic Tree and Microarray Analysis', *Int J Mol Sci*, 17.

Wang, H. X., F. R. Tekpetey, and G. M. Kidder. 2009. 'Identification of WNT/beta-CATENIN signaling pathway components in human cumulus cells', *Mol Hum Reprod*, 15: 11-7.

Wang, Q., T. Stacy, M. Binder, M. Marin-Padilla, A. H. Sharpe, and N. A. Speck. 1996. 'Disruption of the Cbfa2 gene causes necrosis and hemorrhaging in the central nervous system and blocks definitive hematopoiesis', *Proc Natl Acad Sci U S A*, 93: 3444-9.

Wathlet, S., T. Adriaenssens, I. Segers, G. Verheyen, R. Janssens, W. Coucke, P. Devroey, and J. Smitz. 2012. 'New candidate genes to predict pregnancy outcome in single embryo transfer cycles when using cumulus cell gene expression', *Fertil Steril*, 98: 432-9 e1-4.

Weimar, C. H., E. D. Post Uiterweer, G. Teklenburg, C. J. Heijnen, and N. S. Macklon. 2013. 'In-vitro model systems for the study of human embryo-endometrium interactions', *Reprod Biomed Online*, 27: 461-76.

Weinhold, B. 2006. 'Epigenetics: the science of change', *Environ Health Perspect*, 114: A160-7.

Wenzl, R., L. Kiesel, J. C. Huber, and F. Wieser. 2003. 'Endometriosis: a genetic disease', *Drugs Today (Barc)*, 39: 961-72.

Wiechens, N., K. Heinle, L. Englmeier, A. Schohl, and F. Fagotto. 2004. 'Nucleo-cytoplasmic shuttling of Axin, a negative regulator of the Wnt-beta-catenin Pathway', *J Biol Chem*, 279: 5263-7.

Wilcox, A. J., D. D. Baird, and C. R. Weinberg. 1999. 'Time of implantation of the conceptus and loss of pregnancy', *N Engl J Med*, 340: 1796-9.

Wong, K. M., S. Repping, and S. Mastenbroek. 2014. 'Limitations of embryo selection methods', *Semin Reprod Med*, 32: 127-33.

Wu, Christopher, Larry I Lipshultz, and Jason R Kovac. 2016. 'The role of advanced paternal age in modern reproductive medicine', *Asian journal of andrology*, 18: 425.

Wu, H., C. Ding, X. Shen, J. Wang, R. Li, B. Cai, Y. Xu, Y. Zhong, and C. Zhou. 2015. 'Medium-based noninvasive preimplantation genetic diagnosis for human alpha-thalassemias-SEA', *Medicine (Baltimore)*, 94: e669.

Xu, J., R. Fang, L. Chen, D. Chen, J. P. Xiao, W. Yang, H. Wang, X. Song, T. Ma, S. Bo, C. Shi, J. Ren, L. Huang, L. Y. Cai, B. Yao, X. S. Xie, and S. Lu. 2016. 'Noninvasive chromosome screening of human embryos by genome sequencing of embryo culture medium for in vitro fertilization', *Proc Natl Acad Sci U S A*, 113: 11907-12.

Yamaguchi, Y., C. Tayama, J. Tomikawa, R. Akaishi, H. Kamura, K. Matsuoka, N. Wake, H. Minakami, K. Kato, T. Yamada, K. Nakabayashi, and K. Hata. 2019. 'Placenta-specific epimutation at H19-DMR among common pregnancy complications: its frequency and effect on the expression patterns of H19 and IGF2', *Clin Epigenetics*, 11: 113.

Yang, G., R. Zhang, X. Chen, Y. Mu, J. Ai, C. Shi, Y. Liu, C. Shi, L. Sun, N. G. Rainov, H. Li, B. Yang, and S. Zhao. 2011. 'MiR-106a inhibits glioma cell growth by targeting E2F1 independent of p53 status', *J Mol Med (Berl)*, 89: 1037-50.

Yang, L., Q. Lv, W. Chen, J. Sun, Y. Wu, Y. Wang, X. Chen, X. Chen, and Z. Zhang. 2017. 'Presence of embryonic DNA in culture medium', *Oncotarget*, 8: 67805-09.

Yerushalmi, G. M., M. Salmon-Divon, Y. Yung, E. Maman, A. Kedem, L. Ophir, O. Elemento, G. Coticchio, M. Dal Canto, M. Mignini Renzinu, R. Fadini, and A. Hourvitz. 2014. 'Characterization of the human cumulus cell transcriptome during final follicular maturation and ovulation', *Mol Hum Reprod*, 20: 719-35.

Ying, T. H., C. J. Tseng, S. J. Tsai, S. C. Hsieh, H. Z. Lee, Y. H. Hsieh, and D. T. Bau. 2011. 'Association of p53 and CDKN1A genotypes with endometriosis', *Anticancer Res*, 31: 4301-6.

Zegers-Hochschild, F., G. D. Adamson, J. de Mouzon, O. Ishihara, R. Mansour, K. Nygren, E. Sullivan, S. van der Poel, Technology International Committee for Monitoring Assisted Reproductive, and Organization World Health. 2009. 'The International Committee for Monitoring Assisted Reproductive Technology (ICMART) and the World Health Organization (WHO) Revised Glossary on ART Terminology, 2009', *Hum Reprod*, 24: 2683-7.

Zhang, J. 2015. 'Revisiting germinal vesicle transfer as a treatment for aneuploidy in infertile women with diminished ovarian reserve', *J Assist Reprod Genet*, 32: 313-7.

Zhao, Z., H. Shi, J. Li, Y. Zhang, C. Chen, and Y. Guo. 2020. 'Cumulative live birth rates according to the number of oocytes retrieved following the "freeze-all" strategy', *Reprod Biol Endocrinol*, 18: 14.

Zivi, E., D. Barash, E. Aizenman, D. Gibson, and Y. Shufaro. 2014. 'Zygote serine decreased uptake from the fertilization medium is associated with implantation and pregnancy', *J Assist Reprod Genet*, 31: 889-97.

14.0 **Appendix 1. Published abstracts as first author**

Jason C. Parks, Alyssa L. Patton, Blair R. McCallie, Darren K. Griffin, William B. Schoolcraft, Mandy G. Katz-Jaffe. *Secreted Endometrial Microrna Gene Regulators Are Critical For Successful Embryo Implantation*. Presented at 2015 ASRM Conference in Baltimore, Maryland.

Objective: Successful implantation is dependent on the intricate dialogue between a viable embryo and a receptive endometrium. On the maternal side, specific adhesion changes need to occur for blastocyst attachment, in addition to tight regulation of key signaling molecules in the microenvironment of the implanting embryo. This study investigated the mammalian uterine fluid secretome prior to embryo transfer, utilizing two sampling techniques, to examine the microRNAome in association with implantation outcome.

Design: Research study

Materials and Methods: In vivo fertilized zygotes collected from super ovulated female BDF-1 mice were cultured to the blastocyst stage. Hatching blastocysts were either collected for gene expression analysis using qRT-PCR (n=12) or selected for transfer into each uterine horn (n= 4/horn) of a pseudopregnant BDF-1 recipient mouse (n=16). Immediately prior to embryo transfer, a uterine lavage or aspirate was collected (n=32). On Day 16 of embryo development, implantation outcome was noted. Endometrial tissue was also biopsied from pseudopregnant mice not receiving an embryo transfer (n=12). Uterine lavage, aspiration and endometrial tissue samples were analyzed for expression

of 306 miRNAs using the TaqMan® Rodent MicroRNA Array (Thermo Fisher) and analyzed for significance in association with implantation outcome using REST© statistical software (Qiagen).

Results: Analysis of the two uterine fluid sampling techniques revealed no similarities in miRNA expression profiles in relation to implantation. Uterine aspirates that resulted in positive implantation, displayed 18 increased, and 7 decreased miRNAs ($P<0.05$). Notably, mir-101a, a conserved miRNA between human and mouse, showed increased expression in uterine aspirates with positive pregnancy. Expression of miR-101a was observed in receptive endometrial tissue. There are seven known validated target genes for miR-101a including, Akt1, a gene responsible for the mitigation of trophoblast migration. Increased miR-101a expression, as observed in positive outcome uterine aspirates, has been shown to mediate Akt1 activation. Akt1 expression was identified specifically in hatching blastocysts.

Conclusions: The embryo-endometrial interaction is crucial to implantation success. Secreted uterine miRNAs characterize the maternal molecular dialogue, and are internalized by the trophectoderm to function as transcriptomic regulators, either promoting or inhibiting blastocyst development and adhesion. For miR-101a, increased expression mediates blastocyst Akt1 expression thereby improving the likelihood of implantation success. In conclusion, the uterine aspirate miRNAome represents a minimally invasive method to assess the embryo-endometrial interaction.

Jason C Parks, Blair McCallie, Julie A Reisz, Matthew Wither, William B Schoolcraft, Mandy G Katz-Jaffe. *Maternal endometrial secretions 24 hours prior to frozen embryo transfer is predictive of implantation outcome*. Presented at 2016 ASRM Conference in Salt Lake City, Utah.

Objective: It is well known that successful implantation is dependent on the intricate dialogue between a competent embryo and a receptive endometrium. On the maternal side, specific biological changes in adhesion need to occur for blastocyst attachment, while tight regulation of signaling pathways are crucial for the invading embryo. The objective of this study was to examine the uterine fluid milieu in association with implantation outcome 24 hours prior to, and at the time of euploid embryo transfer.

Design: Research study

Materials and methods: Infertile patients (n=48) were recruited with IRB consent prior to an estradiol/progesterone replacement frozen embryo transfer (FET) with euploid blastocysts. Uterine secretions were collected by gentle aspiration (~2-5ul), either 24h prior to, or at the time of FET. Uterine secretome analysis was performed blinded of implantation outcome using qPCR for miRNA analysis (n=12) and mass spectrometry (n=36) for metabolite (UHPLS-MS, Thermo) and protein analysis (LC-MS/MS, Thermo). MiRNA profiles were analyzed by REST© statistical software. MS data was converted with MassMatrix and processed with Maven (Princeton Univ). MS/MS data was examined using Mascot™ (v 2.2) and Scaffold (v 2.06). Validation of target genes was performed

using qPCR on endometrial biopsies (n=14) and surplus cryopreserved blastocysts (n=14) donated with patient consent.

Results: A notable uterine secretome profile of miRNA, metabolites and proteins was significantly associated with a negative, toxic environment both 24hrs prior to, and at the time of embryo transfer ($P<0.05$, >2 fold change). Specifically, 6 maternal miRNAs showed increased expression with negative implantation, including miR-17 ($P<0.05$). A known target gene of miR-17 through negative regulation is VEGFA, a signal protein essential for implantation and secreted by the receiving endometrium as well as the implanting embryo. Validation of VEGFA expression was confirmed in epithelial endometrial cells and individual blastocysts. A total of 12 amino acids displayed significant decreased quantities in the uterine secretome associated with negative implantation ($P<0.05$, >2 fold change) including arginine, essential for blastocyst activation and trophectoderm motility. Additionally, the MUC protein family were observed at increased protein levels with implantation failure ($P<0.05$). MUCIN proteins are epithelial cell surface proteins that have considerable effect on endometrial function, creating a barrier to implantation.

Conclusion: Aberrant maternal uterine miRNA and molecular secretions allow for the characterization of implantation failure both 24 hours prior to, and at the time of FET. This compromised embryo-endometrial dialogue further impacts the transcription levels of key signaling molecules, resulting in significantly lower implantation success. Predicting the maternal molecular microenvironment ahead of embryo transfer may allow for fine tuning of procedures for IVF patients thereby improving implantation outcomes.

Jason C Parks, Michelle Denomme Tignanelli, Nathan McCubbin, Blair McCallie, William Schoolcraft, Mandy Katz-Jaffe. *Advanced paternal age directly impacts placental epigenetic mechanisms*. Presented at 2017 ASRM Conference in San Antonio, Texas.

Objective: The placental epigenome plays a key role in regulating fetal growth and development. Alterations in placental DNA methylation have been associated with adverse pregnancy complications including preterm birth, intrauterine growth restriction and preeclampsia. The KCNQ1OT1 imprinting cluster consists of an imprinting control region (ICR) with paternally expressed KCNQ1OT1 non-coding RNA and numerous maternally expressed protein-coding genes. KCNQ1OT1 ICR methylation loss is directly linked to imprinting disorders in humans. The aim of this study was to investigate the impact of paternal aging on the methylation and expression of the Kcnq1ot1 imprinting cluster in viable embryonic placentas.

Design: Longitudinal research study.

Materials and Methods: Male outbred CF1 mice (n=8) with proven fertility were mated routinely during each animals lifespan (4-15 months) with superovulated young outbred virgin CF1 females (6-9 weeks). Pregnant females were sacrificed on day 16 of fetal development and embryonic placentas were collected for DNA and RNA isolation. Relative expression analysis was performed by qPCR for 10 imprinted genes from the Kcnq1ot1 imprinting cluster (n=24 embryonic placenta, paternal age 4-6 months; n=24 embryonic placenta, paternal age 11-15 months). Imprinted DNA methylation was assessed by targeted bisulfite sequencing at the Kcnq1ot1 ICR (n=24 embryonic placenta,

paternal age 4-6 months; n=24 embryonic placenta, paternal age 11-15 months). Statistical analysis was performed using REST© (Qiagen) and Student's t-test where appropriate, with significance at $p<0.05$.

Results: Decreased expression for Kcnq1ot1 non-coding RNA was observed in embryonic placentas at paternal age 11-15 months, along with increased expression for Nap1l4, Slc22a19, Cdkn1c, and Kcnq1 ($p<0.05$). Dysregulation of imprinted gene expression corresponded with an increase in imprinted DNA methylation at the Kcnq1ot1 ICR in embryonic placentas at paternal age 11-15 months (65.6%) compared to the same males during their youth (4-6 months, 59.0%; $p=0.016$). These results are highly indicative of an aberrant gain of methylation on the typically unmethylated paternal allele at the Kcnq1ot1 ICR, resulting in the loss of paternal Kcnq1ot1 non-coding RNA expression, and a gain of paternal expression for otherwise only maternally expressed protein-coding genes: Nap1l4, Slc22a19, Cdkn1c, and Kcnq1.

Conclusions: While the genome is largely reprogrammed during gametogenesis and early embryogenesis, imprinting domains escape this epigenetic reprogramming. In our study paternal aging was associated with significant epigenetic dysregulation to both ICR DNA methylation and imprinted gene expression at the Kcnq1ot1 domain in embryonic placenta. If these epigenetic changes related to paternal aging are translational, they could be responsible for placental dysfunction and adverse pregnancy outcomes.

Jason C. Parks, Blair R. McCallie, Alyssa L. Patton, Nathan I. McCubbin, William B. Schoolcraft, Mandy G. Katz-Jaffe. *Antioxidant intervention promotes cell survival and redox balance within the ovary and subsequent oocyte resulting in improved IVF outcomes*. Presented at 2018 ASRM Conference in Denver, Colorado.

Objective: The damaging effect of oxidative stress and reactive oxygen species in ovarian aging has been associated with a decrease in follicular quantity and quality. Previously we have reported that antioxidant intervention prior to infertility treatment benefits patient outcomes. The objective of this study was to utilize a murine model to explore the molecular mechanisms underlying this observed clinical benefit.

Design: Research study.

Materials & Methods: Female CF-1 mice were naturally aged for 9 months prior to a daily diet intervention of 4 grams/animal of *Euterpe oleracea* (açaí; sourced from Brazil and biochemically tested for high antioxidant activity). Control mice received the same balanced nutritional feed but without the intervention. All aged mice were subjected to ovarian stimulation prior to collection of MII oocytes and ovarian tissue. Ovaries (n=12) were processed for CodeLink™ Mouse Whole Genome (Applied Microarrays) with Ingenuity Pathway Analysis (Qiagen). QPCR was utilized for microarray validation (n=12) and oocyte gene expression (n=19) with REST 2009 statistical software (Qiagen). Infertility patients (n=209; mean 38.0 ±4.0 years) presenting with ≥1 prior failed IVF cycle, ingested 600mg of natural açaí three times a day for 8-12 weeks prior to routine ovarian

stimulation. Live birth outcomes were analyzed for each patient, with and without açaí, using Fisher's exact test, with significance at $P<0.05$.

Results: Microarray gene expression analysis of murine ovarian tissue revealed significant transcription changes in the açaí intervention group, with the most enriched pathways belonging to apoptotic signaling and oxidation redox ($P<0.05$). QPCR validation confirmed a decrease of pro-apoptotic genes (Fas, Casp9, Bik and Tnf) and increases of pro-survival cell death regulators (Bcl2 and Bcl2l1), as well as increases of antioxidant enzymes (Gclm and Sod2, among others) with açaí intervention ($P<0.05$). Murine MII oocytes in the açaí intervention group were also found to have increased antioxidant gene expression (Gss, Gpx1, Gsr, Gsto1, Gclm, Sod1 and Sod2). Ongoing clinical results continue to show significant improvements in oocyte yield (17.4 ±10.1 vs. 13.7±8.2; $P<0.0001$) and proportion of euploid blastocysts (43.6% vs. 30.3%; $P<0.0001$) for female patients with ≥1 prior failed IVF cycle. Euploid FET (n=138) outcomes for these intervention patients have resulted in a 76.1% live birth rate.

Conclusions: In conclusion, following antioxidant intervention with natural aging, the murine ovarian transcriptome revealed an environment promoting cell survival alongside a decrease in apoptotic signaling, and an increase in antioxidant activity that could be resulting in restoration of ovarian function and oocyte quality. Taken together this offers a molecular explanation for the clinical improvements observed for women with a history of IVF failures, following antioxidant intervention prior to infertility treatment.

JC Parks, BR McCallie, NI McCubbin, DK Griffin, WB Schoolcraft, MG Katz-Jaffe. *Uterine miRNAs reflect the unique microenvironment in an individual murine horn during the window of implantation*. Presented at 2018 SSR Conference in New Orleans, Louisiana.

Successful implantation is dependent on the complex interchange between a viable embryo and a receptive endometrium. On the maternal side, specific adhesion molecules are required for blastocyst attachment, in addition to tight regulation of signaling molecules surrounding the implanting embryo. This study utilized a minimally invasive technique of sampling the mammalian uterine environment, immediately prior to embryo transfer, to examine microRNA expression in association with implantation outcome. In vivo fertilized zygotes collected from super ovulated virgin female BDF-1 mice were cultured to the blastocyst stage. Two hatching, day 5 blastocysts were selected for individual embryo transfer into each uterine horn (n= 1 embryo/horn) of a pseudo pregnant BDF-1 recipient mouse (n=7). Immediately prior to the embryo transfer procedure, a gentle aspiration from the lumen of the uterine horn was performed (n=14). On Day 16 of fetal development, recipient females were sacrificed, and implantation outcome was documented. Uterine aspirates were evaluated for microRNA expression by qPCR (TaqMan®, Thermo Fisher) and analyzed for significance in association with implantation outcome, significance at $P < 0.05$. Six specific microRNAs were chosen based on their known roles as mediators of transcription in association with embryo implantation: miR-22, miR-145, miR-200a, miR-223, miR-3074 and miR-let7b. Analysis of the uterine aspirate revealed significant expression differences in relation to implantation

for miR-22, miR-200a, miR-3074 and miR-let-7b ($P < 0.05$). Specifically, miR-let-7b displayed increased expression ($P < 0.05$) with successful single embryo implantation compared to a negative outcome in the opposite horn of the same female mouse. Increased expression of miR-let7b has been shown to play a regulatory role on the expression of Muc1 during the window of implantation, resulting in the establishment of viable pregnancy (Inyawilert et. al., 2015). In contrast, miR-22, miR-200a and miR-3074 displayed a significant decrease in expression with single embryo implantation ($P < 0.05$) compared to a negative outcome in the opposite horn of the same female mouse. Studies have shown that dysregulation of miR-22 in conjunction with Tiam1/Rac1 signal expression inhibit embryo implantation (Ma HL et. al., 2015). In conclusion, this study has revealed that each uterine horn has a unique microenvironment containing a complex milieu of microRNAs during the window of implantation. Uterine microRNAs represent a minimally invasive means of sampling the embryo-endometrial molecular dialogue, allowing for the prediction of implantation potential which if translatable to the human, could improve IVF success for infertility patients.

Jason C Parks, Blair McCallie, Mary Sweet, Taylor Pini, William B Schoolcraft, Mandy G Katz-Jaffe. *Minimally invasive uterine aspiration 24 hours ahead of embryo transfer characterizes the compromised RIF uterine microenvironment and is predictive of reproductive outcome*. Presented at 2019 ASRM Conference in Philadelphia, Pennsylvania.

Objective: Repeat implantation failure (RIF) is particularly challenging to treat in ART, resulting in limited success even when adequate preparation of the endometrium is established and a transfer is performed with a high grade euploid blastocyst. The objective of this study was to utilize a multidisciplinary approach to decipher the complexity of RIF through investigations of the maternal molecular components ahead of an embryo transfer.

Design: Research study

Materials and methods: Patients were recruited with IRB consent 24 hours prior to a programmed frozen embryo transfer (FET) with a euploid blastocyst. Uterine secretions were collected by gentle aspiration (~2-5ul) under ultrasound guidance and grouped according to reproductive outcomes: Failed euploid FET (RIF patients, ≥3 prior IVF failures) and Positive live birth FET (maternally age-matched patients; mean 36.6 ±3.8 years). Total and small RNA (n = 22) was isolated for sequencing on the NovaSEQ 6000 (Illumina). Reads were aligned to hg38 using GSNAP and analyzed with edgeR (FDR cutoff of 5%; $P<0.01$). Metabolite analysis (n = 20) was performed by UHPLS-MS (Thermo) using MassMatrix and Maven (Princeton Univ). Proteomic analysis (n = 6) involved FASP

digestion and LC-MS/MS, with protein identifications generated by Mascot (v 2.6) and Scaffold (v 4.8.9) (α of 0.05; fold change >1.5 or <0.5).

Results: A unique uterine microenvironment was observed for RIF patients and negative implantation outcomes 24 hours prior to an embryo transfer ($P<0.05$). An interplay of several biological processes were evident in RIF failed aspirates with a focused interest on 13 significantly reduced transcripts, 7 significantly increased maternal miRNAs, 12 significantly decreased amino acids and 16 proteins of significantly altered abundance ($P<0.05$). Specific examples included decreased expression of PLA2G4D ($P<0.0001$) which regulates the eicosanoid pathway, thereby impacting downstream synthesis of prostaglandins like PGE2. Decreased expression of TET1 ($P<0.0001$), an epigenetic regulator required for DNA methylation. Increased expression of miR-17, a known negative regulator of VEGFA, required for successful implantation ($P<0.01$). Decreased quantities of arginine, essential for blastocyst activation and trophectoderm motility ($P<0.05$). Lastly, an increased abundance of SERPING1, a protein associated with inflammation, which regulates complement activation ($P<0.05$).

Conclusion: Analysis of uterine secretions 24 hours prior to FET, allowed for an in-depth molecular characterization of the compromised RIF uterine microenvironment and was predictive of reproductive outcome. The negative influence on key miRNAs and gene transcription levels, in addition to altered amino acid and protein concentrations, were all identified as critical contributors to poor RIF outcomes. Ongoing investigations into the relationships of these molecular networks will lead to the possibility of more effective clinical interventions for this difficult patient population.

Jason C Parks, Mary E Haywood, Blair McCallie, Sue McCormick, William B Schoolcraft, Mandy Katz-Jaffe. *Disruption of NFR2-mediated stress response and DNA repair pathways are associated with limited developmental potential of trisomy embryos.* Presented at 2020 ASRM Virtual Conference.

Objective: Embryonic chromosomal trisomy is recognized as a leading cause of reproductive failure and pregnancy loss in human reproduction. Interestingly, specific trisomy's have differing implantation potential and only a handful of trisomies (chromosome 13, 18, 21, X and Y) will even develop past the first trimester. The aim of this study was to investigate the association between the embryonic transcriptome and a range of embryonic trisomy with differing implantation potentials.

Design: Research study

Materials and methods: Surplus, frozen blastocysts (n = 55) were donated to research with IRB and patient consent. Blastocysts underwent micromanipulation to isolate trophectoderm (TE) cells for transcriptome analysis. In addition to euploid blastocysts (n=17), the following trisomies were identified based on differing implantation potential: trisomy 7 (n=11) and trisomy 11 (n=5) that are most likely to result in implantation failure, as well as trisomy 15 (n=11) and trisomy 22 (n=11) which are able to implant but will always result in miscarriage. Individual TE total RNA (n = 25) was isolated for sequencing on the NovaSEQ 6000 (Illumina). Reads were aligned to hg38 using GSNAP and only reads mapping to non-trisomy chromosomes were included in downstream analysis (genes on chromosomes 7, 11, 15, and 22 were excluded in all samples). Differential gene

expression was analyzed with edgeR and limma (FDR<5%), and interpreted using Ingenuity Pathway Analysis (Qiagen). Validation was performed on additional individual TE samples (n = 30; 6 per group) with gene expression confirmed using Real-Time PCR (ViiA 7 Real-Time PCR System; P<0.05).

Results: An interplay of several biological processes were evident in all trisomy embryo groups compared to euploid, regardless of the specific chromosome involved in the meiotic error, with a total of 389 differentially expressed genes (P<0.05). There was no enrichment for chromosome type or cytoband. Pathway analysis identified a globally inhibited NRF2-mediated stress response including validation of the two central players in the pathway, NRF2 and KEAP1 (P<0.001) and 8 significantly decreased NRF2 targets (regulating key antioxidant and metabolic genes; P<0.05). CLPTM1L, also a target of NRF2, was validated showing increased expression that may result in activation of apoptosis (P<0.05). DNA damage response was also significantly associated with embryonic trisomy (P<0.05). Specific validated genes included confirmation of significant increased expression of BRCA2, PALB2 and ATR, all genes that are essential for DNA damage repair pathways (P<0.0001).

Conclusion: This in-depth molecular characterization of embryonic trisomy concluded that regardless of the individual triploid chromosome, a globally compromised transcriptome was apparent. Significant disruption to the NRF2- mediated stress response and DNA repair pathways were specifically evident in all trisomy embryos, which explains why the vast majority of trisomy conceptions will have limited potential and perish during the early stages of development.

15.0 Appendix 2. Additional publication

McCallie BR, **Parks JC,** Griffin DK, Schoolcraft WB, Katz-Jaffe MG. Infertility diagnosis has a significant impact on the transcriptome of developing blastocysts. Mol Hum Reprod. 2017 Aug 1;23(8):549-556. doi: 10.1093/molehr/gax034.

My personal contribution to this manuscript

I worked closely with Dr. Katz-Jaffe and McCallie on this research study by providing input with regard to the study design and results interpretation. I was also responsible for coordinating the collection of study materials between the research department and the IVF laboratory. I also warmed each of the vitrified embryos, confirmed their viability and finally prepared the samples for storage at -80°C and downstream transcriptome experiments. This manuscript was co-authored by Blair McCallie and myself, with each of us sharing first-authorship.

Molecular Human Reproduction, Vol.23, No.8 pp. 549–556, 2017
Advanced Access publication on June 27, 2017 doi:10.1093/molehr/gax034

molecular human reproduction

ORIGINAL ARTICLE

Infertility diagnosis has a significant impact on the transcriptome of developing blastocysts

Blair R. McCallie[1,2,†*], Jason C. Parks[1,2,†], Darren K. Griffin[2], William B. Schoolcraft[3], and Mandy G. Katz-Jaffe[1,3]

[1]Fertility Labs of Colorado, 10290 Ridgegate Circle, Lone Tree, CO, USA [2]University of Kent, Canterbury CT2 7NJ, UK [3]Colorado Center for Reproductive Medicine, 10290 Ridgegate Circle, Lone Tree, CO, USA

*Correspondence address. E-mail: bmccallie@fcolo.com

Submitted on February 14, 2017; resubmitted on May 24, 2017; editorial decision on June 5, 2017; accepted on June 6, 2017

STUDY QUESTION: Is the human blastocyst transcriptome associated with infertility diagnosis, specifically: polycystic ovaries (PCO), male factor (MF) and unexplained (UE)?

SUMMARY ANSWER: The global blastocyst transcriptome was significantly altered in association with a PCO, MF and UE infertility diagnosis.

WHAT IS KNOWN ALREADY: Infertility diagnosis has an impact on the probability for a successful outcome following an IVF cycle. Limited information is known regarding the relationship between a specific infertility diagnosis and blastocyst transcription during preimplantation development.

STUDY DESIGN, SIZE, DURATION: Blastocysts created during infertility treatment from patients with specific infertility diagnoses (PCO, MF and UE) were analyzed for global transcriptome compared to fertile donor oocyte blastocysts (control).

PARTICIPANTS/MATERIALS, SETTING, METHODS: Surplus cryopreserved blastocysts were donated with patient consent and institutional review board approval. Female patients were <38 years old with male patients <40 years old. Blastocysts were grouped according to infertility diagnosis: PCO ($n = 50$), MF ($n = 50$), UE ($n = 50$) and fertile donor oocyte controls ($n = 50$). Pooled blastocysts were lysed for RNA isolation followed by microarray analysis using the SurePrint G3 Human Gene Expression Microarray. Validation was performed on significant genes of interest using real-time quantitative PCR (RT-qPCR).

MAIN RESULTS AND THE ROLE OF CHANCE: Transcription alterations were observed for all infertility etiologies compared to controls, resulting in differentially expressed genes: PCO = 869, MF = 348 and UE = 473 ($P < 0.05$; >2-fold). Functional annotation of biological and molecular processes revealed both similarities, as well as differences, across the infertility groups. All infertility etiologies displayed transcriptome alterations in signal transducer activity, receptor binding, reproduction, cell adhesion and response to stimulus. Blastocysts from PCO patients were also enriched for apoptotic genes while MF blastocysts displayed enrichment for genes involved in cancer processes. Blastocysts from couples with unexplained infertility displayed transcription alterations related to various disease states, which included mechanistic target of rapamycin (mTOR) and adipocytokine signaling. RT-qPCR validation confirmed differential gene expression for the following genes: BCL2 like 10 (*BCL2L10*), heat shock protein family A member 1A (*HSPA1A*), heat shock protein family A member 1B (*HSPA1B*), activating transcription factor 3 (*ATF3*), fibroblast growth factor 9 (*FGF9*), left-right determination factor 1 (*LEFTY1*), left-right determination factor 2 (*LEFTY2*), growth differentiation factor 15 (*GDF15*), inhibin beta A subunit (*INHBA*), adherins junctions associated protein 1 (*AJAP1*), cadherin 9 (*CDH9*) and laminin subunit alpha 4 (*LAMA4*) ($P < 0.05$; >2-fold).

LARGE SCALE DATA: Not available due to participant privacy.

LIMITATIONS, REASONS FOR CAUTION: Blastocyst samples for microarray analysis required pooling. While this allows for an overall average in each infertility etiology group and can reduce noise from sample-to-sample variation, it cannot give a detailed analysis of each blastocyst within the group.

†These authors contributed equally to this work.

WIDER IMPLICATIONS OF THE FINDINGS: Underlying patient infertility diagnosis has an impact on the blastocyst transcriptome, modifying gene expression associated with developmental competence and implantation potential.

STUDY FUNDING AND COMPETING INTEREST(S): No conflict of interest or outside funding provided.

Key words: polycystic ovaries / male factor / unexplained infertility / transcriptome / gene expression

Introduction

The World Health Organization (WHO) estimates that one out of six couples struggle with infertility, and the origins are equally distributed between male and female. There are many different causes of infertility including, among others, polycystic ovaries (PCO) and male factor (MF). Infertility can be the result of a variety of problems ranging from genetic to hormonal and even environmental. When all known sources have been ruled out, the couple is defined as idiopathic or unexplained.

Polycystic ovary syndrome (PCOS) is the most common endocrine disorder in women of reproductive age and a major cause of female factor infertility (Simms and Pate, 2013). It is the result of hormonal imbalances, typically excess androgen production, which lead to rare or irregular ovulation (Krishnan and Muthusami, 2017). Unlike PCOS, women diagnosed with PCO do not have a metabolic condition but have ovaries with abnormally high follicle counts and can still possess hormonal imbalances. PCO is far more common than PCOS, affecting anywhere from 20% to 30% of the population, and the causes are largely unknown (Koivunen et al., 1999). PCO patients are often infertile due to anovulation, thereby requiring ART to conceive. High miscarriage rates are associated with this infertility phenotype, as well as decreased fertilization after IVF, suggesting poorer quality oocytes and embryos (Hardy et al., 1995).

MF infertility, which is almost always defined as abnormal semen analysis based on WHO guidelines, is solely responsible for 20–30% of human infertility and is a contributing factor in half of all couples presenting for ART (Agarwal et al., 2015). Problems with sperm production can originate from many different factors including hormonal, environmental and even on a physical level within the testicle, causing problems with the seminiferous tubules. These tubules contain the Sertoli cells that act as nourishment for developing germ cells and are the location for spermatogenesis. Poor semen parameters have been shown to result in delayed and failed fertilization, as well as compromised embryo development and quality (Ron-el et al., 1991; Janny and Menezo, 1994).

Unexplained infertility (UE) is diagnosed in about 15–30% of infertile couples and is difficult to treat because the underlying etiology is unknown (Practice Committee of the American Society for Reproductive, 2006). It is defined as the inability to conceive after 12 months of regular, unprotected intercourse and when all recommended fertility assessments fail to reveal any anomaly (Quaas and Dokras, 2008). Patients can present with varying infertility histories including multiple IVF failures, poor embryo development, as well as lengthy periods of infertility. A retrospective review of 45 studies found that couples with this diagnosis have, on average, a 1–4% chance of achieving pregnancy during any given menstrual cycle without utilizing ART (Guzick et al., 1998). Nevertheless, 40–60% will spontaneously conceive within three years (depending on the female partner's age) and this rate can increase to as high as 75% with the use of ART (Galliano and Pellicer, 2015). ART techniques can also potentially help further address the cause of infertility in these patients (i.e. low fertilization rates, embryo fragmentation, abnormal oocytes, etc.) as well as improve time to conception.

A fertilized oocyte must not only facilitate the syngamy of the male and female genomic contributions but also undergo a series of cellular divisions before embryonic genome activation is initiated (Fragouli et al., 2013). Both the timing of the activation, as well as the synchrony of genes activated, must be accurately controlled to produce a blastocyst stage embryo that is viable and developmentally competent for implantation to occur (Latham and Schultz, 2001). In the mouse model, studies have observed two waves of embryonic gene transcription, the first corresponding to zygotic genome activation which occurs at the 1–2 cell stage, and the second occurring during the morula-to-blastocyst transition (Hamatani et al., 2004a). While these transcriptional events are similar in the human embryo, the timing is different with the zygotic genome activation occurring at the 4–8 cell stage (Niakan et al., 2012). Any irregularities during this critical time can lead to embryos that are incompetent and unable to implant.

The interactions between the blastocyst and the uterus that result in successful implantation are directed by an equally complex molecular dialog (Fitzgerald et al., 2008). Uterine receptivity has been extensively studied on all molecular levels, including the cross-talk between the embryo and endometrium which is quite extensive and results in an environment ideal for embryo adhesion and placentation (Mirawet-Valenciano et al., 2015). It has also been shown that viable mouse embryos have a specific gene expression profile that favors uterine attachment and invasion of the maternal endometrium. Chaen et al. found that ovarian estrogen indirectly co-ordinates mouse blastocyst adhesion through integrin activation in the blastocyst (Chaen et al., 2012). Additionally, a mammalian model for blastocyst activity has shown that specific molecular signaling directs either blastocyst activation or dormancy, affecting implantation competency (Hamatani et al., 2004b). Our laboratory has previously reported that differential mouse trophectoderm gene expression following embryo biopsy is associated with murine blastocyst implantation success. Specifically, higher gene expression of UDP-GlcNAc:betaGal beta-1,3-*N*-acetylglucosaminyltransferase 5 (*B3gnt5*), caudal type homeobox 2 (*Cdx2*), eomesodermin (*Eomes*) and wingless-type MMTV integration site family, member 3A (*Wnt3a*) were predictive of sustained implantation. In contrast, decreased gene expression of *Eomes* and *Wnt3a* were associated with absorption or pregnancy loss and decreased gene expression of *B3gnt4* and *Cdx2* were observed with negative outcomes (Parks et al., 2011).

There is limited knowledge of the human preimplantation embryo transcriptome and how it correlates to pregnancy outcomes. Jones et al. examined the transcriptome of human trophectoderm biopsies and identified more than 7000 transcripts expressed exclusively in

viable blastocysts (Jones et al., 2008). A more recent study utilized single-cell RNA sequencing on both human and mouse preimplantation embryos to determine a dataset of genes that are important for pluripotency (Blakeley et al., 2015). Ongoing transcriptome analysis in our laboratory revealed differential gene expression from blastocysts obtained from PCO women compared with donor controls. Over 800 genes were found to be disrupted in these PCO blastocysts in addition to 12 altered protein biomarkers, demonstrating a link between patient infertility phenotype and embryo development (Katz-Jaffe et al., 2010).

The objective of the present study was to further explore the global transcriptome of human blastocysts from patients with differing infertility etiologies, specifically PCO, MF and UE, to uncover novel biological pathways associated with their infertility that may influence downstream implantation outcomes. These findings will further our understanding of the impact of infertility diagnoses on the embryonic molecular signature at the time of implantation, and may lead to refined lab-based and clinical approaches for improving IVF outcomes.

Materials and Methods

Human blastocysts

Surplus, cryopreserved, anonymous, human blastocysts from IVF patients with specific infertility diagnoses were donated with Institutional Review Board (IRB) consent. All embryos were considered to be transferable quality with a grade of 3BB or better on day 5 of embryo development (Gardner and Schoolcraft, 1999). Either slow freezing or vitrification protocols were used to cryopreserve the blastocysts (Veeck et al., 2004; Kuwayama, 2007) which were grouped according to a single distinct infertility diagnosis: $n = 50$ young donor oocyte controls with no MF infertility; $n = 50$ PCO; $n = 50$ MF infertility; and $n = 50$ UE. Every blastocyst used in this study came from a different patient (female <38 years old, male <40 years old) and all patients had successful pregnancies from the same IVF cohort as the blastocyst used for research. Patients diagnosed with PCO had PCO confirmed by ultrasound but did not have any endocrine or metabolic abnormalities, as determined by androgen levels, fasting glucose and insulin levels, and oral glucose tolerance testing. MF infertility patients were all diagnosed based on WHO guidelines as oligoasthenoteratozoospermia with sperm concentration <15 million/ml, motility <32% and <4% normal morphology. UE infertility was defined following a negative fertility workup which included normal semen analysis, normal ovarian reserve testing and normal uterine assessment with no prior failures or missed abortions.

Blastocyst thaw and RNA isolation

Blastocysts were either thawed or warmed using routine laboratory procedures, with an overall 95% survival rate. Blastocysts in each distinct infertility diagnosis group were pooled ($n = 25$ per pool, two pools per group), and RNA was isolated using the PicoPure RNA Isolation Kit (ThermoFisher Scientific, Grand Island, NY, USA) per the manufacturer's instructions with minor modifications. Briefly, blastocysts were lysed in 10 µl of Extraction Buffer before adding one volume of 70% ethanol and binding to a silica-based membrane. Samples were then washed and on-column deoxyribonuclease treated (Qiagen, Valencia, CA, USA) prior to elution in 20 µl and storage at −80°C.

Microarray hybridization

Isolated RNA from each group was reverse transcribed, amplified and labeled using the LowInput QuickAmp Labeling Kit (Agilent Technologies, Santa Clara, CA, USA). Quantification and quality of total RNA was performed using the High Sensitivity RNA ScreenTape on a 4200 TapeStation System (Agilent Technologies). Quantification and specific activity of labeled cRNA was determined using the NanoDrop® ND-1000 spectrophotometer (ThermoFisher Scientific). A total of 600 ng of cRNA was then applied to the SurePrint G3 Human Gene Expression Microarray containing 50 599 biological features (Agilent Technologies) per the manufacturer's instructions and hybridized in a rotating oven for 17 h at 65°C. Arrays were washed and then scanned using a DNA Microarray Scanner C (Agilent Technologies). Feature extraction software was utilized to extract gene expression data (Agilent Technologies).

Real-time quantitative PCR validation

RNA was reverse transcribed using the High-Capacity cDNA Reverse Transcription Kit (ThermoFisher Scientific). cDNA was diluted 1:5 in nuclease-free water and real-time quantitative PCR (RT-qPCR) was performed for validation of specific differentially expressed genes identified from the transcriptome analysis. Absolute expression was quantified relative to a standard curve using slope and PCR efficiencies, and normalized to a stable housekeeping gene, *GAPDH*. Briefly, *Power* SYBR® Green PCR Master Mix (ThermoFisher Scientific) was combined with 5 µM primer mix and 5 µl diluted cDNA for a total volume of 25 µl. The reaction was incubated at 95°C for 10 min, followed by 40 cycles of amplification at 95°C for 15 s and 60°C for 1 min with a final dissociation stage for melt curve analysis.

Statistical analysis

Transcript analysis was performed using GeneSpring software (version 7, Agilent Technologies), including principal component analysis (PCA), unsupervised hierarchical clustering, one-way ANOVA and unpaired *t*-test with Benjamini–Hochberg correction (significance at $P < 0.05$). qPCR analysis was performed with REST 2009 software (Qiagen) which uses the correction for exact PCR efficiencies with mean crossing point deviations between sample and control groups to determine an expression ratio that is tested for significance by a Pair Wise Fixed Reallocation Randomization Test. Significance was defined as $P < 0.05$.

Ethical approval

All participants provided written informed consent and this study was approved by an institutional review board.

Results

The blastocyst transcriptome according to infertility diagnosis

The overall human blastocyst transcriptome contained 33 587 gene transcripts which included numerous splicing variants and isoforms, revealing 13 136 annotated genes. PCA and unsupervised hierarchical clustering distinguished each of the four blastocyst groups by their transcriptomes (Fig. 1). The most significant transcriptome variation was observed in blastocysts derived from infertile PCO patients. Compared to donor controls, significant differences in transcription (>2-fold; $P < 0.05$) were observed for 869 genes in PCO blastocysts, 348 genes in MF blastocysts and 473 genes in blastocysts from couples with UE (Fig. 2). Both upregulation and downregulation were observed in each group: PCO = 647 increased, 222 decreased; MF = 143 increased, 205 decreased; UE = 305 increased, 168 decreased (Table I).

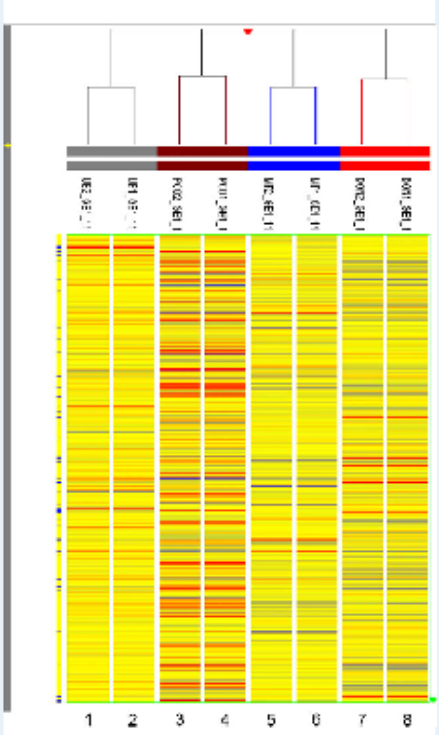

Figure 1 Differential transcriptome profiles based on infertility diagnosis. Human blastocyst transcriptomes from unexplained infertility (UE) (lanes 1 and 2), polycystic ovaries (PCO) (lanes 3 and 4), male factor (MF) (lanes 5 and 6) and control (lanes 7 and 8). Unsupervised hierarchical clustering clearly separated the transcriptomes of the four groups, with the most significant variation in gene expression observed for the PCO group.

Functional annotation of PCO blastocysts was performed using DAVID (https://david.ncifcrf.gov) which revealed significant differences in gene ontology including: cell communication, differentiation and adhesion, reproduction, transcription factor activity, regulation of apoptosis, receptor binding, signal transducer activity and response to hormone stimulus. Pathway analysis identified enriched biological processes with altered transcripts in PCO versus control blastocysts ($P < 0.05$) including gap junction proteins and genes involved in p53 signaling, calcium signaling, transforming growth factor (TGF)-beta signaling, histidine metabolism and apoptosis (Table I).

Transcriptome analysis of MF blastocysts resulted in some common gene ontology differences in relation to PCO blastocysts that included: signal transduction, regulation of apoptosis, cell adhesion, reproduction and receptor binding. Unique differences were also observed for

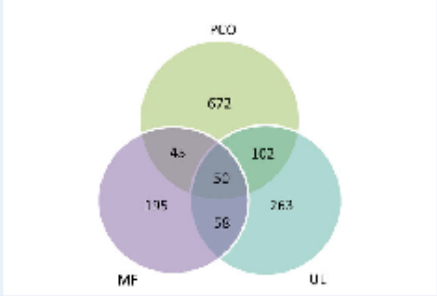

Figure 2 Venn diagram depicting gene overlap of differentially expressed transcripts between the infertility diagnoses groups. $P < 0.05$; >2-fold; one-way ANOVA and unpaired t-test with Benjamini–Hochberg correction. $N = 1385$ genes.

MF including: response to stress, regulation of growth and protein dimerization activity. Pathway analysis of MF versus control blastocysts revealed enrichment in TGF-beta, ErbB, B cell receptor and GnRH signaling (Table I).

Functional annotation of UE blastocysts also had similar outcomes to PCO blastocysts in signal transducer activity, receptor binding, cell differentiation, adhesion and morphogenesis, reproduction and response to stimulus, among others. Unique differences for UE included: oxidoreductase activity, protein dimerization activity and monooxygenase activity. Pathway analysis of UE versus control blastocysts had some similarities (TGF-beta signaling and focal adhesion) compared to the other two groups but many more differences including the affected pathways: type I diabetes, antigen processing, leukocyte migration, autoimmune thyroid disease, systemic lupus erythematosus, mechanistic target of rapamycin (mTOR) signaling and adipocytokine signaling (Table I).

Microarray validation

RT-qPCR was used to validate the microarray data by investigating the mRNA expression levels of genes involved in stress response, apoptosis, cell growth and adhesion and embryonic development. qPCR results confirmed a significantly higher expression of the stress sensing protein activating transcription factor 3 (*ATF3*) in PCO blastocysts compared to donor controls ($P < 0.05$) and lower levels of anti-apoptotic oocyte-inherited gene BCL2 like 10 (*BCL2L10*) ($P < 0.05$) and the heat shock protein family A members 1A and 1B (*HSPA1A* and *HSPA1B*) ($P < 0.05$; Fig. 3). Blastocysts from patients with MF infertility displayed an increased expression of growth differentiating factor 15 (*GDF15*) ($P < 0.05$) and the cell proliferation regulator, inhibin beta A subunit (*INHBA*) ($P < 0.05$; Fig. 4), as observed in the microarray data. Additionally, reduced expression was validated in MF blastocysts for fibroblast growth factor 9 (FGF9) ($P < 0.05$), and left-right determination factors 1 and 2 (*LEFTY1*, *LEFTY2*) ($P < 0.05$; Fig. 4). Three genes were also confirmed to have reduced expression in blastocysts with UE, as observed in the microarray data: adherens junctions associated

Table I Significantly altered transcripts and pathways associated with specific infertility diagnoses.

Infertility diagnosis	# ↑ Genes ($P < 0.05$; >2-fold)	# ↓ Genes ($P < 0.05$; >2-fold)	Enriched pathways ($P < 0.05$; >2-fold)
PCO	647	222	p53 signaling, TGF-beta signaling, apoptosis, histidine metabolism
MF	143	205	TGF-beta signaling, ErbB signaling, GnRH signaling, B cell receptor signaling
UE	305	168	mTOR signaling, autoimmune thyroid disease, systemic lupus erythematosus, Type I diabetes and adipocytokine signaling

PCO, polycystic ovaries; MF, male factor infertility; UE, unexplained infertility; TGF, transforming growth factor; ErbB, epidermal growth factor; mTOR, mechanistic target of rapamycin.
Statistical method: one-way ANOVA and unpaired t-test with Benjamini–Hochberg correction.

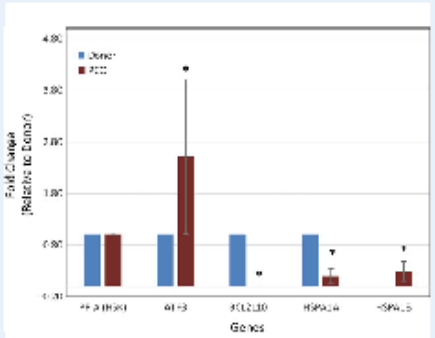

Figure 3 Altered expression of genes involved in apoptosis and stress response in PCO blastocysts. Quantitative PCR (qPCR) was performed to validate expression levels of activating transcription factor 3 (*ATF3*), BCL2 like 10 (*BCL2L10*) and heat shock protein family A members 1A and 1B (*HSPA1A* and *HSPA1B*) in donor control and PCO blastocysts with peptidylprolyl isomerase A (*PPIA*) transcription as the constant internal reference gene. A significant increase in *ATF3* expression was observed, while *BCL2L10*, *HSPA1A* and *HSPA1B* displayed significantly lower expression in PCO blastocysts, compared to donor controls; *$P < 0.05$; pair-wise fixed reallocation randomization test.

protein 1 (*AJAP1*), cadherin 9 (*CDH9*) and laminin subunit alpha 4 (*LAMA4*) (all $P < 0.05$; Fig. 5).

Discussion

This study highlighted that the human blastocyst transcriptome is significantly impacted by the type of patient infertility diagnosis (PCO, MF and UE). All three of the infertility diagnoses shared transcriptome alterations, with PCO blastocysts displaying the greatest transcriptome variation. An altered blastocyst transcriptome has the potential to impact overall developmental competence, contributing to the infertility observed in patients with these etiologies.

The expression of genes involved in stress response and apoptosis were significantly different in PCO blastocysts compared to donor controls, suggesting a PCO environment has a significant impact on the developing blastocyst's transcriptome, including alterations in stress signaling pathways and the regulation of apoptosis. These findings are consistent with those of Wang *et al.*, who reported differential expression of 650 transcripts in the ovaries of women with PCOS compared to normal ovaries and found similar alterations in pathways involved in stress response, apoptosis and regulation of transcription (Wang *et al.*, 2014). A higher expression of *ATF3* and lower expression of *BCL2L10*, *HSPA1A* and *HSPA1B* in PCO blastocysts was observed in this study compared with donor controls. *ATF3*, a stress sensor, increases p53 protein levels and transcription of p53-responsive genes that result in either cell arrest and DNA repair or apoptosis (Yan *et al.*, 2005), thereby maintaining DNA integrity. In the developing embryo, highly regulated apoptotic events are critical for embryo homeostasis and survival. The BCL2 proteins are both anti- and pro-apoptotic; *BCL2L10* is an anti-apoptotic oocyte-inherited transcript and elimination of *BCL2L10* accelerates oocyte death (Guillemin *et al.*, 2009). *HSPA1A* and *B* are involved in embryonic genome activation and decreased expression has been observed in mammalian arrested embryos (Le Masson and Christians, 2011; Pan *et al.*, 2014). Likewise, gene expression analyses of oocytes from PCOS women also revealed reduced expression in these heat shock proteins (Wood *et al.*, 2007). Decreased fertilization rates after IVF as well as a higher risk of miscarriage are associated with the PCO infertility diagnosis. Altered expression levels of each of these genes in PCO may disrupt the normal balance of apoptosis in the preimplantation embryo, with downstream consequences for implantation and developmental outcomes.

Blastocysts derived from MF infertility were significantly altered for TGF-beta and ErbB signaling pathways which are crucial during cell growth and proliferation. *GDF15* is a gene belonging to the TGF-beta superfamily and plays a role in regulating inflammatory and apoptotic pathways. The increased expression observed for *GDF15* in MF blastocysts is associated with numerous disease states including inflammation and oxidative stress. Likewise, *INHBA*, which encodes the same TGF-beta superfamily of proteins, was also found to have increased expression in MF blastocysts. *INHBA* is a negative regulator of gonadal stromal cell proliferation, thus excess expression would lead to inappropriate decreases in cell proliferation which could negatively impact implantation potential. Decreased gene expression in MF blastocysts was observed for *FGF9*, *LEFTY1* and *LEFTY2*. *FGF9* is involved in many biological processes including embryo development, cell growth and morphogenesis. It has been found to be required for stimulating Erk1/2 activation in differentiating spermatagonia

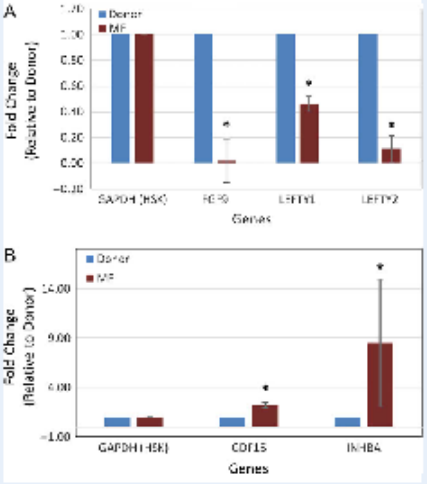

Figure 4 Altered expression of genes involved in cell growth and differentiation in MF blastocysts. qPCR was performed to validate expression levels of growth differentiation factor 15 (*GDF15*), inhibin beta A subunit (*INHBA*), fibroblast growth factor 9 (*FGF9*) and left-right determination factors 1 and 2 (*LEFTY1* and *LEFTY2*) in donor control and MF blastocysts with *GAPDH* transcription as the constant internal reference gene. (**A**) Expression of *FGF9*, *LEFTY1* and *LEFTY2* was significantly lower and (**B**) *GDF15* and *INHBA* significantly higher in MF blastocysts compared to donor controls; $^{*}P < 0.05$; pair-wise fixed reallocation randomization test.

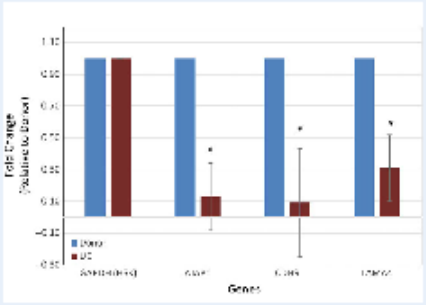

Figure 5 Altered expression of genes involved in cell adhesion and migration in UE blastocysts. qPCR was performed to validate expression levels of adherens junctions associated protein 1 (*AJAP1*), cadherin 9 (*CDH9*) and laminin subunit alpha 4 (*LAMA4*) in donor control and UE blastocysts with *GAPDH* transcription as the constant internal reference gene. All three genes were significantly decreased in expression in UE blastocysts compared to donor controls; $^{*}P < 0.05$; pair-wise fixed reallocation randomization test.

(Tassinari et al., 2015). LEFTY proteins are critical in sustaining pluripotency and implicated in differentiation of embryonic stem cells (Khalkhali-Ellis et al., 2016). Inactive LEFTY has been shown to result in embryos that become entirely mesoderm and fail to develop (Hamada et al., 2002). Poor sperm parameters in MF patients are correlated with fertilization failure and compromised embryo quality and development (Loutradi et al., 2006). Decreases in the expression of these genes could severely impact embryo developmental competence, which is crucial for implantation.

Important pathways, including cell differentiation and morphogenesis, reproduction and response to stress, were affected from blastocysts derived from patients with UE infertility. These pathways affect embryo growth and development as well as cell adhesion and migration. Decreased expression was observed for three genes involved in cell adhesion and migration: *AJAP1*, *CDH9* and *LAMA4*. *AJAP1* has been observed to be decreased in various cancers and interacts with β-catenin complexes that impact cell cycle function and apoptosis (Zeng et al., 2014). The decreased expression observed in UE blastocysts could have a negative impact on the balance of apoptosis, possibly leading to inappropriate expression of genes that affect cellular invasion. *CDH9* belongs to a family of cell adhesion molecules that regulate morphogenesis and are involved in intracellular signaling pathways (Hableib and Nelson, 2006). These cadherins are responsible for cell–cell adhesion during morula compaction, in addition to playing a role in tissue and organ development (Peyrieras et al., 1983). Decreased expression would inhibit the both early embryo development and later fetal development in utero. *LAMA4* is a laminin that mediates the attachment, migration and organization of cells into organized tissues during embryonic development. Laminins are vital for organogenesis and have critical functions in several tissues including skin, muscle and vasculature (Durbeej, 2010). As the etiology of UE infertility is more ambiguous, many adverse outcomes are possible including poor embryo development and IVF failure. The decreased expressed observed in UE blastocysts could have significant consequences for embryo implantation and ongoing development.

The similarities between all infertility groups included transcriptome alterations in signal transducer activity, receptor binding, reproduction, cell adhesion and response to stimulus. These biological and molecular processes are all inter-related and crucial to embryo development and implantation, which are processes characterized by cells that proliferate, migrate and attach. Receptors are generally transmembrane protein molecules that bind to signaling molecules in response to external stimuli. Once a receptor protein receives a signal, a series of biochemical reactions is initiated which conveys those signals across a cell, triggering changes in cell function or state, known as signal transduction. An example of this is Hedgehog (Hh) proteins which are expressed during vertebrate development. Hh signaling has been observed during embryonic development and has significance during the growth of reproductive tissues including the gonad and uterus (Walterhouse et al., 2003). Cellular adhesion, in which cells interact to attach to a surface, regulates signal transduction and is an essential process for embryo implantation into the uterus lining. It is therefore not surprising

that all three infertility diagnoses shared blastocysts with transcriptome alterations in these important biological and molecular processes.

The differences between each infertility group were more remarkable when studying their pathway analyses. Blastocysts from women with PCO were enriched for apoptosis. This is in concordance with data published showing that ovaries from women with PCO have abnormal apoptotic activity and folliculogenesis (Cai *et al.*, 2013). On the other hand, signaling pathways from blastocysts with MF infertility were largely involved in cancer processes. Lian *et al.* also found that infertile men with maturation arrest had hyperactive germ cell proliferation as a result of the inhibition of tumor suppressor *IRF1* by its microRNA, miR-383 (Lian *et al.*, 2010). Interestingly, UE infertility was enriched for pathways involved in mTOR and adipocytokine signaling, both of which are related to various disease states. This could explain some of the difficulties in treating patients with unknown infertility as the cause of their reproductive deficiencies could be the result of anything ranging from environmental to unknown disease risk factors. For example, autoimmune disorders, such as lupus, have been shown to cause a woman's immune system to reject an embryo, thereby preventing implantation into the uterus (Mojarrad *et al.*, 2013).

Conclusion

This novel study suggests that underlying patient infertility diagnosis has an impact on the blastocyst transcriptome, modifying genes that may affect developmental competence and implantation outcomes. Ongoing research determining how transcription alterations are linked to inferior pregnancy outcomes for PCO, MF and UE patients is crucial to improving IVF success. This is especially true for UE patients, as a more defined infertility diagnosis could translate into more targeted clinical management. Understanding how different infertility etiologies contribute to embryo viability may also lead to the development of new laboratory and clinical therapies. An example of this type of clinical advancement is the endometrial receptivity array which identifies endometrial receptivity for patients with repeated implantation failure (Ruiz-Alonso *et al.*, 2013). Further studies could lead to similar advancements, including individualized embryo culture systems and custom stimulation and frozen embryo transfer protocols, thereby improving outcomes for these patients.

Acknowledgements

We would like to acknowledge all the physicians and embryologists at the Colorado Center for Reproductive Medicine for their support in this study. We would also like to acknowledge Alyssa Patton for her assistance collecting material in this study.

Authors' roles

B.R.M. performed all microarray and RT-qPCR experiments and analysis and took the lead in preparing the manuscript. J.C.P. collected all blastocyst samples for all experiments. D.K.G. and W.B.S. provided critical review of the manuscript. M.K.J. designed and oversaw the completion of the study. All authors participated in the editing of the manuscript.

Funding

No conflict outside funding was provided.

Conflict of interest

None declared.

References

Agarwal A, Mulgund A, Hamada A, Chyatte MR. A unique view on male infertility around the globe. *Reprod Biol Endocrinol* 2015;**13**:37.

Blakeley P, Fogarty NM, Del Valle I, Wamaitha SE, Hu TX, Elder K, Snell P, Christie L, Robson P, Niakan KK. Defining the three cell lineages of the human blastocyst by single-cell RNA-seq. *Development* 2015;**142**:3613.

Cai L, Ma X, Liu S, Liu J, Wang W, Cui Y, Ding W, Mao Y, Chen H, Huang J *et al.* Effects of upregulation of Hsp27 expression on oocyte development and maturation derived from polycystic ovary syndrome. *PLoS One* 2013;**8**:e83402.

Chaen T, Konno T, Egashira M, Bai R, Nomura N, Nomura S, Hirota Y, Sakurai T, Imakawa K. Estrogen-dependent uterine secretion of osteopontin activates blastocyst adhesion competence. *PLoS One* 2012;**7**:e48933.

Galliano D, Pellicer A. Potential Etiologies of Unexplained Infertility in Females. In: Schattman GL, Esteves SC, Agarwal A (eds). *Unexplained Infertility*. New York, NY: Springer Science, 2015:141–147.

Durbeej M. Laminins. *Cell Tissue Res* 2010;**339**:259–268.

Fitzgerald JS, Poehlmann TG, Schleussner E, Markert UR. Trophoblast invasion: the role of intracellular cytokine signalling via signal transducer and activator of transcription 3 (STAT3). *Hum Reprod Update* 2008;**14**:335–344.

Fragouli E, Alfarawati S, Spath K, Jaroudi S, Sarasa J, Enciso M, Wells D. The origin and impact of embryonic aneuploidy. *Hum Genet* 2013;**132**:1001–1013.

Gardner D, Schoolcraft W. In-vitro culture of human blastocysts. In: Jansen R, Mortimer D (eds). *Towards Reproductive Certainty: Fertility and Genetics Beyond 1999*. Carnforth: Parthenon Press, 1999:378–388.

Guillemin Y, Lalle P, Gillet G, Guerin JF, Hamamah S, Aouacheria A. Oocytes and early embryos selectively express the survival factor BCL2L10. *J Mol Med (Berl)* 2009;**87**:923–940.

Gurick DS, Sullivan MW, Adamson GD, Cedars MI, Falk RJ, Peterson EP, Steinkampf MP. Efficacy of treatment for unexplained infertility. *Fertil Steril* 1998;**70**:207–213.

Halbleib JM, Nelson WJ. Cadherins in development: cell adhesion, sorting, and tissue morphogenesis. *Genes Dev* 2006;**20**:3199–3214.

Hamada H, Meno C, Watanabe D, Saijoh Y. Establishment of vertebrate left-right asymmetry. *Nat Rev Genet* 2002;**3**:103–113.

Hamatani T, Carter MG, Sharov AA, Ko MS. Dynamics of global gene expression changes during mouse preimplantation development. *Dev Cell* 2004;**6**:117–131.

Hamatani T, Daikoku T, Wang H, Matsumoto H, Carter MG, Ko MS, Dey SK. Global gene expression analysis identifies molecular pathways distinguishing blastocyst dormancy and activation. *Proc Natl Acad Sci USA* 2004b;**101**:10326–10331.

Hardy K, Robinson FM, Paraschos T, Wicks R, Franks S, Winston RM. Normal development and metabolic activity of preimplantation embryos in vitro from patients with polycystic ovaries. *Hum Reprod* 1995;**10**:2125–2135.

Janny L, Menezo YJ. Evidence for a strong paternal effect on human preimplantation embryo development and blastocyst formation. *Mol Reprod Dev* 1994;**38**:36–42.

Jones GM, Cram DS, Song B, Kokkali G, Pantos K, Trounson AO. Novel strategy with potential to identify developmentally competent IVF blastocysts. *Hum Reprod* 2008;**23**:1748–1759.

Katz-Jaffe MG, McCallie BR, Janesch A, Filipovits JA, Schoolcraft WB, Gardner DK. Blastocysts from patients with polycystic ovaries exhibit

altered transcriptome and secretome. *Reprod Biomed Online* 2010;**21**: 520–526.
Khalilhali-Ellis Z, Galat V, Galat Y, Gilgur A, Seftor EA, Hendrix MJ. Lefty glycoproteins in human embryonic stem cells: extracellular delivery route and posttranslational modification in differentiation. *Stem Cells Dev* 2016;**25**:1681–1690.
Koivunen R, Laatikainen T, Tomas C, Huhtaniemi I, Tapanainen J, Martikainen H. The prevalence of polycystic ovaries in healthy women. *Acta Obstet Gynecol Scand* 1999;**78**:137–141.
Krishnan A, Muthusami S. Hormonal alterations in PCOS and its influence on bone metabolism. *J Endocrinol* 2017;**232**:R99–R113.
Kuwayama M. Highly efficient vitrification for cryopreservation of human oocytes and embryos: the Cryotop method. *Theriogenology* 2007;**67**: 73–80.
Latham KE, Schultz RM. Embryonic genome activation. *Front Biosci* 2001;**6**: D748–D759.
Le Masson F, Christians E. HSFs and regulation of Hsp70.1 (Hspa1b) in oocytes and preimplantation embryos: new insights brought by transgenic and knockout mouse models. *Cell Stress Chaperones* 2011;**16**:275–285.
Lian J, Tian H, Liu L, Zhang XS, Li WQ, Deng YM, Yao GD, Yin MM, Sun F. Downregulation of microRNA-383 is associated with male infertility and promotes testicular embryonal carcinoma cell proliferation by targeting IRF1. *Cell Death Dis* 2010;**1**:e94.
Loutradi KE, Tarlatzis BC, Goulis DG, Zepiridis L, Pagou T, Chatzioannou E, Grimbizis GF, Papadimas I, Bontis I. The effects of sperm quality on embryo development after intracytoplasmic sperm injection. *J Assist Reprod Genet* 2006;**23**:69–74.
Miravet-Valenciano JA, Rincon-Bertolin A, Vilella F, Simon C. Understanding and improving endometrial receptivity. *Curr Opin Obstet Gynecol* 2015;**27**:187–192.
Mojarrad M, Hassanzadeh-Nazarabadi M, Tafazoli N. Polymorphism of genes and implantation failure. *Int J Mol Cell Med* 2013;**2**:1–8.
Niakan KK, Han J, Pedersen RA, Simon C, Pera RA. Human pre-implantation embryo development. *Development* 2012;**139**:829–841.
Pan X, Kong D, Liu L, Gao F, Zhang X, Tang B, Li Z. Development block of golden hamster ICSI embryos is associated with decreased expression of HDAC1, HSPA1A and MYC. *Cell Biol Int* 2014;**38**:1280–1290.
Parks JC, McCallie BR, Janesch AM, Schoolcraft WB, Katz-Jaffe MG. Blastocyst gene expression correlates with implantation potential. *Fertil Steril* 2011;**95**:1367–1372.
Peyrieras N, Hyafil F, Louvard D, Ploegh HL, Jacob F. Uvomorulin: a nonintegral membrane protein of early mouse embryo. *Proc Natl Acad Sci USA* 1983;**80**:6274–6277.
Practice Committee of the American Society for Reproductive Medicine. Effectiveness and treatment for unexplained infertility. *Fertil Steril* 2006; **86**:S111–S114.
Quaas A, Dokras A. Diagnosis and treatment of unexplained infertility. *Rev Obstet Gynecol* 2008;**1**:69–76.
Ron-el R, Nachum H, Herman A, Golan A, Caspi E, Soffer Y. Delayed fertilization and poor embryonic development associated with impaired semen quality. *Fertil Steril* 1991;**55**:338–344.
Ruiz-Alonso M, Blesa D, Diaz-Gimeno P, Gomez E, Fernandez-Sanchez M, Carranza F, Carrera J, Vilella F, Pellicer A, Simon C. The endometrial receptivity array for diagnosis and personalized embryo transfer as a treatment for patients with repeated implantation failure. *Fertil Steril* 2013;**100**:818–824.
Sirmans SM, Pate KA. Epidemiology, diagnosis, and management of polycystic ovary syndrome. *Clin Epidemiol* 2013;**6**:1–13.
Tassinari V, Campolo F, Cesarini V, Todaro F, Dolci S, Rossi P. Fgf9 inhibition of meiotic differentiation in spermatogonia is mediated by Erk-dependent activation of Nodal-Smad2/3 signaling and is antagonized by Kit Ligand. *Cell Death Dis* 2015;**6**:e1688.
Veeck LL, Bodine R, Clarke RN, Berrios R, Libraro J, Moschini RM, Zaninovic N, Rosenwaks Z. High pregnancy rates can be achieved after freezing and thawing human blastocysts. *Fertil Steril* 2004;**82**:1418–1427.
Walterhouse DO, Lamm ML, Villavicencio E, Iannaccone PM. Emerging roles for hedgehog-patched-Gli signal transduction in reproduction. *Biol Reprod* 2003;**69**:8–14.
Wang XX, Wei JZ, Jiao J, Jiang SY, Yu DH, Li D. Genome-wide DNA methylation and gene expression patterns provide insight into polycystic ovary syndrome development. *Oncotarget* 2014;**5**:6603–6610.
Wood JR, Dumesic DA, Abbott DH, Strauss JFIII. Molecular abnormalities in oocytes from women with polycystic ovary syndrome revealed by microarray analysis. *J Clin Endocrinol Metab* 2007;**92**:705–713.
Yan C, Lu D, Hai T, Boyd DD. Activating transcription factor 3, a stress sensor, activates p53 by blocking its ubiquitination. *EMBO J* 2005;**24**: 2425–2435.
Zeng L, Fee BE, Rivas MV, Lin J, Adamson DC. Adherens junctional associated protein-1: a novel 1p36 tumor suppressor candidate in gliomas (Review). *Int J Oncol* 2014;**45**:13–17.

16.0 Appendix 3. Additional publication

Katz-Jaffe MG, Lane SL, **Parks JC,** McCallie BR, Makloski R, Schoolcraft WB. Antioxidant Intervention Attenuates Aging-Related Changes in the Murine Ovary and Oocyte. Life (Basel). 2020 Oct 22;10(11):E250. doi: 10.3390/life10110250.

My personal contribution to this manuscript

I worked closely with Dr. Katz-Jaffe on this research study and provided input with regard to the study design and results interpretation. I was responsible for maintaining and monitoring the health of the mouse colony, and worked with Dr. Katz-Jaffe to coordinate ordering animals and reagents as needed. I sacrificed the animals used in this study in accordance with the experimental timeline, and the study materials were collected by me including oocytes and ovaries for -80°C storage. Finally, I contributed to the writing of the materials and methods section of the manuscript.

life

MDPI

Article

Antioxidant Intervention Attenuates Aging-Related Changes in the Murine Ovary and Oocyte

Mandy G. Katz-Jaffe *, Sydney L. Lane, Jason C. Parks, Blair R. McCallie, Rachel Makloski and William B. Schoolcraft

Colorado Center for Reproductive Medicine, Lone Tree, CO 80124, USA; SLane@ColoCRM.com (S.L.L.); JParks@ColoCRM.com (J.C.P.); BMcCallie@ColoCRM.com (B.R.M.); RMakloski@ColoCRM.com (R.M.); BSchoolcraft@ColoCRM.com (W.B.S.)

* Correspondence: MKatz-Jaffe@ColoCRM.com; Tel.: +1-303-788-8300

Received: 15 September 2020; Accepted: 20 October 2020; Published: 22 October 2020

check for updates

Abstract: Advanced maternal age (AMA) is associated with reduced fertility due in part to diminished ovarian follicle quantity, inferior oocyte quality, chromosome aneuploidy, and lower implantation rates. Ovarian aging is accompanied by increased oxidative stress and blunted antioxidant signaling, such that antioxidant intervention could improve reproductive potential. The first aim of this study was to determine the molecular effects of antioxidant intervention in the ovaries and oocytes of aged mice, utilizing a supplement containing only naturally occurring açai (Euterpe oleracea) with an oxygen radical absorbance capacity of 208,628 µmol Trolox equivalent (TE)/100 g indicating high antioxidant activity. Nine month old female CF-1 mice were administered 80 mg/day antioxidants (n = 12) or standard diet (n = 12) for 12 weeks. In the ovary, antioxidant treatment upregulated β-adrenergic signaling, downregulated apoptosis and proinflammatory signaling, and variably affected cell growth and antioxidant pathways ($p < 0.05$). Exogenous antioxidants also increased the oocyte expression of antioxidant genes *GPX1*, *SOD2*, and *GSR* ($p < 0.05$). A feasibility analysis was then conducted on female AMA infertility patients as a proof-of-principle investigation. Patients (n = 121; <45 years old) consented to receiving 600 mg antioxidants three times daily for ≥8 weeks preceding infertility treatment. Preliminary results indicate promising outcomes for AMA patients, warranting further investigation.

Keywords: antioxidants; flavonoids; oxidative stress; advanced maternal age; in vitro fertilization; dietary supplements

1. Introduction

Advanced maternal age (AMA) represents a significant decrease in fertility associated with reduced ovarian follicle quantity and oocyte quality, increased oocyte chromosome aneuploidy, and lower implantation rates [1–3]. Aging is associated with an imbalanced redox state in most organs, including the ovaries, with increased reactive oxygen species (ROS) relative to antioxidant signaling [4,5]. In aged ovaries, this is likely due in part to less activity of naturally occurring antioxidant enzymes [6,7]. Transcriptional changes also contribute to aging effects in a variety of ways. Specifically, antioxidant gene expression decreases in mouse, nonhuman primate, and human oocytes [8–11], altered microRNAs in human blastocysts lead to reduced oxidative defense [12], and granulosa and cumulus cell gene expression important for oocyte maturation is dysregulated [11,13,14]. Aged oocytes are also more sensitive to oxidative stress and likely require a shift in redox balance toward increased antioxidant signaling [15].

The relationship between ROS and antioxidant signaling in the ovary is complex. Ovarian ROS are important mediators of numerous processes including ovulation, corpus luteum formation,

and ovarian angiogenesis [16–19], but they can also be detrimental to ovarian processes such as cumulus–oocyte complex interactions and oocyte maturation [20,21]. Therefore, the correct balance between ROS generation and elimination is essential for optimal ovarian function and fertility [22]. The aging-associated decline in fertility has shown correlation with dysregulated pro- and antioxidant signaling [11,23,24]. Studies utilizing various animal models of induced ovarian oxidative stress provide evidence that antioxidant supplementation combats oxidative damage in the ovary [25–30].

In patients with increased levels of oxidative stress, clinical studies have linked positive pregnancy outcomes with more robust antioxidant signaling. One such study in patients with unexplained infertility found that a higher intake of certain antioxidant nutrients was associated with decreased time to pregnancy [31]. Another study observed a positive correlation between the total antioxidant response measured in maternal blood and pregnancy success following in vitro fertilization (IVF) [32]. Consistent with these studies, elevated circulating or peritoneal ROS are associated with idiopathic infertility [33,34]. Therefore, we hypothesize that augmenting antioxidant signaling may improve ovarian function and fertility.

The primary aim of this study was to determine the effects of antioxidant treatment on gene expression in ovaries and oocytes of aged mice. We utilized the naturally occurring açai berry (*Euterpe oleracea*) as it contains flavonoids that are potent scavengers of oxygen free radicals and ROS, and it shows therapeutic benefit in several studies investigating aging impact [35,36]. Dietary antioxidant supplementation was sufficient to alter gene expression in both ovaries and oocytes. Signaling pathways that are impacted by aging, i.e., antioxidant and apoptosis, were altered by antioxidant treatment. We then evaluated the feasibility of antioxidant administration in patients prior to an IVF cycle and determined that patients were compliant with the antioxidant regimen, where it was found that reproductive outcomes in AMA and younger counterparts were comparable. We conclude that antioxidant supplementation is a feasible and promising strategy to improve ovarian function during reproductive aging, warranting further investigation.

2. Results

2.1. Pathway Analysis of the Aged Murine Ovarian Transcriptome Following Antioxidant Intervention

After 9 months of natural aging, female mice were fed either a control chow diet or the same diet supplemented with antioxidants for 12 weeks, after which they were euthanized for collection of ovaries and oocytes (Figure 1a). Murine ovarian transcriptome analysis revealed that, compared to a control diet, antioxidant treatment altered the expression of many signaling pathways in the ovaries of aged mice as determined by pathway analysis (Figure 2) of the differentially expressed genes (Table S1, Supplementary Materials). Antioxidant administration resulted in upregulated β-adrenergic signaling (dopamine receptor, cardiac β-adrenergic, and cyclin-dependent kinase 5 (CDK5) signaling pathways). Apoptosis signaling was downregulated (induction of apoptosis via the human immunodeficiency virus 1 (*HIV1*) pathway) with reduced expression of tumor necrosis factor receptor superfamily member 1B (*TNFRSF1B*). Cell growth pathways were both upregulated (cyclins and cell-cycle regulation, gap 1 (G1)/synthesis (S) checkpoint regulation, and angiopoietin signaling pathways), and downregulated (transforming growth factor beta (TGFβ) and p38 mitogen-activated protein kinase (MAPK) signaling pathways), suggesting that antioxidant treatment promoted cell-type-specific cell survival and growth.

Antioxidant intervention had anti-inflammatory effects by downregulating proinflammatory pathways (p38 MAPK and B-cell receptor signaling pathways; nuclear factor (NF)-κB signaling, Z-score −0.632). The intervention also had antioxidant effects per microarray findings, i.e., increased expression of the antioxidant gene *PAX4*, but did not result in a significant difference by pathway analysis.

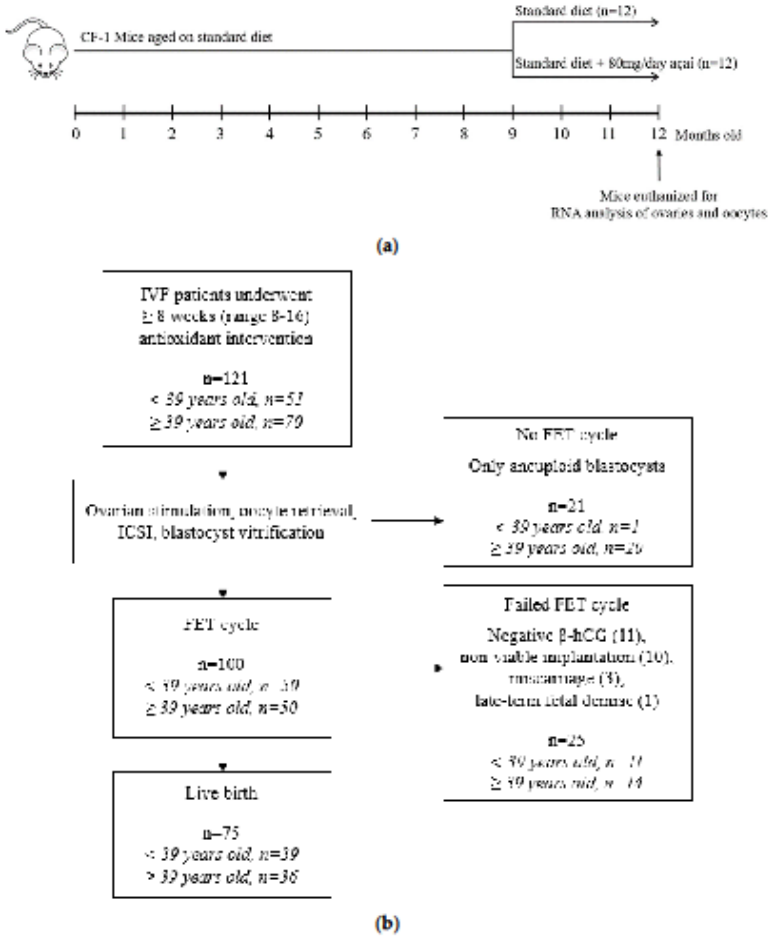

Figure 1. Experimental designs for antioxidant intervention in (a) mice and (b) humans are detailed.

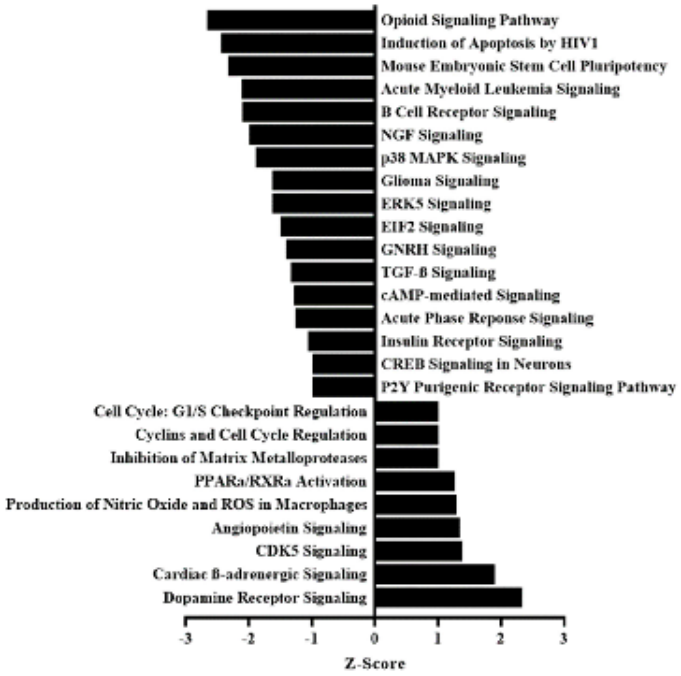

Figure 2. Pathway analysis of the differentially expressed genes in aged murine ovaries following antioxidant intervention. Cellular pathways with altered expression after antioxidant intervention compared to control diet, with $p < 0.05$ and Z-score >1 or <−1, are presented.

2.2. *Differential Gene Expression in the Murine Ovary Following Antioxidant Intervention*

Effects of antioxidant treatment on apoptosis signaling in the ovary were further investigated by qPCR (Figure 3a), and the microarray and qPCR findings were consistent. Expression of tumor necrosis factor (*TNF*)-related genes was lower after antioxidant treatment as determined by both methodologies. The microarray did not report levels of the other genes analyzed by qPCR. Differentially expressed genes by qPCR reflected a shift toward pro-survival and antiapoptotic signaling. Antioxidant intervention downregulated the extracellular-induced apoptotic signaling response, with reduced expression of proapoptotic factors *TNF* and Fas cell-surface death receptor (*FAS*). Intrinsically induced apoptosis was also downregulated by antioxidant treatment, with reduced expression of the proapoptotic factor Bcl-2-interacting killer (*BIK*) and higher expression of pro-survival factors Bcl2-like 1 (*BCL2L1*), B-cell lymphoma 2 apoptosis regulator (*BCL2*), and Bcl-2 homologous antagonist killer (*BAK1*). Consistently, expression of the proapoptosis regulator caspase 9 (*CASP9*) was reduced.

We determined by qPCR that ovarian signaling components important for redox balance were variably affected by antioxidant treatment, with reduced expression of the antioxidant enzymes glutaredoxin (*GLRX*), quiescin sulfhydryl oxidase 1 (*QSOX1*), and protein disulfide isomerase family A member 4 (*PDIA4*), but increased expression of the antioxidant genes glutamate cysteine ligase modifier subunit (*GCLM*) and superoxide dismutase 2 (*SOD2*) (Figure 3a).

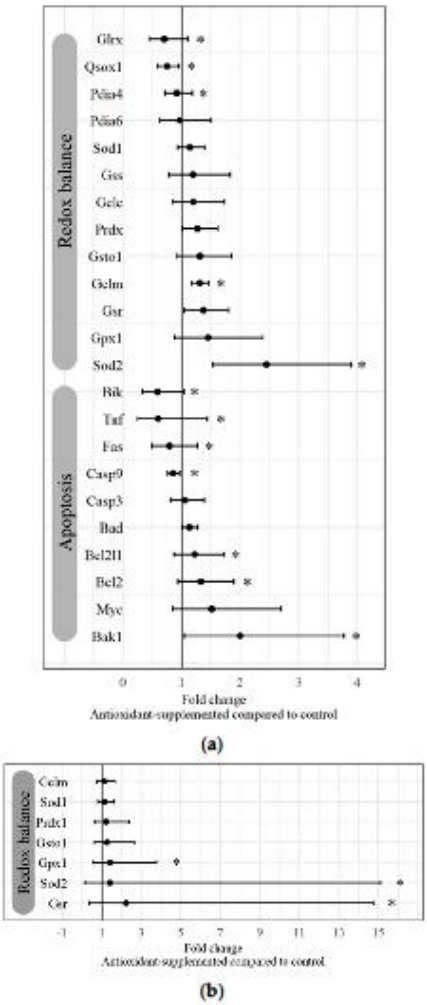

Figure 3. Antioxidant-induced gene expression changes in the aged murine ovary and meiosis II (MII) oocytes. Select genes identified as differentially expressed by microarray and additional genes of interest were analyzed by qPCR. Data are presented as the fold change (± fold change range) of gene expression in (**a**) ovaries ($n = 12$ each) and (**b**) MII oocytes ($n = 19$ each) from antioxidant-treated aged mice compared to aged mice on control diet. * $p < 0.05$ by two-tailed, unpaired *t*-test.

2.3. *Effects of Antioxidant Administration on Murine Oocyte Gene Expression*

Antioxidant intervention altered the gene expression of factors important in redox signaling in murine oocytes (Figure 3b). Expression levels of three important antioxidant genes—glutathione

peroxidase (*GPX1*), *SOD2*, and glutathione reductase (*GSR*)—were markedly higher in oocytes from mice treated with antioxidants compared to control diet.

2.4. Feasibility Analysis after Antioxidant Intervention

To determine feasibility of the antioxidant intervention in a patient cohort, infertility patients were administered antioxidants for 8–16 (mean 9.9 ± 2.2) weeks (variability due to menstrual cycle dates), immediately preceding follicle-stimulating hormone (FSH) administration (Figure 1b). Patients were aged 38.1 ± 3.5 (median 39, range 28–44) years during their antioxidant-supplemented IVF cycle. The patients had normal ovarian reserves as determined by measurement of antral follicle count and follicle-stimulating hormone (FSH) on menstrual cycle day 3 and antimüllerian hormone levels (Table 1). In total, 121 patients were offered the treatment, and all consented and were compliant.

Preimplantation genetic testing for aneuploidy (PGT-A) was performed by array comparative genomic hybridization (aCGH) or next-generation sequencing (NGS; Illumina, San Diego, CA, USA) for detection of whole-chromosome aneuploidy only. Trisomies of chromosomes 15, 16, 19, 21, and 22 and monosomies of chromosomes 15, 16, 18, 19, 21, and 22 each occurred in more than 10% of patients (Figure 4). In total, 21 patients had only aneuploid blastocysts and did not undergo frozen embryo transfer (FET; Figure 1b). The IVF cycles that resulted in only aneuploid blastocysts occurred in women who were significantly older than patients who underwent FET (41.5 ± 1.7 vs. 37.4 ± 3.4 years old, $p < 0.0001$). In patients 39 years or older compared to patients younger than 39, IVF outcomes were similar apart from euploidy rates, which were lower in the older group ($p < 0.0001$; Table 1).

Table 1. Results of proof-of-principle investigation.

	FET Patients <39 Years, *n* = 50	FET Patients ≥39 Years, *n* = 50
Age, years	34.5 ± 2.4	40.3 ± 1.3
Prior failed IVF cycles, *n* (range)	2.1 ± 1.4 (1–8)	1.9 ± 1.4 (1–7)
Baseline ovarian reserve parameters		
AMH, ng/mL	2.9 ± 2.9	2.8 ± 2.1
D3 FSH, ng/mL	8.0 ± 3.4	8.4 ± 3.1
D3 AFC, *n*	16.6 ± 8.3	15.7 ± 8.5
IVF outcomes		
Oocytes collected, *n*	17.4 ± 8.3	17.4 ± 9.2
Total blastocysts, *n*	5.0 ± 2.9	5.2 ± 3.3
Total blastocysts, %	30.4 ± 14.1	33.7 ± 18.3
Euploid blastocysts, *n*	3.0 ± 1.9	2.1 ± 1.6
Euploid blastocysts, %	63.8 ± 24.8	43.4 ± 22.3 *
Embryos transferred	1.5 ± 0.5	1.4 ± 0.5
FET outcomes		
Implantation rate (FHT)	72.0%	75.3%
Negative β-hCG	4 (8%)	7 (14%)
Nonviable implantation	6 (12%)	4 (8%)
Miscarriage	1 (2%)	2 (4%)
Fetal demise at 34 weeks	0 (0%)	1 (2%)
Live birth	39 (78%)	36 (72%)
Twin birth	11 (28%)	9 (24%)

FET, frozen embryo transfer; β-hCG, β-human chorionic gonadotropin; AMH, antimüllerian hormone; FSH, follicle-stimulating hormone; AFC, antral follicle count; D3, menstrual cycle day 3; FHT, fetal heart tones; IVF, in vitro fertilization. Data are presented as means ± SD or number (%) of patients. * $p < 0.0001$ by two-tailed, unpaired *t*-test.

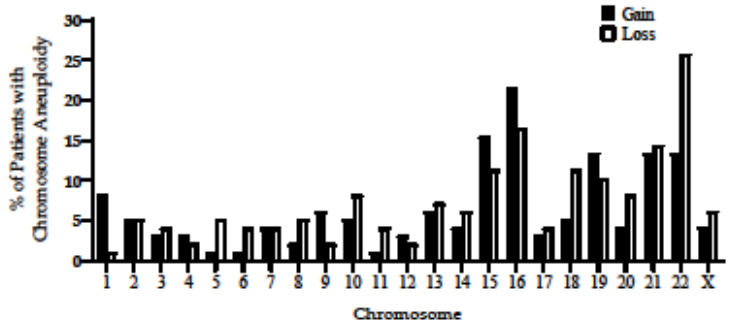

Figure 4. Types of aneuploidies in blastocysts from antioxidant-treated patients (n = 553 blastocysts, 100 IVF cycles). The percentage of patients with a gain or loss of each chromosome is presented.

2.5. Outcomes of FET Following Antioxidant Supplementation

All subjects underwent follow-up after FET procedures, and 75% resulted in live birth (Table 1). In total, 99.3% of cryopreserved embryos survived warming and 1.4 ± 0.5 embryos were transferred per patient according to the physician's direction and their prior infertility history. Cases of reproductive failure included 11 negative β-human chorionic gonadotropin (β-hCG) measurements, seven biochemical pregnancy losses, three pregnancies resulting in first-trimester fetal loss (no products of conception analyzed), and one late-gestation fetal demise due to a placental defect. AMA patients 39 years or older had promising FET outcomes comparable to good-prognosis patients younger than 39 (Table 1).

3. Discussion

Antioxidant supplementation in aged mice was sufficient to impact the ovarian and oocyte transcriptome, specifically, signaling pathways affected by aging. Infertility patients were compliant with the antioxidant regimen prior to an IVF cycle and AMA patients had promising and comparable reproductive outcomes to their younger counterparts. These findings support our hypothesis that reduced antioxidant signaling in the aged ovary can be ameliorated by exogenous antioxidant intervention to enhance reproductive potential.

Following antioxidant administration, the murine ovarian transcriptome reflected an environment with enhanced cell survival and β-adrenergic signaling, decreased apoptotic signaling proinflammatory pathways, and altered antioxidant signaling compared to control aged mice. Upregulated β-adrenergic signaling may contribute to improved ovarian function through changes in follicular development and hormone secretion [37–39], particularly since ovarian sympathetic nerve activity may decline with ovarian aging [40]. The anti-inflammatory effects of antioxidant treatment are consistent with previous reports [41]. Further cell-type-specific investigation into the effects of antioxidant treatment on redox regulation in the ovary is warranted, given that some antioxidant enzymes were upregulated while others were downregulated. A recently published study of nonhuman primates provided insight into ovarian cell-type-specific changes in gene expression with aging [11] and reported increased apoptosis and reduced antioxidants in the ovary, which they localized to granulosa cells. The aged mice in this study showed a similar phenotype to aged nonhuman primates, and antioxidant intervention was sufficient to alter the cellular processes most influenced by aging, i.e., apoptosis and antioxidant signaling. In the whole ovary, the expression of important antioxidant genes was upregulated, including *GCLM*, the modifier subunit of glutamate cysteine ligase (GCL). Decreased activity of GCL is associated with increased oxidative stress and aging-related diminished function in the ovary [42]; thus, we speculate that increased *GCLM* expression reduces oxidative stress and improves ovarian function.

In murine oocytes, expression of key antioxidant genes *SOD2*, *GPX1*, and *GSR* was markedly higher after treatment. Disrupted redox balance associated with aging reduces oocyte competence [22] such that increased expression of these genes in oocytes of antioxidant-supplemented mice could lead to restoration of quality and future developmental competence. Superoxide dismutase is important in meiosis for maintenance of sister chromatid cohesion necessary to prevent segregation errors and aneuploidy [43,44]; thus, its upregulation following antioxidant intervention could reduce meiotic errors. Glutathione peroxidase activation in oocytes has also been associated with enhanced embryonic development [45,46]. The importance of increasing antioxidant enzyme expression in oocytes was highlighted by a recent study that reported downregulation of these genes (including *GPX1* and *GSR*) with aging in the oocytes of nonhuman primates [11]. Restoration of redox balance in the oocyte may be beneficial for maintaining correct epigenetic signatures which are important for euploidy, fertilization potential, and embryo development [47].

On the basis of these observations, infertility patients were recruited for a proof-of-principle investigation of antioxidant supplementation prior to an IVF cycle to analyze its feasibility. In AMA patients 39 years of age or older compared to their younger counterparts, IVF and FET outcomes were similar with the exception of aneuploidy rates that were higher for the AMA patients, as extensively documented in the literature [48]. The 21 patients who did not undergo FET due to aneuploidy were significantly older than the antioxidant-supplemented patients who underwent FET (41.5 ± 1.7 vs. 37.4 ± 3.4 years old, $p < 0.0001$). There was a lack of euploidy in 17.4% of patients, which is in the expected range for women of this age (36.7 ± 3.7 years old, $n = 121$) [49]. Thus, antioxidants did not negate the known effect of advanced maternal aging as women enter their 40s as the most significant risk factor for chromosome aneuploidy. The antioxidant regimen was not detrimental to IVF outcomes, as live birth rates were comparable to typical rates at our clinic and even represent possible improvements [50]. The preliminary findings of this proof-of-principle investigation provide rationale for future studies on the efficacy of antioxidant intervention.

Our findings may have broader implications for antioxidant administration in additional populations. For example, there was elevated anti-inflammatory gene expression in the ovary with antioxidants, suggesting that patients with pathologic ovarian inflammation may benefit from antioxidant treatment. In women with obesity and/or polycystic ovary syndrome, there is evidence that chronic, low-grade inflammation and oxidative stress in both ovarian follicles and the endometrium contribute to anovulation and implantation failure, indicating that these groups may benefit from this intervention [51,52].

There is robust evidence that an imbalanced redox state contributes to the effects of aging, and that oxidative stress and aging are associated with lower fertility. So far, there is a lack of knowledge of the benefits of antioxidant treatment in the preconception period on assisted reproductive technology outcomes. In an aged murine model, antioxidant treatment positively impacted ovarian and oocyte signaling pathways impacted by aging. When the antioxidant supplement was administered to AMA patients prior to an IVF cycle, reproductive outcomes were similar to those in younger counterparts. Antioxidant supplementation is a promising strategy to achieve optimal ovarian function and oocyte quality, warranting further investigation.

4. Materials and Methods

4.1. Murine Antioxidant Intervention Protocol

Female outbred CF-1 mice (Charles River, Wilmington, MA, USA) were housed with a 12 h light/dark cycle and ad libitum access to standard chow diet and water. All animal procedures and protocols were completed in accordance with the Guide for the Care and Use of Laboratory Animals (8th edition) and approved by the Fertility Labs of Colorado Ethics in Research Committee. Mice were naturally aged for 9 months prior to an antioxidant diet intervention of 80 mg açai daily for 12 weeks ($n = 12$; Figure 1a). The açai antioxidant supplement was sourced from a commercial manufacturer

and contained only the naturally occurring açai berry from the palm tree *Euterpe oleracea*. The açai pulp underwent nonthermal dehydration and packaging into vegetable-based cellulose capsules (Ecofruits International Inc., South Jordan, UT, USA). Chemical analysis of the lot by the manufacturer reported a total polyphenol content of 6618 mg gallic acid equivalent (GAE)/100 g, an oxygen radical absorbance capacity (ORAC) of 208,628 µmol Trolox equivalent (TE)/100 g, and negligible microbial contamination. Control mice (n = 12) received the same balanced nutritional feed but without the açai supplementation. After 12 weeks of the antioxidant intervention or control diet, mice were euthanized by cervical dislocation for immediate collection of ovaries or oocytes.

For oocyte collection, mice were superovulated with 5 IU pregnant mare's serum gonadotropin (Sigma G-4877, St. Louis, MO, USA) followed 48 h later by 5 IU hCG (Sigma CG-5). Then, 23 h after hCG administration, animals were euthanized by cervical dislocation, and oviducts were immediately dissected from the abdominal cavity. Cumulus oocyte masses were then isolated from the ampullae in G-MOPS+ (Vitrolife, Stockholm, Sweden) and exposed to hyaluronidase (Sigma H-3757) to denude the cumulus cells and isolate the oocytes for collection.

4.2. Murine RNA Isolation, Transcriptome Analysis, and Quantitative Real-Time PCR

Murine ovaries were harvested from 12 month old mice, and RNA was isolated using the RNeasy mini kit after homogenization with the QiaShredder (Qiagen, Germantown, MD, USA). RNA analysis was carried out with CodeLink™ Mouse Whole Genome Array (Applied Microarrays, Tempe, AZ, USA) and Ingenuity Pathway Analysis (Qiagen).

RNA was isolated from oocytes in meiosis II (MII) using the PicoPure™ RNA Isolation Kit (Applied Biosystems, Foster City, CA, USA) with minor modifications to the manufacturer's protocol. Briefly, oocytes were lysed at 42 °C for 30 min in 10 µL of extraction buffer. One volume of 70% ethanol was mixed with each sample prior to loading onto a preconditioned purification column. Each sample was on-column deoxyribonuclease-treated at room temperature for 15 min (Qiagen). After several washes, RNA was eluted in 20 µL of elution buffer.

For microarray validation and further gene expression investigation in ovaries and MII oocyte gene expression, reverse transcription was performed using the High-Capacity complementary DNA (cDNA) Reverse Transcription Kit (Applied Biosystems). The same extracted RNA samples were used for both ovarian microarray and gene expression. The cDNA was diluted (1:4) in 1× Tris–ethylenediaminetetraacetic acid (EDTA) buffer prior to performing quantitative reverse-transcription PCR (RT-qPCR) on the 7300 Real-Time PCR System (Applied Biosystems). Here, 3 µL of diluted cDNA was combined with 5 µM primer mix and Power SYBR™ Green PCR Master Mix (Applied Biosystems) in a 15 µL final volume and amplified under the following thermal cycling conditions: 95 °C for 10 min, followed by 40 cycles at 95 °C for 15 s and 60 °C for 1 min, and a melt curve stage at 95 °C for 15 s, 60 °C for 1 min, and 95 °C for 15 s. Gene primers are described in Table S2 (Supplementary Materials). For each target gene, relative expression to the stable internal housekeeping gene ribosomal protein L19 (*RPL19*) was determined for sample-to-sample comparisons. The fold change in expression of antioxidant-supplemented vs. control mice was determined using the $2^{-\Delta\Delta CT}$ method.

4.3. Feasibility Analysis of Antioxidant Intervention Protocol and Outcomes

A total of 121 patients undergoing IVF with autologous oocytes consented to participate in this proof-of-principle investigation. All female patients were <45 years and their partners had no severe male factor infertility or requirement for surgically removed sperm. Patients provided informed consent (Health One Institutional Review Board, protocol no. 350763-4) and were not compensated for their participation.

The intervention protocol is described in Figure 1b. Routine IVF protocols were followed as described previously [53]. Patients were administered antioxidants—the same açai supplements described above—orally in 600 mg capsules three times daily according to the variable reported doses of açai pulp administered [54], and compliance was assessed by subjects' verbal confirmation.

The duration of intervention was 8–16 (mean 9.9 ± 2.2) weeks (variability due to menstrual cycle dates), immediately preceding FSH administration. Standard protocols were followed for ovarian stimulation, IVF, and PGT-A.

The primary patient outcomes were indicators of ovarian function and oocyte quality, i.e., the number of oocytes retrieved, blastocyst development, and blastocyst euploidy. The patients underwent follow-up to determine subsequent reproductive outcomes.

4.4. Statistical Analysis

Murine microarray data were analyzed by Ingenuity Pathway Analysis (Qiagen) and pathways with $p < 0.05$ and Z-score >1 or <−1 are reported. Murine qPCR data are presented as fold change compared to control ± the fold change range. Statistical analysis was performed using REST 2009 software (Qiagen)m which uses PCR efficiencies and mean crossing point deviation between the sample and control groups to test for significance via a Pair-Wise Fixed Reallocation Randomization Test© (significance at $p < 0.05$).

Supplementary Materials: The following are available online at http://www.mdpi.com/2075-1729/10/11/250/s1: Table S1. Differentially expressed genes in aged murine ovarian tissue after antioxidant supplementation ($n = 12$); Table S2. Primer sequences for quantitative real-time polymerase chain reaction of ovarian and oocyte genes.

Author Contributions: Conceptualization, M.G.K.-J. and W.B.S.; data curation, M.G.K.-J., S.L.L., and B.R.M.; investigation, M.G.K.-J., J.C.P., B.R.M., and R.M.; writing—original draft, M.G.K.-J. and S.L.L.; writing—review and editing, M.G.K.-J. and S.L.L. All authors have read and agreed to the published version of the manuscript.

Funding: This research received no external funding.

Acknowledgments: We would like to thank Alexander Schauss at the University of Arizona for his guidance and mentorship. We thank Kenneth Jones at the University of Colorado Anschutz Medical Campus and Mary Haywood at the Colorado Center for Reproductive Medicine for their assistance with data analysis. Lastly, we would like to thank the clinical team at the Colorado Center for Reproductive Medicine for their support of this feasibility study.

Conflicts of Interest: The authors declare no conflict of interest. The funders had no role in the design of the study; in the collection, analyses, or interpretation of data; in the writing of the manuscript, or in the decision to publish the results.

Abbreviations

AMA	Advanced maternal age
ROS	Reactive oxygen species
IVF	In vitro fertilization
CASP9	Caspase 9
CDK5	Cyclin-dependent kinase 5
HIV1	Human immunodeficiency virus 1
TNFRSF1B	TNF receptor superfamily member 1B
TGFβ	Transforming growth factor beta
MAPK	Mitogen-activated protein kinase
NF-κB	Nuclear factor kappa light chain enhancer of activated B cells
PAX4	Paired box gene 4
TNF	Tumor necrosis factor
FAS	Fas cell surface death receptor
BIK	Bcl-2-interacting killer
BCL2L1	Bcl-2-like 1
BCL2	B-cell lymphoma 2 apoptosis regulator
BAK1	Bcl-2 homologous antagonist killer
GLRX	Glutaredoxin
QSOX1	Quiescin sulfhydryl oxidase 1
PDIA4	Protein disulfide isomerase family A member 4
GCLM	Glutamate cysteine ligase modifier subunit
SOD2	Superoxide dismutase 2

GPX1	Glutathione peroxidase
GSR	Glutathione reductase
FSH	Follicle stimulating hormone
FET	Frozen embryo transfer
PGT-A	Preimplantation genetic testing for aneuploidy
aCGH	Array comparative genomic hybridization
NGS	Next generation sequencing
β-hCG	Beta-human chorionic gonadotropin
GAE	Gallic acid equivalent
ORAC	Oxygen radical absorbance capacity
TE	Trolox equivalent
RPL19	Ribosomal protein L19

References

1. Eichenlaub-Ritter, U. Oocyte ageing and its cellular basis. *Int. J. Dev. Biol.* **2012**, *56*, 841–852. [CrossRef] [PubMed]
2. Crawford, N.M.; Steiner, A.Z. Age-related Infertility. *Obs. Gynecol. Clin. N. Am.* **2015**, *42*, 15–25. [CrossRef] [PubMed]
3. Llarena, N.; Hine, C. Reproductive Longevity and Aging: Geroscience Approaches to Maintain Long-Term Ovarian Fitness. *J. Gerontol. A Biol. Sci. Med. Sci.* **2020**. [CrossRef] [PubMed]
4. Tarin, J.J. Potential effects of age-associated oxidative stress on mammalian oocytes/embryos. *Mol. Hum. Reprod.* **1996**, *2*, 717–724. [CrossRef] [PubMed]
5. Ruder, E.H.; Hartman, T.J.; Blumberg, J.; Goldman, M.B. Oxidative stress and antioxidants: Exposure and impact on female fertility. *Hum. Reprod. Update* **2008**, *14*, 345–357. [CrossRef]
6. Carbone, M.C.; Tatone, C.; Delle Monache, S.; Marci, R.; Caserta, D.; Colonna, R.; Amicarelli, F. Antioxidant enzymatic defences in human follicular fluid: Characterization and age-dependent changes. *Mol. Hum. Reprod.* **2003**, *9*, 639–643. [CrossRef]
7. Lim, J.; Luderer, U. Oxidative damage increases and antioxidant gene expression decreases with aging in the mouse ovary. *Biol. Reprod.* **2011**, *84*, 775–782. [CrossRef]
8. Steuerwald, N.M.; Bermudez, M.G.; Wells, D.; Munne, S.; Cohen, J. Maternal age-related differential global expression profiles observed in human oocytes. *Reprod. BioMed. Online* **2007**, *14*, 700–708. [CrossRef]
9. Hamatani, T.; Falco, G.; Carter, M.G.; Akutsu, H.; Stagg, C.A.; Sharov, A.A.; Dudekula, D.B.; VanBuren, V.; Ko, M.S.H. Age-associated alteration of gene expression patterns in mouse oocytes. *Hum. Mol. Genet.* **2004**, *13*, 2263–2278. [CrossRef]
10. McCallie, B.R.; Parks, J.C.; Trahan, G.D.; Jones, K.L.; Coate, B.D.; Griffin, D.K.; Schoolcraft, W.B.; Katz-Jaffe, M.G. Compromised global embryonic transcriptome associated with advanced maternal age. *J. Assist. Reprod. Genet.* **2019**, *36*, 915–924. [CrossRef]
11. Wang, S.; Zheng, Y.; Li, J.; Yu, Y.; Zhang, W.; Song, M.; Liu, Z.; Min, Z.; Hu, H.; Jing, Y.; et al. Single-Cell Transcriptomic Atlas of Primate Ovarian Aging. *Cell* **2020**, *180*, 585–600. [CrossRef] [PubMed]
12. McCallie, B.R.; Parks, J.C.; Strieby, A.L.; Schoolcraft, W.B.; Katz-Jaffe, M.G. Human blastocysts exhibit unique microrna profiles in relation to maternal age and chromosome constitution. *J. Assist. Reprod. Genet.* **2014**, *31*, 913–919. [CrossRef] [PubMed]
13. Dumesic, D.A.; Meldrum, D.R.; Katz-Jaffe, M.G.; Krisher, R.L.; Schoolcraft, W.B. Oocyte environment: Follicular fluid and cumulus cells are critical for oocyte health. *Fertil. Steril.* **2015**, *103*, 303–316. [CrossRef] [PubMed]
14. McReynolds, S.; Dzieciatkowska, M.; McCallie, B.R.; Mitchell, S.D.; Stevens, J.; Hansen, K.; Schoolcraft, W.B.; Katz-Jaffe, M.G. Impact of maternal aging on the molecular signature of human cumulus cells. *Fertil. Steril.* **2012**, *98*, 1574–1580. [CrossRef]
15. Mihalas, B.P.; Redgrove, K.A.; McLaughlin, E.A.; Nixon, B. Molecular Mechanisms Responsible for Increased Vulnerability of the Ageing Oocyte to Oxidative Damage. *Oxid. Med. Cell. Longev.* **2017**, *2017*, 4015874. [CrossRef]

16. Fujii, J.; Iuchi, Y.; Okada, F. Fundamental roles of reactive oxygen species and protective mechanisms in the female reproductive system. *Reprod. Biol. Endocrinol.* **2005**, *3*, 43. [CrossRef]
17. Behrman, H.R.; Kodaman, P.H.; Preston, S.L.; Gao, S. Oxidative Stress and the Ovary. *J. Soc. Gynecol. Investig.* **2001**, *8*, S40–S42.
18. Kodaman, P.H.; Behrman, H.R. Endocrine-Regulated and Protein Kinase C-Dependent Generation of Superoxide by Rat Preovulatory Follicles. *Endocrinology* **2001**, *142*, 687–693. [CrossRef]
19. Freitas, C.; Neto, A.C.; Matos, L.; Silva, E.; Ribeiro, A.; Silva-Carvalho, J.L.; Almeida, H. Follicular Fluid redox involvement for ovarian follicle growth. *J. Ovarian Res.* **2017**, *10*, 44. [CrossRef]
20. Tsai-Turton, M.; Luderer, U. Opposing Effects of Glutathione Depletion and Follicle-Stimulating Hormone on Reactive Oxygen Species and Apoptosis in Cultured Preovulatory Rat Follicles. *Endocrinology* **2006**, *147*, 1224–1236. [CrossRef]
21. Jana, S.K.; K, N.B.; Chattapadhyay, R.; Chakravarty, B.; Chaudhury, K. Upper control limit of reactive oxygen species in follicular fluid beyond which viable embryo formation is not favorable. *Reprod. Toxicol.* **2010**, *29*, 447–451. [CrossRef] [PubMed]
22. Yuan, Y.; Wheeler, M.B.; Krisher, R.L. Disrupted Redox Homeostasis and Aberrant Redox Gene Expression in Porcine Oocytes Contribute to Decreased Developmental Competence. *Biol. Reprod.* **2012**, *87*, 78. [CrossRef] [PubMed]
23. Yeh, J.; Bowman, M.J.; Browne, R.W.; Chen, N. Reproductive aging results in a reconfigured ovarian antioxidant defense profile in rats. *Fertil. Steril.* **2005**, *84*, 1109–1113. [CrossRef] [PubMed]
24. Lord, T.; Martin, J.H.; Aitken, R.J. Accumulation of Electrophilic Aldehydes During Postovulatory Aging of Mouse Oocytes Causes Reduced Fertility, Oxidative Stress, and Apoptosis. *Biol. Reprod.* **2015**, *92*, 33. [CrossRef]
25. Xian, Y.; Liang, L.; Qi, S.; Xie, Y.; Song, B.; Ouyang, S.; Xie, Y.; Sun, X.; Wang, W. Antioxidants retard the ageing of mouse oocytes. *Mol. Med. Rep.* **2018**, *18*, 1981–1986. [CrossRef]
26. Lian, H.-Y.; Gao, Y.; Jiao, G.-Z.; Sun, M.-J.; Wu, W.-F.; Wang, T.-Y.; Li, H.; Tan, J.-H. Antioxidant supplementation overcomes the deleterious effects of maternal restraint stress-induced oxidative stress on mouse oocytes. *Reproduction* **2013**, *146*, 559–568. [CrossRef]
27. Song, C.; Peng, W.; Yin, S.; Zhao, J.; Fu, B.; Zhang, J.; Mao, T.; Wu, H.; Zhang, Y. Melatonin improves age-induced fertility decline and attenuates ovarian mitochondrial oxidative stress in mice. *Sci. Rep.* **2016**, *6*, 35165. [CrossRef]
28. Kandemir, Y.B.; Aydin, C.; Gorgisen, G. The effects of melatonin on oxidative stress and prevention of primordial follicle loss via activation of mTOR pathway in the rat ovary. *Cell. Mol. Biol.* **2017**, *63*, 100–106. [CrossRef]
29. Liu, X.; Lin, X.; Mi, Y.; Li, J.; Zhang, C. Grape Seed Proanthocyanidin Extract Prevents Ovarian Aging by Inhibiting Oxidative Stress in the Hens. *Oxid. Med. Cell. Longev.* **2018**, *2018*, 9390810. [CrossRef]
30. Liu, X.; Lin, X.; Zhang, S.; Guo, C.; Li, J.; Mi, Y.; Zhang, C. Lycopene ameliorates oxidative stress in the aging chicken ovary via activation of Nrf2/HO-1 pathway. *Aging* **2018**, *10*, 2016–2036. [CrossRef]
31. Ruder, E.H.; Hartman, T.J.; Reindollar, R.H.; Goldman, M.B. Female dietary antioxidant intake and time to pregnancy among couples treated for unexplained infertility. *Fertil. Steril.* **2014**, *101*, 759–766. [CrossRef]
32. Velthut, A.; Zilmer, M.; Zilmer, K.; Kaart, T.; Karro, H.; Salumets, A. Elevated blood plasma antioxidant status is favourable for achieving IVF/ICSI pregnancy. *Reprod. Biomed. Online* **2013**, *26*, 345–352. [CrossRef] [PubMed]
33. Wang, Y.; Sharma, R.K.; Falcone, T.; Goldberg, J.; Agarwal, A. Importance portance of reactive oxygen species in the peritoneal fluid of women with endometriosis or idiopathic infertility. *Fertil. Steril.* **1997**, *68*, 826–830. [CrossRef]
34. Bedaiwy, M.A.; Falcone, T.; Sharma, R.K.; Goldberg, J.M.; Attaran, M.; Nelson, D.R.; Agarwal, A. Prediction of endometriosis with serum and peritoneal fluid markers: A prospective controlled trial. *Hum. Reprod.* **2002**, *17*, 426–431. [CrossRef] [PubMed]
35. Schauss, A.G.; Wu, X.; Prior, R.L.; Ou, B.; Huang, D.; Owens, J.; Agarwal, A.; Jensen, G.S.; Hart, A.N.; Shanbrom, E. Antioxidant capacity and other bioactivities of the freeze-dried Amazonian palm berry, Euterpe oleraceae mart. (acai). *J. Agric. Food Chem.* **2006**, *54*, 8604–8610. [CrossRef]
36. Kang, J.; Xie, C.; Li, Z.; Nagarajan, S.; Schauss, A.G.; Wu, T.; Wu, X. Flavonoids from acai (Euterpe oleracea Mart.) pulp and their antioxidant and anti-inflammatory activities. *Food Chem.* **2011**, *128*, 152–157. [CrossRef]
37. Merz, C.; Saller, S.; Kunz, L.; Xu, J.; Yeoman, R.R.; Ting, A.Y.; Lawson, M.S.; Stouffer, R.L.; Hennebold, J.D.; Pau, F.; et al. Expression of the beta-2 adrenergic receptor (ADRB-2) in human and monkey ovarian follicles: A marker of growing follicles? *J. Ovarian Res.* **2015**, *8*, 8. [CrossRef]

38. Wheeler, A.G.; Lean, J.; Walker, M. Peripheral progesterone concentrations in the luteal-phase ewe: Effects of a beta-adrenergic receptor antagonist and two beta 2-adrenergic agonists. *J. Endocrinol.* **1988**, *116*, 137–142. [CrossRef]
39. Parillo, F.; Maranesi, M.; Mignini, F.; Marinelli, L.; Di Stefano, A.; Boiti, C.; Zerani, M. Evidence for a dopamine intrinsic direct role in the regulation of the ovary reproductive function: In vitro study on rabbit corpora lutea. *PLoS ONE* **2014**, *9*, e104797. [CrossRef]
40. Cruz, G.; Fernandois, D.; Paredes, A.H. Ovarian function and reproductive senescence in the rat: Role of ovarian sympathetic innervation. *Reproduction* **2017**, *153*, R59–R68. [CrossRef]
41. Xie, C.; Kang, J.; Li, Z.; Schauss, A.G.; Badger, T.M.; Nagarajan, S.; Wu, T.; Wu, X. The açai flavonoid velutin is a potent anti-inflammatory agent: Blockade of LPS-mediated TNF-α and IL-6 production through inhibiting NF-κB activation and MAPK pathway. *J. Nutr. Biochem.* **2012**, *23*, 1184–1191. [CrossRef]
42. Lim, J.; Nakamura, B.N.; Mohar, I.; Kavanagh, T.J.; Luderer, U. Glutamate Cysteine Ligase Modifier Subunit (Gclm) Null Mice Have Increased Ovarian Oxidative Stress and Accelerated Age-Related Ovarian Failure. *Endocrinology* **2015**, *156*, 3329–3343. [CrossRef]
43. Perkins, A.T.; Das, T.M.; Panzera, L.C.; Bickel, S.E. Oxidative stress in oocytes during midprophase induces premature loss of cohesion and chromosome segregation errors. *Proc. Natl. Acad. Sci. USA* **2016**, *113*, E6823–E6830. [CrossRef]
44. Cheng, J.M.; Liu, Y.X. Age-Related Loss of Cohesion: Causes and Effects. *Int. J. Mol. Sci.* **2017**, *18*, 1578. [CrossRef]
45. Fortier, M.E.; Audet, I.; Giguere, A.; Laforest, J.P.; Bilodeau, J.F.; Quesnel, H.; Matte, J.J. Effect of dietary organic and inorganic selenium on antioxidant status, embryo development, and reproductive performance in hyperovulatory first-parity gilts. *J. Anim. Sci.* **2012**, *90*, 231–240. [CrossRef]
46. Xiong, X.; Lan, D.; Li, J.; Lin, Y.; Li, M. Selenium supplementation during *in vitro* maturation enhances meiosis and developmental capacity of yak oocytes. *Anim. Sci. J.* **2018**, *89*, 298–306. [CrossRef]
47. Dattilo, M.; D'Amato, G.; Caroppo, E.; Menezo, Y. Improvement of gamete quality by stimulating and feeding the endogenous antioxidant system: Mechanisms, clinical results, insights on gene-environment interactions and the role of diet. *J. Assist. Reprod. Genet.* **2016**, *33*, 1633–1648. [CrossRef]
48. Mikwar, M.; MacFarlane, A.J.; Marchetti, F. Mechanisms of oocyte aneuploidy associated with advanced maternal age. *Mutat. Res.* **2020**, *785*, 108320. [CrossRef]
49. Franasiak, J.M.; Forman, E.J.; Hong, K.H.; Werner, M.D.; Upham, K.M.; Treff, N.R.; Scott, R.T. The nature of aneuploidy with increasing age of the female partner: A review of 15,169 consecutive trophectoderm biopsies evaluated with comprehensive chromosomal screening. *Fertil. Steril.* **2014**, *101*, 656–663. [CrossRef]
50. Katz-Jaffe, M.G.; McReynolds, S.; Henry, L.; McCubbin, N.; Mann, R.S.; Tucci, R.; McCormick, S.; Schoolcraft, W.B. Age-related pregnancy loss is largely overcome with single euploid embryo transfer. *Fertil. Steril.* **2020**, *114*, e428. [CrossRef]
51. Riley, J.K.; Jungheim, E.S. Is there a role for diet in ameliorating the reproductive sequelae associated with chronic low-grade inflammation in polycystic ovary syndrome and obesity? *Fertil. Steril.* **2016**, *106*, 520–527. [CrossRef] [PubMed]
52. Poston, L.; Igosheva, N.; Mistry, H.D.; Seed, P.T.; Shennan, A.H.; Rana, S.; Karumanchi, S.A.; Chappell, L.C. Role of oxidative stress and antioxidant supplementation in pregnancy disorders. *Am. J. Clin. Nutr.* **2011**, *94*, 1980S–1985S. [CrossRef]
53. Young, D.; Klepacka, D.; McGarvey, M.; Schoolcraft, W.B.; Katz-Jaffe, M.G. Infertility patients with chromosome inversions are not susceptible to an inter-chromosomal effect. *J. Assist. Reprod. Genet.* **2019**, *36*, 509–516. [CrossRef] [PubMed]
54. Alessandra-Perini, J.; Rodrigues-Baptista, K.C.; Machado, D.E.; Nasciutti, L.E.; Perini, J.A. Anticancer potential, molecular mechanisms and toxicity of Euterpe oleracea extract (açaí): A systematic review. *PLoS ONE* **2018**, *13*, e0200101. [CrossRef] [PubMed]

17.0 Appendix 4. Additional publication

Denomme MM, McCallie BR, **Parks JC,** Schoolcraft WB, Katz-Jaffe MG. Epigenetic Dysregulation Observed in Monosomy Blastocysts Further Compromises Developmental Potential. PLoS One. 2016 Jun 7;11(6):e0156980. doi: 10.1371/journal.pone.0156980. eCollection 2016.

My personal contribution to this manuscript

I worked closely with Dr. Katz-Jaffe and Dr. Denomme to coordinate the collection of study materials between the research department and the IVF laboratory. I also warmed the vitrified embryos used in this study, and confirmed their viability prior to preparing them for storage at -80°C and downstream molecular experiments. Finally, I co-wrote and edited sections of the materials and methods section of the manuscript for publication as a co-author.

PLOS | ONE

RESEARCH ARTICLE

Epigenetic Dysregulation Observed in Monosomy Blastocysts Further Compromises Developmental Potential

Michelle M. Denomme[1], Blair R. McCallie[1], Jason C. Parks[1], William B. Schoolcraft[2], Mandy G. Katz-Jaffe[1,2]*

1 Fertility Labs of Colorado, Lone Tree, Colorado, United States of America, 2 Colorado Center for Reproductive Medicine, Lone Tree, Colorado, United States of America

* MKatz-Jaffe@ColoCRM.com

Citation: Denomme MM, McCallie BR, Parks JC, Schoolcraft WB, Katz-Jaffe MG (2016) Epigenetic Dysregulation Observed in Monosomy Blastocysts Further Compromises Developmental Potential. PLoS ONE 11(6): e0156980. doi:10.1371/journal.pone.0156980

Editor: Osman El-Maarri, University of Bonn, Institute of Experimental Hematology and Transfusion Medicine, GERMANY

Received: February 17, 2016

Accepted: May 23, 2016

Published: June 7, 2016

Data Availability Statement: All relevant data are within the paper and its Supporting Information files.

Funding: The authors received no specific funding for this work.

Competing Interests: The authors have declared that no competing interests exist.

Abstract

Epigenetic mechanisms such as DNA methylation regulate genomic imprinting and account for the distinct non-equivalence of the parental genomes in the embryo. Chromosomal aneuploidy, a major cause of infertility, distorts this highly regulated disparity by the presence or absence of chromosomes. The implantation potential of monosomy embryos is negligible compared to their trisomy counterparts, yet the cause for this is unknown. This study investigated the impact of chromosomal aneuploidy on strict epigenetically regulated domains, specifically imprinting control regions present on aneuploid chromosomes. Donated cryopreserved human IVF blastocysts of transferable quality, including trisomy 15, trisomy 11, monosomy 15, monosomy 11, and donor oocyte control blastocysts were examined individually for DNA methylation profiles by bisulfite mutagenesis and sequencing analysis of two maternally methylated imprinting control regions (ICRs), *SNRPN* (15q11.2) and *KCNQ1OT1* (11p15.5), and one paternally methylated imprinting control region, *H19* (11p15.5). Imprinted genes within the regions were also evaluated for transcript abundance by RT-qPCR. Overall, statistically significant hypermethylated and hypomethylated ICRs were found in both the trisomy and monosomy blastocysts compared to controls, restricted only to the chromosome affected by the aneuploidy. Increased expression was observed for maternally-expressed imprinted genes in trisomy blastocysts, while a decreased expression was observed for both maternally- and paternally-expressed imprinted genes in monosomy blastocysts. This epigenetic dysregulation and altered monoallelic expression observed at imprinting control regions in aneuploid IVF embryos supports euploid embryo transfer during infertility treatments, and may specifically highlight an explanation for the compromised implantation potential in monosomy embryos.

Introduction

Embryonic chromosomal aneuploidy is a major cause of human infertility, and likely contributes to most failed conceptions, both natural and IVF. As the most common chromosome abnormality in human reproduction, it is the leading source of miscarriages, stillbirths, and congenital birth defects [1], as well as the largest underlying basis for embryo arrest and implantation failure [2]. Over half of early human IVF embryos are estimated to be affected by whole chromosome imbalances. While it is difficult to definitively decipher the precise frequencies of meiotic and mitotic origins, it is known that the vast majority are a result of maternal meiotic errors in the oocyte, followed distantly by mitotic errors post-fertilization, having paternal meiotic errors in the sperm occurring at the lowest frequency [3, 4].

Aneuploidy can affect any of the twenty-two autosome pairs and the two sex chromosomes. However, trisomy and monosomy errors compromise embryonic development by different means. Trisomy errors involve the gain of a third additional chromosome. Many of the smaller size trisomies will successfully implant, but contribute to pregnancy loss, and only a handful can reach live birth including the widely characterized Down Syndrome (Trisomy 21). Monosomy errors involve the loss of one chromosome from a pair. These embryos predominately do not implant, and rarely reach clinical pregnancy, having Turner Syndrome (XO) the only full monosomy that has the potential to develop to term. This significant disparity reported between pre- and post-implantation frequencies for monosomy embryos has recently been tallied, with 45.7% of preimplantation monosomies in blastocysts reduced to 6.3% of post-implantation monosomies in spontaneous abortuses [5]. The cause for this compromised implantation potential for monosomy embryos compared to their trisomy counterparts is unknown. An increasing number of aneuploidy studies have proposed a relationship between chromosome imbalance and epigenetics, though cause and consequence are still undetermined [6–12].

Epigenetics describes the chromatin modifications that alter the accessibility of genes and regulate gene expression [13]. These chromatin changes allow cells to maintain differential expression despite containing the same genomic material [14]. Gametogenesis and early embryogenesis are critical stages in which genome-wide epigenetic transitions required for early mammalian development are orchestrated [15].

The epigenetic phenomenon known as genomic imprinting restricts gene expression in the embryo to one of the two parental contributions. Disruption to this highly regulated process can lead to developmental and neurological disorders such as Beckwith-Wiedemann Syndrome (BWS), Angelman Syndrome (AS) and Prader-Willi Syndrome (PWS), which are characterized by genetic and epigenetic errors at the *KCNQ1OT1* (BWS), *H19* (BWS) and *SNRPN* (AS and PWS) imprinting control regions (ICRs) [16–22]. Epigenetic mechanisms, including DNA methylation, are criticial for maintaining genomic imprinting regulation. The hypothesis is that chromosomal aneuploidy distorts this highly regulated disparity, with some evidence observed in neoplasia [8, 23].

Our previous investigation of epigenetic modifiers uncovered a hypomethylated state and reduced gene expression limited to the monosomy chromosome [24]. To further analyze the epigenetic effects of aneuploidy, in this study we compared the imprinted DNA methylation profiles and imprinted gene expression levels of three ICRs, *SNRPN*, *H19* and *KCNQ1OT1*, in individual aneuploid blastocysts. Consistent with our expectations, trisomy and monosomy blastocysts had both hyper- and hypomethylated imprinted DNA regions and altered imprinted gene expression when compared to controls. Our results indicate that the dysregulation of genomic imprinting in aneuploid blastocysts, specifically the altered imprinted methylation leading to decreased gene expression observed in monosomy embryos, may contribute to

their reduced implantation potential and support euploid embryo transfer following comprehensive chromosome screening in IVF cycles.

Materials and Methods

Surplus cryopreserved human blastocysts

One hundred and thirty five patients who had undergone fertility treatments at the Colorado Center for Reproductive Medicine (CCRM) donated a total of 170 cryopreserved human blastocysts. All blastocysts were viable and morphologically graded as high transferrable quality ≥3BB on Day 5 of embryonic development [25]. Comprehensive chromosome screening (CCS) was performed by our in-house genetics laboratory at CCRM as previously described [26]. Trisomy 15 (n = 30), monosomy 15 (n = 30), trisomy 11 (n = 30), monosomy 11 (n = 35), and donor oocyte control blastocysts (n = 45) were analyzed. Blastocysts were divided between two experimental models, either imprinted DNA methylation analysis or imprinted gene expression analysis, as described in Table 1.

Ethics statement

Ethics approval was obtained from our associated HCA-HealthONE Institutional Review Board and Western Institutional Review Board. All patients provided informed written consent for their blastocysts to be used in this study and gave permission for researchers to access medical records to obtain embryology and CCS results.

Imprinted DNA methylation analysis by bisulfite mutagenesis

Bisulfite mutagenesis and clonal sequencing of individual human blastocysts was performed as previously described [27, 28]. Briefly, warmed blastocysts were embedded in a 2:1 low melting point agarose and lysis mixture and incubated in SDS lysis buffer overnight in a 50°C waterbath. The following day, the samples were immediately processed for bisulfite mutagenesis or frozen at (-20°C) for a maximum of 5 days. To process, samples were first incubated at 90–95°C for 2.5 minutes and were then denatured for 15 minutes at 37°C in 1 mL of 0.1M NaOH. Bisulfite conversion occurred in 500 μL of 2.5M bisulfite solution under mineral oil in a 50°C waterbath for 3.5 hours. Desulfonation of samples took place at 37°C for 15 minutes in 1 mL of 0.3M NaOH, and the samples were then washed twice in 1 mL of TE buffer and twice in 1 mL of H_2O with shaking.

Table 1. Summary of blastocysts divided among experimental procedures.

Experiment	Embryos	Number of Blastocysts	Number of Patients	Mean Maternal Age	Mean Paternal Age
	Controls	35	13	Donor, <33	39.7 ± 5.2
Imprinted	Trisomy 15	20	20	39.5 ± 3.8	40.0 ± 6.5
DNA	Trisomy 11	20	20	38.7 ± 4.0	39.9 ± 4.4
Methylation	Monosomy 15	20	20	38.3 ± 4.4	37.2 ± 4.3
	Monosomy 11	25	25	39.0 ± 3.0	39.7 ± 4.6
	Controls	10	2	Donor, <33	39.8 ± 1.5
Imprinted	Trisomy 15	10	10	40.5 ± 2.1	41.8 ± 5.5
Gene	Trisomy 11	10	10	37.1 ± 4.4	39.7 ± 6.5
Expression	Monosomy 15	10	10	41.2 ± 2.3	44.8 ± 5.6
	Monosomy 11	10	10	40.9 ± 1.2	42.8 ± 3.2

doi:10.1371/journal.pone.0156980.t001

Table 2. PCR primers and parameters for bisulfite mutagenesis.

Locus	Gene	Primer Name	Primer Sequence (5'-3')	Size (bp)	CpG (#)	SNPs	REF
15q11.2	**SNRPN**	SNRPN-OF	TAGTGTTGTGGGGTTTTAGGG	371	24	Rs220029	[27]
	(U41384)	SNRPN-IF	AGGGAGGGAGTTGGGATTT			G (84.8%) /	
		SNRPN-IR	CACAACAACAAACCTCTAAACATTC			A (15.2%)	
		SNRPN-OR	TACCCACCTCCACCCATATC				
11p15.5	**H19**	H19-OF	AATAATGAGGTGTTTTAGTTTTATGGATG	170	14	Rs2071094	[27, 29]
	(AI087017)	H19-IF	TTGGTTGTAGTTGTGGAAT			C (66.4%) /	
		H19-IR	ACTCCTATAAATATCCTATTCCCAAATAACCCC			A (33.6%)	
		H19-OR	ACTTAAATCCCAAACCATAACACTAAAAC				
11p15.5	**KCNQ1OT1**	KCNQ1OT1-OF	TGTTTTTGTAGTTTATATGGAAGGGTTAA	265	22	Rs56134313	[29, 30]
	(U90095)	KCNQ1OT1-IF	GTTAGGGAAGTTTTAGGGTGTGAAT			G (94.0%) /	
		KCNQ1OT1-IR	AAACATACCAAACCACCCACCTAACAAA			A (6.0%)	
		KCNQ1OT1-OR	CTCACCCCTAAAAACTTAAAACCTC				

OF = outer forward primer, IF = inner forward primer, IR = inner reverse primer, OR = outer reverse primer
94°C for 10 min, 55 cycles of (94°C for 15 sec, 56°C for 20 sec, 72°C for 20 sec), 72°C for 10 min. [27]

doi:10.1371/journal.pone.0156980.t002

For the first round of nested PCR amplification, the agarose bead was added directly to a Hot Start Ready-To-Go (RTG) (GE Healthcare) PCR bead that contained 0.5 μL of each 10 μM gene-specific outer primer, 1 μL of 240 ng/mL transfer RNA and water up to 15 μL. For the second round of nested PCR amplification, 5 μL of first round product was added to a fresh RTG bead mixed with 19 μL water and 0.5 μL of each 10 μM inner primer. *The SNRPN, H19*, and *KCNQ1OT1* PCR bisulfite primers were described previously [27] and can be found in Table 2. Both outer and inner PCR reactions were performed as previously described [27]. Following the second round of PCR amplification, samples were gel extracted, ligated into the pGEM-T EASY vector system (Promega), and transformed into Z-competent DH5α *Escherichia coli* cells (Zymo Research). Following colony PCR amplification, 30 μL of individual clone samples were sent for sequencing at Bio Basic Inc. (Markham, ON, Canada).

Approximately 25–35 clones were sequenced per blastocyst per gene. Methylation patterns were determined using two online software programs (BISMA and QUMA). Identical clones were considered to be representative of one individual DNA strand, and thus were included only once in each blastocyst DNA methylation figure. Total DNA methylation for each gene was calculated as a percentage of the total number of methylated CpGs divided by the total number of CpG dinucleotides. When present, total DNA methylation for each single nucleotide polymorphism (SNP) was calculated separately. For simplicity of analysis, any monosomy blastocyst containing more than one parental SNP within a gene was discarded from the study. Student's *t*-test was used to examine significance for methylation between aneuploid and control blastocysts. A p-value of <0.05 was considered to be statistically significant.

Relative imprinted expression analysis

Total RNA was isolated from individual whole blastocysts for analysis of gene transcript abundance as previously described [31]. Briefly, using the PicoPure RNA Isolation Kit (Molecular Devices), blastocysts were lysed, treated with RNase-free DNase I (Qiagen), washed twice, and eluted in 20 μL elution solution. To generate cDNA template for real-time PCR, reverse transcription was performed using the High Capacity Reverse Transcription cDNA kit (Applied Biosystems).

Table 3. Expression primers and PCR parameters.

Locus	Gene	Primer Name	Primer Sequence (5'-3')	Size (bp)
15q11.2	***SNRPN***	*SNRPN-F*	GCCATATTGGAGTAGCGAGGAA	84
	(NM_003097.3)	*SNRPN-R*	CAATGCAAGCTGGGCAGAA	
	UBE3A	*UBE3A-F*	CAAAAATGGCCCAGACACAGA	119
	(NM_000462.3)	*UBE3A-R*	ACGTGATGGCCTTCAACAATC	
11p15.5	***H19***	*H19-F*	GGAGTGAATGAGCTCTCAGG	308
	(NR_002196.2)	*H19-R*	CTAAGGTGTTCAGGAAGGCC	
	KCNQ1OT1	*KCNQ1OT1-F*	AAAAGCTCCCAACGAGGAA	64
	(NR_002728.3)	*KCNQ1OT1-R*	GGCTCTTGGCTGGGTACA	
	CDKN1C	*CDKN1C-F*	GGCCTCTGATCTCCGATTTC	67
	(NM_000076.2)	*CDKN1C-F*	ACATGGCCCGAGGACTTC	
7p13	***PPIA***	*PPIA-F*	GCTTTGGGTCCAGGAATGG	59
	(NM_001300981.1)	*PPIA-R*	TTGTCCACAGTCAGCAATGG	

F = forward primer, R = reverse primer.

95°c for 10 min, 40 cycles of (95°C for 15 sec, 60°C for 1 min), 95°C for 15 sec, 60°C for 1 min, 95°C for 15 sec, 60°C for 15 sec

doi:10.1371/journal.pone.0156980.t003

Quantitative real-time PCR was performed using the ABI 7300 Real Time PCR System with the Power SYBR Green PCR Master Mix (Applied Biosystems). The quantification of two genes for trisomy 15 and monosomy 15, *SNRPN* and *UBE3A*, and three genes for trisomy 11 and monosomy 11, *H19*, *KCNQ1OT1* and *CDKN1C* were calculated relative to the housekeeping gene, *PPIA* (7p13), which displayed comparatively constant levels of transcription in every sample, and compared to donor control blastocysts. Expression primers and PCR parameters are outlined in Table 3, all primers were designed in-house except for *H19* [32]. The PCR reaction efficiency recorded R^2 values ≥ 0.95 and the correlation coefficient was calculated to be >0.99. Statistical analysis was performed using the Relative Expression Software Tool (REST-2009) (Qiagen). REST software determines an expression ratio that is tested for significance by a Pair Wise Fixed Reallocation Randomization Test [33]. Samples with $p<0.05$ were considered statistically significant.

Results

Blastocysts and imprinting regions

A total of 170 cryopreserved blastocysts were donated with IRB and patient consent, 45 were donor oocyte control blastocysts, while the remaining 125 were aneuploid blastocysts divided between trisomy 15, trisomy 11, monosomy 15 and monosomy 11. A summary of the distribution of blastocysts among experimental procedures, along with mean maternal and paternal ages are outlined in Table 1.

Three defined ICRs were selected for investigation; the *SNRPN* ICR, located on human chromosome 15q11.2, and the *H19* and *KCNQ1OT1* ICRs located adjacently on human chromosome 11p15.5. The *SNRPN* and *KCNQ1OT1* ICRs are maternally methylated in the oocyte and paternally expressed from the unmethylated sperm contribution. The *H19* ICR is reversed, paternally methylated in the sperm and maternally expressed from the unmethylated oocyte contribution. A single nucleotide polymorphism (SNP) was present in all three amplified regions, but at different frequencies: *SNRPN* SNP G (84.8%) / A (15.2%) (Rs220029), *H19* SNP C (66.4%) / A (33.6%) (Rs2071094), and *KCNQ1OT1* SNP G (94.7%) / A (6.3%) (Rs56134313) (S1 Table).

Imprinted DNA methylation in control blastocysts

Each control blastocyst displayed diploid chromosomes representing one inherited methylated allele and one inherited unmethylated allele at all imprinted regions (Fig 1a–1c). Analysis of the twenty blastocysts examined at *SNRPN* revealed an average methylation of 53.7% ± 3.9%. *H19* had an average methylation of 47.3% ± 5.0%, while *KCNQ1OT1* had 50.6% ± 4.2% average methylation. To summarize, all control blastocysts examined had a DNA methylation profile range that was comparable to the expected fifty percent methylation for diploid chromosomes (Fig 1d, S1 Fig, S2 Table).

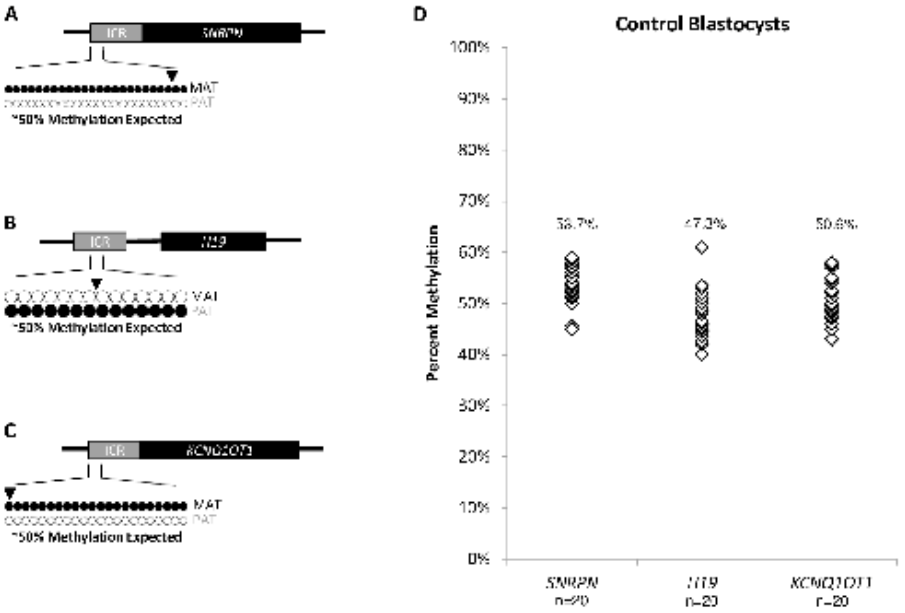

Fig 1. Imprinted DNA methylation profiles of control blastocysts. Black dots represent methylated CpGs, white dots represent unmethylated CpGs. The SNP location is indicated by an arrowhead. "MAT" represents the maternal oocyte-contributed allele; "PAT" represents the paternal sperm-contributed allele. A) Diagram of the *SNRPN* ICR amplified region analyzed on human chromosome 15q11.2 (GenBank: U41384) in control blastocysts, a 371 bp region consisting of 24 assessable CpGs and a G/A SNP (Rs220029). The *SNRPN* ICR is maternally methylated. Approximately 50% methylation is expected, derived from one MAT allele and one PAT allele. B) Diagram of the *H19* ICR amplified region analyzed on human chromosome 11p15.5 (GenBank: AF087017) in control blastocysts, a 170 bp region consisting of 14 assessable CpGs and a A/C SNP (Rs2071094). The *H19* ICR is paternally methylated. Approximately 50% methylation is expected, derived from one MAT allele and one PAT allele. C) Diagram of the *KCNQ1OT1* ICR amplified region analyzed on human chromosome 11p15.5 (GenBank: U90095) in control blastocysts, a 265 bp region consisting of 22 assessable CpGs and a G/A SNP (Rs56134313). The *KCNQ1OT1* ICR is maternally methylated. Approximately 50% methylation is expected, derived from one MAT allele and one PAT allele. D) Summary chart of percent methylation in all control blastocysts at the *SNRPN* (n = 20), *H19* (n = 20), and *KCNQ1OT1* (n = 20) ICRs. Each white diamond represents the methylation percentage for one individual control blastocyst per ICR. Average percent methylation for each cohort is indicated above each gene. Methylation dot diagrams for individual control blastocysts can be found in S1 Fig, and a summary can be found in S2 Table.

doi:10.1371/journal.pone.0156980.g001

Imprinted DNA methylation in trisomy blastocysts

At imprinted regions, a trisomy chromosome is represented by one inherited methylated allele, one inherited unmethylated allele, and a third inherited allele with unknown origin and subsequent unknown methylation status (Fig 2a–2c). Analysis of the trisomy 15 blastocysts at the *SNRPN* ICR revealed an average methylation of 67.0% ± 4.5% ($p<0.001$ compared to controls) among the twenty blastocysts, suggesting a gain of the third additional chromosome from the oocyte for all blastocysts examined (Fig 2d, S2 Fig, S2 Table). *H19* and *KCNQ1OT1* reside on diploid chromosome 11, and thus were unaffected by the trisomy, having 48.5% ± 5.4% ($p = 0.64$), and 52.8% ± 1.8% ($p = 0.26$), respectively, in the five blastocysts examined (Fig 2d, S4 Fig, S2 Table).

Analysis of trisomy 11 blastocysts at *H19* showed 36.8% ± 10.3% ($p<0.001$) average methylation (Fig 2e, S2 Fig, S2 Table). The DNA methylation range for *H19* was broadened due to the high frequency of both SNP polymorphisms at this locus. In the same trisomy 11 blastocysts, *KCNQ1OT1* had 17/20 blastocysts with 63.8% ± 3.6% ($p<0.001$) average methylation, reflecting a gain of the third chromosome from the oocyte, and 3/20 blastocysts with 39.3% ± 4.2% ($p<0.001$) average methylation, indicating a gain of the third chromosome from the sperm (Fig 2e, S2 Fig, S2 Table).

In confirmation of these origins of aneuploidy, both *H19* and *KCNQ1OT1*, located adjacent to each other on chromosome 11, reflect the same gain from the oocyte or sperm in the same individual blastocysts. For example, blastocyst 11T02, 11T08, 11T12 appear to have gained the third chromosome from the sperm at both imprinted loci. *SNRPN* resides on diploid chromosome 15, and was unaffected by the trisomy in all five blastocysts examined, having an average methylation of 51.2% ± 2.5% ($p = 0.20$), comparable to controls (Fig 2e, S4 Fig, S2 Table).

Imprinted DNA methylation in monosomy blastocysts

At imprinted regions, a monosomy chromosome results in a loss of either the inherited methylated allele or loss of the inherited unmethylated allele. Loss of the methylated allele is expected to result in hypomethylation of the ICR in the blastocyst, contributing only from the unmethylated chromosome. Loss of the unmethylated allele is expected to result in hypermethylation of the ICR in the blastocyst, contributing only from the methylated chromosome (Fig 3a–3c).

Analysis of monosomy 15 blastocysts at *SNRPN* revealed 15/20 blastocysts with an average methylation of 2.3% ± 1.0% ($p<0.001$ compared to controls), suggesting the chromosome loss originated from the oocyte, and 5/20 blastocysts with 87.8% ± 3.7% average methylation ($p<0.001$), suggesting the chromosome loss originated from the sperm (Fig 3d, S3 Fig, S2 Table). *H19* and *KCNQ1OT1* reside on diploid chromosome 11 in these blastocysts, and thus were unaffected by the monosomy in all five blastocysts examined, with an average methylation of 48.5% ± 5.4% ($p = 0.64$) and 52.0% ± 3.7% ($p = 0.49$), respectively (Fig 3d, S4 Fig, S2 Table).

Analysis of monosomy 11 blastocysts at *H19* revealed 19/25 blastocysts with an average methylation of 84.6% ± 6.4% ($p<0.001$), suggesting the chromosome loss arose from the oocyte, while 6/25 blastocysts had an average methylation of 4.2% ± 2.9% ($p<0.001$), suggesting the chromosome loss arose from the sperm (Fig 3e, S3 Fig, S2 Table). In the same monosomy 11 blastocysts, *KCNQ1OT1* had 16/25 blastocysts with 4.0% ± 1.6% ($p<0.001$) average methylation, suggesting the chromosome loss originated from the oocyte, and 3/25 blastocysts with 91.3% ± 6.4% ($p<0.001$) average methylation, suggesting the chromosome loss originated from the sperm (Fig 3e, S3 Fig, S2 Table). In confirmation of these results, both *H19* and *KCNQ1OT1* reflected the same origin of loss from the oocyte or sperm in the same individual blastocysts. For example, blastocysts 11M06, 11M10, 11M22 presumably lost the chromosome contributed

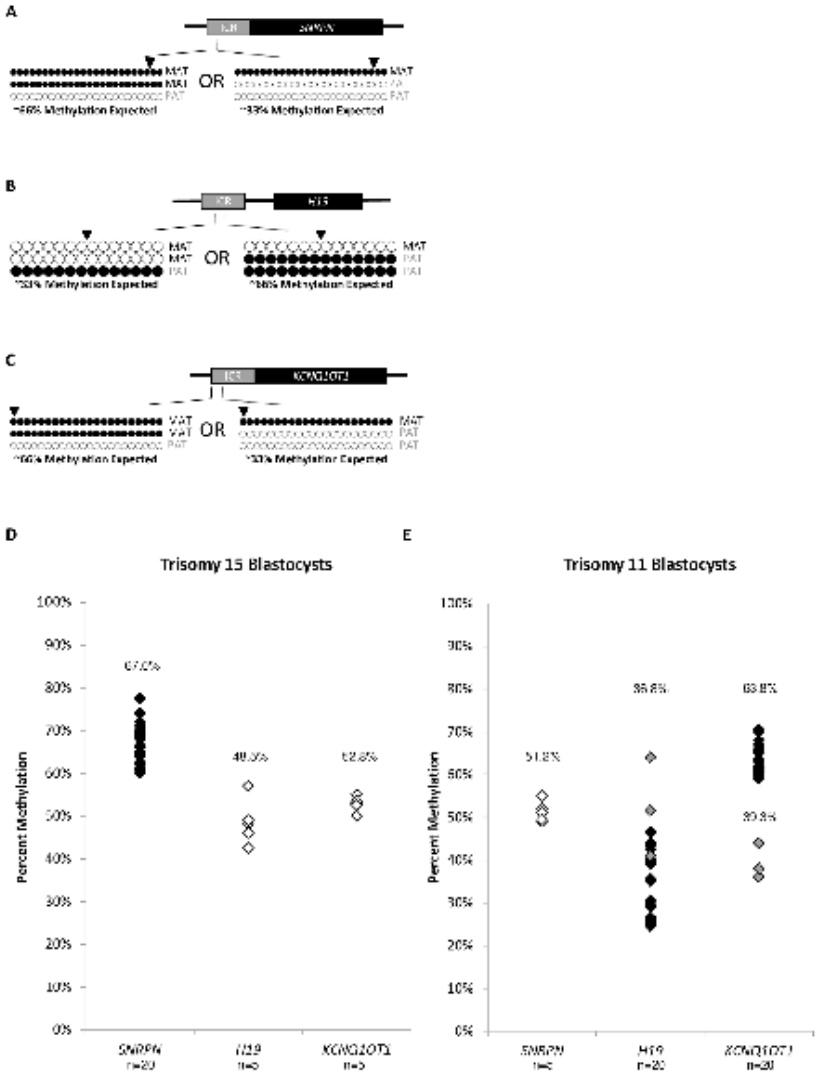

Fig 2. Imprinted DNA methylation profiles of trisomy blastocysts. Black dots represent methylated CpGs, white dots represent unmethylated CpGs. The SNP location is indicated by an arrowhead. "MAT" represents the maternal oocyte-contributed allele; "PAT" represents the paternal sperm-contributed allele. A) Diagram of the *SNRPN* ICR amplified region analyzed in trisomy 15 blastocysts. Approximately 66% methylation is expected with an additional MAT allele. Approximately 33% methylation is expected with an additional PAT allele. B) Diagram of the *H19* ICR amplified region analyzed in trisomy 11

blastocysts. Approximately 33% methylation is expected with an additional MAT allele. Approximately 66% methylation is expected with an additional PAT allele. C) Diagram of the *KCNQ1OT1* ICR amplified region analyzed in trisomy 11 blastocysts. Approximately 66% methylation is expected with an additional MAT allele. Approximately 33% methylation is expected with an additional PAT allele. D) Summary chart of percent methylation in all trisomy 15 blastocysts at the *SNRPN* (n = 20), *H19* (n = 5), and *KCNQ1OT1* (n = 5) ICRs. Black diamonds represent blastocysts with presumable gain of the third chromosome 15 from the oocyte, grey diamonds represent blastocysts with presumable gain of the third chromosome 15 from the sperm. White diamonds represent the methylation percentage for the ICRs on diploid chromosome 11. Average percent methylation for each cohort is indicated. E) Summary chart of percent methylation in all trisomy 11 blastocysts at the *SNRPN* (n = 5), *H19* (n = 20), and *KCNQ1OT1* (n = 20) ICRs. Black diamonds represent blastocysts with presumable gain of the third chromosome 11 from the oocyte, grey diamonds represent blastocysts with presumable gain of the third chromosome 11 from the sperm. White diamonds represent the methylation percentage for the ICR on diploid chromosome 15. Average percent methylation for each cohort is indicated. Methylation dot diagrams for individual trisomy blastocysts and diploid ICRs can be found in S2 and S4 Figs, and a summary can be found in S2 Table.

doi:10.1371/journal.pone.0156980.g002

from the sperm at both imprinted loci. A third subset of 6/25 blastocysts had 47.8% ± 6.9% ($p = 0.25$) average methylation for *KCNQ1OT1*, which was not statistically different from control blastocysts at this imprinted locus. *SNRPN* resides on diploid chromosome 15, and thus was unaffected by the monosomy 11 in all five blastocysts examined having 51.6% ± 2.9% ($p = 0.29$) average methylation (Fig 3e, S4 Fig, S2 Table).

Imprinted gene expression in aneuploid blastocysts

Transcript abundance for trisomy 15 and monosomy 15 blastocysts were compared to control blastocysts at two imprinted genes on human chromosome 15, and normalized to the housekeeping gene, *PPIA* (7p13). *SNRPN* is paternally expressed, while *UBE3A* is maternally expressed in human blastocysts. *UBE3A* was significantly increased in the trisomy 15 blastocysts ($p<0.001$), while *SNRPN* was not statistically altered compared to controls ($p = 0.08$). In the monosomy 15 blastocysts, both *SNRPN* ($p<0.001$) and *UBE3A* ($p<0.001$) were significantly decreased when compared to the control blastocysts (Fig 4a).

In the same way, transcript abundance for trisomy 11 and monosomy 11 blastocysts were compared to control blastocysts at three imprinted genes on human chromosome 11, and normalized to the same housekeeping gene, *PPIA* (7p13). *H19* and *CDKN1C* are maternally expressed, while *KCNQ1OT1* is paternally expressed, in human blastocysts. *H19* ($p<0.01$) was significantly increased in the trisomy 11 blastocysts, while *CDKN1C* trended towards an increase without statistical difference ($p = 0.30$). *KCNQ1OT1* expression was comparable to controls ($p = 0.49$). In the monosomy 11 blastocysts, *H19* ($p<0.05$) was significantly decreased compared to the control group. While no significant difference was observed between the monosomy group and controls at *KCNQ1OT1* ($p = 0.65$) or *CDKN1C* ($p = 0.79$), a trend towards a decrease was evident (Fig 4b).

Discussion

This study was designed to investigate the DNA methylation and imprinted gene expression profiles of imprinting control regions upon altered chromosome constitution in individual human blastocysts. Previously, our group examined the effects of aneuploidy on epigenetic modifications chromosome-wide. In monosomy blastocysts, DNA methylation levels were reduced on the chromosome involved in the error, while trisomy blastocysts showed no difference in DNA methylation compared to diploid controls. Likewise, protein-coding genes found on the specific monosomy chromosome were significantly decreased [24]. On account of these results, we questioned how whole chromosome aneuploidy can affect strict epigenetically regulated domains. Specifically, we questioned whether genomic imprints are maintained despite chromosome-wide reduced methylation levels on these monosomies. To investigate, we

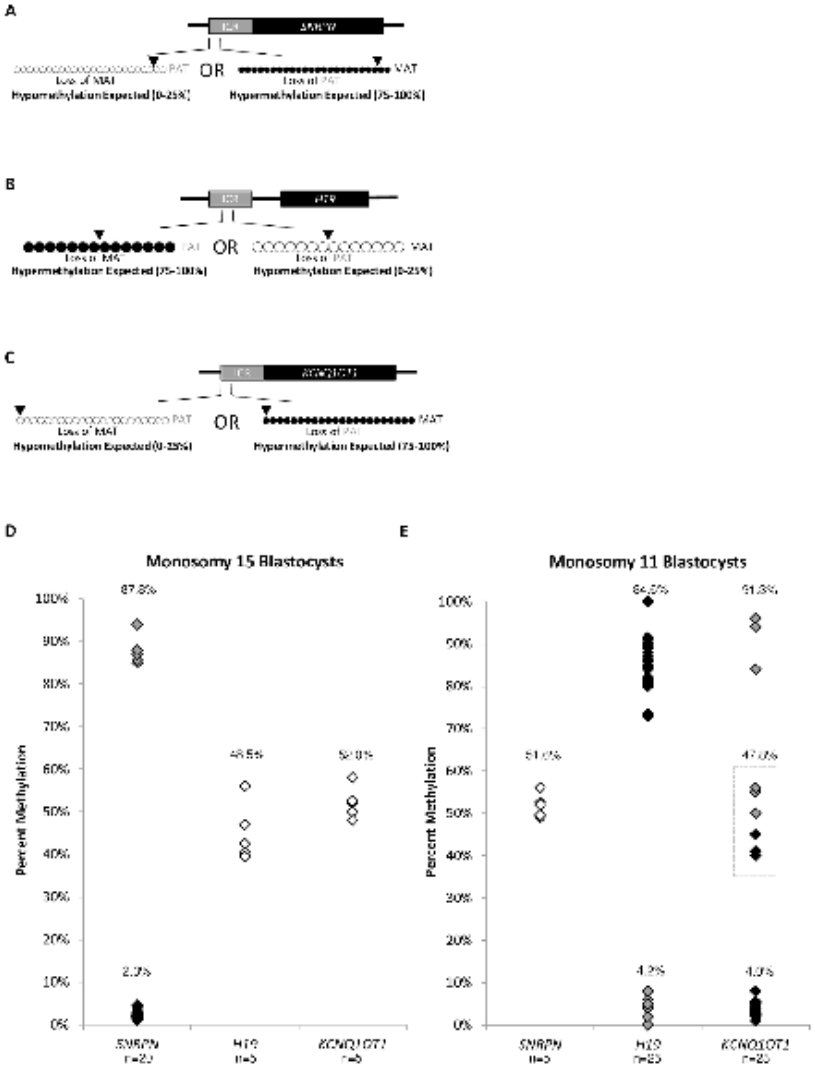

Fig 3. Imprinted DNA methylation profiles of monosomy blastocysts. Black dots represent methylated CpGs, white dots represent unmethylated CpGs. The SNP location is indicated by an arrowhead. "MAT" represents the maternal oocyte-contributed allele; "PAT" represents the paternal sperm-contributed allele. A) Diagram of the *SNRPN* ICR amplified region analyzed in monosomy 15 blastocysts. Hypomethylation (0–25%) is expected with the presence of only the PAT allele. Hypermethylation (75–100%) is expected with the presence of only the MAT allele. B) Diagram of the *H19* ICR amplified region

analyzed in monosomy 11 blastocysts. Hypermethylation (75–100%) is expected with the presence of only the PAT allele. Hypomethylation (0–25%) is expected with the presence of only the MAT allele. C) Diagram of the *KCNQ1OT1* ICR amplified region analyzed in monosomy 11 blastocysts. Hypomethylation (0–25%) is expected with the presence of only the PAT allele. Hypermethylation (75–100%) is expected with the presence of only the MAT allele. D) Summary chart of percent methylation in all monosomy 15 blastocysts at the *SNRPN* (n = 20), *H19* (n = 5), and *KCNQ1OT1* (n = 5) ICRs. Black diamonds represent blastocysts with presumable loss of a chromosome 15 from the oocyte, grey diamonds represent blastocysts with presumable loss of a chromosome 15 from the sperm. White diamonds represent the methylation percentage for the ICRs on diploid chromosome 11. Average percent methylation for each cohort is indicated. E) Summary chart of percent methylation in all monosomy 11 blastocysts at the *SNRPN* (n = 5), *H19* (n = 25), and *KCNQ1OT1* (n = 25) ICRs. Black diamonds represent blastocysts with presumable loss of a chromosome 11 from the oocyte, grey diamonds represent blastocysts with presumable loss of a chromosome 11 from the sperm. White diamonds represent the methylation percentage for the ICR on diploid chromosome 15. The grey dotted box highlights the six blastocysts with unexpected *KCNQ1OT1* methylation profiles. Average percent methylation for each cohort is indicated. Methylation dot diagrams for individual monosomy blastocysts and diploid ICRs can be found in S3 and S4 Figs, and a summary can be found in S2 Table.

doi:10.1371/journal.pone.0156980.g003

compared the DNA methylation profiles of trisomy 15 and 11, as well as monosomy 15 and 11, to control blastocysts. Three confirmed imprinting control regions shown to result in human imprinting disorders when dysregulated were selected for investigation; the *SNRPN* ICR, located on human chromosome 15, and the *H19* and *KCNQ1OT1* ICRs located on human chromosome 11.

Trisomy blastocysts have altered imprinted DNA methylation

All forty trisomy blastocysts that were examined showed methylation profiles away from the expected fifty percent methylation for all imprinting control regions present on the aneuploid chromosome. When more than one single nucleotide polymorphism was evident at a gene within a blastocyst, both methylated and unmethylated DNA strands were often apparent

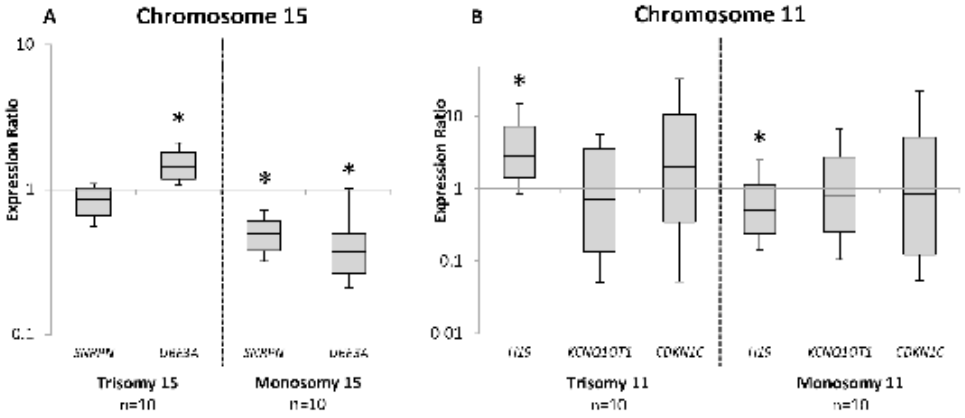

Fig 4. Summary of relative expression for imprinted genes on Chromosome 15 and Chromosome 11 in individual blastocysts. A) Relative gene expression of *SNRPN* and *UBE3A* in control blastocysts (n = 10) compared to trisomy 15 (n = 10) and monosomy 15 (n = 10) blastocysts. B) Relative gene expression of *H19*, *KCNQ1OT1* and *CDKN1C* in control blastocysts (n = 10) compared to trisomy 11 (n = 10) and monosomy 11 (n = 10) blastocysts. Relative expression between control and aneuploid groups was normalized to the housekeeping gene *PPIA* (7p13) using the Relative Expression Software Tool (REST) to determine an expression ratio that was tested for significance by a Pair Wise Fixed Reallocation Randomization Test. Differences were considered to be statistically significant when $p<0.05$, Star "*" denotes statistical significance.

doi:10.1371/journal.pone.0156980.g004

under one SNP designation, highlighting the presence of three contributing chromosomes. Both *SNRPN* and *KCNQ1OT1* had predominantly increased methylation profiles compared to control blastocysts, while *H19* primarily had decreased methylation compared to controls. The *SNRPN* and *KCNQ1OT1* ICRs establish methylation in the oocyte and are unmethylated in the sperm, thus we can presume that the third additional chromosome was gained from the oocyte due to meiotic errors for the majority of blastocysts (20/20 *SNRPN*, 17/20 *KCNQ1OT1*). Likewise, as the *H19* ICR has the reverse imprint, establishing methylation in the sperm and remaining unmethylated in the oocyte, we can again presume that the third additional chromosome was gained primarily from the oocyte (17/20 *H19*). In support of our results, both *H19* and *KCNQ1OT1*, located contiguously on chromosome 11, reflect the same gain from either the oocyte or sperm in the same individual blastocysts. Maternal meiotic errors reportedly do not affect all chromosomes equally, with elevated rates for some chromosomes (including trisomy 15) [4], providing explanation for the observed 100% presumably maternal gain in this cohort of trisomy 15 blastocysts but not in this cohort of trisomy 11 blastocysts.

Importantly, imprinted methylation is altered by the trisomy in all forty aneuploid blastocysts examined, having both increased and decreased methylation detected depending on the ICR and the origin of the third chromosome. The imprinted regions present on diploid chromosomes were unaffected by the presence of the trisomic chromosome and displayed methylation profiles comparable to controls, suggesting that the altered imprinted methylation is restricted to the chromosome involved in the trisomy.

Monosomy blastocysts have altered imprinted DNA methylation

Similar to the trisomy blastocysts, monosomy blastocysts appeared to bias towards presumptive chromosomal loss from the oocyte, likely a consequence of oocyte meiotic errors (15/20 *SNRPN*, 19/25 *H19*, 16/25 *KCNQ1OT1*). In support of these observations, both *H19* and *KCNQ1OT1* again reflected the same loss from the oocyte or sperm in the same individual blastocysts. Meiotic errors in sperm are rare, with only ~5% of sperm identified as aneuploid [34], and paternal error is extremely low in blastocyst biopsies, having a higher frequency in monosomies than in trisomies [4]. In total, 7.5% of the trisomy blastocysts and 24.4% of the monosomy blastocysts examined in this cohort were presumably paternal meiotic in origin.

To summarize, all forty-five monosomy blastocysts that were examined showed altered methylation away from the expected fifty percent methylation in at least one imprinting control region. Unexpectedly, a third subset of imprinted DNA methylation was observed for the *KCNQ1OT1* ICR. In this group, 6/25 blastocysts more closely resembled the methylation profile of controls, while *H19* remained altered in the same individual blastocysts. This suggests that these unpredicted results are restricted to the *KCNQ1OT1* domain. Importantly, due to the monoallelic nature of imprints, some monosomy blastocysts appeared to gain imprinted methylation in at least one ICR compared to controls (for example, 19/25 at *H19*) due to the origin of the single remaining chromosome. Similar to the trisomies examined, imprinted regions present on diploid chromosomes were unaffected by the monosomy and displayed expected methylation profiles, suggesting that the altered methylation is again restricted to the single remaining chromosome involved in the monosomy.

Altered imprinted gene expression in aneuploid blastocysts

Both maternally and paternally expressed genes can reside within imprinted regions, regardless of the origin of ICR methylation. Thus, we further investigated the impact of this observed altered imprinted DNA methylation found in aneuploid blastocysts on the expression of the imprinted genes that exist within the regions.

On human chromosome 15, *SNRPN* is a paternally expressed gene, and *UBE3A* is a maternally expressed gene under control of the same ICR. A significant increase in *UBE3A* was observed in trisomy 15 blastocysts, while *SNRPN* was unaffected compared to controls. All 100% of the trisomy 15 blastocysts examined for imprinted methylation presumably gained an additional methylated maternal chromosome. This third chromosome arising from the oocyte likely increased maternal *UBE3A* expression, while *SNRPN* expression from the paternal contribution remained unaffected.

In the monosomy 15 blastocysts, both *SNRPN* and *UBE3A* were significantly decreased in expression when compared to the control blastocysts. A loss of the oocyte-derived chromosome presumably occurred in 75% of blastocysts, resulting in loss of *UBE3A* expression. The other 25% of blastocysts had presumably lost the sperm-derived chromosome, resulting in loss of *SNRPN* expression. The remaining allele in both scenarios likely was unaffected. Thus, both genes appear decreased in comparison to diploid controls.

On human chromosome 11, *KCNQ1OT1* is a paternally expressed non-coding RNA, while *CDKN1C* is a maternally expression gene within the same ICR. *H19* is a maternally expressed non-coding RNA located at an adjacent ICR. A significant increase in maternally-expressed *H19* was observed in trisomy 11 blastocysts, while a trend towards an increase was also observed for *CDKN1C*. *KCNQ1OT1* was not statistically different from controls. With respect to methylation, 85% of trisomy 11 blastocysts examined for imprinted DNA methylation presumably originated from an additional methylated maternal chromosome, increasing the maternal contribution for *H19* and *CDKN1C* expression, while *KCNQ1OT1* expression from the paternal contribution remained unaffected.

In the monosomy 11 blastocysts, a significant decrease in *H19* was observed, while both *KCNQ1OT1* and *CDKN1C* only trended towards a decrease when compared to the control blastocysts. In 76% of monosomy 11 blastocysts examined for imprinted methylation, the oocyte-derived chromosome was presumably lost, resulting in loss of *H19 and CDKN1C* expression, while the other 24% had presumably lost the sperm-derived chromosome, resulting in loss of *KCNQ1OT1* expression. Again, the remaining allele likely was unaffected in both scenarios. Thus, all three genes appear decreased in comparison to controls, with a statistical significance observed at *H19*.

Overall, the imprinted gene expression results correlated with our expectations from the observed imprinted DNA methylation results in their respective aneuploid blastocysts. Interestingly, the genes present within the *KCNQ1OT1* ICR had more variable expression and did not show statistically significant differences compared to controls. These expression results may further support the concept that the *KCNQ1OT1* region behaves differently than other ICRs at the human blastocyst stage.

All four aneuploid blastocyst groups, independent of the chromosome involved in the error, had significantly altered gene expression in at least one gene, reinforcing the notion that aneuploid blastocysts are not developmentally competent. As imprinted genes are critical for embryonic development, this disrupted imprinted expression likely contributes to the frequent implantation failure observed from aneuploid embryos.

Aneuploidy and other chromosome errors at imprinting control regions

Human imprinting disorders are a consequence of chromosomal mutations, microdeletions or microduplications within the imprinted regions [35], imprinted methylation defects, and uniparental disomy (UPD) [19, 36, 37]. UPD is classified as an inheritance of two chromosome copies (or chromosome regions) from one parent and no copy from the other parent [38]. These occurrences are generally undetectable in common embryo chromosome screening

techniques like array CGH or qPCR on account of normal diploid copy numbers, yet the parental-derived imprinted DNA methylation profile is dramatically affected. Likewise, mutations and microdeletions or microduplications of imprinted regions often go undetected based on the limited region of chromosome affected. The disrupted DNA methylation at these ICRs, however, and resulting aberrant gene expression of the underlying imprinted genes can lead to imprinting disorders, like Beckwith-Wiedemann Syndrome [19, 39], Angelman Syndrome and Prader-Willi Syndrome [22, 37].

A publication using SNP array-based 24-chromosome aneuploidy screening reported that the frequency of UPD in human blastocysts is extremely rare (0.06%) [40]. By comparison, full chromosome aneuploidy of oocytes and preimplantation embryos is exceptionally common in human reproduction [41–48]. In fact, it is estimated that over half of early human IVF embryos are affected by whole-chromosome imbalances [4, 48]. Maternal meiotic errors originating in the oocyte are responsible for the vast majority of these imbalances [3, 4], while the frequency of mitotic errors and the level of embryo mosaicism are still speculative. A recent report from a preimplantation genetic diagnosis (PGD) commercial laboratory observed 30% of blastocysts to be mosaic from a multitude of IVF clinics worldwide [49]. The authors go on to emphasize that blastocyst mosaicism rates vary between IVF clinics, pointing at possible procedure-related effects on post-meiotic chromosome segregation errors. Our in-house genetics laboratory at the Colorado Center for Reproductive Medicine routinely reconfirms diagnosis on aneuploid embryos. A dual trophectoderm biopsy is performed with blinded analysis of prior comprehensive chromosome screening (CCS) aneuploidy results to reveal 96% concordance within an individual blastocyst and only a 4% false-positive rate of mosaic aneuploid embryos.

Our study was the first to investigate if whole-chromosome imbalances impact these imprinting control regions differently than microdeletions, UPDs, or methylation defects restricted to individual ICRs. In fact, this study is also the first to identify an imprinted region, *KCNQ1OT1*, that responds differently to a single whole-chromosome monosomy state in a subset of human blastocysts. Investigations into the rationale for these observations are ongoing. There is a possibility that it could reflect the position of the ICR within the domain, the DNA sequence itself, a combination of both, or some other mechanism in which we are currently unaware. Intriguingly, unlike the *SNRPN* and *H19* ICRs, the *KCNQ1OT1* ICR resides directly inside the coding region of the gene *KCNQ1*. This could create a more susceptible chromatin conformation that would enable targeting of DNA methyltransferase (DNMT) enzymes or tet methylcytosine dioxygenase (TET) machinery resulting in DNA methylation acquisition or loss, respectively, in these monosomy blastocysts. There is also potential that this region has a relaxed imprinted regulation compared to other ICRs at this stage in human development.

Genomic imprinting in human blastocysts

Limited studies have examined genomic imprinting in human blastocysts, focused particularly in relation to the effects of ART treatments (reviewed in [50]). Principally, these studies were performed on poor quality embryos that were not suitable for transfer [51–54], however good quality blastocysts have also revealed an unusually high frequency of aberrant methylation patterns [27, 29, 30]. At the blastocyst stage, 8/12 (67%) high quality transferable blastocysts harbored aberrant methylation for *SNRPN* [27], while 2/5 (40%) [29], and 4/13 (31%) [27], blastocysts displayed aberrant methylation for *KCNQ1OT1*, and 2/14 (14%) blastocysts harboured aberrant *H19* methylation [27]. Conversely, two studies both showed normal *H19* methylation in five blastocysts, respectively [29, 30]. Discrepancies between studies may relate to the small number of embryos analyzed. Notably, while SNP analysis was possible for a select

few, comprehensive chromosome screening was not performed on these embryos prior to these methylation studies.

In contrast, our study which controls for chromosome constitution, suggests that diploid blastocysts harbor imprinted methylation profiles within the expected normal range, while trisomy and monosomy blastocysts have altered methylation at these imprinted loci. Combined with inherent underlying infertility, this provides a possibility that human blastocyst methylation errors are more closely linked to chromosomal aneuploidy than the infertility treatments themselves.

Conclusions

All trisomy blastocysts examined showed a methylation profile consistent with a third inherited chromosome for at least one ICR, presumably originating in the oocyte for the majority of the blastocysts. This supports known literature that maternal meiotic errors are the most common cause of trisomies. Significantly increased and decreased ICR methylation compared to controls contributed to altered imprinted gene expression. All imprinted genes examined in trisomy blastocysts had either significantly increased expression or comparable expression to controls, providing one explanation as to why trisomy embryos have the ability to continue into post-implantation development, but mostly fail to develop to term.

All monosomy blastocysts examined showed a methylation profile consistent with a loss of an inherited chromosome. This chromosome loss is also presumably originating in the oocyte for the majority of the blastocysts, emphasizing that maternal meiotic errors are also the most common cause of monosomies. Significant hypermethylated and hypomethylated ICRs compared to controls contributed to altered imprinted gene expression. By contrast to their trisomy counterparts, all monosomy blastocysts exhibited significantly decreased expression in at least one imprinted gene, with a downward trend observed in all imprinted genes analyzed. This loss of imprinted gene expression may equally contribute to an explanation as to why monosomy embryos cannot progress further than the preimplantation period of development, contributing to their compromised developmental potential.

Supporting Information

S1 Fig. Imprinted DNA methylation profiles of individual control blastocysts. Imprinted DNA methylation analysis in twenty individual control blastocysts at the A) *SNRPN* ICR, B) *H19* ICR, C) *KCNQ1OT1* ICR. Each line is a unique DNA strand amplified within an individual blastocyst. Black dots represent methylated CpGs, white dots represent unmethylated CpGs. Blastocyst ID is indicated above-left of the diagram, in which "C##" represents control blastocyst number. SNP ID and percent methylation is indicated above-right of the diagram. When more than one SNP is present, a SNP ID and percent methylation is indicated separately for each SNP.
(TIF)

S2 Fig. Imprinted DNA methylation profiles of individual trisomy blastocysts. Imprinted DNA methylation analysis in twenty individual trisomy 15 blastocysts at the A) *SNRPN* ICR; and twenty individual trisomy 11 blastocysts at the B) *H19* ICR, and C) *KCNQ1OT1* ICR. Each line is a unique DNA strand amplified within an individual blastocyst. Black dots represent methylated CpGs, white dots represent unmethylated CpGs. Blastocyst ID is indicated above-left of the diagram, in which "15T##" represents trisomy 15 blastocyst number, and "11T##" represents trisomy 11 blastocyst number. SNP ID and percent methylation is indicated above-right of the diagram. When more than one SNP is present, a SNP ID and percent methylation

is indicated separately for each SNP. Blastocysts with ID and percent methylation denoted in grey are presumable chromosome gain from the sperm.
(TIF)

S3 Fig. Imprinted DNA methylation profiles of individual monosomy blastocysts. Imprinted DNA methylation analysis in twenty individual monosomy 15 blastocysts at the A) *SNRPN* ICR; and twenty-five individual monosomy 11 blastocysts at the B) *H19* ICR, and C) *KCNQ1OT1* ICR. Each line is a unique DNA strand amplified within an individual blastocyst. Black dots represent methylated CpGs, white dots represent unmethylated CpGs. Blastocyst ID is indicated above-left of the diagram, in which "15M##" represents monosomy 15 blastocyst number, and "11M##" represents monosomy 11 blastocyst number. SNP ID and percent methylation is indicated above-right of the diagram. When more than one SNP is present, a SNP ID and percent methylation is indicated separately for each SNP. Blastocysts with ID and percent methylation denoted in grey are presumable chromosome loss from the sperm. The grey boxes highlight the six blastocysts with *KCNQ1OT1* methylation profiles comparable to controls.
(TIF)

S4 Fig. Diploid imprinted DNA methylation profiles of individual aneuploid blastocysts. Diploid imprinted DNA methylation analysis in five trisomy 11 and five monosomy 11 blastocysts at the A) *SNRPN* ICR, and five trisomy 15 and five monosomy 15 blastocysts at the B) *H19* ICR, C) *KCNQ1OT1* ICR. Each line is a unique DNA strand amplified within an individual blastocyst. Black dots represent methylated CpGs, white dots represent unmethylated CpGs. Blastocyst ID is indicated above-left of the diagram, in which "15T##" represents trisomy 15 blastocyst number, "15M##" represents monosomy 15 blastocyst number, "11T##" represents trisomy 11 blastocyst number, and "11M##" represents monosomy 11 blastocyst number. SNP ID and percent methylation is indicated above-right of the diagram. When more than one SNP is present, a SNP ID and percent methylation is indicated separately for each SNP.
(TIF)

S1 Table. SNP frequencies among blastocyst groups. A single nucleotide polymorphism (SNP) was present in all three amplified regions, but at different frequencies: *SNRPN* SNP G (84.8%) / A (15.2%) (Rs220029), *H19* SNP C (66.4%) / A (33.6%) (Rs2071094), and *KCNQ1OT1* SNP G (94.7%) / A (6.3%) (Rs56134313).
(TIF)

S2 Table. Methylation results per blastocyst. An overview table indicating DNA methylation percentages for all relevant ICRs per blastocyst. C## = Control blastocyst, 15T## = Trisomy 15 blastocyst, 11T## = Trisomy 11 blastocyst, 15M## = Monosomy 15 blastocyst, 11M## = Monosomy 11 blastocyst, Grade = numeric:alpha:alpha score for blastocyst degree of expansion and hatching status: ICM development: TE development [25], Vit = vitrification freezing, SNP = single nucleotide polymorphism, light grey sections = presumable paternal gain or loss originating from the sperm, dark grey sections = unexpected subset of methylation profiles at *KCNQ1OT1*.
(TIF)

Author Contributions

Conceived and designed the experiments: MD MKJ. Performed the experiments: MD BM JP. Analyzed the data: MD BM MKJ. Contributed reagents/materials/analysis tools: MD BM JP WS MKJ. Wrote the paper: MD MKJ.

References

1. Hassold T, Hall H, Hunt P. The origin of human aneuploidy: where we have been, where we are going. Hum Mol Genet. 2007; 16 Spec No. 2: R203–8. Epub 2007/10/04. 16/R2/R203 [pii] doi: 10.1093/hmg/ddm243 PMID: 17911163.
2. Alfarawati S, Fragouli E, Colls P, Stevens J, Gutierrez-Mateo C, Schoolcraft WB, et al. The relationship between blastocyst morphology, chromosomal abnormality, and embryo gender. Fertil Steril. 2011; 95 (2):520–4. Epub 2010/06/12. S0015-0282(10)00600-X [pii] doi: 10.1016/j.fertnstert.2010.04.003 PMID: 20537630.
3. Rabinowitz M, Ryan A, Gemelos G, Hill M, Baner J, Cinnioglu C, et al. Origins and rates of aneuploidy in human blastomeres. Fertil Steril. 2012; 97(2):395–401. Epub 2011/12/27. S0015-0282(11)02810-X [pii] doi: 10.1016/j.fertnstert.2011.11.034 PMID: 22195772.
4. McCoy RC, Demko ZP, Ryan A, Banjevic M, Hill M, Sigurjonsson S, et al. Evidence of Selection against Complex Mitotic-Origin Aneuploidy during Preimplantation Development. PLoS Genet. 2015; 11(10): e1005601. Epub 2015/10/23. doi: 10.1371/journal.pgen.1005601 PGENETICS-D-15-01371 [pii]. PMID: 26491874; PubMed Central PMCID: PMC4619652.
5. Rodriguez-Purata J, Lee J, Whitehouse M, Moschini RM, Knopman J, Duke M, et al. Embryo selection versus natural selection: how do outcomes of comprehensive chromosome screening of blastocysts compare with the analysis of products of conception from early pregnancy loss (dilation and curettage) among an assisted reproductive technology population? Fertil Steril. 2015; 104(6):1460–6 e12. Epub 2015/09/12. S0015-0282(15)01761-6 [pii] doi: 10.1016/j.fertnstert.2015.08.007 PMID: 26361205.
6. Tuck-Muller CM, Narayan A, Tsien F, Smeets DF, Sawyer J, Fiala ES, et al. DNA hypomethylation and unusual chromosome instability in cell lines from ICF syndrome patients. Cytogenet Cell Genet. 2000; 89(1–2):121–8. Epub 2000/07/15. 15590 [pii] 15590. PMID: 10894953.
7. Davidsson J, Veerla S, Johansson B. Constitutional trisomy 8 mosaicism as a model for epigenetic studies of aneuploidy. Epigenetics Chromatin. 2013; 6(1):18. Epub 2013/07/03. 1756-8935-6-18 [pii] doi: 10.1186/1756-8935-6-18 PMID: 23816241; PubMed Central PMCID: PMC3704342.
8. Davidsson J. The epigenetic landscape of aneuploidy: constitutional mosaicism leading the way? Epigenomics. 2014; 6(1):45–58. Epub 2014/03/04. doi: 10.2217/epi.13.78 PMID: 24579946.
9. Viana J, Pidsley R, Troakes C, Spiers H, Wong CC, Al-Sarraj S, et al. Epigenomic and transcriptomic signatures of a Klinefelter syndrome (47,XXY) karyotype in the brain. Epigenetics. 2014; 9(4):587–99. Epub 2014/01/31. 27806 [pii] doi: 10.4161/epi.27806 PMID: 24476718; PubMed Central PMCID: PMC4121369.
10. Sailani MR, Santoni FA, Letourneau A, Borel C, Makrythanasis P, Hibaoui Y, et al. DNA-Methylation Patterns in Trisomy 21 Using Cells from Monozygotic Twins. PLoS One. 2015; 10(8):e0135555. Epub 2015/09/01. doi: 10.1371/journal.pone.0135555 PONE-D-15-12331 [pii]. PMID: 26317209; PubMed Central PMCID: PMC4552626.
11. Lim JH, Kim DJ, Lee DE, Han JY, Chung JH, Ahn HK, et al. Genome-wide microRNA expression profiling in placentas of fetuses with Down syndrome. Placenta. 2015; 36(3):322–8. Epub 2015/01/18. S0143-4004(14)00920-5 [pii] doi: 10.1016/j.placenta.2014.12.020 PMID: 25595853.
12. McCallie BR, Parks JC, Stieby AL, Schoolcraft WB, Katz-Jaffe MG. Human blastocysts exhibit unique microrna profiles in relation to maternal age and chromosome constitution. J Assist Reprod Genet. 2014; 31(7):913–9. Epub 2014/04/25. doi: 10.1007/s10815-014-0235-y PMID: 24760722; PubMed Central PMCID: PMC4096874.
13. Jaenisch R, Bird A. Epigenetic regulation of gene expression: how the genome integrates intrinsic and environmental signals. Nat Genet. 2003; 33 Suppl:245–54. Epub 2003/03/01. doi: 10.1038/ng1089 [pii]. PMID: 12610534.
14. Herrera LA, Prada D, Andonegui MA, Duenas-Gonzalez A. The epigenetic origin of aneuploidy. Curr Genomics. 2008; 9(1):43–50. Epub 2008/03/01. doi: 10.2174/138920208783884883 PMID: 19424483; PubMed Central PMCID: PMC2674307.
15. Rodenhiser D, Mann M. Epigenetics and human disease: translating basic biology into clinical applications. CMAJ. 2006; 174(3):341–8. Epub 2006/02/01. 174/3/341 [pii] doi: 10.1503/cmaj.050774 PMID: 16446478; PubMed Central PMCID: PMC1373719.
16. Shuman C, Beckwith JB, Smith AC, Weksberg R. Beckwith-Wiedemann Syndrome. 1993. Epub 2010/03/20. NBK1394 [bookaccession]. PMID: 20301568.
17. Sparago A, Cerrato F, Vernucci M, Ferrero GB, Silengo MC, Riccio A. Microdeletions in the human H19 DMR result in loss of IGF2 imprinting and Beckwith-Wiedemann syndrome. Nat Genet. 2004; 36 (9):958–60. Epub 2004/08/18. doi: 10.1038/ng1410 [pii]. PMID: 15314640.
18. Prawitt D, Enklaar T, Gartner-Rupprecht B, Spangenberg C, Oswald M, Lausch E, et al. Microdeletion of target sites for insulator protein CTCF in a chromosome 11p15 imprinting center in Beckwith-

Wiedemann syndrome and Wilms' tumor. Proc Natl Acad Sci U S A. 2005; 102(11):4086–90. Epub 2005/03/04. 0500037102 [pii] doi: 10.1073/pnas.0500037102 PMID: 15743916; PubMed Central PMCID: PMC554791.

19. Weksberg R, Nishikawa J, Caluseriu O, Fei YL, Shuman C, Wei C, et al. Tumor development in the Beckwith-Wiedemann syndrome is associated with a variety of constitutional molecular 11p15 alterations including imprinting defects of KCNQ1OT1. Hum Mol Genet. 2001; 10(26):2989–3000. Epub 2001/12/26. PMID: 11751681.

20. Weksberg R, Shuman C, Smith AC. Beckwith-Wiedemann syndrome. Am J Med Genet C Semin Med Genet. 2005; 137C(1):12–23. Epub 2005/07/13. doi: 10.1002/ajmg.c.30058 PMID: 16010676.

21. Nicholls RD, Saitoh S, Horsthemke B. Imprinting in Prader-Willi and Angelman syndromes. Trends Genet. 1998; 14(5):194–200. Epub 1998/06/05. S0168-9525(98)01432-2 [pii]. PMID: 9613204.

22. Horsthemke B. Structure and function of the human chromosome 15 imprinting center. J Cell Physiol. 1997; 173(2):237–41. Epub 1997/11/20. doi: 10.1002/(SICI)1097-4652(199711)173:2<237::AID-JCP28>3.0.CO;2-B [pii] 10.1002/(SICI)1097-4652(199711)173:2<237::AID-JCP28>3.0.CO;2-B. PMID: 9365529.

23. Haas OA. Is genomic imprinting involved in the pathogenesis of hyperdiploid and haploid acute lymphoblastic leukemia of childhood? Acta Genet Med Gemellol (Roma). 1996; 45(1–2):239–42. Epub 1996/01/01. PMID: 8872038.

24. McCallie BR PJ, Streiby A, Schoolcraft WB, Katz-Jaffe MG, editor Abstract: Hypomethylation of monosomy chromosomes may reflect decreased implantation potential. 70th American Society of Reproductive Medicine Annual Meeting; 2014 September 2014; Hawaii: Fertility & Sterility.

25. Gardner DK S W. In vitro culture of human blastocysts. In: Jansen M, editor. Toward Reproductive Certainty: Fertility and Genetics Beyond 1999: UK: Parthenon Publishing London; 1999. p. 378–88.

26. Yang Z, Liu J, Collins GS, Salem SA, Liu X, Lyle SS, et al. Selection of single blastocysts for fresh transfer via standard morphology assessment alone and with array CGH for good prognosis IVF patients: results from a randomized pilot study. Mol Cytogenet. 2012; 5(1):24. Epub 2012/05/04. 1755-8166-5-24 [pii] doi: 10.1186/1755-8166-5-24 PMID: 22551456; PubMed Central PMCID: PMC3403960.

27. White CR, Denomme MM, Tekpetey FR, Feyles V, Power SG, Mann MR. High Frequency of Imprinted Methylation Errors in Human Preimplantation Embryos. Sci Rep. 2015; 5:17311. Epub 2015/12/03. srep17311 [pii] doi: 10.1038/srep17311 PMID: 26626153; PubMed Central PMCID: PMC4667293.

28. Denomme MM, Zhang L, Mann MR. Single oocyte bisulfite mutagenesis. J Vis Exp. 2012;(64:). Epub 2012/07/12. 4046 [pii] doi: 10.3791/4046 PMID: 22782232; PubMed Central PMCID: PMC3471283.

29. Khoueiry R, Ibala-Romdhane S, Al-Khtib M, Blachere T, Lornage J, Guerin JF, et al. Abnormal methylation of KCNQ1OT1 and differential methylation of H19 imprinting control regions in human ICSI embryos. Zygote. 2013; 21(2):129–38. Epub 2012/02/04. S0967199411000694 [pii] doi: 10.1017/S0967199411000694 PMID: 22300968.

30. Ibala-Romdhane S, Al-Khtib M, Khoueiry R, Blachere T, Guerin JF, Lefevre A. Analysis of H19 methylation in control and abnormal human embryos, sperm and oocytes. Eur J Hum Genet. 2011; 19(11):1138–43. Epub 2011/06/10. ejhg201199 [pii] doi: 10.1038/ejhg.2011.99 PMID: 21654730; PubMed Central PMCID: PMC3198154.

31. Parks JC, McCallie BR, Janesch AM, Schoolcraft WB, Katz-Jaffe MG. Blastocyst gene expression correlates with implantation potential. Fertil Steril. 2011; 95(4):1367–72. Epub 2010/09/25. S0015-0282(10)02286-7 [pii] doi: 10.1016/j.fertnstert.2010.08.009 PMID: 20864103.

32. Berteaux N, Lottin S, Monte D, Pinte S, Quatannens B, Coll J, et al. H19 mRNA-like noncoding RNA promotes breast cancer cell proliferation through positive control by E2F1. J Biol Chem. 2005; 280(33):29625–36. Epub 2005/06/30. M504033200 [pii] doi: 10.1074/jbc.M504033200 PMID: 15985428.

33. Pfaffl MW, Horgan GW, Dempfle L. Relative expression software tool (REST) for group-wise comparison and statistical analysis of relative expression results in real-time PCR. Nucleic Acids Res. 2002; 30(9):e36. Epub 2002/04/25. PMID: 11972351; PubMed Central PMCID: PMC113859.

34. Templado C, Vidal F, Estop A. Aneuploidy in human spermatozoa. Cytogenet Genome Res. 2011; 133(2–4):91–9. Epub 2011/02/02. 000323795 [pii] doi: 10.1159/000323795 PMID: 21282942.

35. Horsthemke B. In brief: genomic imprinting and imprinting diseases. J Pathol. 2014; 232(5):485–7. Epub 2014/01/08. doi: 10.1002/path.4326 PMID: 24395592.

36. Cooper WN, Luharia A, Evans GA, Raza H, Haire AC, Grundy R, et al. Molecular subtypes and phenotypic expression of Beckwith-Wiedemann syndrome. Eur J Hum Genet. 2005; 13(9):1025–32. Epub 2005/07/07. 5201463 [pii] doi: 10.1038/sj.ejhg.5201463 PMID: 15999116.

37. Nicholls RD, Knoll JH, Butler MG, Karam S, Lalande M. Genetic imprinting suggested by maternal heterodisomy in nondeletion Prader-Willi syndrome. Nature. 1989; 342(6247):281–5. Epub 1989/11/16. doi: 10.1038/342281a0 PMID: 2812027.

38. Robinson WP. Mechanisms leading to uniparental disomy and their clinical consequences. Bioessays. 2000; 22(5):452–9. Epub 2000/05/08. doi: 10.1002/(SICI)1521-1878(200005)22:5<452::AID-BIES7>3.0.CO;2-K [pii] 10.1002/(SICI)1521-1878(200005)22:5<452::AID-BIES7>3.0.CO;2-K. PMID: 10797485.

39. Choufani S, Shuman C, Weksberg R. Beckwith-Wiedemann syndrome. Am J Med Genet C Semin Med Genet. 2010; 154C(3):343–54. Epub 2010/08/31. doi: 10.1002/ajmg.c.30267 PMID: 20803657.

40. Gueye NA, Devkota B, Taylor D, Pfundt R, Scott RT Jr., Treff NR. Uniparental disomy in the human blastocyst is exceedingly rare. Fertil Steril. 2014; 101(1):232–6. Epub 2013/10/03. S0015-0282(13)03017-3 [pii] doi: 10.1016/j.fertnstert.2013.08.051 PMID: 24083874.

41. Delhanty JD, Griffin DK, Handyside AH, Harper J, Atkinson GH, Pieters MH, et al. Detection of aneuploidy and chromosomal mosaicism in human embryos during preimplantation sex determination by fluorescent in situ hybridisation, (FISH). Hum Mol Genet. 1993; 2(8):1183–5. Epub 1993/08/01. PMID: 8401499.

42. Munne S, Lee A, Rosenwaks Z, Grifo J, Cohen J. Diagnosis of major chromosome aneuploidies in human preimplantation embryos. Hum Reprod. 1993; 8(12):2185–91. Epub 1993/12/01. PMID: 8150922.

43. Kamiguchi Y, Rosenbusch B, Stenzik K, Mikamo K. Chromosomal analysis of unfertilized human oocytes prepared by a gradual fixation-air drying method. Hum Genet. 1993; 90(5):533–41. Epub 1993/01/01. PMID: 8428752.

44. Iwarsson E, Lundqvist M, Inzunza J, Ahrlund-Richter L, Sjoblom P, Lundkvist O, et al. A high degree of aneuploidy in frozen-thawed human preimplantation embryos. Hum Genet. 1999; 104(5):376–82. Epub 1999/07/08. PMID: 10394928.

45. Wilton L, Voullaire L, Sargeant P, Williamson R, McBain J. Preimplantation aneuploidy screening using comparative genomic hybridization or fluorescence in situ hybridization of embryos from patients with recurrent implantation failure. Fertil Steril. 2003; 80(4):860–8. Epub 2003/10/15. S0015028203011622 [pii]. PMID: 14556801.

46. Fragouli E, Wells D, Thornhill A, Serhal P, Faed MJ, Harper JC, et al. Comparative genomic hybridization analysis of human oocytes and polar bodies. Hum Reprod. 2006; 21(9):2319–28. Epub 2006/05/18. del157 [pii] doi: 10.1093/humrep/del157 PMID: 16704993.1

47. Fragouli E, Escalona A, Gutierrez-Mateo C, Tormasi S, Alfarawati S, Sepulveda S, et al. Comparative genomic hybridization of oocytes and first polar bodies from young donors. Reprod Biomed Online. 2009; 19(2):228–37. Epub 2009/08/29. PMID: 19712560.

48. Schoolcraft WB, Fragouli E, Stevens J, Munne S, Katz-Jaffe MG, Wells D. Clinical application of comprehensive chromosomal screening at the blastocyst stage. Fertil Steril. 2010; 94(5):1700–6. Epub 2009/11/27. S0015-0282(09)03875-8 [pii] doi: 10.1016/j.fertnstert.2009.10.015 PMID: 19939370.

49. Munne S, Grifo J, Wells D. Mosaicism: "survival of the fittest" versus "no embryo left behind". Fertil Steril. 2016. Epub 2016/02/02. S0015-0282(16)00051-0 [pii] doi: 10.1016/j.fertnstert.2016.01.016 PMID: 26827669.

50. Denomme MM, Mann MR. Genomic imprints as a model for the analysis of epigenetic stability during assisted reproductive technologies. Reproduction. 2012; 144(4):393–409. Epub 2012/09/08. REP-12-0237 [pii] doi: 10.1530/REP-12-0237 PMID: 22956517.

51. Shi X, Chen S, Zheng H, Wang L, Wu Y. Abnormal DNA Methylation of Imprinted Loci in Human Preimplantation Embryos. Reprod Sci. 2014; 21(8):978–83. Epub 2014/01/11. 1933719113519173 [pii] doi: 10.1177/1933719113519173. PMID: 24406788; PubMed Central PMCID: PMC4126214.

52. Chen SL, Shi XY, Zheng HY, Wu FR, Luo C. Aberrant DNA methylation of imprinted H19 gene in human preimplantation embryos. Fertil Steril. 2010; 94(6):2356–8, 8 e1. Epub 2010/03/23. S0015-0282(10)00248-7 [pii] doi: 10.1016/j.fertnstert.2010.01.120 PMID: 20303482.

53. Geuns E, De Rycke M, Van Steirteghem A, Liebaers I. Methylation imprints of the imprint control region of the SNRPN-gene in human gametes and preimplantation embryos. Hum Mol Genet. 2003; 12(22):2873–9. Epub 2003/09/23. doi: 10.1093/hmg/ddg315 [pii]. PMID: 14500540.

54. Geuns E, De Temmerman N, Hilven P, Van Steirteghem A, Liebaers I, De Rycke M. Methylation analysis of the intergenic differentially methylated region of DLK1-GTL2 in human. Eur J Hum Genet. 2007; 15(3):352–61. Epub 2007/01/11. 5201759 [pii] doi: 10.1038/sj.ejhg.5201759 PMID: 17213841.

18.0 Appendix 5. Additional publication

Denomme MM, McCallie BR, **Parks JC,** Schoolcraft WB, Katz-Jaffe MG. Alterations in the sperm histone-retained epigenome are associated with unexplained male factor infertility and poor blastocyst development in donor oocyte IVF cycles. Hum Reprod. 2017 Dec 1;32(12):2443-2455. doi: 10.1093/humrep/dex317.

My personal contribution to this manuscript

I worked closely with Dr. Katz-Jaffe and Dr. Denomme to coordinate the collection of study materials between the research department and the IVF laboratory. I also performed sperm count and motility for samples donated to research, and prepared them for storage at -80°C and downstream epigenetic experiments. Finally, I co-wrote and edited sections of the materials and methods section of the manuscript for publication as a co-author.

Human Reproduction, Vol.32, No.12 pp. 2443–2455, 2017
Advanced Access publication on October 26, 2017 doi:10.1093/humrep/dex317

human reproduction ORIGINAL ARTICLE *Infertility*

Alterations in the sperm histone-retained epigenome are associated with unexplained male factor infertility and poor blastocyst development in donor oocyte IVF cycles

Michelle M. Denomme[1], Blair R. McCallie[1], Jason C. Parks[1], William B. Schoolcraft[2], and Mandy G. Katz-Jaffe[1,2,*]

[1]Fertility Labs of Colorado, 10290 Ridgegate Circle, Lone Tree CO, 80124, USA [2]Colorado Center for Reproductive Medicine, 10290 Ridgegate Circle, Lone Tree CO, 80124, USA

*Correspondence address: E-mail: MKatz-Jaffe@ColoCRM.com

Submitted on May 17, 2017; resubmitted on August 24, 2017; accepted on October 2, 2017

STUDY QUESTION: Is there a distinct sperm histone-retained epigenetic signature in unexplained male factor infertility patients resulting in compromised blastocyst development?

SUMMARY ANSWER: Using only donor oocyte IVF cycles, sperm DNA methylation patterns and miRNA profiles were significantly altered in normozoospermic patients resulting in poor blastocyst development, reflecting a subset of unexplained male factor infertility.

WHAT IS KNOWN ALREADY: Aberrant sperm DNA methylation has been associated with known male factor infertility, particularly noted in oligozoospermic patients. Unexplained male factor infertility remains a significant proportion of *in vitro* fertilization failures having unknown underlying physiology.

STUDY DESIGN, SIZE, DURATION: Sperm samples ($n = 40$) and blastocysts ($n = 48$) were obtained during fertile donor oocyte IVF cycles with normozoospermic parameters, thereby excluding known female and male infertility factors. Samples were divided into two groups based on blastocyst development (Good Group = ≥20% embryos with D5 grade 'AA' blastocysts, and ≥60% embryos of transferable quality on D5 and D6; Poor Group = ≤10% embryos with D5 grade 'AA' blastocysts, and ≤40% embryos of transferable quality on D5 and D6).

PARTICIPANTS/MATERIALS, SETTING, METHODS: Samples were obtained from patients undergoing IVF treatments with informed consent and institutional review board approval. The Infinium HumanMethylation450 BeadChip microarray was used to identify histone-retained CpG island genes and genomic regions showing differences in sperm DNA methylation between the Good Group and the Poor Group. Pathway and gene network analysis for the significantly altered genes was performed, and targeted DNA methylation validation was completed for 23 genes and two imprinting control regions. Sperm miRNA profiles were assessed using the TaqMan® Human MicroRNA Array Card, with corresponding blastocyst mRNA gene expression examined by qRT-PCR.

MAIN RESULTS AND THE ROLE OF CHANCE: Our study is the first to investigate unexplained male factor infertility while significantly eliminating confounding female factors from our sample population by using only young fertile donor oocytes. We identified 1634 CpG sites located at retained histone CpG island regions that had significant sperm DNA methylation differentials between the two embryogenesis groups ($P < 0.05$). A largely hypermethylated profile was evident in the Good Group, with a small but distinct and statistically significant shift ($P < 0.05$) observed in the Poor Group. Genes involved in embryonic development were highly represented among histone-retained CpG sites with decreased methylation in the Poor Group ($P < 0.05$). Ten significantly altered sperm miRNAs ($P < 0.05$), correlated with altered target gene mRNA expression in the blastocysts from the Poor Group ($P < 0.05$). Taken together, significantly impacted sperm miRNA and target transcript levels in blastocysts from the Poor Group may contribute alongside aberrant sperm DNA methylation to the compromised blastocyst development observed.

LIMITATIONS, REASONS FOR CAUTION: Our examination of CpG island regions restricted to retained histones represents only a small part of the sperm epigenome. The results observed are descriptive and further studies are needed to elucidate the functional effects of differential sperm DNA methylation on unexplained male factor infertility and blastocyst development.

WIDER IMPLICATIONS OF THE FINDINGS: Slight epigenetic changes in sperm may have a cumulative effect on fertility and embryonic developmental competence. Knowledge of sperm epigenetics and inheritance has important implications for future generations, while providing evidence for potential causes of unexplained male factor infertility.

STUDY FUNDING/COMPETING INTEREST(S): No external funding was used for this study. None of the authors have any competing interest.

Key words: DNA methylation / epigenetics / sperm / blastocyst / unexplained infertility

Introduction

Infertility is a complex disorder encompassing a broad range of physical, structural, hormonal, genetic and environmental causes. It can impact either the male or female counterpart as well as the couple collectively as a pair. While many origins of infertility are well characterized, as many as half (37–58%) of all cases are diagnosed as unexplained, having the standard infertility testing fail to find a cause (Moghissi and Wallach, 1983; Irvine, 1998; Hamada *et al.*, 2012). The introduction of *in vitro* fertilization (IVF) and intracytoplasmic sperm injection (ICSI) bypasses male infertility, thus eliminating the majority of barriers to fertilization but concurrently preventing an explanation for their cause. Unexplained (idiopathic) male factor (MF) infertility remains a significant proportion ranging from 6% to 27% of IVF failures having unknown underlying physiology (Moghissi and Wallach, 1983; Hamada *et al.*, 2011).

Epigenetics refers to chromatin modifications, including DNA methylation, histone modifications and non-coding RNAs, that alter the accessibility of genes and regulate gene expression without changes to the DNA sequence (Jaenisch and Bird, 2003). Sperm epigenetic marks have been implicated in zygotic functions post-fertilization, and may contribute to embryonic development and offspring health (Nanassy and Carrell, 2008; Kumar *et al.*, 2013). However, the precise epigenetic signature that is heritable in human gametes is still under debate, likewise the function of human sperm epigenetic inheritance in the early embryo remains largely unknown.

During gametogenesis and early embryogenesis the methylome is reprogrammed as genome-wide epigenetic transitions are orchestrated, shifting the embryo into a totipotent state (Rodenhiser and Mann, 2006). Some regions, like imprinted genes and repetitive elements, can preserve their methylation signature from the parental gametes through to the developing embryo. Additional inheritance from the sperm DNA methylation landscape may be essential for both fertilization of the oocyte and viability of the early embryo (Carrell and Hammoud, 2010; Dada *et al.*, 2012; Jenkins and Carrell, 2012). Non-coding RNAs have been detected in sperm (Pessot *et al.*, 1989; Krawetz, 2005) including microRNAs (Amanai *et al.*, 2006; Yan *et al.*, 2008). However, the necessity of human sperm-borne RNAs for fertilization and embryogenesis remains under debate (Sendler *et al.*, 2013; Cui *et al.*, 2015).

Sperm DNA is primarily packaged tightly within the sperm head by protamines (Oliva and Dixon, 1991; Dadoune, 1995), which is conducive to a largely hypermethylated genome and a transcriptionally silent state. The localization and modification of retained histones (5–15% in humans) may reflect regions important for early embryonic development (Gatewood *et al.*, 1987; Hammoud *et al.*, 2009; Miller *et al.*, 2010), including developmental genes, transcription factors, microRNAs (miRNAs) and imprinted genes. Abnormal sperm DNA methylation signatures have largely been associated with MF infertility, particularly noted in oligozoospermic patients and observed at imprinted and developmental genes located at retained histones (Hammoud *et al.*, 2010, 2011). This has led to further investigations of genome-wide sperm epigenetic patterns in MF cases (Houshdaran *et al.*, 2007; Jenkins *et al.*, 2015, 2016a; Dere *et al.*, 2016), and recently expanded to unexplained infertility (Aston *et al.*, 2015; Urdinguio *et al.*, 2015; Jenkins *et al.*, 2016b).

As epigenetic aberrations have been highly implicated in known MF infertility, we hypothesize that there is a lesser, but still distinct, abnormal sperm epigenetic signature in unexplained infertility patients resulting in compromised embryogenesis and outcome. The aim of this study was to use DNA methylation analysis of the histone-retained sperm CpG island regions, combined with sperm miRNA profiling, to improve the knowledge of sperm epigenetics and provide evidence for potential causes of unexplained male factor infertility.

Materials and Methods

Ethical approval

Semen samples were obtained from 40 men, and surplus, cryopreserved blastocysts were donated from sixteen couples, that underwent IVF treatments at the Colorado Center for Reproductive Medicine, after informed consent and Institutional Review Board approval.

Sample selection

Semen analysis ($n = 40$) was performed in accordance with World Health Organization guidelines (Cooper *et al.*, 2010). Only normozoospermic samples from young donor oocyte IVF cycles were included in the study. Sperm samples ($n = 20$) were selected for the good quality embryo group ('Good Group'), based on inclusion criteria of ≥20% embryos with D5 grade 'AA' blastocysts, and ≥60% embryos of transferable quality (grade ≥'3BB') on Day 5 and Day 6 collectively. Likewise, sperm samples ($n = 20$) were selected for the poor quality embryo group ('Poor Group'), based on inclusion criteria of ≤10% embryos with D5 grade 'AA' blastocysts, and ≤40% embryos of transferable quality on Day 5 and Day 6 collectively. Semen samples were prepared by a two-layer (90–45%) PureSperm density-gradient centrifugation (Nidacon,

Gothenburg, Sweden) with subsequent swim-up concentrating technique to collect the viable progressively motile portion. A somatic cell lysis step (0.1% SDS, 0.5% Triton X-100 in H_2O) was employed to remove round cell contamination, and clean motile sperm samples were diluted to 5×10^6 sperm and stored at −80°C.

Blastocysts (n = 48) from donor oocyte IVF cycles with normozoospermic parameters were scored based on inner cell mass and trophectoderm quality (Gardner and Schoolcraft, 1999). All blastocysts included in the study were morphologically graded as high, transferrable quality (grade ≥ '3BB').

Table I Summary of patient samples.

	Paternal age (years)	Semen parameters			
		Volume (mL)	Motility (%)	Count (million/mL)	Total motile count (million/mL)
Good Group	40.3 ± 1.3	2.9 ± 0.3	60.3% ± 3.1%	126.9 ± 14.1	221.7 ± 32.2
Poor Group	42.0 ± 1.1	3.4 ± 0.3	61.1% ± 2.6%	134.5 ± 18.8	290.4 ± 48.5
Significance (*t*-test); $P < 0.05$	0.311	0.306	0.851	0.753	0.255
	Maternal Age (years)	**Embryo Quality**			
		Oocytes Retrieved (#)	**Oocytes Fertilized (% of retrieved)**	**Grade D5 'AA' Blastocysts (% of fertilized)**	**Transferable D5&D6 Blastocysts (% of fertilized)**
Good Group	<33; donor oocyte	25.6 ± 1.7	93.3% ± 2.3%	36.5% ± 3.0%	73.0% ± 2.4%
Poor Group	<33; donor oocyte	20.8 ± 2.3	93.2% ± 2.2%	0.8% ± 0.4%	20.9% ± 2.3%
Significance (*t*-test); $P < 0.05$		0.101	0.965	**<0.001**	**<0.001**

Value after the ± reflect standard error of the mean. Bold values indicate statistically significant differences between groups.
Good Group: n = 25 couples; 20 sperm samples, 24 blastocyst samples.
Poor Group: n = 28 couples; 20 sperm samples, 24 blastocyst samples.

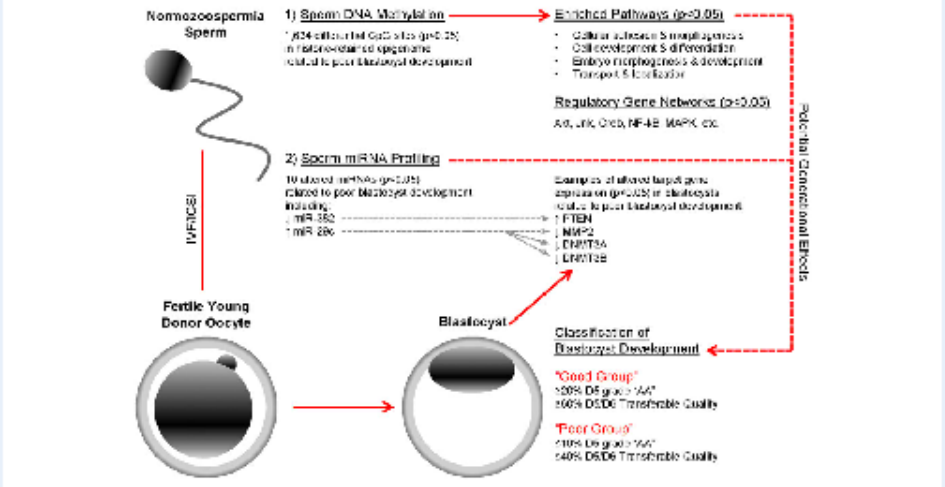

Figure 1 Experimental outline and results summary. Normozoospermia sperm samples in donor oocyte IVF cycles resulted in either good quality (Good Group) or poor quality (Poor Group) embryogenesis. In the Poor Group, aberrant sperm DNA methylation in histone-retained regions was enriched for genes involved in critical developmental pathways and regulatory gene networks, while altered sperm miRNAs corresponded to altered target gene transcript levels in blastocysts, reflecting the poor blastocyst development observed.

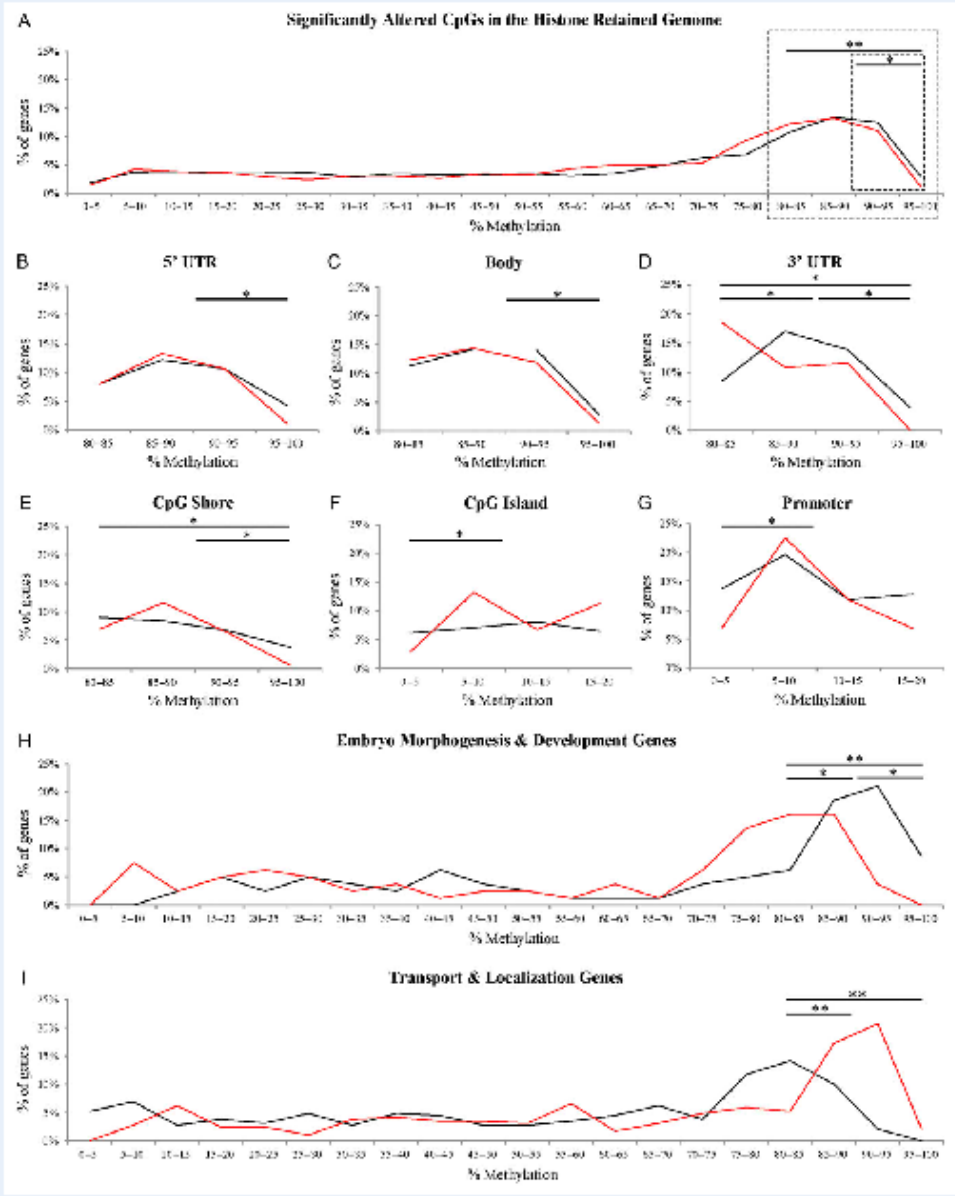

Figure 2 Sperm DNA methylation profiles of statistically significant genes for the histone-retained genome and across defined genomic regions. Mean methylation (β-values) for all significantly altered genes between the Good Group (black lines) and the Poor Group (red lines) distributed into 5% methylation intervals for (**A**) the histone-retained genome (1634 CpGs), (**B–E**) hypermethylated genomic regions: 5′UTR (189 CpGs), body (1185

Sperm methylation array analysis

Isolated DNA from sperm samples ($n = 12$) using the QiaAMP DNA Mini Kit (Qiagen, Valencia CA) was bisulfite converted with the EZ DNA Methylation-Direct Kit (Zymo Research, Irvine CA) for hybridization to an Infinium HumanMethylation450 BeadChip microarray (Illumina, San Diego CA) according to manufacturer's protocols. Beta values (β-values; range 0–1) and significant differential methylation was determined by calculating 'DiffScores' at a significance level of $P < 0.05$ (GenomeStudio, Illumina). After the removal of SNP containing probes, the β-value distribution was examined for histone-retained regions (Hammoud *et al.*, 2009), and then dissected further across defined genomic regions provided by Illumina (CpG island, CpG shore, CpG shelf, promoter-associated, TSS1 500 [TSS: transcriptional start site], TSS200, 5′UTR [UTR: untranslated region], first exon, body, 3′UTR).

Sperm methylation pathway and gene network analyses

Using DAVID 6.8 (Database for Annotation, Visualization and Integrated Discovery) (Huang da *et al.*, 2009a; 2009b), gene ontology (GO) term enrichment with a *P*-value of <0.05 and a Benjumini score of <0.05 were included to account for multiple comparison corrections. Interaction gene networks were constructed using Ingenuity® Pathway Analysis (IPA®; Qiagen), a tool which uncovers the significance of omics data within the context of biological systems.

Sperm targeted DNA methylation analysis

Methylation validation on normozoospermic samples ($n = 16$) was performed by targeted bisulfite sequencing at two imprinting control regions and 23 developmental or significant genes. Briefly, sperm samples underwent DNA isolation using the QiaAMP DNA Mini Kit (Qiagen). Bisulfite mutagenesis was performed using the EZ DNA Methylation-Direct kit (Zymo Research), with PCR amplification of 100 ng converted DNA in Illustra™ Hot Start Mix Ready-To-Go (RTG) PCR beads (GE Healthcare, Buckinghamshire UK). PCR bisulfite primers can be found in Supplementary Table SI. Individual clones were sent for sequencing (Bio Basic Inc., Markham ON, Canada). Methylation percentage for each gene was calculated as the number of methylated CpGs divided by the total number of CpG dinucleotides.

Sperm microRNA analysis

RNA isolation and qRT-PCR was performed on normozoospermic samples ($n = 12$) using TaqMan® Human MicroRNA Arrays (Applied Biosystems, U.S.A.) according to the manufacturer's instructions. Briefly, samples were reverse transcribed using the Megaplex™RT Primers Human Primer Pool A and the TaqMan® MicroRNA Reverse Transcription Kit (Life Technologies, U.S.A.). Quantitative real-time PCR was performed after preamplification using the TaqMan® Human MicroRNA Array Card and run on the ABI7900HT Fast Real-Time PCR System. Cycle thresholds were analyzed using RQ Manager 1.2.1 (Life Technologies). The Poor Group was analyzed relative to the Good Group using the internal constant, *MammU6*. A list of differentially expressed miRNAs was uploaded into miRTarBase (http://mirtarbase.mbc.nctu.edu.tw/) to identify predicted target genes for blastocyst gene expression.

Blastocyst relative mRNA gene expression analysis

Total RNA was isolated from individual blastocysts ($n = 48$) for analysis of transcript abundance as previously described (Parks *et al.*, 2011). Samples were treated with RNase-free DNase I (Qiagen), and the High Capacity Reverse Transcription cDNA kit (ThermoFisher Scientific, U.S.A.). Quantitative real-time PCR was performed using the ABI 7300 Real Time PCR System with Power SYBR Green PCR Master Mix (ThermoFisher Scientific). The quantification of seven genes was calculated relative to the housekeeping gene, *ACTB* (β-actin), which displayed comparatively constant levels of transcription in every sample. The Poor Group was analyzed relative to the Good Group. Expression primers are outlined in Supplementary Table SII.

Statistical analyses

Significant differential methylation for the sperm methylation array analysis was determined by an Illumina custom algorithm for calculating 'DiffScores' [*P*-value =1/(10^(ABS(DiffScore)/10))] which employed a Benjamini-Hochberg corrected false discovery rate (FDR) approach for multiple testing correction. The algorithm transforms FDR values by the following equation: [$-10\log_{10}$ (q-value FDR)], such that a transformed FDR value of 13 = 0.05, 20 = 0.01, 30 = 0.001, and a significance level of 0.05 was employed similar to other recent publications (Urdinguio *et al.*, 2015; Dere *et al.*, 2016). A power analysis was calculated to detect methylation differences of 2% with a standard deviation of 4%, resulting in a required sample size of 63 in each group to achieve a power of 80%. With the sample size of 6 as available in our two groups for the sperm methylation array, this would translate into an observed power of 14% for this study. Pathway analysis was assessed using DAVID 6.8, where a modified Fisher Exact *P*-value of $P < 0.05$ were considered significant GO term enrichment for 'Biological Processes', and a Benjamini value of 0.05 was used to correct enrichment *P*-values to control false discovery rate. Student's *t*-test was used to examine significance for targeted sperm methylation validation between groups where $P < 0.05$ was considered to be statistically significant. The Relative Expression Software Tool (REST 2009) (Qiagen) was used for mRNA and miRNA gene expression analyses. The determined expression ratio was tested for significance by a Pair Wise Fixed Reallocation Randomization Test (Pfaffl *et al.*, 2002).

Results

Patient outcomes and experimental design

A summary of average patient ages, semen parameters and embryo development can be found in Table I, with an experimental outline and results summary found in Fig. 1. The IVF cycles were defined as one of two groups, sperm resulting in good quality (Good Group) or poor quality (Poor Group) blastocyst development. The only statistical difference between groups was observed at the blastocyst stage based on the inclusion criteria (D5 grade 'AA': Good = 37%, Poor = 1%; $P < 0.001$; Transferable quality on D5 and D6: Good = 73%, Poor = 21%; $P < 0.001$).

CpGs), 3′UTR (130 CpGs), CpG shore (345 CpGs), (**F**,**G**) hypomethylated genomic regions: CpG island (311 CpGs), promoter (102 CpGs), (**H**) genes involved in embryo development and morphogenesis (81 CpGs) and (**I**) genes involved in transport and localization (290 CpGs). Statistics were performed for hypermethylated regions [80–100%], [80–90%], [90–100%] and hypomethylated regions [0–20%], [0–10%], [10–20%]. Statistical significance of $P < 0.05$ is denoted by *, and statistical significance of $P < 0.001$ is denoted by **.

Table II Enriched biological processes for statistically significant genes.

GO term	Term	# of genes	Methylation INCREASE in Poor Group: *P*-value	Methylation DECREASE in Poor Group: *P*-value	# of genes
GO:0048598	Embryonic morphogenesis	0			41
GO:0009790	Embryo development	0			51
GO:0009952	Anterior/posterior pattern specification	0			18
GO:0048568	Embryonic organ development	0			27
GO:0003002	Regionalization	0			23
GO:0051049	Regulation of transport	83			0
GO:0032879	Regulation of localization	105			0
GO:0051234	Establishment of localization	175			0
GO:0006810	Transport	169			0
GO:0051179	Localization	205			0
GO:0044765	Single-organism transport	128			0
GO:1902578	Single-organism localization	133			0
GO:0022610	Biological adhesion	77			68
GO:0007155	Cell adhesion	76			67
GO:0031589	Cell-substrate adhesion	16			18
GO:0030154	Cell differentiation	144			142
GO:0030182	Neuron differentiation	61			62
GO:0048731	System development	163			163
GO:0009653	Anatomical structure morphogenesis	108			111
GO:0007275	Multicellular organism development	179			180
GO:0044707	Single-multicellular organism process	215			212
GO:0048468	Cell development	84			96
GO:0048666	Neuron development	49			55
GO:0032502	Developmental process	198			203
GO:0031175	Neuron projection development	43			47
GO:0030030	Cell projection organization	61			66
GO:0000904	Cell morphogenesis involved in differentiation	40			45
GO:0048856	Anatomical structure development	195			198
GO:0022008	Neurogenesis	71			67
GO:0048699	Generation of neurons	68			64
GO:0048869	Cellular developmental process	156			152
GO:0044767	Single-organism developmental process	197			197
GO:0007399	Nervous system development	95			94
GO:0032989	Cellular component morphogenesis	60			63
GO:0000902	Cell morphogenesis	55			60
GO:0048812	Neuron projection morphogenesis	31			31
GO:0032501	Multicellular organismal process	235			235
GO:0031344	Regulation of cell projection organization	33			29
GO:0030036	Actin cytoskeleton organization	32			34
GO:0030029	Actin filament-based process	38			39
GO:0007010	Cytoskeleton organization	51			58
GO:0051128	Regulation of cellular component organization	83			97
GO:0065009	Regulation of molecular function	99			113
GO:0016043	Cellular component organization	0			210
GO:0044699	Single-organism process	414			397
GO:0044763	Single-organism cellular process	383			370
GO:0065008	Regulation of biological quality	136			116
GO:0071840	Cellular component organization or biogenesis	0			213

P-value significance
P < 0.00001
P < 0.0001
P < 0.001
P < 0.01
P < 0.05
P ≥ 0.05 (N/A)

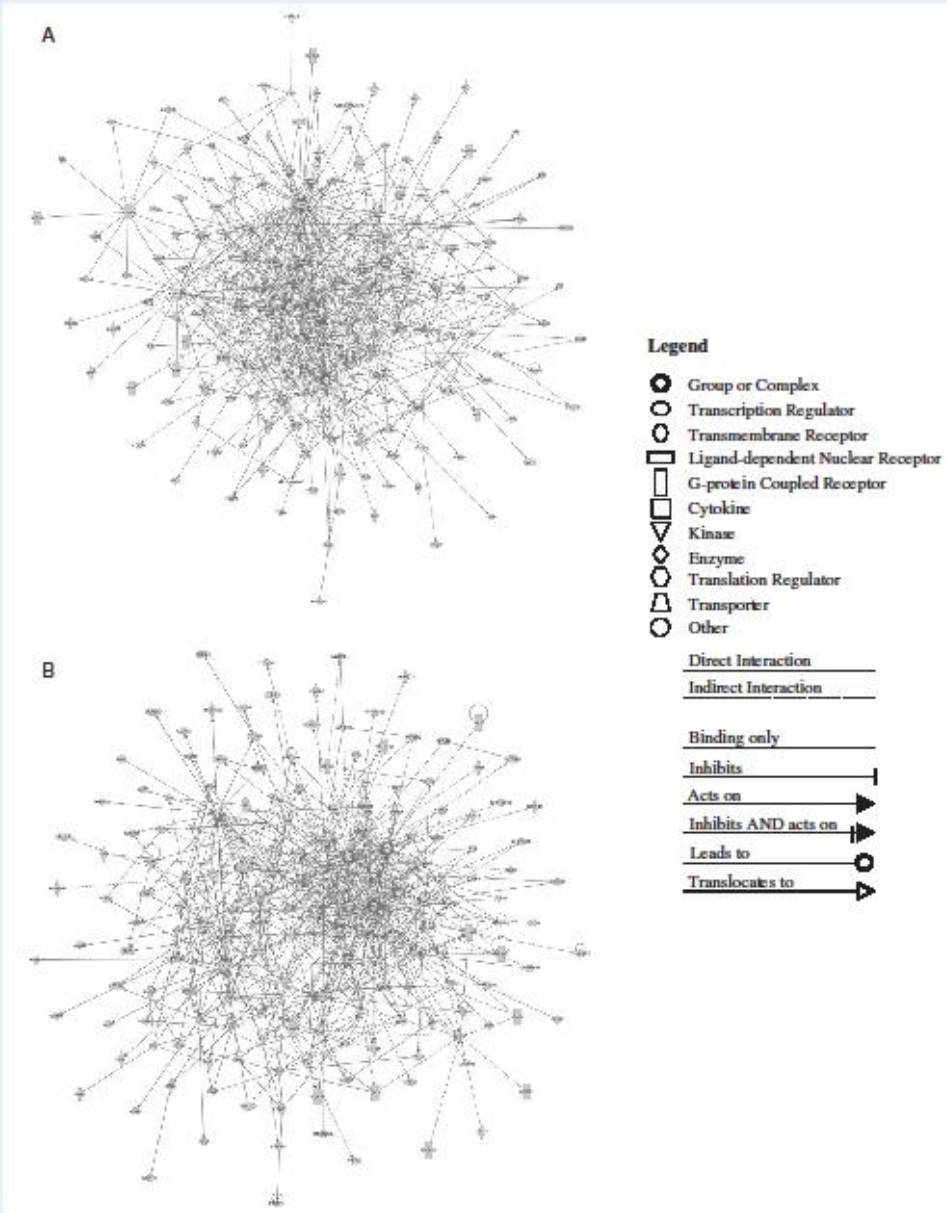

Figure 3 Regulatory gene networks identified for statistically significant genes. Top gene interaction networks generated from lists of genes with (**A**) increased methylation or (**B**) decreased methylation in the Poor Group.

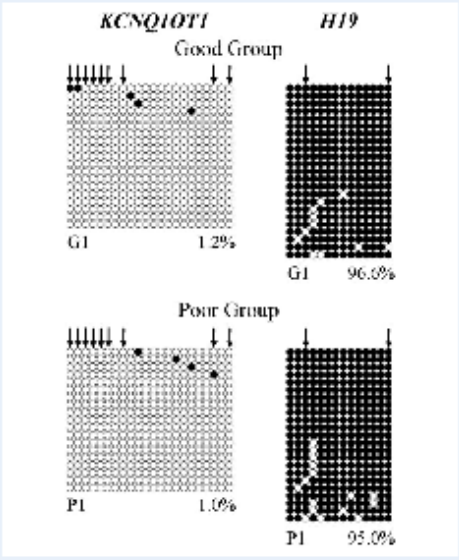

Figure 4 Representative sperm DNA methylation profiles at two imprinting control regions. A representation of targeted DNA methylation analysis in individual normozoospermic samples ($n = 6$) at the paternally expressed *KCNQ1OT1* ICR; hypomethylated (Good Group: 1.2%; Poor Group: 1.0%), and the paternally methylated *H19* ICR; hypermethylated (Good Group: 96.6%; Poor Group: 95.0%). No statistical difference was found between groups. Each line is a unique DNA strand amplified within the sperm sample. Black dots represent methylated CpGs, white dots represent unmethylated CpGs. Sperm ID is indicated below-left of the image. Percent methylation is indicated below-right of the image. Arrows indicate the CpG directly targeted by an Infinium HumanMethylation450 BeadChip probe, none of which were statistically significant between groups in the array dataset.

Histone-Retained Sperm DNA Methylation Profiles

The sperm methylation array data resulted in 1634 CpG probe sites that were statistically different between the two groups ($P < 0.05$) at retained histones (Fig. 1) (Hammoud et al., 2009). The β-value distribution was examined for all retained histones, and then separated across defined genomic regions. In the Good Group, a predominantly hypermethylated profile was evident, consistent with previous reports (Smallwood et al., 2011; Dere et al., 2016), having >40% of all CpG sites presenting with ≥80% methylation (≥0.8 β-value). A small but distinct and statistically significant shift away from expected methylation levels was observed in the samples attained from the Poor Group ($P < 0.05$) (Fig. 2A). This shift was uniformly observed for the Poor Group among specific genomic regions that possessed primarily hypermethylated CpGs (Fig. 2B–E). By contrast, a primarily hypomethylated profile was observed for the Good Group at CpG islands and regions close to the promoter, having >30% of CpG sites presenting with ≤20% methylation (≤0.2 β-value). A statistically significant shift away from expected methylation levels was observed in the samples attained from the Poor Group ($P < 0.05$). This shift for the Poor Group was consistent among two genomic regions with primarily hypomethylated CpGs (Fig. 2F and G).

Gene ontology and regulatory network analysis

Genes with significant differential methylation at CpG probe sites ($P < 0.05$) showing increased (576 genes) or decreased (562 genes) methylation in the Poor Group were used for biological process GO term analysis. Genes enriched for cellular adhesion and morphogenesis were significant in both sets, as well as a variety of other cellular development and differentiation processes ($P < 0.05$) (Table II, Fig. 1). Notably, genes enriched for transport and localization were highly represented among those with significantly increased CpG methylation in the Poor Group, while genes involved in embryonic morphogenesis and development were highly represented among those with significantly decreased CpG methylation in the Poor Group. Enriched genes listed in the 'embryo morphogenesis' and 'embryo development' categories highlighted a hypermethylated pattern among the sperm samples in the Good Group, with a small but significant methylation loss for these genes in the Poor Group ($P < 0.05$) (Fig. 2H). Interestingly, enriched genes listed in the 'transport' and 'localization' categories highlighted an opposite shift for hypermethylated CpGs ($P < 0.05$) (Fig. 2I).

The same gene lists for increased and decreased methylation in the Poor Group were targeted for bioinformatics analysis to construct regulatory networks (Fig. 3A and B). Many pathways were found in common between the two methylation lists, including Akt, Jnk, Creb, NF-kB and MAPK. However, different players within these complexes were either increased or decreased in the Poor Group, impacting the overall gene network function (Supplementary Table SIII).

Targeted sperm DNA methylation validation

Less than ten percent of known human imprinted genes (7%; 7/97) were represented within the methylation array dataset with at least one significantly altered CpG site (range: 1–3 CpG sites). Likewise, examination of 10 known gametic differentially methylated regions (gDMRs; *PLAGL1*, *GRB10*, *PEG10*, *MEST*, *PEG13*, *H19*, *KCNQ1OT1*, *SNRPN*, *PEG3*, *GNAS*) did not reveal any aberrant imprinted methylation patterns. This was further confirmed by targeted bisulfite sequencing, observing no statistical difference between groups at two defined imprinting control regions (ICRs), the paternally expressed *KCNQ1OT1* ICR and the paternally methylated *H19* ICR (Fig. 4).

Twenty-three genes were also selected for further methylation validation at the individual CpG level. Three distinct patterns of methylation were observed: (i) hypermethylation (80–100%) in both groups, (ii) hypomethylation (0–20%) in both groups and (iii) variable methylation in both groups (Fig. 5). Two genes were selected for evaluation in a larger cohort of sperm samples on account of their consistent and discernable methylation differential between groups; *ANKRD53* and *MAPT* (Fig. 6 and Supplementary Fig. S1).

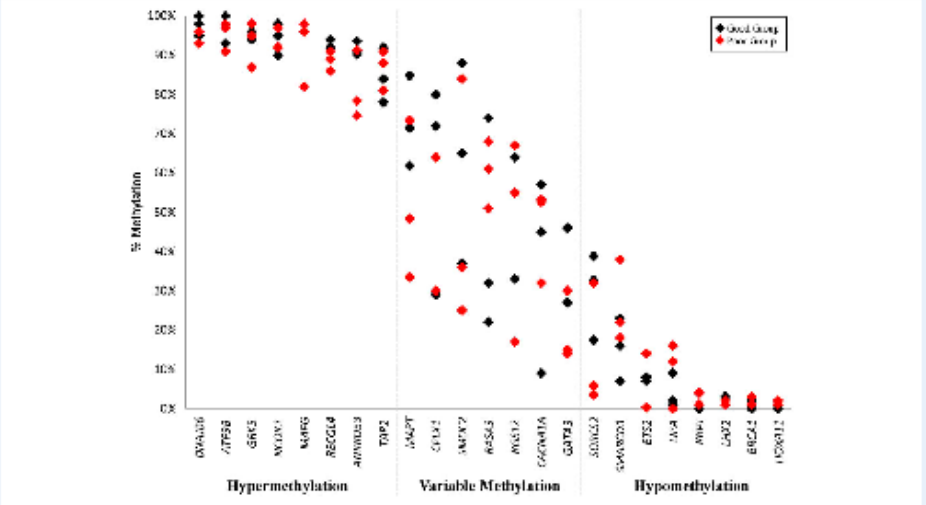

Figure 5 Sperm DNA methylation validation for both groups at select genes. Targeted DNA methylation analysis in individual normozoospermic samples ($n = 6$) at 23 genes. Black diamonds represent sperm from the Good Group, and red diamonds represent sperm from the Poor Group. Each diamond is positioned at the average percent methylation for the individual sperm sample. Three methylation patterns are observed: hypermethylation in both groups, hypomethylation in both groups and variable methylation in both groups.

Sperm microRNA profiling

The miRNA profiles of the two sperm groups were investigated and 10 miRNAs were found to be significantly altered, including one that was exclusively expressed in the sperm from the Good Group (*miR-325*), and one that was exclusively expressed in the sperm from the Poor Group (*miR-873*). In addition, five were significantly down-regulated (*let-7d, miR-371–3p, miR-382, miR-516a-5p, miR-523*), while three were significantly up-regulated (*miR-139–5p, miR-29c, miR-520d-5p*) in the Poor Group ($P < 0.05$) (Figs 1 and 7A).

Blastocyst mRNA gene expression

Targeted mRNA transcript levels in individual blastocysts revealed seven genes with significant alterations in the Poor Group ($P < 0.05$) (Figs 1 and 7B). Increased *miR-29c* in the sperm from the Poor Group negatively targets the *de novo* methyltransferase enzymes in humans. Significant decreases in both *DNMT3A* and *DNMT3B* transcripts were found in the blastocysts from the Poor Group. This miRNA also negatively targets *MMP2*, a matrix metalloproteinase gene important for implantation, showing significantly reduced expression. Decreased *miR-382* negatively targets *PTEN*, a negative regulator of the PI3K/AKT signaling pathway essential for embryonic gene activation. A corresponding increase in expression of *PTEN* was observed in the blastocysts from the Poor Group. A significant increase was also identified for *TDG*, a thymine DNA glycosylase required for defense against genetic mutation and for active DNA demethylation, while significant decreases were detected for the pluripotency gene *POU5F1*, required for proper preimplantation development, and *DNMT1*, the methyltransferase enzyme required for DNA methylation maintenance.

Discussion

The molecular mechanisms resulting in male infertility are poorly understood, and a large proportion of cases are deemed unexplained, or idiopathic, as standard testing fails to find a cause. Gametogenesis and early embryogenesis are important stages for genome-wide epigenetic transitions, providing a period in which disruption to normal epigenetic regulatory pathways would greatly affect gamete maturation as well as embryo development. Increasing evidence suggests that sperm DNA methylation is an important mark, with a direct association with poor semen parameters, often manifesting at developmental genes and imprinted regions (Hammoud *et al.*, 2010, 2011). Similar disturbances to male epigenetic reprogramming may also contribute to unexplained male factor infertility and to the poor embryonic development observed in these cases (Aston *et al.*, 2015; Urdinguio *et al.*, 2015; Jenkins *et al.*, 2016a,b). To address the association between unexplained MF infertility and epigenetics, we selected sperm samples having normal semen parameters and young donor oocyte cycles to eliminate known male and female factors.

The histone-retained CpG island regions of the sperm epigenome did not exhibit a statistically significant difference when examined in its entirety between the two groups, which indicated no correlation

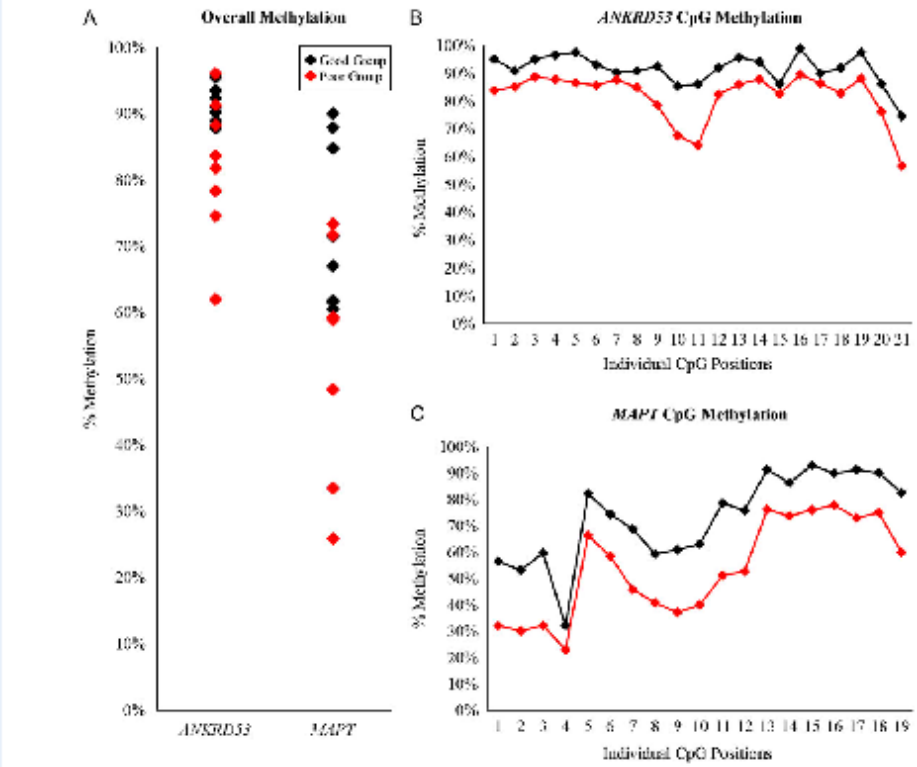

Figure 6 Sperm DNA methylation percentages at *ANKRD53* and *MAPT*. Targeted DNA methylation analysis in individual normozoospermic samples ($n = 16$) at *ANKRD53* and *MAPT*. Black diamonds represent sperm from the Good Group, and red diamonds represent sperm from the Poor Group. (**A**) Each diamond is positioned at the average percent methylation for the individual sperm sample. (**B**) Average percent methylation is distributed by the 21 CpG positions at *ANKRD53* for both groups (Good Group: 91.6%; Poor Group: 82.0%; $P < 0.05$). (**C**) Average percent methylation is distributed by the 19 CpG positions at *MAPT* for both groups (Good Group: 73.1%; Poor Group: 53.8%; $P < 0.05$).

between overall DNA methylation levels and quality of embryos (Benchaib et al., 2005). Rather, a small (~5–10%) but distinct and statistically significant shift away from the expected methylation profile was observed in correlation with poor blastocyst development. The biological significance of this small methylation shift is still unknown, though existing data suggests that subtle epigenetic changes are associated with complex disease phenotypes (Leenen et al., 2016), and therefore may have greater translational consequences, resulting in a cumulative effect on fertility and subsequent embryonic developmental capacity.

An even distribution between increased methylation and decreased methylation was observed with poor blastocyst development, in agreement with a previous report (Urdinguio et al., 2015). Gene ontology analysis revealed an enrichment of genes involved in cellular adhesion and morphogenesis similar to other publications (Aston et al., 2015; Hammoud et al., 2015; Urdinguio et al., 2015), as well as expansive processes involving cell development, differentiation and organization. Genes in these pathways impact cell-to-cell interactions including sperm-oocyte fusion, embryonic genome activation, implantation potential and embryonic differentiation. As affirmation, enrichment for genes involved in embryo morphogenesis and development were found to be the utmost significant pathway in the population of CpG sites with decreased methylation. Regulatory networks illustrated a surplus of pathways that were common between the gene lists for increased and decreased methylation. Yet, the genes within these pathways were primarily distinct between lists, indicating that the methylation alterations at these genes are collectively driving the changes observed in the unexplained MF infertility group. Aberrant methylation at these critical genes, impacting the overall gene network function, conceivably leads to the observed compromised embryogenesis.

Three distinct patterns of methylation were observed in the genes selected for validation: hypermethylation, hypomethylation and

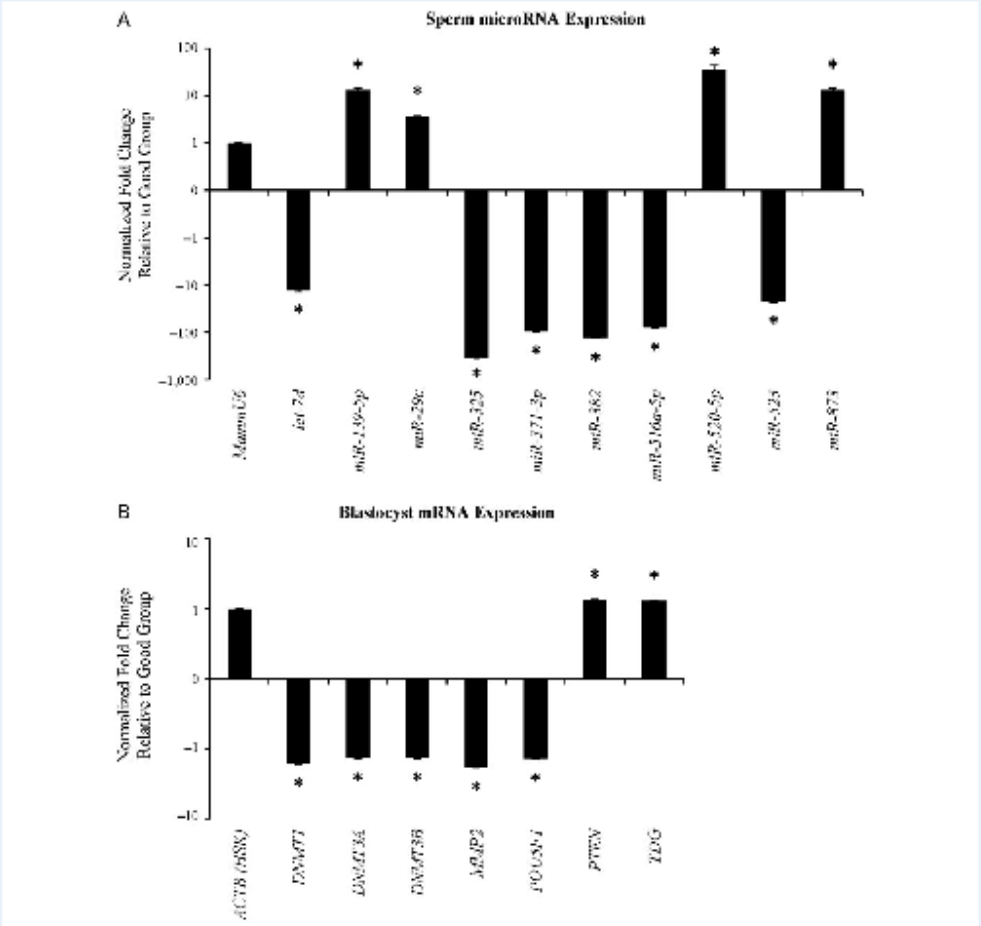

Figure 7 miRNA and mRNA gene expression changes in the Poor Group. Transcript abundance for (**A**) sperm miRNA expression, and (**B**) blastocyst mRNA expression. Normalized fold change relative to the Good Group and to the internal constant *MammU6* for miRNA expression, and to the housekeeping gene *ACTB* for mRNA expression. Statistical significance of $P < 0.05$ is denoted by an asterisk.

variable methylation. Sperm resulting in poor blastocyst development appeared to be more prone to increased epigenetic heterogeneity, similar to studies of known MF infertility (Benchaib *et al.*, 2005; Kuhtz *et al.*, 2014; Jenkins *et al.*, 2015; Laurentino *et al.*, 2015). The biological consequences of these small alterations are unclear, but they may impact the active global DNA demethylation of the paternal genome after fertilization, or disrupt the fidelity of DNA methylation maintenance at vital paternally inherited loci.

Altered sperm methylation correlated with altered paternal miRNA profiles in samples resulting in poor blastocyst development. Mature spermatozoa are transcriptionally quiescent, but lingering transcripts including small non-coding RNAs exist (Amanai *et al.*, 2006; Yan *et al.*, 2008), and their aberrant presence or absence could be indicative of abnormal development, function, or fertility. Growing evidence indicates a potential role for these paternal miRNAs in early embryo development (Krawetz, 2005). Increased paternal sperm miRNA levels correlated with higher rates of good-quality embryos, implantation, pregnancy and live birth in unexplained male infertility patients (Cui *et al.*, 2015). In our study, ten miRNAs were identified as significantly altered in association with poor blastocyst development, with corresponding alterations to target genes involved in embryonic genome activation, blastocyst implantation and DNA methylation. This

dysregulation of sperm-borne miRNAs or their targets may also be a source of the observed compromised blastocyst development.

Epigenetic reprogramming events in both the gametes and the early embryo are designed to prevent epigenetic defects from being inherited. However, erroneous generational epigenetic inheritance of aberrant methylation and miRNA signatures from a compromised sperm population, facilitated by IVF/ICSI, may occur and contribute to gene expression alterations and ultimately poor embryo quality. Having eliminated the influence of female factor infertility by using only young fertile donor oocytes, significantly altered methylation profiles enriched at developmental loci were observed in normozoospermic samples resulting in poor blastocyst development, reflecting a subset of unexplained male factor infertility. The improved knowledge of sperm epigenetics and epigenetic inheritance from studies such as ours have important implications for future generations, while providing evidence for potential causes of unexplained male factor infertility and support modified counseling and clinical management.

Supplementary data

Supplementary data are available at *Human Reproduction* online.

Acknowledgements

The authors would like to acknowledge Dr. Kenneth Jones from the University of Colorado for his help in bioinformatics.

Authors' roles

M.M.D. participated in study design, and executed analyses of the 450 K array data and pathway analyses, performed the targeted DNA methylation experiments and analyses, and took the lead in manuscript drafting and editing. B.R.M. executed the miRNA and mRNA expression experiments and analyses, and participated in manuscript drafting. J.C.P. collected and prepared sperm and blastocyst samples for all the experiments as well as participated in manuscript drafting. W.B.S. provided critical manuscript review and editing, and M.G.K-J designed and oversaw the completion of the study, participated in critical discussion and in manuscript drafting and editing.

Funding

No external funding was used for this study.

Conflict of interest

None declared.

References

Amanai M, Brahmajosyula M, Perry AC. A restricted role for sperm-borne microRNAs in mammalian fertilization. *Biol Reprod* 2006;**75**:877–884.

Aston KI, Uren PJ, Jenkins TG, Horsager A, Cairns BR, Smith AD, Carrell DT. Aberrant sperm DNA methylation predicts male fertility status and embryo quality. *Fertil Steril* 2015;**104**:1388–1397. e1381–1385.

Benchaib M, Braun V, Ressnikof D, Lornage J, Durand P, Niveleau A, Guerin JF. Influence of global sperm DNA methylation on IVF results. *Hum Reprod* 2005;**20**:768–773.

Carrell DT, Hammoud SS. The human sperm epigenome and its potential role in embryonic development. *Mol Hum Reprod* 2010;**16**:37–47.

Cooper TG, Noonan E, von Eckardstein S, Auger J, Baker HW, Behre HM, Haugen TB, Kruger T, Wang C, Mbizvo MT *et al.* World Health Organization reference values for human semen characteristics. *Hum Reprod Update* 2010;**16**:231–245.

Cui L, Fang L, Shi B, Qiu S, Ye Y. Spermatozoa micro ribonucleic acid-34c level is correlated with intracytoplasmic sperm injection outcomes. *Fertil Steril* 2015;**104**:312–317. e311.

Dada R, Kumar M, Jesudasan R, Fernandez JL, Gosalvez J, Agarwal A. Epigenetics and its role in male infertility. *J Assist Reprod Genet* 2012;**29**:213–223.

Dadoune JP. The nuclear status of human sperm cells. *Micron* 1995;**26**:323–345.

Dere E, Huse S, Hwang K, Sigman M, Boekelheide K. Intra- and inter-individual differences in human sperm DNA methylation. *Andrology* 2016;**4**:832–842.

Gardner DK, Schoolcraft WB. In vitro culture of human blastocysts. In: Jansen M (ed). *Toward Reproductive Certainty: Fertility and Genetics Beyond 1999*. UK: Parthenon Publishing London, 1999, 378–388.

Gatewood JM, Cook GR, Balhorn R, Bradbury EM, Schmid CW. Sequence-specific packaging of DNA in human sperm chromatin. *Science* 1987;**236**:962–964.

Hamada A, Esteves SC, Agarwal A. Unexplained male infertility: potential causes and management. *Hum Androl* 2011;**1**:2–16.

Hamada A, Esteves SC, Nizza M, Agarwal A. Unexplained male infertility: diagnosis and management. *Int Braz J Urol* 2012;**38**:576–594.

Hammoud SS, Low DH, Yi C, Lee CL, Oatley JM, Payne CJ, Carrell DT, Guccione E, Cairns BR. Transcription and imprinting dynamics in developing postnatal male germline stem cells. *Genes Dev* 2015;**29**:2312–2324.

Hammoud SS, Nix DA, Hammoud AO, Gibson M, Cairns BR, Carrell DT. Genome-wide analysis identifies changes in histone retention and epigenetic modifications at developmental and imprinted gene loci in the sperm of infertile men. *Hum Reprod* 2011;**26**:2558–2569.

Hammoud SS, Nix DA, Zhang H, Purwar J, Carrell DT, Cairns BR. Distinctive chromatin in human sperm packages genes for embryo development. *Nature* 2009;**460**:473–478.

Hammoud SS, Purwar J, Pflueger C, Cairns BR, Carrell DT. Alterations in sperm DNA methylation patterns at imprinted loci in two classes of infertility. *Fertil Steril* 2010;**94**:1728–1733.

Houshdaran S, Cortessis VK, Siegmund K, Yang A, Laird PW, Sokol RZ. Widespread epigenetic abnormalities suggest a broad DNA methylation erasure defect in abnormal human sperm. *PLoS One* 2007;**2**:e1289.

Huang da W, Sherman BT, Lempicki RA. Bioinformatics enrichment tools: paths toward the comprehensive functional analysis of large gene lists. *Nucleic Acids Res* 2009a;**37**:1–13.

Huang da W, Sherman BT, Lempicki RA. Systematic and integrative analysis of large gene lists using DAVID bioinformatics resources. *Nat Protoc* 2009b;**4**:44–57.

Irvine DS. Epidemiology and aetiology of male infertility. *Hum Reprod* 1998;**13**:33–44.

Jaenisch R, Bird A. Epigenetic regulation of gene expression: how the genome integrates intrinsic and environmental signals. *Nat Genet* 2003;**33**:245–254.

Jenkins TG, Aston KI, Hotaling JM, Shamsi MB, Simon L, Carrell DT. Teratozoospermia and asthenozoospermia are associated with specific epigenetic signatures. *Andrology* 2016a;**4**:843–849.

Jenkins TG, Aston KI, Meyer TD, Hotaling JM, Shamsi MB, Johnstone EB, Cox KJ, Stanford JB, Porucznik CA, Carrell DT. Decreased fecundity and sperm DNA methylation patterns. *Fertil Steril* 2016b;**105**:51–57. e51–53.

Jenkins TG, Aston KI, Trost C, Farley J, Hotaling JM, Carrell DT. Intra-sample heterogeneity of sperm DNA methylation. *Mol Hum Reprod* 2015;**21**:313–319.

Jenkins TG, Carrell DT. The sperm epigenome and potential implications for the developing embryo. *Reproduction* 2012;**143**:727–734.

Krawetz SA. Paternal contribution: new insights and future challenges. *Nat Rev Genet* 2005;**6**:633–642.

Kuhtz J, Schneider E, El Hajj N, Zimmermann L, Fust O, Linek B, Seufert R, Hahn T, Schorsch M, Haaf T. Epigenetic heterogeneity of developmentally important genes in human sperm: implications for assisted reproduction outcome. *Epigenetics* 2014;**9**:1648–1658.

Kumar M, Kumar K, Jain S, Hassan T, Dada R. Novel insights into the genetic and epigenetic paternal contribution to the human embryo. *Clinics (Sao Paulo)* 2013;**68**:5–14.

Laurentino S, Beygo J, Nordhoff V, Kliesch S, Wistuba J, Borgmann J, Buiting K, Horsthemke B, Gromoll J. Epigenetic germline mosaicism in infertile men. *Hum Mol Genet* 2015;**24**:1295–1304.

Leenen FA, Muller CP, Turner JD. DNA methylation: conducting the orchestra from exposure to phenotype? *Clin Epigenetics* 2016;**8**:92.

Miller D, Brinkworth M, Iles D. Paternal DNA packaging in spermatozoa: more than the sum of its parts? DNA, histones, protamines and epigenetics. *Reproduction* 2010;**139**:287–301.

Moghissi KS, Wallach EE. Unexplained infertility. *Fertil Steril* 1983;**39**:5–21.

Nanassy L, Carrell DT. Paternal effects on early embryogenesis. *J Exp Clin Assist Reprod* 2008;**5**:2.

Oliva R, Dixon GH. Vertebrate protamine genes and the histone-to-protamine replacement reaction. *Prog Nucleic Acid Res Mol Biol* 1991;**40**:25–94.

Parks JC, McCallie BR, Janesch AM, Schoolcraft WB, Katz-Jaffe MG. Blastocyst gene expression correlates with implantation potential. *Fertil Steril* 2011;**95**:1367–1372.

Pessot CA, Brito M, Figueroa J, Concha II, Yanez A, Burzio LO. Presence of RNA in the sperm nucleus. *Biochem Biophys Res Commun* 1989;**158**:272–278.

Pfaffl MW, Horgan GW, Dempfle L. Relative expression software tool (REST) for group-wise comparison and statistical analysis of relative expression results in real-time PCR. *Nucleic Acids Res* 2002;**30**:e36.

Rodenhiser D, Mann M. Epigenetics and human disease: translating basic biology into clinical applications. *CMAJ* 2006;**174**:341–348.

Sendler E, Johnson GD, Mao S, Goodrich RJ, Diamond MP, Hauser R, Krawetz SA. Stability, delivery and functions of human sperm RNAs at fertilization. *Nucleic Acids Res* 2013;**41**:4104–4117.

Smallwood SA, Tomizawa S, Krueger F, Ruf N, Carli N, Segonds-Pichon A, Sato S, Hata K, Andrews SR, Kelsey G. Dynamic CpG island methylation landscape in oocytes and preimplantation embryos. *Nat Genet* 2011;**43**:811–814.

Urdinguio RG, Bayon GF, Dmitrijeva M, Torano EG, Bravo C, Fraga MF, Bassas L, Larriba S, Fernandez AF. Aberrant DNA methylation patterns of spermatozoa in men with unexplained infertility. *Hum Reprod* 2015;**30**:1014–1028.

Yan W, Morozumi K, Zhang J, Ro S, Park C, Yanagimachi R. Birth of mice after intracytoplasmic injection of single purified sperm nuclei and detection of messenger RNAs and MicroRNAs in the sperm nuclei. *Biol Reprod* 2008;**78**:896–902.

19.0 Appendix 6. Additional publication

Denomme MM, McCallie BR, **Parks JC,** Booher K, Schoolcraft WB, Katz-Jaffe MG. Inheritance of epigenetic dysregulation from male factor infertility has a direct impact on reproductive potential. Fertil Steril. 2018 Aug;110(3):419-428.e1. doi: 10.1016/j.fertnstert.2018.04.004. Epub 2018 Jun 28.

My personal contribution to this manuscript

I worked closely with Dr. Katz-Jaffe and Dr. Denomme to coordinate the collection of study materials between the research department and the IVF laboratory. I also performed sperm count and motility for samples donated to research, and prepared them for storage at -80°C and downstream epigenetic experiments. Finally, I co-wrote and edited sections of the materials and methods section of the manuscript for publication as a co-author.

ORIGINAL ARTICLE: ANDROLOGY

Inheritance of epigenetic dysregulation from male factor infertility has a direct impact on reproductive potential

Michelle M. Denomme, Ph.D.,[a] Blair R. McCallie, B.Sc.,[a] Jason C. Parks, B.Sc.,[a] Keith Booher, Ph.D.,[b] William B. Schoolcraft, M.D.,[c] and Mandy G. Katz-Jaffe, Ph.D.[a,c]

[a] Fertility Labs of Colorado, Lone Tree, Colorado; [b] Zymo Research Corp., Irvine, California; and [c] Colorado Center for Reproductive Medicine, Lone Tree, Colorado

Objective: To evaluate the epigenetic consequence on the methylome and subsequent transcriptome in euploid blastocysts of male-factor (MF) infertility patients.
Design: Methylome and transcriptome analysis on individual oligoasthenoteratozoospermia (OAT [MF]) blastocysts.
Setting: Infertility clinic.
Patient(s): Clinical data from 128 couples presenting with OAT (MF) and 118 maternal age–matched control (no MF) subjects undergoing infertility treatment from 2010 to 2014, along with 72 surplus cryopreserved blastocysts donated from 33 couples with their informed consents.
Intervention(s): None.
Main Outcome Measure(s): Methyl Maxi-Seq (Zymo Research) was used to determine genome-wide DNA methylation, and small cell number RNA-Seq was used to examine the global transcriptome. Validation experiments were performed with the use of pyrosequencing or quantitative real-time polymerase chain reaction. Statistical analysis used Student *t* test, analysis of variance in R, Fisher exact test, and pairwise fixed reallocation randomization test where appropriate, with significance at $P<.05$.
Result(s): Clinical pregnancy rates were similar between OAT (MF) patients and control (no MF) subjects after euploid embryo transfer. However, the miscarriage rate for OAT (MF) patients was significantly higher (14.7% vs. 2.2%; $P<.05$). Methylome and transcriptome analyses of individual blastocysts revealed significant alterations in 1,111 CpG sites and 469 transcripts, respectively ($P<.05$). Pathway analysis elucidated genes involved in "regulation of cellular metabolic process" as universally affected. Validation of the genome-wide approaches was performed for *SBF1* and *SLC6A9* ($P<.05$).
Conclusion(s): Methylation and transcription aberrations in individual OAT (MF) blastocysts illustrate an epigenetic consequence of MF infertility on embryogenesis, significantly altering key developmental genes and affecting embryonic competence. This epigenetic dysregulation provides an explanation for the reduced reproductive potential in OAT (MF) patients despite euploid blastocyst transfers. (Fertil Steril® 2018;110:419–28. ©2018 by American Society for Reproductive Medicine.)
El resumen está disponible en Español al final del artículo.

Key Words: Male factor, PGT-A, methylome, transcriptome, epigenetic dysregulation

Discuss: You can discuss this article with its authors and other readers at https://www.fertstertdialog.com/users/16110-fertility-and-sterility/posts/31847-25761

Male-factor (MF) infertility contributes to one-half of all infertility cases worldwide [1, 2]. It is typically identified during assisted reproductive technology (ART) procedures by means of standardized semen parameter analyses assessing sperm concentration, motility, and morphology [3]. This conventional measurement continues to be the only routine test to diagnose this condition, even though it is known that such descriptive assessments cannot account for all aspects of sperm quality, such as chromatin organization and integrity. Compromised quality of the male gamete is known to affect fertilization potential, cleavage divisions, and embryo grade [4, 5], and is associated with an increase in aneuploidy [6], miscarriage [7], and negative pregnancy outcomes.

Received February 8, 2018; revised March 28, 2018; accepted April 3, 2018; published online June 28, 2018.
M.M.D. has nothing to disclose. B.R.M. has nothing to disclose. J.C.P. has nothing to disclose. K.B. is an employee of Zymo Research Corp. W.B.S. has nothing to disclose. M.G.K.-J. has nothing to disclose.
Reprint requests: Mandy G. Katz-Jaffe, Ph.D., Colorado Center for Reproductive Medicine, 10290 Ridgegate Circle, Lone Tree, Colorado 20124 (E-mail: mkatz-jaffe@coloorm.com).

Fertility and Sterility® Vol. 110, No. 3, August 2018 0015-0282/$36.00

https://doi.org/10.1016/j.fertnstert.2018.04.004

Recent evidence suggests that the sperm epigenetic status could also play a role in the etiology of miscarriage (8, 9). Epigenetic reprogramming events occur during gametogenesis and early embryogenesis, including DNA methylation erasure, acquisition, and maintenance (10). Some regions, such as imprinted genes and repetitive elements, can preserve their methylation signature from the parental gametes through to the developing embryo (11). Epigenetic inheritance from the sperm DNA methylation landscape is essential for both proper fertilization of the oocyte and viability of the early embryo, whereby disruption could largely affect embryonic development. A number of studies in both humans and nonhuman animal models have highlighted the importance of a "paternal factor" in miscarriage (9,12–15), but the causality between sperm DNA integrity and embryo development after implantation remains unexplained. There is a wide array of evidence linking MF infertility and aberrant sperm epigenetic signatures (16–21), but little is known about the inherited effects after fertilization (22, 23). Nevertheless, evidence suggests that aneuploidy affects epigenetic regulation, resulting in hypomethylation and genetic instability in blastocysts (24).

The introduction of intracytoplasmic sperm injection (ICSI) circumvents conventional MF infertility, thus eliminating the majority of barriers to fertilization. Sperm are selected for ICSI based on the best possible combination of motility and normal gross morphology. However, this does not ensure the genetic or epigenetic integrity of the sperm, and disruptions may play a significant role in impairing the development of the embryo after fertilization. The incorporation of preimplantation genetic testing for aneuploidy (PGT-A) has proved to be successful in improving embryo selection by removing abnormal chromosomal contributions, and randomized controlled trials have shown increases in sustained implantation and delivery rates (25–29).

The present study explored the clinical outcomes of PGT-A for oligoasthenoteratozoospermia (OAT [MF]) patients after a euploid blastocyst transfer. More importantly, it investigated the generational epigenetic effects of severe MF infertility by examining the global methylome and subsequent transcriptome of blastocysts derived from OAT (MF) infertility patients.

MATERIALS AND METHODS

Patient Selection

IVF cycle data and pregnancy outcomes were collected from couples (n = 246) that underwent frozen euploid blastocyst transfers at the Colorado Center for Reproductive Medicine from 2010 to 2014. Surplus cryopreserved blastocysts (n = 72) were donated from couples (n = 33) 5+ years after their infertility treatment with their informed consents and Institutional Review Board approval (WIRB study no. 1145350).

OAT (MF) was defined as motility <40%, morphology <3%, count <20 million/mL, and total motile count (TMC) <13 million/mL. OAT (MF) infertility patients (n = 128) and maternal age–matched control subjects with normozoospermia (no MF; n = 118), underwent routine infertility treatment during a similar time frame in the IVF laboratory. Ovarian stimulation, oocyte retrieval, ICSI, embryo culture, trophectoderm biopsy, PGT-A, and vitrification procedures were routinely performed as previously reported (30). Euploid blastocysts were warmed and transferred in a subsequent frozen embryo transfer. Statistical analysis for ovarian reserve, IVF cycle data, and pregnancy outcomes included Student *t* test with significance at $P<.05$.

PGT-A

Trophectoderm biopsies underwent cell lysis and DNA amplification with the use of Taqman quantitative real-time polymerase chain reaction (qPCR) (31). The copy number for all 22 pairs of autosomes and two sex chromosomes was characterized with the use of standard methods of relative quantification (32). This PCR methodology has demonstrated 98.6% accuracy (31, 33). Only embryos diagnosed as euploid 46XX or 46XY with sufficient confidence were deemed to be suitable for transfer. Limitations of qPCR methodology include the inability to detect mosaicism, chromosome segmental imbalances, and structural rearrangements.

Blastocyst Grading

Blastocysts included in the study were scored based on inner cell mass and trophectoderm quality (34), and were all morphologically graded as high, transferrable quality (grade ≥ 3BB). Blastocysts were divided into two groups based on semen parameter analysis at the time of oocyte retrieval. Blastocysts (n = 36) were selected for the control group based on the inclusion criteria of motility ≥40%, morphology ≥3%, count 20 million/mL, and TMC ≥ 13 million/mL, and donor oocyte. Blastocysts (n = 36) were selected for the OAT (MF) group based on the inclusion criteria of motility <40%, morphology <3%, count <20 million/mL, and TMC <13 million/mL.

Whole-Genome Bisulfite Sequencing

Trophectoderm biopsies (~5–10 cells; ~60 pg DNA) from individual blastocysts (n = 6) underwent whole genome bisulfite sequencing with the use of the Methyl Maxi-Seq platform (Zymo Research). Extremely-low-input library preparation of the samples with the use of the Pico Methyl-Seq Library Prep Kit (Zymo Research) was followed by amplification steps to add adapter sequences, PCR purification (DNA Clean & Concentrator 5; Zymo Research), and sequencing on the Illumina HiSeq 2500 platform. Sequence reads were identified with the use of standard Illumina base-calling software with a 5× minimum read count filter and theoretical resolution for detection at 20%, and bisulfite sequence data alignments were performed with the use of the alignment software Bismark (www.bioinformatics.babraham.ac.uk/projects/bismark/), between OAT (MF) and control (no MF) groups. Index files were constructed with the use of the entire reference genome, hg19. The methylation level of each cytosine was estimated as the number of reads reporting a C, divided by the total number of reads reporting a C or T. Quantification of the statistical significance of the methylation difference was determined with the use of the Student *t* test, where $P<.05$ was deemed to be significant. A limitation to the study is that a correction for multiple comparisons was not performed owing to the low

starting material in individual blastocysts combined with the small sample size and lack of statistical power.

Whole-Transcriptome RNA-Seq

Individual blastocysts (n = 11) underwent RNA isolation with the use of the Picopure RNA Isolation Kit (Molecular Devices), and library preparation with the use of the Low Input Library Prep Kit (Clontech) followed by small-cell-number RNA-Seq run on the Illumina HiSeq 4000 with the use of the 1 × 50 bp platform. Reads generated were mapped to the human genome (hg19) with the use of gSNAP, gene expression (values expressed as fragments per kilobase per million [FPKM]) derived by Cufflinks, and differential expression analyzed by means of analysis of variance in R. Owing to low input RNA and inherent variability therein, a significance cutoff of $P<.05$ was used. In addition, to remove false positives at or near baseline expression levels, a strict expression cutoff of 5 FPKM was used, where one of the means (either the control mean or the treatment mean) must be ≥5 FPKM.

Biologic Processes Pathway Analysis

Pathway analysis was assessed with the use of DAVID 6.8 (Database for Annotation, Visualization, and Integrated Discovery) (35, 36) for four independent gene lists significantly altered in OAT (MF): hypermethylated, hypomethylated, decreased transcription, and increased transcription. A modified Fisher exact P value of <.05 was considered to indicate significant GO term enrichment for "biologic processes." A limitation to the study is that a correction for multiple comparisons was not performed owing to the low starting material in individual blastocysts combined with the small sample size, which resulted in a lack of statistical power and may affect the interpretation of the pathway analysis.

Targeted Bisulfite Pyrosequencing for Validation

Bisulfite conversion of individual blastocyst genomic DNA and pyrosequencing analysis was performed as previously described (37) with negative and positive control samples included. Briefly, genomic DNA (~600 pg) of individual blastocysts (n = 30) were isolated with the use of the QIAamp DNA Micro Kit (Qiagen) and modified with the use of the EZ DNA Methylation-Gold Kit (Zymo Research). Converted DNA was directly used as the template for nested PCR amplification with the use of a universal reverse biotinylated primer in the second round. Two genes, *SBF1* and *SLC6A9*, were chosen for validation by means of pyrosequencing, based on both their methylome and transcriptome results as well as their reported biologic roles. The DNA methylation assays investigated six CpG sites for *SBF1* and eight CpG sites for *SLC6A9*. Primers for methylation analysis (CpG) were designed with the use of the PyroMark Assay Design Software v.2.0.1.15 (Qiagen) and are provided with PCR parameters in Supplemental Table 1a (available online at www.fertstert.org). Pyrosequencing reactions were performed in a Pyromark Q24 Advanced system (Pyrosequencing) with the Pyromark Q24 Advanced CpG Kit (Qiagen). The DNA methylation level was calculated as a ratio of the C to T peaks at a given CpG site with the use of PyroMark Q24 Advanced Software v.3.0.0. (Qiagen). Student t test was used for targeted blastocyst methylation validation, where $P<.05$ was considered to be statistically significant.

Relative Expression Analysis with the Use of PCR for Validation

Total RNA was isolated from individual blastocysts (n = 24) for analysis of transcript abundance as previously described (38). Briefly, samples were treated with RNase-free DNase I (Qiagen), and then reverse transcribed using the High Capacity Reverse Transcription cDNA kit (Thermo Fisher Scientific). The ABI 7300 Real Time PCR System was used to perform quantitative real-time PCR with Power SYBR Green PCR Master Mix (ThermoFisher Scientific). The quantification of the two genes, *SBF1* and *SLC6A9*, were calculated relative to the housekeeping gene, *GAPDH*. The OAT (MF) group was analyzed relative to the Control (no MF) group. Expression primers and PCR parameters are outlined in Supplemental Table 1b (available online at www.fertstert.org). The Relative Expression Software Tool (REST 2009; Qiagen) was used for mRNA gene expression analysis. The determined expression ratio was tested for significance by a pairwise fixed reallocation randomization test (39) where $P<.05$ was considered to be statistically significant.

RESULTS

IVF Cycle Outcomes

A summary of patient information and IVF cycle outcomes is provided in Table 1. The two groups, OAT (MF) and control (no MF), were defined based on semen parameters at the time of oocyte retrieval. As such, statistical differences were observed based on the MF inclusion criteria as outlined in the Materials and Methods section. Conversely, number of oocytes retrieved and fertilized remained similar between groups, as did number of blastocysts biopsied, proportion of euploid blastocysts, blastocyst survival after vitrification, and the number of euploid blastocysts transferred. Likewise, there were no significant differences between the patient groups for patient ages or ovarian reserve, except for anti-müllerian hormone levels, which were statistically better for the OAT (MF) group (control [no MF]: 2.3 ng/mL; OAT [MF]: 3.2 ng/mL; $P=.014$).

As for frozen embryo transfer (FET) outcomes, there were no significant differences detected between the two infertility groups for biochemical pregnancy or clinical pregnancy rates, with a trend indicating a lower live birth rate for the OAT (MF) patients. However, a significant increase was observed for first-trimester pregnancy loss after ultrasound detection of fetal heart tone in OAT (MF) infertility patients compared with the maternal age–matched control (no MF) subjects after the transfer of a euploid blastocyst (control [no MF]: 2.2%; OAT [MF]: 14.7%; $P=.002$).

TABLE 1

Patient statistics and IVF cycle outcomes.

Variable	Control (no MF) (n = 118)	OAT (MF) (n = 128)	*P* value
Semen parametes			
Motility (%)	58.0% ± 14.1%	12.1% ± 12.8%	<.001[a]
Count (million/mL)	93.4 ± 77.3	4.8 ± 7.8	<.001[a]
Total motile count (million/mL)	166.6 ± 159.8	2.4 ± 5.0	<.001[a]
Morphology (%)	3.2% ± 1.9%	1.1% ± 1.2%	<.001[a]
Patient information			
Paternal age (y)	39.6 ± 5.3	41.0 ± 8.4	.132
Maternal age (y)	36.9 ± 3.6	36.4 ± 3.6	.282
Maternal BMI (kg/m^2)	24.0 ± 4.4	24.0 ± 4.5	.915
Antral follicle count (n#)	16.8 ± 9.1	19.1 ± 10.4	.088
AMH (ng/mL)	2.3 ± 2.0	3.2 ± 3.1	.014[a]
Day 3 FSH (mIU/mL)	7.8 ± 3.5	7.6 ± 3.8	.743
Day 3 E_2 (pg/mL)	40.9 ± 25.4	41.0 ± 29.7	.960
IVF cycle data			
Oocytes retrieved (n)	19.7 ± 8.6	19.8 ± 8.7	.984
Oocytes fertilized (n)	12.6 ± 5.8	12.0 ± 6.3	.476
Blastocysts biopsied (n)	5.8 ± 3.8	5.4 ± 4.3	.546
Proportion of euploid blastocysts (%)	57.1% ± 22.9%	59.7% ± 24.6%	.413
Blastocyst survival after vitrification (%)	98.4% ± 9.5%	99.0% ± 7.8%	.485
Euploid blastocysts transferred per FET (n)	1.6 ± 0.5	1.6 ± 0.5	.939
Cycle outcomes			
Biochemical pregnancy rate (%)	88.5% (100/113)	87.5% (112/128)	.814
Clinical pregnancy rate (%)	78.8% (89/113)	79.7% (102/128)	.860
Miscarriage rate, 1st trimester after FHT (%)	2.2% (2/89)	14.7% (15/102)	.002[a]
Live birth rate per transfer (%)	77.0% (87/113)	68.0% (87/128)	.120

Note: AMH = antimüllerian hormone; BMI = body mass index; FET = frozen embryo transfer; FHT = fetal heart tone; IVF = in vitro fertilization; MF = male factor; OAT = oligoasthenoteratozoospermia.
[a] Statistically significant *P* value.

Denomme. Epigenetic errors and miscarriage in MF. Fertil Steril 2018.

Global Methylome

After whole-genome bisulfite sequencing on trophectoderm biopsies, the bisulfite conversion rate was >97%, and averages for the samples included >747 million read pairs, 45% mapping efficiency, >10 million unique CpGs, with 48× average CpG coverage. Sequencing data displayed methylation profiles that were shifted toward hypomethylation (28.8% methylation in OAT [MF] vs. 18.7% methylation in control [no MF]; $P<.05$) with a notable methylation increase for statistically significant CpG probe sites in the OAT (MF) group (n = 1,111 CpGs; $P<.05$; Fig. 1). These results are within the expected range for blastocyst-stage embryos, which exhibit an overall hypomethylated state around ~20% (40, 41). A total of 726 CpGs (representing 287 genes) were significantly hypermethylated in the OAT (MF) group compared with control (no MF). Of these, 264 CpGs (122 genes) were characterized as "strongly hypermethylated," signifying a 33%–100% increase in methylation relative to the control (no MF) samples. Similarly, 385 CpGs (representing 156 genes) were significantly hypomethylated. Of these, 154 CpGs (66 genes) were characterized as "strongly hypomethylated," with a 33%–100% decrease in methylation. With very small starting input, the genome coverage was adversely affected, which is a limitation to the study. In relation to genomic features, gene body coverage was fairly consistent for all samples (76%–86%), whereas promoters (42%–73%), and CpG islands (29%–59%) showed more variable coverage across the samples (Supplemental Fig. 1, available online at www.fertstert.org).

The list of genes with altered CpG methylation underwent pathway analysis for "Biologic Process." Regulation of signaling (59 genes; $P<.01$), and positive regulation of cellular metabolic process (53 genes; $P<.05$), are the two processes with the greatest number of significantly hypermethylated genes, and would largely affect embryonic development with increased methylation resulting in subsequent decreased gene expression. Conversely, the greatest number of significantly hypomethylated genes revealed negative regulation of cellular metabolic process (28 genes; $P<.01$), and establishment of protein localization (23 genes, $P<.05$), two processes that would directly affect embryonic development with decreased methylation and increased gene expression (Table 2). A list of significantly altered genes involved in positive or negative regulation of cellular metabolic process is provided in Supplemental Table 2 (available online at www.fertstert.org).

Global Transcriptome

Following small-cell-number RNA-Seq on individual blastocysts, the filtered reads distribution averaged 51 million single-end reads, with an average of 2,614 megabases yield and yield quality of ≥89% Q30 bases, with a mean quality score of 37.48. The global transcriptome data resulted in 469 significantly altered transcripts ($P<.05$) in the OAT

FIGURE 1

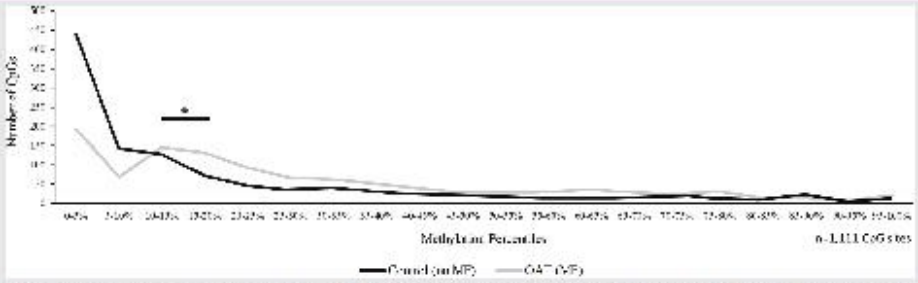

Methylation distribution for statistically significant CpGs. Methylation percentage for all significantly altered CpG sites (n = 1,111) between the control (no male factor [MF]) group (*black line*) and the OAT (MF) group (*gray line*) distributed into 5% methylation intervals. Statistics were performed for hypomethylated regions [0%–20%], [0%–10%], and [10%–20%]. *Statistical significance of $P<.05$.

Denomme. Epigenetic errors and miscarriage in MF. Fertil Steril 2018.

TABLE 2

Enriched biologic processes for statistically significant genes in OAT (MF).

GO term	Term	No. of genes	*P* value
Hypermethylated			
GO:0043087	regulation of GTPase activity	20	<.005
GO:0023051	regulation of signaling	59	<.01
GO:1904062	regulation of cation transmembrane transport	9	<.05
GO:0031325	positive regulation of cellular metabolic process	53	<.05
GO:0034220	ion transmembrane transport	22	<.05
GO:0030516	regulation of axon extension	5	<.05
GO:0060538	skeletal muscle organ development	7	<.05
Hypomethylated			
GO:0030029	actin filament-based process	16	<.0001
GO:1903827	regulation of cellular protein localization	13	<.0005
GO:0006461	protein complex assembly	21	<.005
GO:0031324	negative regulation of cellular metabolic process	28	<.005
GO:0099536	synaptic signaling	11	<.01
GO:0045184	establishment of protein localization	23	<.05
GO:0051270	regulation of cellular component movement	12	<.05
GO:0019725	cellular homeostasis	12	<.05
GO:0051960	regulation of nervous system development	11	<.05
GO:0031327	negative regulation of cellular biosynthetic process	17	<.05
GO:0060548	negative regulation of cell death	12	<.05
Decreased transcription			
GO:0009893	positive regulation of cellular metabolic process	16	<.005
GO:0008104	protein localization	14	<.01
GO:0042325	regulation of phosphorylation	10	<.01
GO:0031401	positive regulation of protein modification process	8	<.05
GO:0016055	Wnt signaling pathway	5	<.05
GO:0032880	regulation of protein localization	7	<.05
GO:0040011	locomotion	9	<.05
Increased transcription			
GO:0048857	neural nucleus development	6	<.0005
GO:0046034	ATP metabolic process	8	<.005
GO:0006090	pyruvate metabolic process	5	<.01
GO:0046907	intracellular transport	22	<.01
GO:0032787	monocarboxylic acid metabolic process	10	<.05
GO:0010565	regulation of cellular ketone metabolic process	5	<.05

Note: ATP = adenosine triphosphate; other abbreviations as in Table 1.

Denomme. Epigenetic errors and miscarriage in MF. Fertil Steril 2018.

FIGURE 2

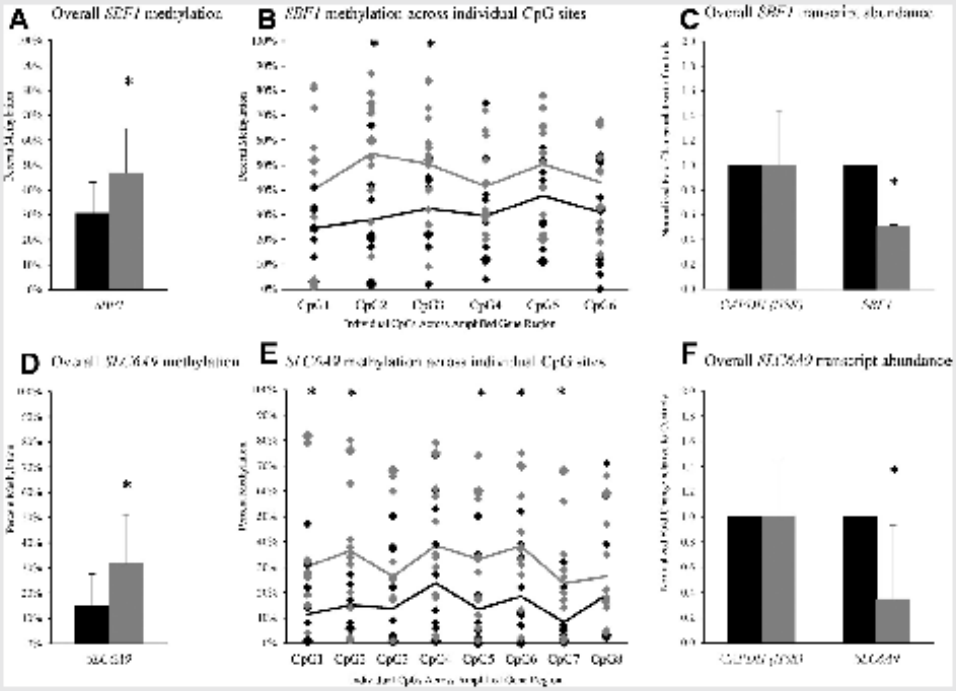

Blastocyst *SBF1* and *SLC6A9* methylation and transcription levels. (**A**) Overall methylation percentage for *SBF1* in the control (no male factor [MF]) group compared with the OAT (MF) group (31% vs. 47%; $P<.05$) in individual blastocysts. Black bars represent overall average methylation or transcript abundance for the control (no MF) group; grey bars represent the OAT (MF) group. Error bars represent SD. (**B**) Methylation percentage for the six CpG sites across the amplified *SBF1* region in individual blastocysts. Significant increases were observed for CpG positions 2 and 3 ($P<.05$). Black lines represent average methylation along the amplified regions for the control (no MF) group; gray lines represent the OAT (MF) group. (**C**) Overall transcript abundance for *SBF1*. Normalized fold change for the OAT (MF) group (0.51; $P<.05$) is relative to the control (no MF) group and to the housekeeping (HSK) gene *GAPDH*. (**D**) Overall methylation percentage for *SLC6A9* in the control (no MF) group compared with the OAT (MF) group (15% vs. 32%; $P<.05$) in individual blastocysts. (**E**) Methylation percentage for the eight CpG sites across the amplified *SLC6A9* region in individual blastocysts. Significant increases were observed for CpG positions 1, 2, 5, 6, and 7 ($P<.05$). (**F**) Overall transcript abundance for *SLC6A9*. Normalized fold change for the OAT (MF) group (0.34; $P<.05$) is relative to the control (no MF) group and to the HSK gene *GAPDH*. Black diamonds represent the methylation level for each individual blastocyst in the Control (no MF) group at each CpG position along the amplified regions; grey diamonds represent the OAT (MF) group. *Statistical significance of $P<.05$.

Denomme. Epigenetic errors and miscarriage in MF. Fertil Steril 2018.

(MF) group. Of these, 404 genes had significantly increased gene expression and 65 genes had significantly decreased gene expression (Supplemental Table 3, available online at www.fertstert.org).

Pathway analysis for biologic processes included positive regulation of metabolic process (16 genes; $P<.01$) with the greatest number of genes with significantly decreased gene expression, and intracellular transport (22 genes; $P<.01$) for those with significantly increased expression (Table 2).

Validation of genome-wide approaches. Overall, 462 CpG sites exhibited statistically significant methylation changes ($P<.05$) corresponding to 423 genes with transcription changes. From these, 118 CpGs were hypermethylated with a corresponding decrease in transcription at 105 genes, and 46 CpGs were hypomethylated with an increase in transcription at 41 genes. A subset of 21 genes was found to be statistically significant in both the methylome and the transcriptome data. Of these, two genes were chosen for validation of the genome-wide approaches that were significantly altered in both methylome and transcriptome results and identified as genes associated with spermatogenesis and embryogenesis. Pyrosequencing data confirmed hypermethylation along the amplified *SBF1* region, with an average methylation for the control (no MF) group at 31% and a statistically significant increase to 47% for the OAT (MF) group ($P<.05$; Fig. 2A). When analyzed individually by CpG site,

significant increases were observed for CpG positions 2 and 3 ($P<.05$; Fig. 2B). With increased methylation, a subsequent decreased transcription is predicted and was observed for the *SBF1* transcript to 0.51 normalized fold change in the OAT (MF) blastocysts relative to control (no MF; $P<.05$; Fig. 2C).

Significant hypermethylation was also observed along the amplified *SLC6A9* region. An average methylation of 15% was observed for the control (no MF) group, with a statistically significant increase to 32% for the OAT (MF) group ($P<.05$) (Fig. 2D). The CpG positions 1, 2, 5, 6, and 7 were identified as significantly altered when analyzed by individual CpG site ($P<.05$; Fig. 2E). A subsequent decreased transcription is predicted and was observed for the *SLC6A9* transcript to 0.34 normalized fold change in the OAT (MF) blastocysts relative to control (no MF; $P<.05$; Fig. 2F), confirming the overall genome-wide results.

DISCUSSION

The molecular basis of MF infertility is poorly understood. Semen parameter analysis, while identifying errors in count, motility, and morphology, does not account for other underlying genetic or epigenetic aspects of MF infertility. Likewise, ICSI circumvents fertilization failure for MF cases, but it also does not select against all possible deleterious effects arising from defective sperm DNA.

Risks of implantation failure and repeated miscarriage are increased in couples with MF infertility [42–44]. One study evaluating high-magnification sperm selection observed an increase in miscarriage rate from 1/12 (8.3%) in the non-MF group to 3/8 (37.5%) in the OAT (MF) group, although owing to limited sample numbers this statistic was not significant ($P=.138$) [45]. Nevertheless, the percentage of higher-quality spermatozoa was significantly lower in patients with OAT (MF; 11% vs. 17%; $P=.001$) and significantly higher in patients with ongoing pregnancy compared with those with miscarriage (23% vs. 11%; $P=.007$). PGT-A testing has revealed higher rates of aneuploidy in embryos derived from spermatozoa with increased chromosomal alterations, and this is exacerbated in OAT (MF) infertility cases [46], again highlighting that ICSI is not sufficient to exclude chromosome errors.

In this study, we strategically eliminated detectable aneuploidy in OAT (MF) blastocysts by performing PGT-A on trophectoderm biopsies and only frozen euploid embryo transfers. Results showed that clinical pregnancy rates were similar between MF patients and non-MF control subjects after euploid embryo transfer. Overall, OAT (MF) infertility patients experienced significant clinical benefit following the transfer of a frozen euploid blastocyst. Nevertheless, the miscarriage rate for maternal age–matched couples presenting with OAT (MF) infertility diagnosis was significantly higher (14.7% vs. 2.2%; $P=.002$) and may represent the disturbance of other developmental variables that are essential for ongoing healthy fetal development.

Alternate paternal factors may influence embryonic development and clinical pregnancy rates, despite euploid embryo transfer, such as sperm epigenetics. The association between aberrant sperm DNA methylation patterns and compromised semen parameters suggests that disturbances in male germline epigenetic reprogramming contribute to this problem. In particular, there have been various demonstrations that methylation errors are present at developmental genes and imprinted loci in men with oligospermia [16,19–21]. However, there is minimal information on the possible consequences that fertilization with sperm harboring methylation errors may have on embryo development, implantation, gestation, and offspring. In a study that analyzed DNA methylation at imprinted loci in ART-derived conceptuses and matched paternal sperm DNA samples, identical alterations were observed in both paired samples in 7/17 cases (41%) [22], demonstrating a direct inheritance of these alterations. Importantly, the imprinting errors were more prevalent in patients with oligospermia.

Evaluation of the methylome and subsequent transcriptome in high-grade individual blastocysts derived from OAT (MF) patients in the present study revealed significant alterations in >1,000 CpG sites and >400 transcripts. The use of only transferrable-quality blastocysts bypasses most effects on preimplantation development, so these significant methylation patterns and expression level changes may instead be responsible for the compromised IVF outcomes and increased miscarriage rate observed in this population.

Pathway analysis elucidated the functional effects of these methylation and expression changes. Interestingly, "regulation of cellular metabolic process" appeared to be universally affected in both sets of results, albeit with alterations to independent genes. Although it is a broad term, hypermethylation of genes involved in positive regulation of cellular metabolic process, as well as hypomethylation of genes involved in its negative regulation, may ultimately affect embryogenesis in a similar manner. Positive regulation of metabolic process was enriched in both the hypermethylated gene list and the corresponding decreased-transcription gene list from OAT (MF) samples. For genes with aberrant increased transcription, more specific metabolic processes were highlighted, including adenosine triphosphate, pyruvate, monocarboxylic acid, and regulation of cellular ketone metabolic process.

Although a large number of CpG sites exhibited increased DNA methylation in the OAT (MF) group, we did not observe a corresponding number of decreased transcripts overall. Rather, a greater number of genes exhibited increased gene expression in the OAT (MF) group. Ultimately, methylation and transcription do not always correlate on a genome-wide scale. One explanation is that the CpG sites assessed are not the ones solely controlling gene expression. The CpG density surrounding the significantly altered site plays a large role in gene regulation. Likewise, the sites may not overlap the positions for transcription-factor binding or enhancers. Also, there are additional epigenetic influences on gene expression, including histone modifications and noncoding RNAs, which we were not able to examine in this study. Necessarily, global DNA methylation–dependent changes in gene expression do not correlate exactly owing to all the other levels of gene regulation acting simultaneously on the genome.

Furthermore, although transcription is a snapshot of present occurrences in the blastocyst, DNA methylation can represent either a memory of a previous status or precondition for future events. Thus, alterations in methylation at the blastocyst stage may instead affect gene expression at later stages of development and in specific tissues depending on location and gene function.

Nevertheless, among the subset of genes with aberrant methylation and corresponding directional transcription changes, two relevant genes were selected for validation studies. High intersample methylation variability was observed, likely a consequence of the dynamic and active methylation reprogramming process occurring at the blastocyst stage. This heterogeneity was expected and has been previously reported (47, 48). Further evaluation of parental source revealed that this variability exists even for those blastocysts derived from the same patients. The *SBF1* protein is highly expressed in the seminiferous tubules of the testes, and mice that are *SBF1* homozygous null are characterized by azoospermia (49). The abnormal increase in *SBF1* methylation and subsequent decrease in expression in blastocysts derived from OAT (MF) sperm is most likely a remnant of compromised spermatogenesis. The *SLC6A9* gene encodes the GLYT1 protein, and has been reported to be essential for cell volume regulation in preimplantation mouse embryos (50, 51). Glycine transport via GLYT1 is also present and essential in human embryos (52). Aberrant decreased *SLC6A9* expression due to increased methylation may result in cell volume dysregulation in the blastocysts derived from OAT (MF) sperm or play a larger role in later events such as implantation.

In summary, this novel study investigated the outcomes of euploid blastocyst transfers for OAT (MF) infertility cases. The miscarriage rate for patients presenting with this infertility diagnosis was significantly higher than for non-MF control subjects, despite maternal age–matched and euploid blastocyst transfer. Furthermore, methylation and transcription aberrations in individual OAT (MF) blastocysts illustrate a consequence of severe MF infertility on epigenetic events occurring during embryogenesis, significantly altering key developmental genes. Taken together, inheritance of epigenetic dysregulation from compromised spermatogenesis in OAT (MF) patients has a direct impact on subsequent embryonic competence and provides an explanation for increased miscarriage rates and reduced reproductive potential.

Acknowledgments: The authors thank Dr. Kenneth Jones from the University of Colorado for his help in pathway analysis.

REFERENCES

1. Agarwal A, Mulgund A, Hamada A, Chyatte MR. A unique view on male infertility around the globe. Reprod Biol Endocrinol 2015;13:37.
2. Chandra A, Martinez GM, Mosher WD, Abma JC, Jones J. Fertility, family planning, and reproductive health of U.S. women: data from the 2002 National Survey of Family Growth. Vital Health Stat 2005;23:1–160.
3. Cooper TG, Noonan E, von Eckardstein S, Auger J, Baker HW, Behre HM, et al. World Health Organization reference values for human semen characteristics. Hum Reprod Update 2010;16:231–45.
4. Loutradi KE, Tarlatzis BC, Goulis DG, Zepiridis L, Pagou T, Chatzioannou E, et al. The effects of sperm quality on embryo development after intracytoplasmic sperm injection. J Assist Reprod Genet 2006;23:69–74.
5. Chapuis A, Gala A, Ferrieres-Hoa A, Mullet T, Bringer-Deutsch S, Vintejoux E, et al. Sperm quality and paternal age: effect on blastocyst formation and pregnancy rates. Basic Clin Androl 2017;27:2.
6. Ramasamy R, Scovell JM, Kovac JR, Cook PJ, Lamb DJ, Lipshultz LI. Fluorescence in situ hybridization detects increased sperm aneuploidy in men with recurrent pregnancy loss. Fertil Steril 2015;103:906–9.e1.
7. Puscheck EE, Jeyendran RS. The impact of male factor on recurrent pregnancy loss. Curr Opin Obstet Gynecol 2007;19:222–8.
8. El Hajj N, Zechner U, Schneider E, Tresch A, Gromoll J, Hahn T, et al. Methylation status of imprinted genes and repetitive elements in sperm DNA from infertile males. Sex Dev 2011;5:60–9.
9. Jenkins TG, Carrell DT. The sperm epigenome and potential implications for the developing embryo. Reproduction 2012;143:727–34.
10. Rodenhiser D, Mann M. Epigenetics and human disease: translating basic biology into clinical applications. CMAJ 2006;174:341–8.
11. Denomme MM, Mann MR. Genomic imprints as a model for the analysis of epigenetic stability during assisted reproductive technologies. Reproduction 2012;144:393–409.
12. Marchetti F, Lowe X, Bishop J, Wyrobek AJ. Absence of selection against aneuploid mouse sperm at fertilization. Biol Reprod 1999;61:948–54.
13. Carrell DT, Liu L, Peterson CM, Jones KP, Hatasaka HH, Erickson L, et al. Sperm DNA fragmentation is increased in couples with unexplained recurrent pregnancy loss. Arch Androl 2003;49:49–55.
14. Slama R, Bouyer J, Windham G, Fenster L, Werwatz A, Swan SH. Influence of paternal age on the risk of spontaneous abortion. Am J Epidemiol 2005;161:816–23.
15. Curley JP, Mashoodh R, Champagne FA. Epigenetics and the origins of paternal effects. Horm Behav 2011;59:306–14.
16. Jenkins TG, Aston KI, Hotaling JM, Shamsi MB, Simon L, Carrell DT. Teratozoospermia and asthenozoospermia are associated with specific epigenetic signatures. Andrology 2016;4:843–9.
17. Du Y, Li M, Chen J, Duan Y, Wang X, Qiu Y, et al. Promoter-targeted bisulfite sequencing reveals DNA methylation profiles associated with low sperm motility in asthenozoospermia. Hum Reprod 2016;31:24–33.
18. Montjean D, Ravel C, Benkhalifa M, Cohen-Bacrie P, Berthaut I, Bashamboo A, et al. Methylation changes in mature sperm deoxyribonucleic acid from oligozoospermic men: assessment of genetic variants and assisted reproductive technology outcome. Fertil Steril 2013;100:1241–7.
19. Hammoud SS, Purwar J, Pflueger C, Cairns BR, Carrell DT. Alterations in sperm DNA methylation patterns at imprinted loci in two classes of infertility. Fertil Steril 2010;94:1728–33.
20. Kobayashi H, Sato A, Otsu E, Hiura H, Tomatsu C, Utsunomiya T, et al. Aberrant DNA methylation of imprinted loci in sperm from oligospermic patients. Hum Mol Genet 2007;16:2542–51.
21. Marques CJ, Costa P, Vaz B, Carvalho F, Fernandes S, Barros A, et al. Abnormal methylation of imprinted genes in human sperm is associated with oligozoospermia. Mol Hum Reprod 2008;14:67–74.
22. Kobayashi H, Hiura H, John RM, Sato A, Otsu E, Kobayashi N, et al. DNA methylation errors at imprinted loci after assisted conception originate in the parental sperm. Eur J Hum Genet 2009;17:1582–91.
23. Jenkins TG, Aston KI, James ER, Carrell DT. Sperm epigenetics in the study of male fertility, offspring health, and potential clinical applications. Syst Biol Reprod Med 2017;63:69–76.
24. McCallie BR, Parks JC, Patton AL, Griffin DK, Schoolcraft WB, Katz-Jaffe MG. Hypomethylation and genetic instability in monosomy blastocysts may contribute to decreased implantation potential. PLoS One 2016;11:e0159507.
25. Dahdouh EM, Balayla J, Garcia-Velasco JA. Comprehensive chromosome screening improves embryo selection: a meta-analysis. Fertil Steril 2015;104:1503–12.

26. Yang Z, Liu J, Collins GS, Salem SA, Liu X, Lyle SS, et al. Selection of single blastocysts for fresh transfer via standard morphology assessment alone and with array CGH for good prognosis IVF patients: results from a randomized pilot study. Mol Cytogenet 2012;5:24.
27. Rubio C, Bellver J, Rodrigo L, Castillon G, Guillen A, Vidal C, et al. In vitro fertilization with preimplantation genetic diagnosis for aneuploidies in advanced maternal age: a randomized, controlled study. Fertil Steril 2017; 107:1122–9.
28. Forman EJ, Upham KM, Cheng M, Zhao T, Hong KH, Treff NR, et al. Comprehensive chromosome screening alters traditional morphology-based embryo selection: a prospective study of 100 consecutive cycles of planned fresh euploid blastocyst transfer. Fertil Steril 2013;100:718–24.
29. Scott RT Jr, Upham KM, Forman EJ, Hong KH, Scott KL, Taylor D, et al. Blastocyst biopsy with comprehensive chromosome screening and fresh embryo transfer significantly increases in vitro fertilization implantation and delivery rates: a randomized controlled trial. Fertil Steril 2013;100: 697–703.
30. Schoolcraft WB, Katz-Jaffe MG. Comprehensive chromosome screening of trophectoderm with vitrification facilitates elective single-embryo transfer for infertile women with advanced maternal age. Fertil Steril 2013;100: 615–9.
31. Treff NR, Tao X, Ferry KM, Su J, Taylor D, Scott RT Jr. Development and validation of an accurate quantitative real-time polymerase chain reaction-based assay for human blastocyst comprehensive chromosomal aneuploidy screening. Fertil Steril 2012;97:819–24.
32. Schmittgen TD, Livak KJ. Analyzing real-time PCR data by the comparative C(T) method. Nat Protoc 2008;3:1101–8.
33. Treff NR, Su J, Tao X, Levy B, Scott RT Jr. Accurate single cell 24 chromosome aneuploidy screening using whole genome amplification and single nucleotide polymorphism microarrays. Fertil Steril 2010;94:2017–21.
34. Gardner DK, Schoolcraft WB. In vitro culture of human blastocysts. In: Jansen R, Mortimer D, editors. Towards reproductive certainty: fertility and genetics beyond 1999. London: Parthenon; 1999:378–88.
35. Huang da W, Sherman BT, Lempicki RA. Systematic and integrative analysis of large gene lists using DAVID bioinformatics resources. Nat Protoc 2009;4: 44–57.
36. Huang da W, Sherman BT, Lempicki RA. Bioinformatics enrichment tools: paths toward the comprehensive functional analysis of large gene lists. Nucleic Acids Res 2009;37:1–13.
37. Huntriss J, Woodfine K, Huddleston JE, Murrell A, Picton HM. Analysis of DNA methylation patterns in single blastocysts by Pyrosequencing. Methods Mol Biol 2015;1315:259–70.
38. Denomme MM, McCallie BR, Parks JC, Schoolcraft WB, Katz-Jaffe MG. Alterations in the sperm histone-retained epigenome are associated with unexplained male factor infertility and poor blastocyst development in donor oocyte IVF cycles. Hum Reprod 2017;32:2443–55.
39. Pfaffl MW, Horgan GW, Dempfle L. Relative expression software tool (REST) for group-wise comparison and statistical analysis of relative expression results in real-time PCR. Nucleic Acids Res 2002;30:e36.
40. Smallwood SA, Tomizawa S, Krueger F, Ruf N, Carli N, Segonds-Pichon A, et al. Dynamic CpG island methylation landscape in oocytes and preimplantation embryos. Nat Genet 2011;43:811–4.
41. Smith ZD, Chan MM, Mikkelsen TS, Gu H, Gnirke A, Regev A, et al. A unique regulatory phase of DNA methylation in the early mammalian embryo. Nature 2012;484:339–44.
42. Caseiro AL, Regalo A, Pereira E, Esteves T, Fernandes F, Carvalho J. Implication of sperm chromosomal abnormalities in recurrent abortion and multiple implantation failure. Reprod Biomed Online 2015;31:481–5.
43. Burrello N, Vicari E, Shin P, Agarwal A, De Palma A, Grazioso C, et al. Lower sperm aneuploidy frequency is associated with high pregnancy rates in ICSI programmes. Hum Reprod 2003;18:1371–6.
44. Bernardini LM, Costa M, Bottazzi C, Gianaroli L, Magli MC, Venturini PL, et al. Sperm aneuploidy and recurrent pregnancy loss. Reprod Biomed Online 2004;9:312–20.
45. Vingris L, Setti AS, de Almeida Ferreira Braga DP, de Cassia Savio Figueira R, Iaconelli A, Borges E. Sperm morphological normality under high magnification predicts laboratory and clinical outcomes in couples undergoing ICSI. Hum Fertil (Camb) 2015;18:81–6.
46. Sanchez-Castro M, Jimenez-Macedo AR, Sandalinas M, Blanco J. Prognostic value of sperm fluorescence in situ hybridization analysis over PGD. Hum Reprod 2009;24:1516–21.
47. Arányi T, Paldi A. The constant variation: DNA methylation changes during preimplantation development. FEBS Lett 2006;580:6521–6.
48. Smallwood SA, Lee HJ, Angermueller C, Krueger F, Saadeh H, Peat J, et al. Single-cell genome-wide bisulfite sequencing for assessing epigenetic heterogeneity. Nat Methods 2014;11:817–20.
49. Firestein R, Nagy PL, Daly M, Huie P, Conti M, Cleary ML. Male infertility, impaired spermatogenesis, and azoospermia in mice deficient for the pseudophosphatase Sbf1. J Clin Invest 2002;109:1165–72.
50. Steeves CL, Baltz JM. Regulation of intracellular glycine as an organic osmolyte in early preimplantation mouse embryos. J Cell Physiol 2005;204: 273–9.
51. Steeves CL, Hammer MA, Walker GB, Rae D, Stewart NA, Baltz JM. The glycine neurotransmitter transporter GLYT1 is an organic osmolyte transporter regulating cell volume in cleavage-stage embryos. Proc Natl Acad Sci U S A 2003;100:13982–7.
52. Hammer MA, Kolajova M, Leveille M, Claman P, Baltz JM. Glycine transport by single human and mouse embryos. Hum Reprod 2000;15:419–26.

Fertility and Sterility®

SUPPLEMENTAL FIGURE 1

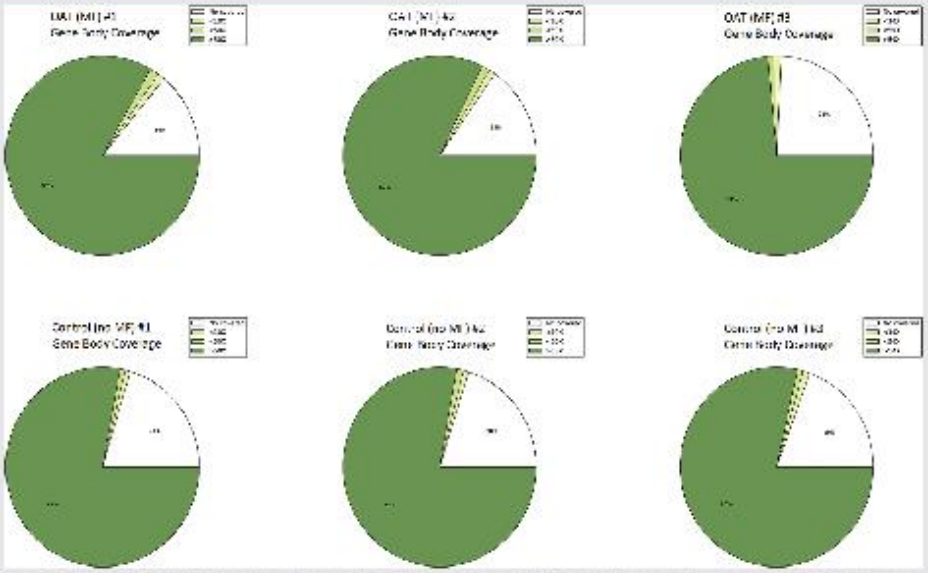

Genomic features of individual blastocyst whole genome bisulfite sequencing results. Pie charts for gene body, promoter, and pG island coverage for oligoasthenoteratozoospermia (OAT; male factor [MF]) compared with control (no MF). Coverage was divided into >50×, <50×, <10×, and no coverage.

Denomme. Epigenetic errors and miscarriage in MF. Fertil Steril 2018.

20.0 Appendix 7. Additional publication

Pini T, **Parks J,** Russ J, Dzieciatkowska M, Hansen KC, Schoolcraft WB, Katz-Jaffe M. Obesity significantly alters the human sperm proteome, with potential implications for fertility. J Assist Reprod Genet. 2020 Apr;37(4):777-787. doi: 10.1007/s10815-020-01707-8. Epub 2020 Feb 5.

My personal contribution to this manuscript

I worked closely with Dr. Katz-Jaffe and Dr. Pini to coordinate the collection of study materials between the research department and the IVF laboratory. I also performed sperm count and motility for samples donated to research, and prepared them for storage at -80°C and downstream epigenetic experiments. Finally, I co-wrote and edited sections of the materials and methods section of the manuscript for publication as a co-author.

Journal of Assisted Reproduction and Genetics (2020) 37:777–787
https://doi.org/10.1007/s10815-020-01707-8

GAMETE BIOLOGY

Obesity significantly alters the human sperm proteome, with potential implications for fertility

T. Pini[1] · J. Parks[1] · J. Russ[1] · M. Dzieciatkowska[2] · K. C. Hansen[2] · W. B. Schoolcraft[1] · M. Katz-Jaffe[1]

Received: 3 October 2019 / Accepted: 30 January 2020 / Published online: 5 February 2020

Abstract

Purpose In men, obesity may lead to poor semen parameters and reduced fertility. However, the causative links between obesity and male infertility are not totally clear, particularly on a molecular level. As such, we investigated how obesity modifies the human sperm proteome, to elucidate any important implications for fertility.

Methods Sperm protein lysates from 5 men per treatment, classified as a healthy weight (body mass index (BMI) ≤25 kg/m^2) or obese (BMI ≥30 kg/m^2), were FASP digested, submitted to liquid chromatography tandem mass spectrometry, and compared by label-free quantification. Findings were confirmed for several proteins by qualitative immunofluorescence and a quantitative protein immunoassay.

Results A total of 2034 proteins were confidently identified, with 24 proteins being significantly ($p < 0.05$) less abundant (fold change < 0.05) in the spermatozoa of obese men and 3 being more abundant (fold change > 1.5) compared with healthy weight controls. Proteins with altered abundance were involved in a variety of biological processes, including oxidative stress (GSS, NDUFS2, JAGN1, USP14, ADH5), inflammation (SUGT1, LTA4H), translation (EIF3F, EIF4A2, CSNK1G1), DNA damage repair (UBEA4), and sperm function (NAPA, RNPEP, BANF2).

Conclusion These results suggest that oxidative stress and inflammation are closely tied to reproductive dysfunction in obese men. These processes likely impact protein translation and folding during spermatogenesis, leading to poor sperm function and subfertility. The observation of these changes in obese men with no overt andrological diagnosis further suggests that traditional clinical semen assessments fail to detect important biochemical changes in spermatozoa which may compromise fertility.

Keywords Obesity · Reproduction · Spermatozoa · Fertility · Proteome · LC-MS/MS

Introduction

Excessive body weight continues to be a growing problem in the twenty-first century; estimates of overweight and obesity (i.e., a body mass index (BMI) of ≥ 25 kg/m^2) in adults remain high at 38.9% globally [1]. In the USA, 37.8% of men of reproductive age (20–59 years) are obese (BMI ≥30 kg/m^2 [2]), highlighting that this population is at risk for experiencing co-morbidities of obesity. As the sequelae of excessive body weight have been investigated, it has become clear that obesity has significant negative implications for fertility. In men, this often manifests as poor semen parameters including below average sperm motility, concentration, and normal morphology [3–5]. In addition, obese men are significantly less likely to conceive naturally within 12 months of trying [6, 7]. Paternal obesity has further been shown to impact the fertility of the subsequent generation in rodent studies, with male offspring demonstrating poor semen parameters and reduced fertilization rates [8, 9]. These data emphasize the negative effects of obesity on male fertility, and highlight the need to further understand the mechanisms underlying these effects and investigate possible solutions.

While obesity is clearly linked to poor semen parameters, diagnosis of the latter remains centered around basic semen

Electronic supplementary material The online version of this article (https://doi.org/10.1007/s10815-020-01707-8) contains supplementary material, which is available to authorized users.

✉ T. Pini
tpini@fcolo.com

[1] Colorado Center for Reproductive Medicine, Lone Tree, CO 80124, USA

[2] School of Medicine Biological Mass Spectrometry Facility, University of Colorado, Aurora, CO 80045, USA

assessment [10]. Assays evaluating basic parameters such as sperm motility, concentration, and morphology may fail to detect obesity-derived changes in spermatozoa operating at the molecular level. Previous studies support this idea, demonstrating that spermatozoa from obese men have altered abundances of a handful of proteins despite being largely normozoospermic (i.e., complying with World Health Organization standards for sperm motility, morphology, and concentration) [11, 12]. However, these studies employed two-dimensional difference gel electrophoresis (2D-DIGE), a proteomic method with good sensitivity, but limitations of low reproducibility, narrow dynamic range, and poor separation of highly hydrophobic or acidic/basic proteins [13]. In comparison, proteomic analysis of samples by liquid chromatography tandem mass spectrometry (LC-MS/MS) offers high sensitivity, with improvements in dynamic range and accurate analysis of proteins regardless of hydrophobicity or isoelectric point [14]. Combined with the use of label-free quantification, LC-MS/MS offers robust and reliable identification of proteomic differences in complex samples, including human spermatozoa [15]. While a previous study by Liu et al. [16] used LC-MS/MS to investigate the sperm proteome of obese men, this was limited to a small sample size ($n = 3$ men), incorporated the complicating factor of severe asthenozoospermia and did not appear to control for relevant factors such as diabetes or smoking. In contrast, we sought to analyze clinically normal samples from a well-controlled population of obese men. Such a deep exploration of the human sperm proteome in the context of obesity could provide insight into the mechanistic links between obesity and infertility, as well as offering more information for clinical assessment of semen parameters, and potential pathways to improve semen quality.

In this context, we performed an in depth proteomic analysis of clinically normal human spermatozoa from healthy weight and obese men using LC-MS/MS. We present a comprehensive sperm proteome investigating the impacts of obesity on a molecular level and discern potential implications for male fertility.

Materials & methods

Chemicals

All chemicals were purchased from Sigma Aldrich (St Louis, MI) unless otherwise stated and were of HPLC grade. Antibodies used for immunofluorescence were purchased from Santa Cruz Biotechnology (Dallas, TX) and Thermo Fisher Scientific (Waltham, MA). Antibodies used for the quantitative protein immunoassay were purchased from Novus Biologicals (Centennial, CO).

Ethical approval

Semen was collected with consent from patients at the Colorado Center for Reproductive Medicine (Lone Tree, CO) and approval from the Western Institutional Review Board (Puyallup, WA, protocol number 20142468).

Patient selection, semen processing, and statistical analysis

Human semen was collected on the day of oocyte retrieval. Men were selected based on age (<50) and BMI (control = BMI < 25 kg/m^2, obese = BMI > 30 kg/m^2). Patients were excluded if they smoked tobacco or had a history of diabetes, hypertension, testicular injuries, or other significant medical conditions. Only men with clinically normal semen were recruited; applied cut offs included semen concentration > 15 × 10^6 spermatozoa/mL, sperm motility > 20%, normal morphology (strict Kruger criteria [17]) ≥ 1%, and DNA fragmentation (terminal deoxynucleotidyl transferase (TdT) dUTP nick-end labeling (TUNEL) assay) < 16% (if measured). Samples with significant somatic cell contamination were excluded. Routine clinical data, including age, BMI, semen concentration, motility, morphology, and DNA fragmentation, were subjected to statistical analysis by Student's two-tailed t test employing an α of 0.05. Values for sperm concentration and motility were obtained from the ejaculate used for proteomic analysis.

Ejaculates were collected by masturbation, allowed to liquefy, and separated on a 90%/45% PureSperm gradient (Nidacon) to remove somatic cells and isolate viable spermatozoa. Sperm pellets were washed twice with G-IVF (Vitrolife) supplemented with 5 mg/mL serum protein supplement (SAGE media) in preparation for intracytoplasmic sperm injection (ICSI). Following ICSI, surplus washed semen was either cryopreserved (proteome, $n = 5$ men per treatment) or immediately underwent processing for qualitative immunofluorescence or the quantitative protein immunoassay as described below. For cryopreservation, washed ejaculates were centrifuged (300×g, 10 min) to remove G-IVF, resuspended 1:1 (v/v) in TEST-yolk buffer (12% (v/v) glycerol, 20% (v/v) egg yolk, 10 μg/mL gentamicin sulfate, Irvine Scientific), and suspended in liquid nitrogen vapor for 20 min before immersion in liquid nitrogen. Samples were stored at −80 °C and thawed by shaking in a 37 °C water bath for 2 min prior to proteomic analysis.

Preparation of sperm cell lysates

Frozen thawed samples were further washed (300×g, 10 min, 2×) with Dulbecco's phosphate buffered saline (PBS, without calcium and magnesium, Gibco) to remove TEST-yolk buffer and any remaining serum protein supplement. Sperm pellets were resuspended in an equal volume of lysis buffer (10 mM tris, 2% (w/v) sodium dodecyl sulfate (SDS), cOmplete mini

EDTA free protease inhibitor cocktail) and incubated for 1 h at room temperature with regular vortexing. Lysates were centrifuged (7500×*g*, 15 min), and both the supernatant and pellet were retained. Cell pellets were solubilized in 200 μL 8 M urea, 100 mM ammonium bicarbonate (U-ABC), vortexed for 20 min, and centrifuged (14,000×*g*, 10 min). Both supernatants were snap frozen and stored at − 80 °C until further processing.

FASP digestion

Samples were individually prepared for mass spectrometry using filter aided sample preparation (FASP). Cell lysate and solubilized pellet supernatant were combined for each sample, the mixture applied to a 30 kDa filter unit (Vivacon, Sartorius; pre-washed with U-ABC) containing 200 μL U-ABC, and centrifuged (14,000×*g*, 15 min). SDS was removed by 3 washes with 200 μL U-ABC (13,000×*g*, 15 min). Proteins were reduced (10 mM dithiothreitol, 30 min, room temperature) and alkylated (50 mM iodoacetamide, 30 min, room temperature, in the dark), washed with U-ABC and 50 mM ammonium bicarbonate and trypsin digested (sequencing grade modified trypsin, 1:50 enzyme:protein, in 0.02% (v/v) protease max/50 mM ammonium bicarbonate, 16 h at 37 °C). Peptides were washed and eluted with consecutive washes of 50 mM ammonium bicarbonate and 0.1% (v/v) formic acid (FA) (13,000×*g*, 10 min). Digested peptides were dried to minimum volume in a vacuum centrifuge, resuspended in 150 μL 0.5% (v/v) FA and applied to activated STAGE (STop and Go Extraction) tips [18] (activated with 80% (v/v) acetonitrile, 0.5% (v/v) FA, and equilibrated with 0.1% (v/v) FA) containing C18 resin (binding capacity ~ 10 μg). Samples were reapplied to tips 3 times to ensure saturation of resin (1500×*g*, 1 min) and washed (0.1% (v/v) FA, 1500×*g*, 2 min) to remove any remaining contaminants. Peptides were eluted (80% (v/v) acetonitrile, 0.5% (v/v) FA), dried to minimum volume in a vacuum centrifuge, and resuspended with 0.1% (v/v) FA prior to injection.

Liquid chromatography tandem mass spectrometry

All samples ($n = 5$ per treatment) were run in duplicate to account for any between-run variation. Samples were analyzed on a Q Exactive HF quadrupole orbitrap mass spectrometer (Thermo Fisher Scientific, Waltham, MA) coupled to an Easy nLC 1000 UHPLC (Thermo Fisher Scientific) through a nanoelectrospray ion source. Peptides were separated on a self-made C18 analytical column (100 μm internal diameter, ×20 cm length) packed with 2.7 μm Phenomenex Cortecs particles. After equilibration with 3 μL 5% (v/v) acetonitrile and 0.1% (v/v) formic acid, the peptides were separated by a 240-min linear gradient from 4% (v/v) to 30% (v/v) acetonitrile with 0.1% (v/v) formic acid at 400 nL/min. LC mobile phase solvents and sample dilutions used 0.1% (v/v) formic acid in water (buffer A) and 0.1% formic acid (v/v) in acetonitrile (buffer B) (Optima™ LC/MS, Fisher Scientific, Pittsburgh, PA). Data acquisition was performed using the instrument supplied Xcalibur™ (v 4.0) software. The mass spectrometer was operated in the positive ion mode, in the data–dependent acquisition mode. Full MS scans were obtained with a range of m/z 300–1600, a mass resolution of 120,000 at m/z 200, and a target value of 1.00E+06 with the maximum injection time of 50 ms. HCD collision was performed on the 15 most significant peaks, and tandem mass spectra were acquired at a mass resolution of 30,000 at m/z 200 and a target value of 1.00E+05, with a maximum injection time of 100 ms. Isolation of precursors was performed with a window of 1.2 Th. The dynamic exclusion time was 20 s. The normalized collision energy was 32. Precursor ions with single, unassigned, or eight and higher charge states were excluded from fragmentation selection.

Protein identification

MS/MS spectra were extracted from raw data files and converted into Mascot generic files (.mgf) using Proteome Discoverer (v 2.2, Thermo Fisher Scientific). Mascot generic files were batch searched using an in-house Mascot server (v 2.6, Matrix Science), against the SwissProt database (release date February 2018, 20,333 entries), with taxonomy set to *Homo sapiens*. Search parameters included trypsin as the protease, allowing up to 1 missed cleavage, carbamidomethyl cysteine as a fixed modification, acetylation of N-terminal proteins, oxidation of methionine and proline, and N-terminal pyroglutamate as variable modifications, MS peak tolerance of 15 ppm, MS/MS fragment ion tolerance of 25 ppm, and peptide charges of 1+, 2+, and 3+ and #C13C of 1.

Label-free quantification of protein abundance and statistical analysis

Mascot .dat files were loaded into (v 4.8.9, Proteome Software Inc.) for ID validation and quantitative analysis. Peptide and protein identifications were accepted if they were established at greater than 95% or 99% probability by the Peptide Prophet [19] and Protein Profit [20] algorithms, respectively. Positive protein identifications also required a minimum of 2 unique peptides. Proteins that contained similar peptides and could not be differentiated based on MS/MS analysis alone were grouped to satisfy the principles of parsimony. False discovery rate (FDR) was calculated within Scaffold, using peptide and protein probabilities calculated by Peptide Prophet and Protein Profit algorithms. Quantitative comparisons employed normalized weighted spectra (NWS) using experiment-wide protein grouping, and treatment groups were compared using a Student's two-tailed *t* test within Scaffold, with an α of 0.05. Data were exported to Excel and ranked by fold change; only samples with a fold change of ≥ 1.5 or ≤ 0.5 were further considered as significant. To further enhance the validity of

the quantitative comparison, a minimum NWS cutoff of 5 was applied to the patient group with the highest abundance of each protein (i.e., NWS below 5 was accepted if present in the patient group with significantly reduced protein abundance).

Gene ontology and protein network interactions

Identified proteins were further characterized using PANTHER (www.patherdb.org, v 14.0) for gene ontology and STRING (www.string-db.org, v 11.0) to identify protein network interactions. In both cases, species was specified as *Homo sapiens*.

Qualitative immunofluorescence

Qualitative immunofluorescence was performed to corroborate a representative selection of proteins which were significantly differentially abundant in the sperm proteome of obese men (GSS and NDUFS2). Samples used for immunofluorescence were obtained from new cohorts of control and obese patients ($n = 3$ per treatment, under the same inclusion/exclusion criteria as previously stated) to ensure that findings could be generalized to a different population of patients. Fresh post-ICSI samples were washed (300×*g*, 10 min) with PBS, diluted to 50×10^6 spermatozoa/mL, and gently smeared on poly-L-lysine-coated slides. Slides were air dried and stored at −20 °C until use. Slides were allowed to warm to room temperature and fixed/permeabilized in 100% ice cold methanol for 1 min. Slides were blocked with 5% (v/v) goat serum in PBS and 0.1% (v/v) Tween 20 (PBST) for 60 min, then treated with primary antibody (1:50 dilution, Supplemental Table S1) diluted in 5% (v/v) goat serum in PBST for 1.5 h. Slides were washed 4 times for 5 min each in PBST, then incubated with a FITC-conjugated goat anti-mouse secondary antibody (1:100 dilution, Supplemental Table S1) diluted in 5% (v/v) goat serum in PBST for 1.5 h. Slides were washed 4 times for 5 min each in PBST, then mounted in Fluoroshield with DAPI and immediately imaged using an Olympus BX52 fluorescent microscope and Coolsnap HQ camera, running Metamorph software (v 7.7.0.0). All images were captured under a × 60 objective, with a standardized exposure time (10 s), and a consistent display range was set for each target using ImageJ (v 1.52a). Target localization and signal strength were qualitatively assessed in all samples.

Orthogonal validation of differentially abundant proteins

A quantitative immunoassay was performed as orthogonal validation for a representative selection of proteins which were significantly differentially abundant in the sperm proteome of obese men (ADH5, GSS, LTA4H). Samples used for the immunoassay were obtained from new cohorts of control and obese patients ($n = 5$ per treatment, under the same inclusion/exclusion criteria as previously stated) to ensure that findings could be generalized to a different population of patients. Fresh post-ICSI samples were washed (300×*g*, 10 min) with PBS, the supernatant discarded, and the pellet snap frozen and stored at −80 °C. Pellets were lysed as above, protein concentration assessed by Qubit assay (Thermofisher), and lysates diluted to a standardized concentration (200 μg/mL for LTA4H or 800 μg/mL for ADH5, GSS) in 0.1× sample buffer (Protein Simple). Relative protein amounts were quantified using the automated Jess Simple Western protein immunoassay (Protein Simple), employing capillary based separation and chemiluminescent detection according to manufacturer's directions. Briefly, samples were diluted with a fluorescent master mix containing DTT (final concentration 40 mM) and reduced (100 °C, 10 min). Proteins were electrophoretically separated by size, labeled with primary and secondary antibodies (Supplemental Table S1), and imaged using chemiluminescence. Fluorescent internal standards were used for quality control, and within-capillary total protein normalization was performed to account for any differences in protein loading. In addition, both positive (HeLa or Jurkat cell lysates) and negative (HeLa or Jurkat cell lysates with no primary antibody) controls were included to confirm appropriate performance of each antibody. All samples were run in duplicate for each protein target ($n = 10$ replicates per treatment). Relative protein amounts were assessed using the corrected area of chemiluminescent peaks and analyzed by Student's two-tailed *t* test, with an α of 0.05.

Results

Clinical data

There were no significant differences between control and obese patients in terms of age, semen concentration, motility, normal morphology, or DNA fragmentation (Table 1). In all cases, patients were considered to have clinically normal semen according to cut offs described (Supplemental Table S2). Average BMI was significantly higher in the obese compared with the control group (33.0 ± 0.6 vs 23.9 ± 0.4 kg/m^2, $p < 0.001$).

Identification of proteins by LC-MS/MS and general characterization

A total of 606, 078 peptides (FDR 0.52%) corresponding to 2034 proteins (FDR 0.00%) were identified in the combined control and obese datasets after applying confidence cut offs (peptide (95%) and protein confidence (99%), minimum 2 unique peptides per protein, Supplemental Table S3). By

Table 1 Clinical data of patients providing ejaculated semen for LC-MS/MS analysis

Parameter	Control (BMI < 25)		Obese (BMI > 30)		*P* value
	Mean ± SEM	Range	Mean ± SEM	Range	
Age	38.2 ± 2.2	33–46	41.0 ± 2.1	35–46	0.379
Body mass index (kg/m^2)	23.9 ± 0.4	22.4–24.9	33.0 ± 0.6	31.2–34.7	*0.000002*
Semen concentration (spermatozoa/mL)	$93.2 \times 10^6 \pm 13.3 \times 10^6$	$69–137 \times 10^6$	$83.5 \times 10^6 \pm 28.3 \times 10^6$	$18–189 \times 10^6$	0.764
Total motility (%)	64.6 ± 0.1	42–77	59.8 ± 0.1	26–78	0.675
Normal morphology (%)[a]	3.0 ± 0.9	1–5	2.8 ± 0.6	1–4	0.856
DNA fragmentation (%)[b]	3.4 ± 2.5	0–13	3.3 ± 0.2	3–4	0.959

[a] Based on Kruger classification [1], assessed on Diff Quik stained slides

[b] Based on TUNEL assay using In Situ Cell Death Detection Kit (Roche Diagnostics), percentage of spermatozoa with DNA strand breaks (i.e., positive staining)

Highlighted to show a significant *p* value (i.e. less than 0.05)

manual comparison with published human proteomes [16, 21–24], the vast majority of these proteins have previously been identified in human spermatozoa (2019/2034, 99.3%). All proteomic data has been made publically available via PRIDE (project accession number PXD014849).

GO analysis of all identified proteins (Supplemental Table S4) showed that the molecular functions of most identified proteins fall under either catalytic activity (GO:0003824, 633 proteins, 30.5% of total) or binding (GO:0005488, 490 proteins, 23.6% of total). Over 80% of proteins were involved in the following biological processes: metabolic process (GO:0008152, 575 proteins, 27.7% of total), cellular component organization or biogenesis (GO:0071840, 333 proteins, 16.1% of total), localization (GO:0051179, 302 proteins, 14.6% of total), biological regulation (GO:0065007, 270 proteins, 13.0% of total), or cellular process (GO:0009987, 222 proteins, 10.7% of total). A wide range of protein classes were identified, with hydrolase (PC00121, 223 proteins, 10.8% of total), oxidoreductase (PC00176, 141 proteins, 6.8% of total), nucleic acid binding (PC00171, 134 proteins, 6.5% of total), transferase (PC00220, 130 proteins, 6.3% of total), cytoskeletal protein (PC00085, 108 proteins, 5.2% of total), and enzyme modulator (PC00095, 105 proteins, 5.1% of total) being the most common.

The 50 most abundant proteins included protein families such as tubulins, dyneins, and heat shock proteins. The major interaction categories of these highly abundant proteins revealed by STRING analysis included metabolic processes (glycolysis, oxidative phosphorylation, beta oxidation of fatty acids), histones, structural proteins, sperm motility, sperm capacitation, and fertilization.

Quantitative differences in the global sperm proteome of obese men

From a total of 2034 proteins, 27 had significantly different abundance in obese compared with control samples (Supplemental Table S5). Of these 27 proteins, 3 were significantly more abundant in spermatozoa of obese men (fold change $\geq 1.5, p < 0.05$), while 24 were significantly less abundant (fold change $\leq 0.5, p < 0.05$) compared with control spermatozoa (Table 2). Proteins with the most significant fold changes included protein jagunal homolog 1 (JAGN1), NADH dehydrogenase [ubiquinone] iron-sulfur protein 2 (NDUFS2), leukotriene A-4 hydrolase (LTA4H), eukaryotic initiation factor 4A-II (EIF4A2), and glutathione synthetase (GSS).

Qualitative immunofluorescence

Qualitative immunofluorescence of representative proteins confirmed abundance changes observed by LC-MS/MS (Fig. 1). GSS showed very strong signal in control spermatozoa, mostly restricted to the equatorial and post acrosomal region, while spermatozoa from obese men displayed only weak signal. NDUFS2 showed moderate signal in spermatozoa from obese men, as both an equatorial band, post acrosomal and midpiece staining, and control spermatozoa showed only dim signal with similar localization.

Orthogonal validation by quantitative protein immunoassay

Changes in protein abundance of ADH5, GSS, and LTA4H were confirmed by orthogonal validation using a Jess Simple Western protein immunoassay (Supplemental figure 1). Both ADH5 and GSS were confirmed to be significantly less abundant in spermatozoa of obese patients compared with controls (ADH5 control 66,160 ± 7641 vs obese 31,855 ± 4666 arbitrary units, $p = 0.001$; GSS control 175,907 ± 13,420 vs obese 107,161 ± 14,068 arbitrary units, $p = 0.002$). While the 63 kDa isoform of LTA4H was similar between control and obese patients, the 73 kDa isoform was significantly less

Table 2 Proteins identified by LC-MS/MS with significantly different abundance (by normalized weighted spectra) in spermatozoa from control (BMI < 25) vs obese (BMI > 30) men

Gene symbol	Protein name	Mean control	Mean obese	*p* value	Fold change (obese/control)
JAGN1	Protein jagunal homolog 1	4.87	8.46	0.04	1.7
NDUFS2	NADH dehydrogenase [ubiquinone] iron-sulfur protein 2, mitochondrial	13.85	21.53	0.00052	1.6
NUP35	Nucleoporin NUP53	20.39	31.10	0.041	1.5
BANF2	Barrier-to-autointegration factor-like protein	16.36	8.88	0.031	0.5
MPC1	Mitochondrial pyruvate carrier 1	11.76	5.34	0.027	0.5
USP14	Ubiquitin carboxyl-terminal hydrolase 14	10.65	4.98	0.016	0.5
RAB18	Ras-related protein Rab-18	8.09	3.77	0.042	0.5
EIF3F	Eukaryotic translation initiation factor 3 subunit F	7.49	3.58	0.039	0.5
SUGT1	Protein SGT1 homolog	16.20	6.87	0.017	0.4
FAHD2A	Fumarylacetoacetate hydrolase domain-containing protein	8.50	3.45	0.026	0.4
CCDC189	Coiled-coil domain-containing protein 189	8.06	3.43	0.0031	0.4
ADH5	Alcohol dehydrogenase class-3	13.62	6.09	<0.0001	0.4
CSNK1G1	Casein kinase I isoform gamma-1	13.41	4.48	0.012	0.3
NAPA	Alpha-soluble NSF attachment protein	8.50	2.45	0.0017	0.3
KIAA1324	UPF0577 protein KIAA1324	7.20	2.10	0.005	0.3
UBE4A	Ubiquitin conjugation factor E4 A	6.19	2.08	0.011	0.3
NT5C	5′(3′)-deoxyribonucleotidase, cytosolic type	6.33	1.98	0.028	0.3
SKP1	S-phase kinase-associated protein 1	6.22	1.79	0.026	0.3
LRRC74A	Leucine-rich repeat-containing protein 74A	10.37	2.01	0.0013	0.2
TTC12	Tetratricopeptide repeat protein 12	8.87	1.86	0.012	0.2
ATIC	Bifunctional purine biosynthesis protein PURH	6.73	1.55	0.0021	0.2
C1orf100	Uncharacterized protein C1orf100	6.35	1.06	0.0022	0.2
GLOD4	Glyoxalase domain-containing protein 4	6.76	1.08	<0.0001	0.2
RNPEP	Aminopeptidase B	7.52	0.68	0.0053	0.09
GSS	Glutathione synthetase	5.81	0.53	0.00019	0.09
EIF4A2	Eukaryotic initiation factor 4A-II	5.11	0.43	0.0048	0.08
LTA4H	Leukotriene A-4 hydrolase	5.09	0.37	0.00079	0.07

abundant in spermatozoa of obese men (control 126,432 ± 4737 vs obese 93, 436 ± 8151 arbitrary units, $p = 0.003$).

Discussion

Using LC-MS/MS, we identified 27 proteins which are significantly different in abundance in the spermatozoa of obese men compared with men of a healthy weight. These results demonstrate that excessive body weight has implications in the male reproductive tract, leading to significant alterations in the sperm proteome. We believe that these alterations are truly a reflection of obesity, as patient cohorts did not differ in any other relevant factors (e.g., age, semen parameters, tobacco use), and patients with complicating factors (e.g., diabetes, oligozoospermia) were excluded. Interestingly, while clinical semen analysis showed no significant differences in semen parameters, mass spectrometric analysis demonstrated significant changes to the sperm proteome, suggesting that even obese men with no severe andrological pathologies may have important molecular alterations to their spermatozoa. The proteomic data gathered in this study suggest possible mechanisms by which the spermatozoa of obese men may be negatively impacted (Fig. 2).

Proteins with altered abundance in the spermatozoa of obese men are involved in a diverse range of processes, yet their common roles serve to highlight how obesity may impact both spermatogenesis and mature sperm function. While mature spermatozoa are thought to be largely transcriptionally silent, changes in protein abundance while spermatozoa are fully transcriptionally active (i.e., during spermatogenesis) are likely to have wide ranging and significant impacts. Several proteins with decreased abundance in spermatozoa from obese men had important roles in transcription and translation, including the eukaryotic translation initiation factors EIF3F and EIF4A2. EIF3F is a subunit of the eIF3 complex, which is involved in mRNA recruitment to initiate protein synthesis.

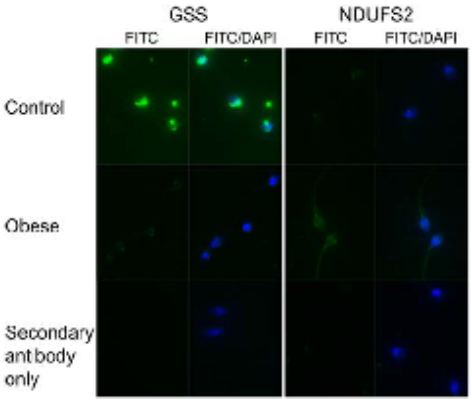

Fig. 1 Representative images of qualitative immunofluorescence. Spermatozoa from control (BMI < 25 kg/m^2) or obese (BMI > 30 kg/m^2) men were incubated with antibodies against GSS or NDUFS2 and a FITC-conjugated secondary antibody. DAPI staining was included to identify all spermatozoa. A secondary antibody only control was included to assess non-specific binding

EIF3F specifically inhibits protein synthesis at the translational level [25], and the decreased expression of this protein in cancer cells protects them from apoptosis [26]. In comparison, EIF4A2 is involved in mRNA silencing via micro RNAs [27]. Expression of casein kinase 1 gamma 1 (CSNK1G1) was also decreased; it is a prolific signaling molecule, involved in hedgehog, NFκB, p53, PI3K/AKT, and Wnt signaling cascades [28], all of which impact transcription and translation of their various downstream targets. The observed reduced abundance of these regulators of transcription and translation demonstrates that obesity may have significant implications for gene expression during spermatogenesis.

Obesity creates a chronic inflammatory state in the body, driven by interactions between adipose tissue and the immune system [29]. This inflammatory state undoubtedly impacts the testes, where increased levels of pro-inflammatory cytokines, inflammation markers, and macrophage infiltration are observed as a result of chronic obesity [30–33]. Inflammation occurring in the testes of obese men may be reflected in, and to some extent explained by, the proteomic alterations we observed. We found reduced levels of SUGT1 (alias SGT1), a co-chaperone of HSP90 with roles in Akt signaling [34], centromere function [35], and regulation of NLRP3 inflammasomes [36]. Obesity is associated with increased expression of NLRP3 [37], and as the SUGT1-HSP90 complex is responsible for maintaining these inflammasomes in a repressed state, limited levels of SUGT1 could potentially lead to an aberrant immune response and auto-activation of inflammatory pathways [36]. Interestingly, leukotriene A4 hydrolase (LTA4H) was also reduced in abundance in the spermatozoa of obese men. LTA4H has both pro- and anti-inflammatory roles, catalyzing the production of the pro-inflammatory mediator leukotriene B4 and degrading the chemoattractant peptide PGP [38]. Due to its potent capacity for degrading PGP, reduced abundance of this protein could help to sustain local inflammation in the testes. Interestingly, both the production and activity of LTA4H is reduced by acrolein [39], a byproduct of lipid peroxidation, which could be produced by developing spermatozoa undergoing oxidative stress [40]. While inflammation associated with obesity is primarily propelled by adipose tissue, reduced levels of SUGT1 and LTA4H could help to maintain inflammation in the testes of obese men.

Chronic low level inflammation contributes to oxidative stress, another significant side effect of obesity [41]. This state of oxidative stress is again locally observed in the testes of obese males, reflected by higher concentrations of both reactive

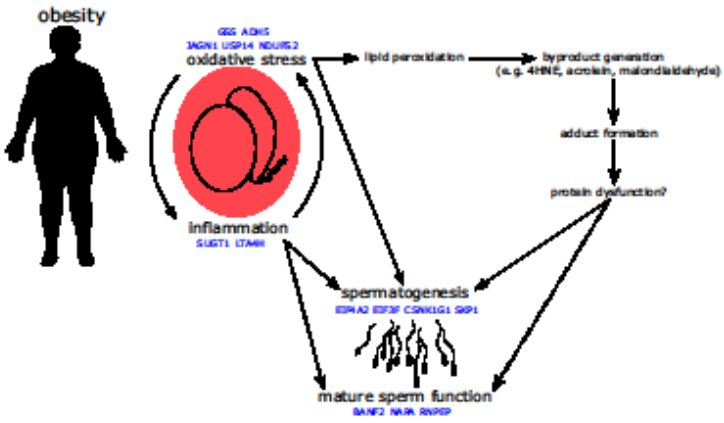

Fig. 2 Obesity creates systemic inflammation and oxidative stress, two closely inter-related processes. When occurring locally in the testes, these processes may impact spermatogenesis and mature sperm function either directly, or indirectly, via the formation of protein/reactive byproduct adducts and subsequent protein dysfunction

oxygen species (ROS) in spermatozoa [5, 42, 43] and products of lipid peroxidation in testicular tissues [44–46]. These products of lipid peroxidation (e.g., 4HNE, acrolein, malondialdehyde) cause further problems by forming protein adducts which may alter protein structure and function, potentially in a deleterious manner [47]. Only 3 proteins were observed at a higher abundance in the spermatozoa of obese men, and 2 of these, NDUFS2 and JAGN1, may have important interactions with oxidative stress and its corollaries. NDUFS2, a component of mitochondrial complex I, forms adducts with lipid peroxidation products under conditions of oxidative stress [48, 49], potentially modifying its structure and/or function and causing mitochondrial dysfunction. Such an alteration could help to explain increases in mitochondrial ROS production [50] and the aberrant mitochondrial function observed in the spermatozoa of obese men [51, 52]. The heightened expression of JAGN1 observed in spermatozoa is likely due to induction of the unfolded protein response during spermatogenesis as a result of endoplasmic reticulum (ER) stress [53], a commonly observed side effect of obesity, driven in part by oxidative stress [54]. We also observed a reduction in USP14, a proteasome-associated deubiquitinating enzyme, which ties together both oxidative and ER stress. Inhibition of USP14 increases degradation of proteins adducted by lipid peroxidation byproducts, enhancing cellular resistance to oxidative stress [55]. In addition, silencing of USP14 activates the ER-associated degradation pathway, increasing breakdown of unfolded proteins in the ER [56]. USP14 was similarly found to be decreased in spermatozoa of obese, asthenozoospermic men [16]. Thus, while increased levels of NDUFS2 and JAGN1 may be causes and symptoms of oxidative stress, reduced levels of USP14 may be a mechanism for coping with oxidative stress, by allowing for increased breakdown of protein adducts and clearance of unfolded proteins.

The loss of antioxidant capacity is another hallmark of obesity [57]. The tripeptide thiol antioxidant glutathione has been found at reduced levels in serum and various body tissues of obese individuals [58–60]. Of note, low glutathione levels have also been observed in the semen of men with various infertility diagnoses [61, 62]. Intriguingly, we saw reduced levels of glutathione synthetase (GSS), which catalyzes the final step of glutathione synthesis. Reduced availability of GSS may directly limit glutathione synthesis, leaving spermatozoa from obese men vulnerable to oxidative damage. We also observed significantly decreased levels of ADH5 (alias GSNOR) in spermatozoa from obese men. ADH5 maintains the balance of GNSO formation and protein nitrosylation, without producing reactive intermediates or end products, thus representing a significant element of cellular antioxidant defense [63]. This activity of ADH5 also contributes to the maintenance of an intracellular glutathione pool; thus, the combined effect of reduced abundance of both GSS and ADH5 may significantly weaken glutathione-based antioxidant defenses in spermatozoa from obese men.

Several proteins which were less abundant in the spermatozoa of obese men compared with men of a healthy weight have important roles in a mature sperm function. NSF attachment protein alpha (NAPA, alias alpha-SNAP) plays a direct and indispensable role in the acrosome reaction [64, 65]. While NAPA is shed from the acrosome during exocytosis, anti-NAPA antibodies limit sperm-zona pellucida binding, suggesting that NAPA may also play a role in zona recognition and binding [66]. Aminopeptidase B (RNPEP, alias APB) is an exopeptidase which cleaves pro-neuropeptides into their active forms [67], and has previously been identified in the sperm acrosome [68]. Interestingly, both the pro-neuropeptide pro-enkephalin and its cleavage product met-enkephalin have also been detected in the human sperm head, and met-enkephalin has been shown to have significant positive effects on sperm motility [69]. While no direct links between RNPEP and the processing of pro-enkephalin in spermatozoa have been described, there is a strong possibility that this may be the exopeptidase responsible. In addition to sperm motility, RNPEP may also impact zona recognition; its inhibition in *Xenopus laevis* spermatozoa reduced vitelline membrane binding by 50% [70]. Barrier to autointegration factor 2 (BANF2, alias BAF-L) is a nuclear protein which, along with BANF1, is expressed in spermatids and retained in mature ejaculated spermatozoa, unlike many other nuclear proteins [71, 72]. BANF2 is highly expressed in the testes and is proposed to regulate the function of BANF1, which has roles in chromatin structure, segregation, and post-mitotic nuclear assembly [73]. These characteristics suggest that BANF2 may be important for maintaining nuclear shape in mature spermatozoa and formation of the male pro-nucleus following fertilization [72]. The reduced levels of NAPA, RNPEP, and BANF2 we observed could help to explain why obese males exhibit poor sperm motility, a deficient response to acrosome challenge [74, 75], reduced zona pellucida binding [76], and slower pronuclear fusion to achieve syngamy following fertilization [77].

Conclusion

We have shown that obesity significantly impacts the human sperm proteome, potentially to the detriment of important spermatogenic processes and the function of mature spermatozoa. These changes may be both symptoms of and contributors to the inflammation and oxidative stress associated with obesity, and may help to explain why obese men may have altered semen parameters, potentially leading to altered fertility. It is noteworthy that these changes were detected in obese men with no significant andrological diagnoses, indicating the failure of traditional clinical semen assessment to recognize molecular changes which could potentially compromise fertility. While some of the problems created by paternal obesity

may be overcome by ART, the swathe of implications following fertilization remains to be rigorously investigated. In addition, efforts should be directed toward the implementation of treatments to correct or limit the observed changes when weight loss prior to conception is neither practical nor realistic.

Acknowledgments The authors thank patients for their generous donation of samples.

Authors' roles T. Pini contributed to the experimental design, sample preparation, data acquisition, data analysis, drafting, and revision of the manuscript. J. Parks and J. Russ contributed to sample preparation. M. Dzieciatkowska and K.C. Hansen contributed to data acquisition and data analysis. W.B. Schoolcraft and M. Katz-Jaffe contributed to the experimental design. All authors critically revised the manuscript and gave final approval for publication.

Funding information This project was fully funded by the Colorado Center for Reproductive Medicine.

Compliance with ethical standards

Conflict of interest The authors declare that they have no conflicts of interest.

Ethical approval All procedures performed in studies involving human participants were in accordance with the ethical standards of the research committee (Western Institutional Review Board, protocol number 20142468) and with the 1964 Helsinki declaration and its later amendments or comparable ethical standards. Informed consent was obtained from all individual participants included in the study.

References

1. Organization WH. Prevalence of overweight among adults, BMI ≥ 25, age-standardized, estimates by WHO region. Global Health Observatory data repository. 2017.
2. Hales C, Carroll M, Fryar C, Ogden C. Prevalence of obesity among adults and youth: United States, 2015–2016: National Center for Health Statistics2017 Contract No.: 288.
3. Oliveira JBA, Petersen CG, Mauri AL, Vagnini LD, Renzi A, Petersen B, et al. Association between body mass index and sperm quality and sperm DNA integrity. A large population study. Andrologia. 2018;50(3):e12889.
4. Ramaraju GA, Teppala S, Prathigudupu K, Kalagara M, Thota S, Kota M, et al. Association between obesity and sperm quality. Andrologia. 2018;50(3):e12888.
5. Taha EA, Sayed SK, Gaber HD, Abdel Hafez HK, Ghandour N, Zahran A, et al. Does being overweight affect seminal variables in fertile men? Reprod BioMed Online. 2016;33(6):703–8.
6. Ramlau-Hansen CH, Thulstrup AM, Nohr EA, Bonde JP, Sørensen TIA, Olsen J. Subfecundity in overweight and obese couples. Hum Reprod. 2007;22(6):1634–7.
7. Sallmén M, Sandler DP, Hoppin JA, Blair A, Baird DD. Reduced fertility among overweight and obese men. Epidemiology. 2006;17(5):520–3.
8. McPherson NO, Fullston T, Bakos HW, Setchell BP, Lane M. Obese father's metabolic state, adiposity, and reproductive capacity indicate son's reproductive health. Fertil Steril. 2014;101(3):865–73.e1.
9. Fullston T, Palmer NO, Owens JA, Mitchell M, Bakos HW, Lane M. Diet-induced paternal obesity in the absence of diabetes diminishes the reproductive health of two subsequent generations of mice. Hum Reprod. 2012;27(5):1391–400.
10. Kliesch S. Diagnosis of male infertility: diagnostic work-up of the infertile man. Eur Urol Suppl. 2014;13(4):73–82.
11. Kriegel TM, Heidenreich F, Kettner K, Pursche T, Hoflack B, Grunewald S, et al. Identification of diabetes- and obesity-associated proteomic changes in human spermatozoa by difference gel electrophoresis. Reprod BioMed Online. 2009;19(5):660–70.
12. Paasch U, Heidenreich F, Pursche T, Kuhlisch E, Kettner K, Grunewald S, et al. Identification of increased amounts of eppin protein complex components in sperm cells of diabetic and obese individuals by difference gel electrophoresis. Mol Cell Proteomics. 2011;10(8):M110.
13. Magdeldin S, Enany S, Yoshida Y, Xu B, Zhang Y, Zureena Z, et al. Basics and recent advances of two dimensional- polyacrylamide gel electrophoresis. Clin Proteomics. 2014;11(1):16.
14. Feugang JM, Liao SF, Willard ST, Ryan PL. In-depth proteomic analysis of boar spermatozoa through shotgun and gel-based methods. BMC Genomics. 2018;19(1):62.
15. Codina M, Estanyol JM, Fidalgo MJ, Ballescà JL, Oliva R. Advances in sperm proteomics: best-practise methodology and clinical potential. Expert Rev Proteomics. 2015;12(3):255–77.
16. Liu Y, Guo Y, Song N, Fan Y, Li K, Teng X, et al. Proteomic pattern changes associated with obesity-induced asthenozoospermia. Andrology. 2015;3(2):247–59.
17. Kruger TF, Menkveld R, Stander FSH, Lombard CJ, Van Der Merwe JP, van Zyl JA, et al. Sperm morphologic features as a prognostic factor in in vitro fertilization. Fertil Steril. 1986;46(6):1118–23.
18. Rappsilber J, Ishihama Y, Mann M. Stop and go extraction tips for matrix-assisted laser desorption/ionization, nanoelectrospray, and LC/MS sample pretreatment in proteomics. Anal Chem. 2003;75(3):663–70.
19. Keller A, Nesvizhskii AI, Kolker E, Aebersold R. Empirical statistical model to estimate the accuracy of peptide identifications made by MS/MS and database search. Anal Chem. 2002;74(20):5383–92.
20. Nesvizhskii AI, Keller A, Kolker E, Aebersold R. A statistical model for identifying proteins by tandem mass spectrometry. Anal Chem. 2003;75(17):4646–58.
21. Amaral A, Castillo J, Ramalho-Santos J, Oliva R. The combined human sperm proteome: cellular pathways and implications for basic and clinical science. Hum Reprod Update. 2014;20(1):40–62.
22. Zhou T, Wang G, Chen M, Zhang M, Guo Y, Yu C, et al. Comparative analysis of macaque and human sperm proteomes: insights into sperm competition. Proteomics. 2015;15(9):1564–73.
23. Bogle OA, Kumar K, Attardo-Parrinello C, Lewis SEM, Estanyol JM, Ballescà JL, et al. Identification of protein changes in human spermatozoa throughout the cryopreservation process. Andrology. 2017;5(1):10–22.
24. Schiza C, Korbakis D, Jarvi K, Diamandis EP, Drabovich AP. Identification of TEX101-associated proteins through proteomic measurement of human spermatozoa homozygous for the missense variant rs35033974. Mol Cell Proteomics. 2019;18(2):338–51.
25. Marchione R, Leibovitch S, Lenormand J-L. The translational factor eIF3f: the ambivalent eIF3 subunit. Cell Mol Life Sci. 2013;70(19):3603–16.
26. Shi J, Kahle A, Hershey JWB, Honchak BM, Warneke JA, Leong SPL, et al. Decreased expression of eukaryotic initiation factor 3f deregulates translation and apoptosis in tumor cells. Oncogene. 2006;25:4923.
27. Meijer HA, Kong YW, Lu WT, Wilczynska A, Spriggs RV, Robinson SW, et al. Translational repression and eIF4A2 activity

are critical for microrna-mediated gene regulation. Science. 2013;340(6128):82–5.
28. Schittek B, Sinnberg T. Biological functions of casein kinase 1 isoforms and putative roles in tumorigenesis. Mol Cancer. 2014;13(1):231.
29. de Heredia FP, Gómez-Martínez S, Marcos A. Obesity, inflammation and the immune system. Proc Nutr Soc. 2012;71(2):332–8.
30. Xiang J, Bian C, Wan X, Zhang Q, Huang S, Wu D. Sleeve gastrectomy reversed obesity-induced hypogonadism in a rat model by regulating inflammatory responses in the hypothalamus and testis. Obes Surg. 2018;28(8):2272–80.
31. Huang G, Yuan M, Zhang J, Li J, Gong D, Li Y, et al. IL-6 mediates differentiation disorder during spermatogenesis in obesity-associated inflammation by affecting the expression of Zfp637 through the SOCS3/STAT3 pathway. Sci Rep. 2016;6:28012.
32. Fan W, Xu Y, Liu Y, Zhang Z, Lu L, Ding Z. Obesity or overweight, a chronic inflammatory status in male reproductive system, leads to mice and human subfertility. Front Physiol. 2018;8:1117.
33. Wagner IV, Klöting N, Atanassova N, Savchuk I, Spröte C, Kiess W, et al. Prepubertal onset of obesity negatively impacts on testicular steroidogenesis in rats. Mol Cell Endocrinol. 2016;437:154–62.
34. Gao G, Kun T, Sheng Y, Qian M, Kong F, Liu X, et al. SGT1 regulates Akt signaling by promoting beta-TrCP-dependent PHLPP1 degradation in gastric cancer cells. Mol Bio Rep. 2013;40(4):2947–53.
35. Niikura Y, Kitagawa R, Ogi H, Kitagawa K. SGT1-HSP90 complex is required for CENP-A deposition at centromeres. Cell Cycle. 2017;16(18):1683–94.
36. Mayor A, Martinon F, De Smedt T, Pétrilli V, Tschopp J. A crucial function of SGT1 and HSP90 in inflammasome activity links mammalian and plant innate immune responses. Nat Immunol. 2007;8(5):497–503.
37. Rheinheimer J, de Souza BM, Cardoso NS, Bauer AC, Crispim D. Current role of the NLRP3 inflammasome on obesity and insulin resistance: a systematic review. Metab - Clin Exp. 2017;74:1–9.
38. Snelgrove RJ, Jackson PL, Hardison MT, Noerager BD, Kinloch A, Gaggar A, et al. A critical role for LTA4H in limiting chronic pulmonary neutrophilic inflammation. Science. 2010;330(6000):90–4.
39. Noerager BD, Xu X, Davis VA, Jones CW, Okafor S, Whitehead A, et al. A potential role for acrolein in neutrophil-mediated chronic inflammation. Inflammation. 2015;38(6):2279–87.
40. Bromfield EG, Aitken RJ, McLaughlin EA, Nixon B. Proteolytic degradation of heat shock protein A2 occurs in response to oxidative stress in male germ cells of the mouse. Mol Hum Reprod. 2017;23(2):91–105.
41. Vincent HK, Taylor AG. Biomarkers and potential mechanisms of obesity-induced oxidant stress in humans. Int J Obes. 2005;30:400.
42. Tunc O, Tremellen K. Oxidative DNA damage impairs global sperm DNA methylation in infertile men. J Assisted Reprod Genet. 2009;26(9):537–44.
43. Pullston T, Shehadeh H, Sanderman LY, Kang WX, Wu LL, Robker RL, et al. Female offspring sired by diet induced obese male mice display impaired blastocyst development with molecular alterations to their ovaries, oocytes and cumulus cells. J Assisted Reprod Genet. 2015;32(5):725–35.
44. Alhashem F, Alkhateeb M, Sakr H, Alshahrani M, Alsunaidi M, Elrefaey H, et al. Exercise protects against obesity induced semen abnormalities via downregulating stem cell factor, upregulating Ghrelin and normalizing oxidative stress. EXCLI J. 2014;13:551–72.
45. Gujjala S, Putakala M, Gangarapu V, Nukala S, Bellamkonda R, Ramaswamy R, et al. Protective effect of *Caralluma fimbriata* against high-fat diet induced testicular oxidative stress in rats. Biomed Pharmacother. 2016;83:167–76.
46. Atilgan D, Parlaktas BS, Uluocak N, Erdemir F, Kilic S, Erkorkmaz U, et al. Weight loss and melatonin reduce obesity-induced oxidative damage in rat testis. Adv Urol. 2013;2013:6.
47. Barnes S, Shonsey Erin M, Eliuk Shannon M, Stella D, Barrett K, Srivastava Om P, et al. High-resolution mass spectrometry analysis of protein oxidations and resultant loss of function. Biochem Soc Trans. 2008;36(5):1037–44.
48. Zhao Y, Miriyala S, Miao L, Mitov M, Schnell D, Dhar SK, et al. Redox proteomic identification of HNE-bound mitochondrial proteins in cardiac tissues reveals a systemic effect on energy metabolism after doxorubicin treatment. Free Radic Biol Med. 2014;72:55–65.
49. Wen J-J, Garg N. Oxidative modification of mitochondrial respiratory complexes in response to the stress of *Trypanosoma cruzi* infection. Free Radic Biol Med. 2004;37(12):2072–81.
50. de Mello AH, Costa AB, Engel JDG, Rezin GT. Mitochondrial dysfunction in obesity. Life Sci. 2018;192:26–32.
51. Fariello RM, Pariz JR, Spaine DM, Cedenho AP, Bertolla RP, Fraietta R. Association between obesity and alteration of sperm DNA integrity and mitochondrial activity. BJU Int. 2012;110(6):863–7.
52. Vignera S, Condorelli Rosita A, Vicari E, Calogero AE. Negative effect of increased body weight on sperm conventional and non-conventional flow cytometric sperm parameters. J Androl. 2013;33(1):53–8.
53. Nosak C, Silva PN, Sollazzo P, Kyung-Mee M, Odisho T, Foster LJ, et al. JAGN1 is induced in response to ER stress and regulates proinsulin biosynthesis. PLoS One. 2016;11(2).
54. Tripathi YB, Pandey V. Obesity and endoplasmic reticulum (ER) stresses. Front Immunol. 2012;3:240.
55. Lee B-H, Lee MJ, Park S, Oh D-C, Elsasser S, Chen P-C, et al. Enhancement of proteasome activity by a small-molecule inhibitor of USP14. Nature. 2010;467:179–86.
56. Nagai A, Kadowaki H, Maruyama T, Takeda K, Nishitoh H, Ichijo H. USP14 inhibits ER-associated degradation via interaction with IRE1α. Biochem Biophys Res Commun. 2009;379(4):995–1000.
57. Fernández-Sánchez A, Madrigal-Santillán E, Bautista M, Esquivel-Soto J, Morales-González Á, Esquivel-Chirino C, et al. Inflammation, oxidative stress, and obesity. Int J Mol Sci. 2011;12(5).
58. Norris KM, Okie W, Kim WK, Adhikari R, Yoo S, King S, et al. A high-fat diet differentially regulates glutathione phenotypes in the obesity-prone mouse strains DBA/2J, C57BL/6J, and AKR/J. Nutr Res. 2016;36(12):1316–24.
59. Ozaydin A, Onaran I, Yesim TE, Sargin H, Avsar K, Sultuybek G. Increased glutathione conjugate transport: a possible compensatory protection mechanism against oxidative stress in obesity? Int J Obes. 2006;30(1):134–40.
60. Pastore A, Ciampalini P, Tozzi G, Pecorelli L, Passarelli C, Bertini E, et al. All glutathione forms are depleted in blood of obese and type 1 diabetic children. Pediatr Diabetes. 2011;13(3):272–7.
61. Atig F, Raffa M, Habib B-A, Kerkeni A, Saad A, Ajina M. Impact of seminal trace element and glutathione levels on semen quality of Tunisian infertile men. BMC Urol. 2012;12(1):6.
62. Ochsendorf FR, Buhl R, Bästlein A, Beschmann H. Glutathione in spermatozoa and seminal plasma of infertile men. Hum Reprod. 1998;13(2):353–9.
63. Rizza S, Filomeni G. Chronicles of a reductase: biochemistry, genetics and physio-pathological role of GSNOR. Free Radic Biol Med. 2017;110:19–30.
64. Bátiz LF, De Blas GA, Michaut MA, Ramírez AR, Rodríguez F, Ratto MH, et al. Sperm from Hyh mice carrying a point mutation in αSNAP have a defect in acrosome reaction. PLoS One. 2009;4(3):e4963.
65. De Blas GA, Roggero CM, Tomes CN, Mayorga LS. Dynamics of SNARE assembly and disassembly during sperm acrosomal exocytosis. PLoS Biol. 2005;3(10):e323.

66. Brahmanaju M, Shoeb M, Laloraya M, Kumar PG. Spatio-temporal organization of Vam6P and SNAP on mouse spermatozoa and their involvement in sperm–zona pellucida interactions. Biochem Biophys Res Commun. 2004;318(1):148–55.
67. Hwang SR, O'Neill A, Bark S, Foulon T, Hook V. Secretory vesicle aminopeptidase B related to neuropeptide processing: molecular identification and subcellular localization to enkephalin- and NPY-containing chromaffin granules. J Neurochem. 2006;100(5):1340–50.
68. Cadel S, Foulon T, Viron A, Balogh A, Midol-Monnet S, Noël N, et al. Aminopeptidase B from the rat testis is a bifunctional enzyme structurally related to leukotriene-A(4) hydrolase. Proc Natl Acad Sci U S A. 1997;94(7):2963–8.
69. Subirán N, Candenas L, Pinto FM, Cejudo-Roman A, Agirregoitia E, Irazusta J. Autocrine regulation of human sperm motility by the met-enkephalin opioid peptide. Fertil Steril. 2012;98(3):617–25.e3.
70. Kubo H, Kotani M, Yamamoto Y, Hazato T. Involvement of sperm proteases in the binding of sperm to the vitelline envelope in *Xenopus laevis*. Zool Sci. 2008;25(1):80–7.
71. de Mateo S, Castillo J, Estanyol JM, Ballescà JL, Oliva R. Proteomic characterization of the human sperm nucleus. Proteomics. 2011;11(13):2714–26.
72. Razan AE, Marine P, Romain B, Guy L, Yasmina A, Vincent A, et al. LEM-domain proteins are lost during human spermiogenesis but BAF and BAF-L persist. Reproduction. 2017;154(4):387–401.
73. Tifft KE, Segura-Totten M, Lee KK, Wilson KL. Barrier-to-autointegration factor-like (BAF-L): a proposed regulator of BAF. Exp Cell Res. 2006;312(4):478–87.
74. Samavat JMS, Natali IPD, Degl'Innocenti SMS, Filimberti EMS, Cantini GPD, Di Franco AMS, et al. Acrosome reaction is impaired in spermatozoa of obese men: a preliminary study. Fertil Steril. 2014;102(5):1274–81.e2.
75. Fan Y, Liu Y, Xue K, Gu G, Fan W, Xu Y, et al. Diet-induced obesity in male C57BL/6 mice decreases fertility as a consequence of disrupted blood-testis barrier. PLoS One. 2015;10(4).
76. Fullston T, McPherson NO, Owens JA, Kang WX, Sanderman LY, Lane M. Paternal obesity induces metabolic and sperm disturbances in male offspring that are exacerbated by their exposure to an "obesogenic" diet. Physiol Rep. 2015;3(3):e12336.
77. Binder NK, Hannan NJ, Gardner DK. Paternal diet-induced obesity retards early mouse embryo development, mitochondrial activity and pregnancy health. PLoS One. 2012;7(12).